Non-Invasive Investigation of Arctic Hunter-Gatherer Archaeological Landscapes Using Combined Remote Sensing and Near Surface Geophysics

By

David Bryce Landry

A thesis submitted to the Faculty of Graduate Studies of

The University of Manitoba

in partial fulfillment of the degree of

Doctor of Philosophy

Department of Anthropology

University of Manitoba

Winnipeg, Manitoba, Canada

Copyright © 2018, David Bryce Landry

Abstract

This dissertation aims to test and evaluate new applications of non-invasive remote sensing and geophysical technologies at three archaeological sites (LdFa-1; LeDx-42; and LbDt-1) located in the interior region of southern Baffin Island, Nunavut. LdFa-1 and LeDx-42 are both Paleo-Inuit occupation sites, while LbDt-1 is one of only two known chert quarry sites in this region. Methods used at these three Paleo-Inuit sites include terrestrial laser scanning, radar imaging, electromagnetic resistivity and conductivity mapping, and magnetic susceptibility mapping. The methods are examined for both their effectiveness in archaeological fieldwork, and their investigative value on lower relief hunter-gatherer sites. The results of these tests are presented through four original research manuscripts.

Developing and integrating a non-invasive multi-method approach to site investigation in the Arctic facilitates efficient in-field data acquisition and allows for less reliance on wide-scale excavation and extended field seasons. Because weather can be an unpredictable factor on site accessibility in the deep interior regions, entire field seasons can, and have been derailed despite best planning efforts and sufficient funding. As such, it is vital that these technologies enable us to collect valuable data within a limited amount of time. Remote sensing and geophysical survey data were collected, processed, analysed, and interpreted in both field and lab settings throughout this project. Because the motivations of this project are heavily methodological in nature, the analytical approach of this dissertation focuses on the ways to integrate these methods and interpretations within pre-established archaeological frameworks.

The results of this study demonstrate that non-invasive, multi-method investigation of Arctic hunter-gatherer sites is an effective approach to derive detailed archaeological data without the need for wide-scale excavation. With these data, I was able to more clearly interpret and understand Paleo-Inuit toolstone use and transport patterns beginning at a quarry and then extending across southern Baffin Island's interior and coastal regions. The combined subsurface imaging and surveys proved to be the most effective way to locate, identify, and investigate anthropogenic features in these complex Arctic environments, and ultimately the resulting information they acquired has enhanced our overall understanding of Paleo-Inuit lifeways in this region.

Acknowledgements

I would like to take the time to wholeheartedly thank all those who have been a vital part in the efforts and completion of this PhD dissertation. First and foremost, my heartfelt thanks go to my advisor, Dr. Brooke Milne. Brooke has been a guiding light throughout my entire graduate tenure. Since first accepting me for my Masters in 2011, and then encouraging me to further pursue a PhD, Brooke has always challenged me in ways I never thought possible, and has never lacked confidence in my abilities, even when I stumbled time and time again. She has been a never-ending source for information, and her expertise in Arctic prehistory continues to amaze me. Brooke has always been there to talk me through struggles and keep me focused on the project at hand. It will be hard to forget how many times simply meeting face-to-face could seemingly solve all my life's problems. I could not have asked for a better advisor, mentor, and now, lifelong friend.

Second, I would like to thank my excellent committee members, Dr. Ian Ferguson, Dr. Robert Park, and Dr. Mostafa Fayek. Their support, advice, and training along the way was stellar and always appreciated. They were always quick to reply to my email requests and provided countless amounts of constructive comments and edits on my dissertation and manuscript drafts over the years. Their expertise across multiple areas of research provided me with the valuable interdisciplinary skillset essential to the completion of this dissertation. I would also like to thank my external examiner, Dr. Douglas Bamforth. His comments and suggestions on my dissertation and during my defence required me to think about the broader implications of my research, and for that, I again offer my profound thanks.

Throughout the past four and a half years, I have had the pleasure of working alongside some incredible people. I would like to give many thanks to all of the field crews who worked with Brooke and myself, including Mostafa Fayek, Bob Park, Ian Ferguson, Mulu Serzu, and Rachel ten Bruggencate. Even though we only managed to get into the field for about eight total days, I was able to collect the data I did because of these hardworking and fantastic researchers. Moreover, each and every one of them made the delays in Ottawa, and weeks spent stuck in Iqaluit all the more bearable.

Conducting my PhD coursework at the University of Calgary through the Western Deans Agreement program allowed me to meet and work with more wonderful people whom I would like to acknowledge. Both Dr. Peter Dawson and Dr. Gerry Oetelaar welcomed me into their classes, and provided me with a new and exciting outlook on North American archaeology, and the many possibilities of using technology and digital spaces in the field. My time spent in Calgary would not have been as enjoyable as it was if it were not for meeting such good people as Colleen Hughes, and Tyler Murchie. I always benefitted from our long discussions and walks around campus, and am so glad to have made such friends while I was away from home. Finally, I am forever grateful to my Aunt Bonnie and Uncle Pete for opening their home to me while I began this 4-month endeavour in Calgary. They truly let me into their family I always felt embraced.

To all my friends and family, I cannot thank you enough for your everlasting love, support, and patience. From phone calls home, to late night movies, game nights, and long discussions over coffee, you have all been there for me since the start. To my brother Stephen, and sister-in-law Lorissa, thank you for always keeping a smile on my face. To Rachel ten

Bruggencate, Amy Scott, Nitasha Ali, and Sölmundur Pálsson, you have each had an everlasting impact on my life and I will always cherish that.

Great big thanks goes to my wonderful partner Deirdre. She has been there for me since the beginning and I love celebrating every moment of this with her. Through all the ebbs and flows of these past few years of writing, she has remained a constant source of happiness and love. With all my heart, thank you.

And finally, Mom and Dad, I couldn't have done this without your encouragement, help, and guidance along the way. You have always been there for me and stayed positive no matter the choices I make in life. For all the hard work you've put in, love you've given me, and kindness you've shown me over the years, I dedicate this dissertation to you.

This research would not have been possible without the support from the University of Manitoba, the Department of Anthropology, and Faculty of Graduate Studies. This research was graciously funded by the following agencies and programs: Social Sciences and Humanities Research Council of Canada's Insight Grant Program (#435-2012-1176; Milne, Fayek, Park, Stenton); the Canada Foundation for Innovation – John R. Evans Leaders Fund Project (#25071; Milne); the Manitoba Research and Innovation Fund (Milne); the Manitoba Heritage Grants Program (#12F-H145; Milne); the Polar Continental Shelf Project (Natural Resources Canada, Earth Sciences Sector, Project #647-13), the Social Sciences and Humanities Research Council Doctoral Award (Landry); University of Manitoba Graduate Fellowship (Landry); Northern Scientific Training Program (Landry); and the University of Manitoba, Faculty of Graduate Studies SSHRC Graduate Enhancement of Tri-Council Stipends Scholarship (Landry).

Final thanks go to anyone I might have missed. I want you to know that I am very grateful for even the smallest contribution and support towards my research. Without all these people in my life, this dissertation would not have been possible. A sincere thanks to everyone.

Table of Contents

Abstract ii

Acknowledgements iii

Table of Contents v

List of Tables x

List of Figures xi

List of Equations xix

List of Acronyms xx

Use of Copyrighted Material xxi

Chapter 1. Introduction 1

1.1 Preamble 1

1.2 Study Area, Motivations and Objectives, and Sites 5

1.3 Integrated Methods and Case Study 9

1.3.1 Case Study 1 10

1.3.2 Case Study 2 11

1.3.3 Case Study 3 11

1.3.4 Case Study 4 12

1.4 Significance of Research 13

1.5 Dissertation Framework 14

1.6 Works Cited – Chapter 1 15

Chapter 2. Eastern Arctic Prehistory, Study Area, and Remote Sensing and Geophysics in an Arctic Environment 26

2.1 Human Occupation of Southern Baffin Island 26

2.2 Study Sites 30

2.2.1 LdFa-1 30

2.2.2 LeDx-42 32

2.2.3 LbDt-1 33

2.3 Physical Environment of Interior Southern Baffin Island 36

2.3.1 Physiography 36
2.3.2 Climate 36
2.3.3 Geology 37
2.4 Subsistence and Material Resources 43
2.5 Remote Sensing and Geophysical Methods 44
2.5.1 Arctic Geophysical and Remote Sensing Studies 44
2.5.2 Terrestrial Laser Scanning Surveys 46
2.5.3 Magnetometer and Gradiometer Surveys 48
2.5.4 Electromagnetic Surveys 50
2.5.5 Ground Penetrating Radar Surveys 53
2.6 Works Cited – Chapter 2 55
Chapter 3. Combined Geophysical Approach in a Complex Arctic Archaeological Environment: A Case Study from the LdFa-1 Site, Southern Baffin Island, Nunavut 73
Abstract 74
3.1 Introduction 75
3.2 Southern Baffin Island and the LdFa-1 Area 5 Survey Site 78
3.3 Geophysical Methods 80
3.3.1 Magnetometer/Gradiometer 80
3.3.2 EM31 82
3.4 Survey and Configuration 83
3.5 Data Reduction and Results 85
3.6 Geophysical Responses 89
3.6.1 Apparent Conductivity 89
3.6.2 TMF and Vertical Magnetic Gradient 89
3.6.3 Apparent Susceptibility Responses 80
3.7 Interpretation 93
3.8 Discussion 91
3.8.1 Archaeological Studies at LdFa-1 94

3.8.2 Implications for Archaeological Studies in a Complex Arctic Environment 95

3.9 Conclusions 97

3.10 Works Cited – Chapter 3 97

Chapter 4. Manual Point Cloud Classification and Extraction for Hunter-Gatherer Feature Investigation: A Test Case from Two Low-Arctic Paleo-Inuit Sites 106

Abstract 107

4.1 Introduction 108

4.2 Study Sites and Methods 111

4.2.1 LdFa-1 and LeDx-42 111

4.2.2 Parameter Values 112

4.2.3 Processing Sequence 114

4.3 Results 117

4.4 Discussion 122

4.5 Conclusions 124

4.6 Works Cited – Chapter 4 125

Chapter 5. Integrated Geophysical Techniques for the Archaeological Investigation of LbDt-1, a Paleo-Inuit Quarry Site in the Interior of Southern Baffin Island, Nunavut, Canada. 130

Abstract 131

5.1 Introduction 132

5.2 LbDt-1 134

5.3 Remote-Sensing and Geophysical Methods 137

5.3.1 Terrestrial Laser Scanning 137

5.3.2 Ground Penetrating Radar Imaging 139

5.3.3 Electromagnetic Imaging 142

5.4 Survey Configuration and Measurements 144

5.5 TLS Data Processing and Results 147

5.6 GPR Data Processing and Results 151

5.6.1 Unprocessed GPR Responses 151
5.6.2 GPR Data Processing Steps 155
5.6.3 GPR Response of the Chert Flake Deposit 157
5.6.4 Deeper GPR Responses 160
5.7 Electromagnetic Survey Data Processing and Results 161
5.7.1 Raw IP and Q Responses 161
5.7.2 Two-Layer Inversions of the IP Data 164
5.8 Integration of Remote Sensing and Geophysical Results 167
5.9 Discussion and Conclusions 171
5.9.1 Remote Sensing and Geophysical Interpretations 172
5.9.2 Archaeological Significance and Conclusions 174
5.10 Works Cited – Chapter 5 175
Chapter 6. Combining Remote Sensing, Geophysics, and Lithic Provenance and Reduction to Understand Long-Term Continuity in Paleo-Inuit Chert Quarrying and Seasonal Inland Travels on Southern Baffin Island, NU. 185
Abstract 186
6.1 Introduction 187
6.1.1 Archaeological Background 189
6.1.1.1 Chert on Southern Baffin Island 190
6.1.1.2 Quarries and Lithic Technology 192
6.1.1.3 Southern Baffin Island Quarries 194
6.2 Materials and Methods 196
6.2.1 Sites 196
6.2.1.1 LbDt-1 196
6.2.1.2 LdFa-1 199
6.2.1.3 LeDx-42 200
6.2.2 Geophysical Analysis and Test Excavation at LbDt-1 200
6.3 LbDt-1, Quarrying, and Inland Mobility on Southern Baffin Island 202
6.4 Conclusion 204

6.5	Works Cited – Chapter 6	205
Chapter 7.	Discussion and Conclusions	214
7.1	Research Objectives and Results	214
7.2	Contributions to the Study of Archaeology and Arctic Sciences	218
7.3	Non-Invasive Approach to Archaeology and the Way of the Future	219
7.4	Works Cited – Chapter 7	224
Appendix A:	Contributions of Collaborating Authors	230

List of Tables

4.1 Parameters and ranges used to fingerprint and define each surface material from LdFa-1 and LeDx-42. A combination of the four parameters can identify and isolate each material from the original point clouds.

List of Figures

Figure 1.1 Map of southern Baffin Island, Nunavut, Canada, noting the locations of three Paleo-Inuit sites, LdFa-1; LeDx-42; and LbDt-1.

Figure 2.1 Photograph taken from above the northern part of Mingo Lake looking across the LdFa-1 site (left) (Photo credit: Dr. Brooke Milne). The topographic site map (right) derived from the 2008 total station survey of the site, covers the foreground area of the photograph.

Figure 2.2 Photograph taken from above the northern part of Mingo River across from LeDx-42 site area (left) (Photo credit: Dr. Brooke Milne). The topographic site map (right) derived from the 2013 TLS survey of the site (Scale in meters). A portion of the river's edge has been topographically mapped during the TLS survey, and can be seen in the site map.

Figure 2.3 Photograph taken from above the eastern shore of the Hone River, across from LbDt-1 (left) (Photo credit: Dr. Brooke Milne). The upper component topographic site map (right) derived through TLS surveys from 2015 (Scales in meters). A portion of the river's edge has been topographically mapped during the TLS survey and can be seen in the site map.

Figure 2.4 Photograph of naturally occurring chert nodules within the limestone layers that outcrops at LbDt-1.

Figure 2.5 Map indicating the locations of archaeological sites LdFa-1, LeDx-42, and LbDt-1 within the spatial geological context of the Precambrian Batholith and the Ordovician sedimentary bedrock. (Sandford and Grant 2000).

Figure 2.6 Correlation at the formation level of the Ordovician stratigraphy on southern Baffin Island and northeastern Melville Peninsula (Zhang & Lavoie 2013).

Figure 2.7 Photographs of Units 2 and 3 from the Amadjuak Group with identification of the units based on the descriptions by Sandford and Grant (2000). a) Eroded and exposed limestone outcrop of Unit 2 at LbDt-1. The height of the outcrop is ~5 m. The outcrop includes embedded chert nodules. b) Photograph of an outcrop of Unit 3, near LdDx-2. Photograph is taken looking north towards Amadjuak Lake. The height of the ridge formed by the limestone outcrop is ~10 m and the length of the ridge on the photograph is ~1.0 km.

Figure 3.1 Northern Canada and Greenland, with Baffin Island and LdFa-1 site map inset (modified from Park, 2008). The LdFa-1 map shows the areas defined at the complex site and defined features of interest and excavation units. The current study is located in Area 5.

Figure 3.2 Photograph of LdFa-1 Area 5 showing the 20m by 20m geophysical survey grid. Note the relatively thick vegetation covering parts of the surface.

Figure 3.3 Relative sensitivity of the apparent conductivity and apparent susceptibility response of a LIN instrument: left-hand vertical axes show normalized depth, the ratio of the depth to coil spacing, and right-hand vertical axes show the equivalent depths for an EM31 instrument operated at 1m elevation. Equations for the sensitivity functions can be found in Fitterman and Labson (2005).

Figure 3.4 (a) Temporal magnetic field fluctuations recorded at the Mingo Lake base station and the Iqaluit Magnetic Observatory on 15 July 2014. The black bar along the top shows the time of the actual magnetic field survey. (b) Contour map of raw TMF data over the survey grid. (c) Contour map of corrected TMF data over the survey grid.

Figure 3.5 Contour maps of the final geophysical survey results from LdFa-1 Area 5. The maps show the TMF, magnetic gradient, apparent susceptibility and apparent conductivity responses. The interpolation and contouring is based on variogram analysis of the data and the apparent conductivity maps include a nugget effect variance of approximately 10% of the scale. Apparent magnetic susceptibility values were derived from the InPhase responses using conversion factors of ka (SI) = 2.95 × 10_3ΔI (ppt) for the HD mode and ka (SI) = 9.51 × 10_3ΔI (ppt) for

the VD mode. These factors provide an exact susceptibility for a uniform Earth model. Apparent susceptibility and apparent conductivity maps show only the relative values of the parameters. “A”, “B” and “C” denote locations of interest.

Figure 3.6 (a and b) Shaded relief maps of the TMF and VD apparent susceptibility in LdFa-1 Area 5 with base-map overlay indicating the location of the previous test units, caribou trails and response areas of interest A, B and C. (c and d) Surface map of the TMF and VD apparent susceptibility response.

Figure 4.1 Archaeological sites LdFa-1 and LeDx-42 situated on a Google Earth landsat image with southern Baffin Island inset. Sites are located near lakes Mingo and Amadjuak, southern Baffin Island, NU.

Figure 4.2 Step-by-step classification sequence from original point cloud dataset to the individually classified elements, using open source LAStools and CloudCompare software.

Figure 4.3 Bottom: Original colour point clouds of LdFa-1 and LeDx-42. Top: Colour classified point clouds using our processing sequence. Colours correspond to the following materials: Blue – Water/Snow; Light Green – Low-vegetation; Dark Green – Medium-vegetation; Red – High-vegetation; Grey – Gravel; Orange – Exposed Outcrop; Yellow – Stone Boulders. Note that the scanner positioning in LeDx-42 caused the shadowed areas in the point clouds.

Figure 4.4 Top: Original point cloud sample from LdFa-1. Bottom: Extracted stone boulders from the point cloud and layered on top of a surface contour map. Arrows indicating the location of stone tent rings near the right side of the map. Scale is in meters.

Figure 4.5 Top: Original point cloud sample from LeDx-42. Gaps in the data represent the location of the laser scanner stations and are indicated by S1 and S2. The exposed stone outcrops on the surface are also outlined in orange. Bottom: Extracted stone boulders from point cloud and layered on top of surface contour map. Stone clusters are found radiating from the points

of highest elevation near the left side of the map, away from the hummocky tundra seen on the right. Scale is in meters.

Figure 5.1 Figure 5.1 Map of southern Baffin Island indicating the location of the archaeological site, LbDt-1, inset with map of northern Canada and Greenland.

Figure 5.2 Oblique aerial photograph of LbDt-1 showing the upper and lower site components. Survey grid 1 (13 m×44 m), grid 2 (6 m×20 m) and grid 3 (8 m×15 m) are noted, along with the survey lines (L) 1 and 2 and the locations of test pits (TP) 1 and 2. The extensive surface chert deposit appears within the yellow dashed ellipse.

Figure 5.3 Photographs from LbDT-1. **a** Surface view of the chert flake deposit. Note the grass growing within the deposit. **b** Photograph of 0.25×0.25 m area of the surface chert deposit. Scale bar divisions are centimeters. **c** Test pit 1, located in grid 2 within the dense chert flake deposit. **d** Test pit 2 which is located on line 1 outside the chert flake deposit.

Figure 5.4 LIN apparent conductivity and apparent susceptibility sensitivity functions and two-layer responses. **a, b** The relative sensitivity of apparent conductivity and apparent susceptibility responses for the vertical dipole (VD) and horizontal dipole (HD) modes. The left axis shows normalised depth, and the right axes show the actual depth for an EMP-400 instrument operated at 10 cm elevation. Note that all responses are plotted using the convention that the sign of the transmitter signal at the receiver coil is positive. **c, d** The apparent conductivity and apparent susceptibility responses for a two-layer structure containing an upper layer of increasing thickness for an EMP-400 instrument operated at 10 cm elevation. The conductivity and susceptibility of the upper layer are a factor of ten higher than the same parameters in the lower layer.

Figure 5.5 Photograph looking north from near the (0 N, 3 E) on grid 1. The locations of grid 2 and test pits TP1 and TP2 are shown. Note the absence of grass from the surface deposits of gravel.

Figure 5.6 TLS images of grid 1. **a** Restored colour image of the grid. The yellow dashed line indicates the surface outline of the visible chert flake deposit, and the blue dashed line indicates the surface outline of the visible gravel deposit. **b** Density

image of point classifications representing chert flakes with surface cortex. **c** Density image of point classifications representing grass. The circular gap in data centred on (31 N, 3 E) indicates the area where the TLS instrument was situated and points did not consistently overlap. Darker shade points indicate greater density of nearby neighbours in (**b**) and (**c**).

Figure 5.7 Topographic surface map of grid 1, using the TLS point cloud relative x,y,z, coordinate data. Gridding is based on natural neighbour interpolation and 5-cm cell sizes. The local topographic lows (around 15 N) correlate with the dark patches on the restored colour image seen in Figure 5.6**a**. A larger reflector is visible at (4–5 E, 0 N), along with a few residual data artefacts at the scanner position (0E, 34 N).

Figure 5.8 Raw and processed GPR responses from near Test Pits TP 1 and TP2 shown using a gray-shaded display. Shaded rectangles show approximate extent of each test pit. The depth scale is based on a dielectric constant of k=9. **a**, **b** Raw GPR data for 20 m long profiles containing TP1 (left) in an area of the chert deposit and TP2 (right) in a background area (see Figure 5.2). Labels indicate particular features of the GPR response: A, diffraction hyperbolas created by heterogeneities in the in-filled test pit; B, zone of extremely dense clutter caused by scattering at the ground surface creates a fuzzy texture when plotted at the scale shown; C, a zone of more discrete diffraction hyperbolas with cusps at the surface; D, diffractions from termination of a subhorizontal reflector; E, zones of more discrete diffraction hyperbolas with cusps at the surface. **c**, **d** The same profiles following standard GPR processing. Note the increase in the continuity of the deeper reflections. **e**, **f** Early time part of the processed GPR radargrams (0–15 ns). Arrows labelled F indicate the direct arrival with the long arrow pointing to the positive central peak of the recorded pulse and the short arrows to the negative side-lobes. Arrows labelled G indicate an early-time negative-polarity reflection with the long arrow pointing to the negative main peak and the short arrows to the positive side-lobes.

Figure 5.9 Processed GPR responses for grid 1. Depths are based on dielectric constant of k=9.9. a Perspective view from the southwest showing line 1. The upper surface

corresponds to the amplitude response at 19 cm depth averaged over a depth range of 18 cm. Arrows on the vertical section indicate south-dipping reflectors. b View of line 1 at increased vertical exaggeration with the location of the top of additional depth slices marked. Arrows indicate south-dipping reflectors. c Enlarged view of first 16 ns of the line 1 response. Arrows indicate negative-polarity reflection interpreted to be the base of the debitage deposit. d Horizontal amplitude slices with black dashed line showing the surface distribution of chert and blue dashed line showing the distribution of gravel. The top of slice 1 is at 2 ns (or 10 cm depth) and the response averages over 2 ns. It highlights the amplitude of the negative polarity reflection. Slice 2 is at 6 ns (or 30 cm depth) and averages over 2 ns. Note the generally low amplitude reflections from the debitage and gravel deposits. Slice 3 is at 12 ns (or 60 cm depth) and averages over 6 ns. It highlights deeper reflections and shows the structures present at shallow depth in the north part of section (from 35 to 44 N) are mostly confined to more shallow depth.

Figure 5.10 Comparison of GPR signals from representative locations of LdBt-1 using wiggle trace format. The background results are for an area with mainly soil at the surface whereas the remaining plots are for areas with gravel or chert flakes at the surface. Note that a deflection to the left corresponds to a black colour in Figures 5.8 and 5.9.

Figure 5.11 EMP-400 16,000 Hz Q and IP responses plotted in terms of apparent conductivity (upper panels) in mS m−1 and apparent susceptibility (lower panels) in SI.

Figure 5.12 Results of two-layer magnetic susceptibility inversions. **a** Statistics of the inversion process showing for the different interface depths the correlation of susceptibility in the two layers (upper panel), the mean value of susceptibility in each layer and the standard deviation of susceptibility in each layer. **b** The contours of susceptibility in each layer for the optimal model with an interface depth of 20 cm. **c** Variograms of the spatial variation of susceptibility in the upper and lower layer. The fitted variograms were used to produce the contoured results in (b).

Figure 5.13 Multi-method imaging of the debitage deposit. Areas labelled (a) and (b) represent the estimated surface extent of the chert debitage and gravel distributions, respectively. a TLS surface point cloud image of grid 1 and grid 2. b Depth to the base of surface layer as indicated by primary reflection in the GPR response. The reflector depth results show a wider distribution of a thick (>9 cm) layer beneath the visible debitage deposit. In contrast, the depth of the reflector beneath the visible gravel deposit is relatively shallow (<4 to 7 cm) and is fairly distinct in the southern portion of grid 1 and parts of grid 2. c Near-surface radar slice (2– 4 ns) showing location of reflections from the base of the chert layer. d Magnetic susceptibility in upper 20 cm showing relatively low values in the debitage and gravel deposits.

Figure 5.14 Two-layer magnetic susceptibility results overlain on the GPR section for the 3-m E line of grid 1. The high susceptibility values in the lower layer at the north end of the line are spatially correlated with deepening GPR reflections and high susceptibility values in the upper layer.

Figure 6.1 Location of sites LbDt-1, LdDx-2, LdFa-1, and LeDx-42 situated within inland southern Baffin Island.

Figure 6.2 Photographs of Units 2 and 3 from the Amadjuak Group with identification of the units based on the descriptions by Sandford and Grant (2000). a) Eroded and exposed limestone outcrop of Unit 2 at LbDt-1. The height of the outcrop is ~5 m. The outcrop includes embedded chert nodules. b) Photograph of an outcrop of Unit 3, near LdDx-2. Photograph is taken looking north towards Amadjuak Lake. The height of the ridge formed by the limestone outcrop is ~10 m and the length of the ridge on the photograph is ~1.0 km.

Figure 6.3 Exposed chert embedded in the limestone outcrop at LbDt-1. Arrows point to loose nodules weathered out of the limestone.

Figure 6.4 Oblique aerial image of the LbDt-1 quarry site. The focus of this study takes place within the Upper Component noted on the image; however, the exposed limestone outcrop is featured within the Lower Component.

Figure 6.5 Photograph showing a small close-up section of the dense chert flake deposit at the LbDt-1 quarry site.

Figure 6.6 Satellite image indicating the approximate location of the LbDt-1 lithic quarry. Note that it sits within the Upper Ordovician Amadjuak Formation, approximately 1 km north of the Cumberland Batholith. Inset map of southern Baffin Island is included at top right.

List of Equations

Eq. 1. $S_{\sigma HD}(r,z) = 2 - 4\left(\frac{z}{r}\right)\left(4\left(\frac{z}{r}\right)^2 + 1\right)^{-1/2}$

Eq. 2. $S_{\sigma VD}(r,z) = 4\left(\frac{z}{r}\right)\left(4\left(\frac{z}{r}\right)^2 + 1\right)^{-3/2}$

Eq. 3. $S_{\kappa HD}(r,z) = -12\frac{z}{r}\left(4\left(\frac{z}{r}\right)^2 + 1\right)^{-5/2}$

Eq. 4. $S_{\kappa VD}(r,z) = 12\frac{z}{r}\left(3 - 8\left(\frac{z}{r}\right)^2\right)\left(4\left(\frac{z}{r}\right)^2 + 1\right)^{-7/2}$

Eq. 5. $v \sim 2S$

Eq. 6. $\kappa_{aHD} = 2I_{HD} \cdot (I_{HD} + 1)^{-1}$

Eq. 7. $\kappa_{aVD} = 2I_{VD} \cdot (I_{VD} - 1)^{-1}$

Eq. 8. $I_{HD} = \frac{-\kappa_1}{2+\kappa_1}\left[R_{\kappa HD}(r,h) - R_{\kappa HD}(r,h+z_1)\right] + \frac{-\kappa_2}{2+\kappa_2}\left[R_{\kappa HD}(h+z_1)\right]$

Eq. 9. $I_{VD} = \frac{-\kappa_1}{2+\kappa_1}\left[R_{\kappa VD}(r,h) - R_{\kappa VD}(r,h+z_1)\right] + \frac{-\kappa_2}{2+\kappa_2}\left[R_{\kappa VD}(h+z_1)\right]$

Eq. 10. $\kappa_1 = 1.706 I_{HD} + 4.1096 I_{VD}$

Eq. 11. $\kappa_2 = -3.3334 I_{HD} - 1.3589 I_{VD}$

List of Acronyms

3D	Three-Dimensional
ASTt	Arctic Small Tool tradition
EM	Electromagnetic
EMP	Electromagnetic Profiler
ERI	Electrical Resistivity Imaging
GPR	Ground Penetrating Radar
HD	Horizontal Dipole
IP	InPhase
LIN	Low Induction Number
Q	Quadrature
RGB	Red, Green, Blue
TLS	Terrestrial Laser Scanning
VD	Vertical Dipole

Use of Copyrighted Material

Chapter 3 of this dissertation is reproduced with minor modifications from "Landry, D. B., Ferguson, I. J., Milne, S. B., Park, R. W. (2015). Combined Geophysical Approach in a Complex Arctic Archaeological Environment: A Case Study from the LdFa-1 Site, Southern Baffin Island, Nunavut. *Archaeological Prospection* 22(3): 157-170".

Chapter 4 of this dissertation is reproduced with minor modifications from "Landry, D. B., Milne, S. B., Park, R. W., Ferguson, I. J., Fayek, M. (2016). Manual Point Cloud Classification and Extraction for Hunter-Gatherer Feature Investigation: A Test Case from Two Low Arctic Paleo-Inuit Sites. *Open Archaeology* 2(1): 232-242, DOI: 10.1515/opar-2016-0017".

Chapter 5 of this dissertation is reproduced with minor modifications from "Landry, D. B., Ferguson, I. J., Milne, S. B., Serzu, M., Park, R. W. (2018) Integrated Geophysical Techniques for the Archaeological Investigation of LbDt-1, a Paleo-Inuit Quarry Site in the Interior of Southern Baffin Island, Nunavut, Canada", *Journal of Archaeological Method and Theory* DOI: https://doi.org/10.1007/s10816-018-9370-6

Chapter 6 of this dissertation is reproduced with minor modifications from "Landry, D. B., Milne, S. B., ten Bruggencate, R. E. (Accepted) "Combining Remote Sensing, Geophysics, and Lithic Provenance and Reduction to Understand Long-Term Continuity in Paleo-Inuit Chert Quarrying and Seasonal Inland Travels on Southern Baffin Island, NU." *Quaternary International*.

Chapter 1

Introduction

1.1 Preamble

The aim of this dissertation is to develop, test, and evaluate new methodological applications of non-invasive remote sensing and geophysical technologies at three archaeological sites located on southern Baffin Island, Nunavut (see Figure 1.1). Digital remote sensing and geophysics, including terrestrial laser scanning (TLS), magnetics, electrical resistivity imaging (ERI), and ground-penetrating radar (GPR), have been integrated into archaeological site investigations in North and South America, (e.g. Conyers et al. 2008; Conyers 2010; 2013; 2016; Dalan 2008; Dalan and Banerjee 1998; Dawson et al. 2011; 2013; Eastaugh and Taylor 2005; 2011; Eastaugh et al. 2013; Hodgetts et al. 2011; 2017; Landry et al. 2015; 2016; Urban 2012; Urban et al. 2012; Pluckhahn and Thompson 2012; Randall 2014; Wolff and Urban 2013 etc.), Europe, (e.g. Barton 2009; Brewly et al. 2005; Chase et al. 2012; Conyers et al. 2013; Gaffney et al. 2007; Gaffney et al. 2012; Guidi et al. 2014; Keay et al. 2009; Smekalova et al. 1993 etc.) and in the Middle East, Asia, and Africa, (e.g. Al-kheder et al. 2009; Conyers 2010; Lambers et al. 2007; Lerma et al. 2010; Ronghui and Yilin 1992; Rüther et al. 2009; Urban et al. 2014a/b etc.) all with impressive results. The digital surface and subsurface data derived through their use have fundamentally changed the way archaeological surveying and mapping are conducted, and how data and results can be represented given the unparalleled precision and unique interpretative power these technologies afford (McCoy and Ladefoged 2009). Furthermore, recent technological advancements in computer hardware and software have made it easier to develop new analytical procedures for processing and interpreting these digital datasets (Dawson and Levy 2016; Landry et al 2016; Thompson et al. 2011). It is not surprising then, that the

current and potential future use of these technologies and the results they can produce for archaeological research continues to generate significant interest among academics, stakeholder communities, and the general public alike (Watterson 2015).

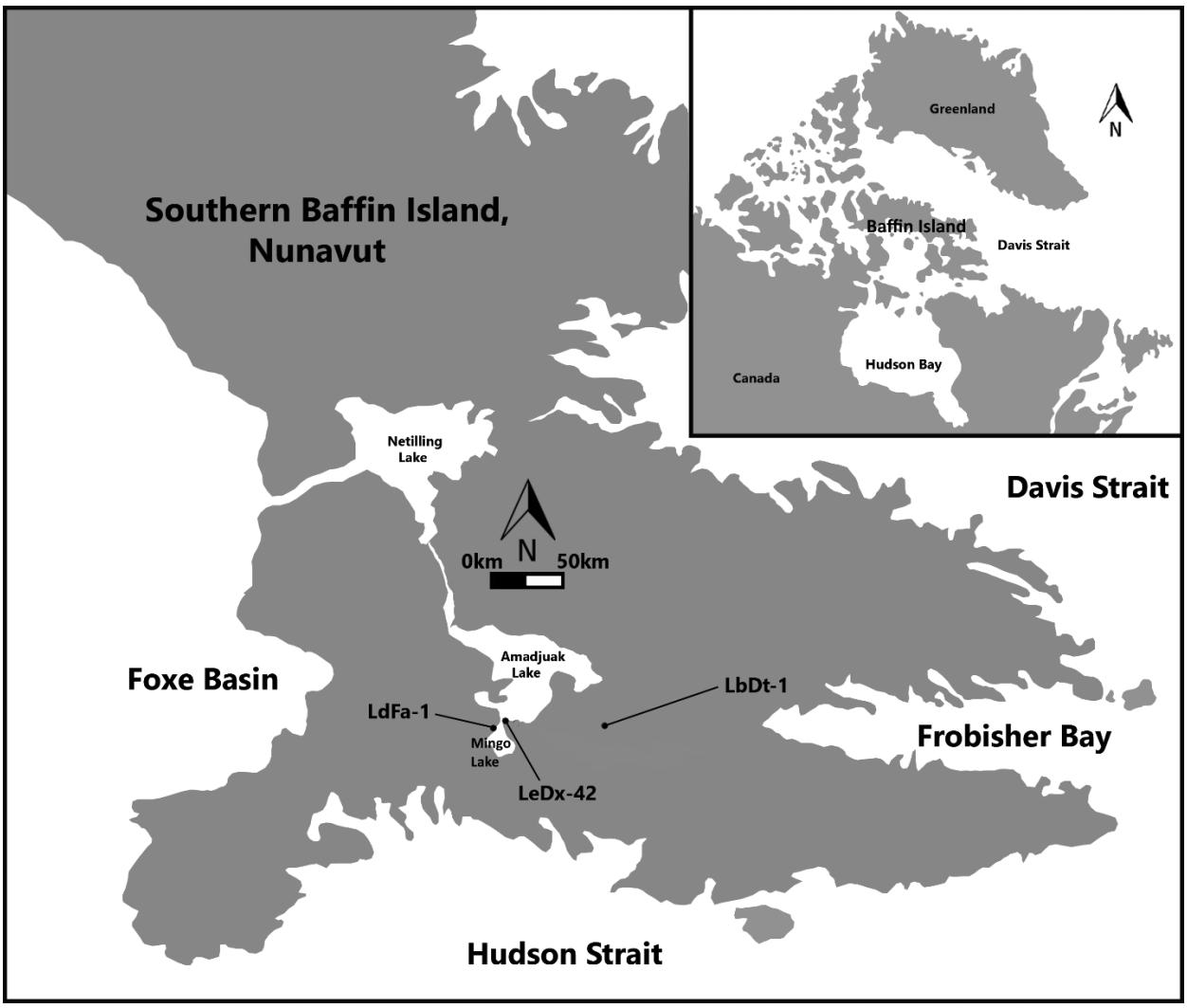

Figure 1.1. Map of southern Baffin Island, Nunavut, Canada, noting the locations of three Paleo-Inuit sites, LdFa-1; LeDx-42; and LbDt-1.

Remote sensing and near-surface geophysical methods were introduced into archaeological practice in Europe in the mid-twentieth century, when investigative interests shifted towards the integration of methodologies used more commonly in the natural sciences; with this came the active recruitment of physicists, geologists, and environmental scientists into the discipline (Aspinall et al. 2008; Bevan 1983; Clark 1986; Conyers 2010; Scollar et al. 1990). In their earliest applications, particularly throughout Britain and France, remote sensing and geophysical methods were being tested at archaeological sites to determine whether such technologies could identify common anomalies as they related to past human activities. These early attempts helped set precedents for the use of non-invasive technologies in investigating archaeological sites, the location of metal artifacts, and the delineation of large-scale near- and sub-surface features (i.e., walls, foundations etc.). The application of remote sensing and geophysics in archaeology was primarily focused on prospection, intended to isolate areas of investigation and reduce the physical extent of full-scale excavation. The fact these technologies could gather site information without the need for full-scale excavation increased fieldwork efficiency and, ultimately, helped to preserve many sites in situ (Tabbagh 1986:576).

The growing popularity of remote sensing and geophysics, and their use in Europe was facilitated, in part, by their successful application in the investigation of large sites including those dating to the Neolithic, Classical, Bronze age, and Iron age periods (e.g. Ard et al. 2014; Batt and Dockrill 1998; Tabbagh 1986). Over time, use of these technologies was encouraged in fieldwork and in research design by European academic, and consulting archaeologists (Aspinall 1991; Gaffney and Gater 2006).

Despite the early implementation of remote sensing and geophysics in archaeological research within Europe, the adoption of these techniques for investigative purposes among North

American archaeologists were not as wide spread until the late-twentieth and early-twenty-first centuries. This delay is noted to be in part due to the extent and nature of archaeological site remains in North America, which tend to consist of more ephemeral occupations characteristic of mobile hunter-gatherers, and the need to develop research designs tailored to investigating such sites (Gibson 1989; Johnson 2006; Urban 2012). Many of these early archaeological sites have been disturbed by centuries of farming and development, and material remains made out of metal were less common among North American prehistoric sites, which together, limited the efficacy of early remote sensing and geophysical technologies in archaeological site prospection.

With improvements in instrument sensitivity, including the ability to detect smaller surface and subsurface anomalies, it is now possible to examine features associated with more ephemeral occupations commonly attributed to hunter-gatherer sites (Landry et al. 2015, In Press; Hodgetts et al. 2016), including smaller-scale geophysical anomalies such as hearth features, subsurface household depressions, fired rock, and midden deposits (Gibson 1989; Glencross et al. 2017; Hodgetts et al. 2016). With these improvements, the application of remote sensing and geophysics in archaeological site investigation, including regions such as the North American Arctic, is becoming more commonplace (Eastaugh et al. 2013; Hodgetts and Eastaugh 2017; Hodgetts et al. 2011; 2017; Landry et al. 2015; 2018; Urban 2012; Urban et al. 2012; Wolff and Urban 2013; Viberg *et al.* 2009).

Since early 2000, the use of remote sensing and geophysics has helped to shift the archaeological discourse primarily from prospection to interpretation, and to heritage conservation and research design. Collectively, the use of these investigative methods and technologies now falls within the context of archaeogeosciences (e.g., Dawson et al. 2013; Valls et al. 2016; Conyers 2016). Archaeologists focus on the potential of these techniques within the

context of interdisciplinary research relying on collaboration with environmental scientists to develop new investigative approaches and procedures (Landry et al. 2015; 2016; 2018). This encourages archaeologists to rethink how digital datasets created through remote sensing and geophysics can be effective interpretative tools in archaeological contexts around the world, and especially for sites that are vulnerable to damage or loss due to natural or anthropogenic forces, including climate change. Overall, there has been a shift in how archaeologists use remote sensing and geophysics from "ad-hoc" to "inquiry based" foci (Conyers 2016; Kvamme 2003; Thompson et al. 2011).

1.2 Study Area, Motivations and Objectives, and Sites

The earliest human populations to live in the Arctic are known archaeologically as the Palaeo-Eskimos. This name – Palaeo-Eskimo – was coined by early investigators and was meant to refer to the fact that these earlier populations lived in the same place as today's Inuit peoples (McGhee 1996). Given the perceived pejorative connotation associated with the name "Eskimo," archaeologists, such as Friesen (2015), prefer to refer to these earliest inhabitants as Paleo-Inuit. It is important to understand, however, that using this term does not imply any direct cultural continuity, genetic or otherwise, with today's Inuit populations. Following Friesen (2015), I also use the term Paleo-Inuit.

On southern Baffin Island, the Paleo-Inuit comprise two distinct yet related cultures – Pre-Dorset (ca. 4,000 – 2,500 BP) and Dorset (ca. 2,500 – 1,100 BP). These populations traveled seasonally between inland and coastal areas to acquire seasonally available subsistence and material resources available in each locale (Milne 2003; Milne et al. 2012). Sites included in this study are principally located in the island's deep interior and the results derived from analysis of

them and their associated remains make an important contribution to the ongoing study of terrestrial land use by these earliest Nunavummiut (see Milne et al. 2012).

The types of Paleo-Inuit sites considered in this study are essential to evaluate the effective application of remote sensing and geophysics in their investigation. Many sites are multi-component wherein Paleo-Inuit populations, as well as later Thule Inuit, came to the same locations repeatedly due to the strategic location these places afforded in the acquisition of a particular resource (e.g. caribou, waterfowl, lithic raw material). Specifically, LdFa-1 and LeDx-42 are located on the banks of Mingo Lake and the Mingo River, respectively. These sites each see frequent caribou traffic as the animals cross these waterways making both ideal hunting locations (Milne et al. 2012, 2013). Other inland sites, such as MaDv-11 (Mosquito Ridge), were located to harvest larger numbers of geese during the annul moult (Milne and Donnelly 2004). Lastly, LbDt-1 and LdDx-1 are two inland quarries where chert was readily acquired by Paleo-Inuit toolmakers (Milne 2015, 2016; ten Bruggencate et al. 2016, 2017). The fact this essential raw material is geologically localized to the intermediate zone separating the southern Baffin Island's coastal and interior regions, means both quarries likely had a strong influence on the routes Paleo-Inuit peoples traveled since both were used to acquire chert toolstone (ten Bruggencate 2015; 2016). While subsistence and material resource acquisition was an important focus for all Paleo-Inuit peoples traveling between southern Baffin Island's inland and coast, the centrality of the interior and the relative ease with which it could be accessed from all coastal uplands made it an ideal location for inter-regional interaction and socialization (Milne 2003; Stenton 1989). Maintaining social contact among small-scale, nomadic hunter-gatherer populations is essential for basic population viability (MacDonald 1999; MacDonald and Hewlett 1999; Milne 2008). Among the Inuit, visiting is an important part of day-to-day life

(Boas 1964; Stenton 1989). Seasonal gatherings in the deep interior likely were an essential part of Paleo-Inuit life as well thus the repeated occupation of large habitation sites like LdFa-1 and LeDx-42 is not at all surprising (Milne 2008; Milne et al. 2012, 2013; Milne and Park 2016).

The motivations for this study are to develop a multi-method approach to site investigation that uses technologies to streamline data acquisition in the field, and that are capable of dealing with contingencies common to working in the Arctic. Because weather has such an unpredictable influence on site accessibility in all Arctic locations, entire field seasons can, and have been derailed despite extensive planning and sufficient funding in place. The nature of these technologies, however, enables a significant amount data collection to occur within a limited amount of time, meaning researchers rarely leave empty handed provided they can arrive at the site even if for a very short amount of time (e.g., Landry et al. 2015).

While there are some challenges to using these kinds of technologies in extreme environments (e.g., Al-kheder et al. 2009; Dawson et al. 2013; Entwistle 2009), they allow archaeologists to continue exploring a site digitally through systematic post-processing and filtering workflows conducted in a lab (Doneus et al. 2008; Entwistle 2009; Landry et al. 2016). Ultimately, this possibility allows archaeologists to worry less about logistical constraints on their research by providing a way to reduce the need for lengthy surveys while still capturing high quality data without the need for invasive and wide-scale excavation.

The multi-method approach presented in this study demonstrates how non-invasive digital datasets, derived from remote sensing and geophysical survey, can be combined with conventional archaeological data, and directly linked to broader archaeological interpretations and theory. This approach helps reduce ambiguity in interpretations since it allows for complementary datasets to be considered. In addition, the efficient and detailed recording of sites

using these methods informs archaeologists of potential areas of interest, and aims to simplify data collection in future field programs. Ultimately, these are important considerations given the remoteness of Arctic archaeological sites, the rapidly changing climate and site conditions, and the immense logistical costs associated with working on them.

These motivations have led me to address the following four objectives in this dissertation: (1) to evaluate the role of archaeogeophysical survey for the discernment of natural and anthropogenic features on hunter-gatherer archaeological sites in the deep interior of southern Baffin Island; (2) to develop and test an accessible method that allows archaeologists to spatially isolate and analyse surface elements from a massive 3D point cloud dataset produced by terrestrial laser scanning; (3) to use a combination of remote sensing and geophysical datasets (surface and subsurface) to develop methodologies that can be employed for the non-invasive study of lithic quarries;, and (4), to identify and understand long-term mobility and resource exploitation patterns through the synthesis of three Paleo-Inuit site investigations in the deep interior of southern Baffin Island.

To meet these objectives, I examine remote sensing and geophysics data acquired from three Paleo-Inuit sites on southern Baffin Island: LdFa-1; LeDx-42, and, LbDt-1. Since none of the specific instruments used in this study had been previously tested in Arctic field condition before, a large part of this study was focused on basic field testing in local conditions present at Paleo-Inuit sites in the study area. LdFa-1 provides an ideal multi-component Paleo-Inuit site to test the capabilities of terrestrial laser scanning and magnetics across a complex environment. Here, features and artifacts are found scattered across the surface of a diverse landscape. The site includes a combination of excavated and unexcavated areas. At this location, remote sensing and geophysical investigation is used to identify and map unknown components both on the surface,

and near-surface layers. LeDx-42 represents a surficially amorphous site with many unknown features. Here, surface laser scanning is used to help locate areas of interest and potential feature markings on the landscape. Finally, LbDt-1 is a massive lithic quarry that spans two separate components. Here, a multi-method approach is used to provide insight into the extent of activities that took place, and demonstrate the potential application of a non-invasive investigative methods to understand the spatial expansiveness of archaeological lithic quarries.

1.3 Integrated Methods and Case Studies

This dissertation presents a non-invasive multi-method approach tested at three Paleo-Inuit sites. Terrestrial laser scanning (TLS), electrical resistivity imaging (ERI), electromagnetics (EM), and ground-penetrating-radar (GPR) were tested and applied to examine the utility of their results. The integration of some, or all, of these methodologies during a site investigation allows for the unique optimization of instrumentation focused towards the collection of particular datasets and presentation of results. Additionally, the use of multiple methods at a range of site types helps provide a baseline of effectiveness for future work on sites in this region, and elsewhere.

The four case study manuscripts presented can be grouped into two categories. Case studies in Chapters 3, 4, and 5 demonstrate the specific use of individual remote sensing and geophysical methods to investigate Paleo-Inuit sites in the interior of southern Baffin Island. The case study presented in chapter 6 shows the integration of both remote sensing and geophysical methods to investigate small-scale hunter-gatherer sites, including quarries, and how use of the results can link to a broader understanding of mobility and resource-use patterns. The case studies are as follows:

1.3.1 Case Study 1

Presented in the first case study (Chapter 3) is the survey, processing, and analysis of the complex Arctic landscape at LdFa-1 using a combined magnetic and electromagnetic approach to define the physical characteristics of both large- and small-scale anthropogenic anomalies. Measurements were made with a GEM Systems Overhauser magnetometer-gradiometer and Geonics EM31 instrument, and a survey configuration was designed to map the total magnetic field, magnetic susceptibility and electrical conductivity responses of the underlying soils. Defined data-reduction methods were an integral part of this study and were used following each survey to produce final responses related closely to the subsurface physical properties of Area 5, and six different geophysical responses were presented in the results of the study. This study shows the significance of reduced interpretational ambiguity made available by the use of complementary non-invasive geophysical datasets, and demonstrates the value of geophysical investigation in a complex Arctic archaeological environment and its potential role in providing information on subsurface archaeological features.

"**Landry, D.B.**, Ferguson, I.J., Milne, S.B., Park, R.W. (2015). Combined Geophysical Approach in a Complex Arctic Archaeological Environment: A Case Study from the LdFa-1 Site, Southern Baffin Island, Nunavut. *Archaeological Prospection* 22(3): 157-170."

1.3.2 Case Study 2

Case study 2 (Chapter 4) focuses on acquiring analytical and interpretive outcomes from large-scale remote sensing datasets through a manual approach using a combination of spectral and intensity measurements collected through typical active sensor TLS (i.e. intensity and RGB

values). This study illustrates the use of TLS data collected in 2013 from LdFa-1 and LeDx-42 to develop a manual point cloud classification approach using open source software (i.e. LAStools and CloudCompare). This approach is applied throughout this study using Paleo-Inuit site point clouds in order to demonstrates its value within hunter-gatherer research, as effective uses of large TLS datasets for extracting and improving our analytical capabilities for low relief site features remains limited.

"**Landry, D.B.**, Milne, S.B., Park, R.W., Ferguson, I.J., Fayek, M. (2016). Manual Point Cloud Classification and Extraction for Hunter-Gatherer Feature Investigation: A Test Case from Two Low Arctic Paleo-Inuit Sites. *Open Archaeology* 2(1): 232-242, DOI: 10.1515/opar-2016-0017."

1.3.3 Case Study 3

Case study 3 (Chapter 5) presents a large-scale non-invasive investigation of the archaeological toolstone quarry deposit at LbDt-1 from an integrated technologies perspective. Geophysical and remote sensing methods from studies 1 and 2 are combined in this study to investigate anthropogenic and geological features in the surface and subsurface layers of the Upper Component at LbDt-1. The models derived from three overlapping surveys provide complementary information making it possible to highlight the complexities of the chert deposit, and derive valuable information about the depth and distribution of the chert both on the surface and subsurface. This study explores the anthropogenic development of this *in-situ* deposit, and the preferential activities spaces used by the Paleo-Inuit at this site.

"**Landry, D.B.**, Ferguson, I.J., Milne, S.B., Serzu, M., Park, R.W. (2018) Integrated Geophysical Techniques for the Archaeological Investigation of LbDt-1, a Paleo-Inuit Quarry Site in the Interior of Southern Baffin Island, Nunavut, Canada." *Journal of Archaeological Method and Theory* DOI: https://doi.org/10.1007/s10816-018-9370-6.

1.3.4 Case Study 4

The fourth and final case study is presented in Chapter 6. It synthesizes four datasets acquired using remote sensing, geophysics, lithic provenance, and reduction analysis from the noted sites. Particular attention is paid to understanding how the Paleo-Inuit used the LbDt-1 quarry and how visits to this important site over time influenced lithic reduction activities at LdFa-1 and LeDx-42. Combining the remote sensing and geophysics results from studies 1, 2, and 3, with previous archaeological investigations at these sites demonstrates the importance of chert toolstone quarries throughout the southern Baffin Island region for both the Pre-Dorset and Dorset peoples.

"**Landry, D.B.**, Milne, S.B., ten Bruggencate, R. E. (Accepted) Combining Remote Sensing, Geophysics, and Lithic Provenance and Reduction to Understand Long-Term Continuity in Paleo-Inuit Chert Quarrying and Seasonal Inland Travels on Southern Baffin Island, NU. *Quaternary International*.

1.4 Significance of Research

This research project is the first of its kind to be conducted on southern Baffin Island, and is unique in its focus on a comprehensive analytical and interpretive application of remote

sensing and geophysics in this region of the Arctic. The results from this project have important implications for a broader area of study: they contribute to the development of low-relief and ephemeral hunter-gatherer site investigations; they provide a wide range of testable archaeogeophysical and remote sensing applications in a complex environmental setting; and they add to the limited literature focused on a non-descriptive analysis of hunter-gatherer lithic procurement sites (i.e., quarries) as part of a technological organization (e.g., Bamforth 1991; 2006; Burke 2007; Byrd et al. 2009; Root 1997).

In addition, the application of this multi-method approach can dramatically shift future research design, decreasing the amount of time spent manually mapping and testing surrounding site landscapes and providing a means to monitor and manipulate *in situ* features post investigation. This type of detailed collection of surface and subsurface data serves as a baseline for future comparative mapping at these sites. It also allows researchers to track active excavations, or even more importantly, to track the degradation of archaeological sites due to physical processes that include erosion and rapidly thawing permafrost throughout the Arctic (e.g., Barr 2007, 2009; Colette 2007; Colette and Cassar 2007; Heritage 2008; Hodgetts and Eastaugh 2017; Wolff and Urban 2013).

Lastly, when applicable, openly sourced software is used to process and analyse data collected from sites throughout this project. Every successful application and dissemination of these software packages and the techniques used helps to make them more accessible to a more general audience and readily comparable to people using the same, or similar approaches around the world.

1.5 Dissertation Framework

This dissertation includes seven chapters. Chapter 2 provides background information about the landscape, geology, resources, and the natural and anthropogenic components of the inland archaeological sites included in this study. Applications of remote sensing and geophysics in an Arctic context are also discussed.

Chapters 3 presents a published peer-reviewed original research manuscript on the topic of electromagnetic and magnetic susceptibility instrumentation and its use on a complex Arctic environment. This chapter discusses the required optimization and reduction of digital datasets in order to reveal the potential improvement possible in the geophysical investigation of Paleo-Inuit archaeological sites in this region.

Chapter 4 discusses the application of a new technique using terrestrial laser scanning to investigate surface features at two different inland archaeological sites through a published peer-reviewed original manuscript. This investigative method is discussed as a manual approach that can be used in the field to help determine areas of interest on archaeological sites, and to efficiently map small scale features in detail.

Chapter 5 consists of a research manuscript presently under provisional acceptance with revisions in the Journal of Archaeological Method and Theory that discusses a multi-method approach to non-invasive Paleo-Inuit site investigation. Specifically, the study presented in this chapter focuses on the potential of applying remote sensing and geophysics as investigative tools at a large-scale lithic quarry located in the interior region of southern Baffin Island.

Chapter 6 is the final manuscript submitted for publication in a special issue of Quaternary International. This contribution derives from a peer-reviewed conference presentation at the Arctic Science Summit Meetings 2017 in Prague, Czech Republic (Landry et

al. 2017). This study presents a synthesis of the remote sensing, geophysical, and archaeological data from the LbDt-1 lithic quarry site, and uses the results as a proxy to discuss land use, and resource procurement and transportation throughout the interior region of southern Baffin Island. Chapter 7 summarizes this study and presents its conclusions. The Appendix provides information about the contribution of each author to these research studies.

1.6 Works Cited – Chapter 1

Al-kheder, S., Al-shawabkeh, Y., and Haala, N. 2009. Developing a documentation system for desert palaces in Jordan using 3D laser scanning and digital photogrammetry. *Journal of Archaeological Science*, 36, 537-546.

Ard, V., Mathé, V., Lévêque, F., and Camus, A. 2014. A comprehensive magnetic survey of a Neolithic causewayed enclosure in West-central France for the interpretation of archaeological features. *Archaeological Prospection*, 22(1), 21-32. DOI: 10.1002/arp.1495

Aspinall, A. 1991. New developments in geophysical prospection. In *Proceedings of the British Academy*, (Vol. 71, pp. 233-244).

Aspinall, A., Gaffney, C., and Conyers, L. 2008. Archaeological prospection – the first fifteen years. *Archaeological Prospection*, 15(4), 241-245.

Bamforth, D. B. 1991. Technological organization and hunter-gatherer land use: a California example. *American Antiquity*, *56*(2), 216-234.

Bamforth, D. B. 2006. The Windy Ridge quartzite quarry: hunter-gatherer mining and hunter-gatherer land use on the North American continental divide. *World Archaeology*, 38(3), 511-527.

Barton, J. 2009. 3D laser scanning and the conservation of earthen architecture: a case study at the UNESCO World Heritage Site Merv, Turkmenistan. *World Archaeology*, 41(3), 489-504.

Barr, S. 2007. The effects of climate change on cultural heritage in the polar regions. In *Heritage at Risk*. ICOMOS World Report 2006/2007 on Monuments and Sites in Danger.

Barr, S. 2009. Protecting cultural heritage and community roots. In *Climate Change and Arctic Sustainable Development*. Paris, France: United Nations Educational, Scientific and Cultural Organization.

Batt, C. M., and Dockrill, S. J. 1998. Magnetic moments in prehistory: Integrating magnetic measurements with other archaeological data from the Scatness multiperiod settlement. *Archaeological Prospection*, *5*(4), 217-227.

Bewley, R. H., Crutchley, S. P., and Shell, C. A. 2005. New light on an ancient landscape: lidar survey in the Stonehenge World Heritage Site. *Antiquity*, 79(305), 636-647.

Bevan, B. W. 1983. Electromagnetics for mapping buried earth features. *Journal of Field Archaeology*, *10*(1), 47-54.

Boas, F. 1964. *The central eskimo*. (Original Publication 1888.) Lincoln: University of Nebraska Press.

Bryd, B. F., Young, D. C., and McGuire, K. R. 2009. Pavement, quarries, Gypsum period residential stability, and Trans-Holocene settlement systems of the Mohave Desert: a case study at Fort Irwin. *Journal of California and Great Basin Anthropology*, 29(2), 121-144.

Burke, A. L. 2007. Quarry source areas and the organization of stone tool technology: a view from Quebec. *Archaeology of Eastern North America*, 35, 63-80.

Chase, A. F., Chase, D. Z., Fisher, C. T., Leisz, S. J., and Weishampel, J. F. 2012. Geospatial revolution and remote sensing LiDAR in Mesoamerican archaeology. In *Proceedings of the National Academy of Sciences (PNAS)*, 109(32), 12916-12921.

Clark, A. J. 1986. Archaeological geophysics in Britain. *Geophysics*, *51*(7), 1404-1413.

Colette A. 2007. *Case Studies on Climate Change and World Heritage.* (Paris: UNESCO World Heritage Centre).

Colette, A., and Cassar, M. 2007. Climate change and world heritage: report on predicting and managing the impacts of climate change on world heritage, and strategy to assist states parties to implement appropriate management responses.

Conyers, L. B. 2010. Ground-penetrating radar for anthropological research. *Antiquity*, 84(323), 175-184.

Conyers, L. B. 2013. *Ground-penetrating radar for archaeology*. AltaMira Press.

Conyers, L. B. 2016. *Interpreting ground-penetrating radar for archaeology*. Routledge.

Conyers, L. B., Ernenwein, E. G., Grealy, M., and Lowe, K. M. 2008. Electromagnetic conductivity mapping for site prediction in meandering river floodplains. *Archaeological Prospection*, 15(2), 81-91.

Conyers, L. B., Daniels, J. M., Haws, J. A., and Benedetti, M. M. 2013. An upper Palaeolithic landscape analysis of coastal Portugal using ground- penetrating radar. *Archaeological Prospection*, 20(1), 45-51.

Dalan, R. A. 2008. A review of the role of magnetic susceptibility in archaeogeophysical studies in the USA: recent developments and prospects. *Archaeological prospection*, *15*(1), 1-31.

Dalan, R. A., and Banerjee, S. K. 1998. Solving archaeological problems using techniques of soil magnetism. *Geoarchaeology*, *13*(1), 3-36.

Dawson, P., Levy, R., and Lyons N. 2011. 'Breaking the fourth wall': 3D virtual worlds as tools for knowledge repatriation in archaeology. *Journal of Social Archaeology,* 11(3), 387-402.

Dawson, P., Bertulli, M. M., Levy, R., Tucker, C., Dick, L., and Cousins, P. L. 2013. Application of 3D laser scanning to the preservation of Fort Conger, a historic polar research base on northern Ellesmere Island, Arctic Canada. *Arctic,* 66(2), 147-158.

Dawson, P., and Levy, R. 2016. From science to survival: Using virtual exhibits to communicate the significance of polar heritage sites in the Canadian Arctic. *Open Archaeology*, *2*(1).

Doneus, M., Briese, C., Fera, M., and Janner, M. 2008. Archaeological prospection of forested areas using full-waveform airborne laser scanning. *Journal of Archaeological Science*, *35*(4), 882-893.

Eastaugh, E., and Taylor, J. 2005. Geophysical survey of the Dorset Palaeoeskimo site of Point Riche. *Newfoundland and Labrador Studies*, *20*(1).

Eastaugh, E., and Taylor, J. 2011. Settlement size and structural complexity: A case study in geophysical survey at Phillip's Garden, Port au Choix. In M. A. P. Renouf (Ed.), *The Cultural Landscapes of Port au Choix, Interdisciplinary Contributions to Archaeology*, (pp. 178-188). Springer Science + Business Media, LLC. DOI 10.1007/ 978-1-4419-8324-4_9.

Eastaugh, E., Ellis, C., Hodgetts, L., Keron, J. 2013. Problem based magnetometer survey at the Late Archaic Davidson Site (AhHk-54) in Southwestern Ontario. *Canadian Journal of Archaeology/Journal Canadien D'Archaéologie*, 37, 274–301.

Heritage. 2008. *Climate Change and the Historic Environment.* London: English Heritage.

Entwistle, J. A., McCaffrey, K. J. W., and Abrahams, P. W. 2009. Three-dimensional (3D) visualisation: the application of terrestrial laser scanning in the investigation of historical Scottish farming townships. *Journal of Archaeological Science*, 36(3), 860-866.

Friesen, T. M. 2015. On the naming of Arctic archaeological traditions: The case for Paleo-Inuit. *Arctic*, 68(3), iii-iv.

Gaffney, C. F., and Gater, J. 2006. *Revealing the buried past: geophysics for archaeologists*. Tempus.

Gaffney, V. L., Thomson, K., and Fitch, S. 2007. *Mapping Doggerland: the Mesolithic landscapes of the southern North Sea*. Archaeopress.

Gaffney, C., Gaffney, V., Neubauer, W., Baldwin, E., Chapman, H., Garwood, P., and Hinterleitner, A. 2012. The Stonehenge hidden landscapes project. *Archaeological Prospection*, *19*(2), 147-155.

Glencross, B., Warrick, G., Eastaugh, E., Hawkins, A., Hodgetts, L., and Lesage, L. 2017. Minimally invasive research strategies in Huron-Wendat archaeology: Working toward a sustainable archaeology. *Advances in Archaeological Practice*, *5*(2), 147-158.

Guidi, G., Russo, M., and Angheleddu, D. 2014. 3D survey and virtual reconstruction of archeological sites. *Digital Applications in Archaeology and Cultural Heritage*, 1, 55-69.

Hodgetts, L., and Eastaugh, E. 2017. The role of magnetometry in managing Arctic archaeological sites in the face of climate change. *Advances in Archaeological Practice*, *5*(2), 110-124.

Hodgetts, L., Dawson, P., and Eastaugh, E. 2011. Archaeological magnetometry in an Arctic setting: a case study from Maguse Lake, Nunavut. *Journal of Archaeological Sciences*, 38, 1754–1762. DOI:10.1016/j.jas.2011.03.007.

Johnson, J. K. 2006. *Remote Sensing in Archaeology: An Explicitly North American Perspective* (pp. 1-16). Tuscaloosa: The University of Alabama Press.

Keay, S., Earl, G., Hay, S., Kay, S., Ogden, J., and Strutt, K. D. 2009. The role of integrated geophysical survey methods in the assessment of archaeological landscapes: the case of Portus. *Archaeological Prospection*, *16*(3), 154-166.

Kvamme, K. 2003. Geophysical surveys as landscape archaeology. *American Antiquity*, 68(3), 435–457.

Lambers, K., Eisenbeiss, H., Sauerbier, M., Kauferschmidt, D., Gaisecker, T., Sotoodeh, S., and Hanusch, T. 2007. Combining photogrammetry and laser scanning for the recording and modelling of the Late Intermediate Period site of Pinchango Alto, Palpa, Peru. *Journal of Archaeological Sciences*, 34, 1702-1712.

Landry, D. B., Ferguson, I. J., Milne, S. B., and Park, R. W. 2015. Combined geophysical approach in a complex Arctic archaeological environment: A case study from the LdFa-1 site, southern Baffin Island, Nunavut. *Archaeological Prospection*, *22*(3), 157-170.

Landry, D. B., Milne, S. B., Park, R. W., Ferguson, I. J., and Fayek, M. 2016. Manual point cloud classification and extraction for hunter-gatherer feature investigation: A test case from two low arctic Paleo-Inuit sites. *Open Archaeology*, *2*(1), 232-242.

Landry, D. B., Ferguson, I. J., Milne, S. B., Serzu, M., and Park, R. W. 2018. Integrated geophysical techniques for the archaeological investigation of LbDt-1, a Paleo-Inuit quarry site in the interior of southern Baffin Island, Nunavut, Canada. *Journal of Archaeological Method and Theory* DOI: https://doi.org/10.1007/s10816-018-9370-6.

Landry, D. B., Milne, S. B., and ten Bruggencate, R. E. (Accepted) Combining Remote Sensing, Geophysics, and Lithic Provenance and Reduction to Understand Long-Term Continuity in Paleo-Inuit Chert Quarrying and Seasonal Inland Travels on Southern Baffin Island, NU. *Quaternary International.*

Landry, D. B., Milne, S. B., Park, R. W., Ferguson, I. J., ten Bruggencate, R., Fayek, M., and Serzu, M. 2017. Quarries, caribou, and seasonal inland travels: understanding Pre-Dorset and Dorset culture adaptations on southern Baffin Island, Nunavut. Paper presented at the Arctic Science Summit Meeting, April 4-7, Prague, Czech Republic.

Lerma, J. L., Navarro, S., Cabrelles, M., and Villaverde, V. 2010. Terrestrial laser scanning and close range photogrammetry for 3D archaeological documentation: the Upper Palaeolithic Cave of Parpallo´ as a case study. *Journal of Archaeological Sciences*, 37, 499-507.

MacDonald, D. H. 1999. Modeling Folsom mobility, mating strategies, and technological organization in the northern Plains. *The Plains Anthropologist*, 141-161.

MacDonald, D. H., and Hewlett, B. S. 1999. Reproductive interests and forager mobility. *Current Anthropology*, *40*(4), 501-524.

Milne, S. B. 2003. Identifying Pre-Dorset structural features on southern Baffin Island: Challenges and considerations for alternative sampling methods. *Inuit Studies*, 27(1-2), 67-90.

Milne, S. B. 2008. Archaeological investigations in the Mingo lake district of southern Baffin Island: Assessing Palaeo-Eskimo culture continuity and change. Permit report covering the work conducted under Nunavut Territory Archaeologist Permit No. 07-014. Department of Culture, Language, Elders and Youth, Government of Nunavut, Igloolik, Nunavut.

Milne, S. B. 2015. Chert Sourcing and Palaeo-Eskimo Stone Tool Technology: Permit Report on Work Conducted Under Nunavut Archaeological Permit No. 2015-21A. Department of Culture, Language, Elders and Youth, Government of Nunavut, Igloolik, Nunavut.

Milne, S. B. 2016. Chert Sourcing and Paleo-Eskimo Stone Tool Technology: Report on Work Conducted Under Nunavut Archaeological Permit No. 2015-21A. Department of Culture, Language, Elders and Youth, Government of Nunavut, Igloolik, Nunavut.

Milne, S. B., and Donnelly, S.M. 2004. Going to the birds: examining the importance of avian resources to Pre-Dorset subsistence strategies on southern Baffin Island. *Arctic Anthropology*, 41(1), 90–112.

Milne, S. B., and Park, R. W. 2016. Pre-Dorset Culture. In M. Friesen and O. Mason (Eds.), *The Oxford Handbook of the Prehistoric Arctic*. Oxford University Press. DOI: 10.1093/oxfordhb/9780199766956.001.0001.

Milne, S. B., Park, R. W., and Stenton, D. R. 2012. Dorset culture land use strategies and the case of inland southern Baffin Island. *Canadian Journal of Archaeology/Journal Canadien D'Archéologie*, 36(2), 267-288.

Milne, S.B., Park R. W., and Stenton, D. R. 2013. For caribou, chert, and company: understanding mobility among the Palaeo-Eskimos of Baffin Island, Arctic Canada. In Mobility, Transition, and Change in Prehistory and Antiquity. Proceedings of the Graduate Archaeology Organisation Conference on the Fourth and Fifth of April 2008 at Hertford College, Oxford, UK, Preston PR, Schorle K (eds). British Archaeological Reports, International Series, Archaeopress: Oxford; 49–61.

McCoy, M. D., and Ladefoged, T. N. 2009. New developments in the use of spatial technology in archaeology. *Journal of Archaeological Research*, *17*(3), 263-295.

McGhee, R. 1996. *Ancient people of the Arctic*. Vancouver: UBC Press.

Pluckhahn, T. J., and Thompson, V. D. 2012. Integrating LiDAR data and conventional mapping of the Fort Center site in south-central Florida: A comparative approach. *Journal of Field Archaeology*, 37(4), 289-301.

Randall, A. 2014. LiDAR-aided reconnaissance and reconstruction of lost landscapes: An example of freshwater shell mounds (ca. 7500-500 cal b.p.) in northeastern Florida. *Journal of Field Archaeology*, 39(2), 162-179.

Ronghui, L., and Yilin, W. 1992. An Overview of Archaeo-Seismological Studies in China. *Journal of Seismological Research*, *4*, 012.

Root, M. J. 1997. Production for Exchange at the Knife River Flint Quarries, North Dakota. *Lithic Technology*, 22, 33-50.

Rüther, H., Chazan, M., Schroeder, Ralph., Neeser, R., Held, C., Walker, S. J., Matmon, A., and Horwitz, L. K. 2009. Laser scanning for conservation and research of African cultural heritage sites: the case study of Wonderwerk Cave, South Africa. *Journal of Archaeological Science*, 36, 1847-1856.

Scollar, I., Tabbagh, A., Hesse, A., and Herzog, I. 1990. *Archaeological prospecting and remote sensing*. Cambridge University Press.

Smekalova, T., Voss, O., and Abrahamsen, N. 1993. Magnetic investigation of iron-smelting centres at Snorup, Denmark. *Archaeologia Polona*, *31*, 83-103.

Stenton, D. R. 1989. Terrestrial adaptations of Neo-Eskimo coastal-marine hunters on southern Baffin Island, NWT. Unpublished Ph.D. dissertation, University of Alberta, Edmonton.

Tabbagh A. 1986. Applications and advantages of the Slingram electromagnetic method for archaeological prospecting. *Geophysics*, 51(3), 576–584.

ten Bruggencate, R. E., Milne, S. B., Fayek, M., Park, R. W., and Stenton, D. R. 2015. Characterization of chert artifacts and two newly identified chert quarries on southern Baffin Island. *Lithic Technology*, 40(3), 189-198.

ten Bruggencate, R. E., Stup, J. P., Milne, S. B., Stenton, D. R., Park, R. W., and Fayek, M. 2016. A human-centered GIS approach to modeling mobility on southern Baffin Island, Nunavut, Canada. *Journal of Field Archaeology*, 41(6), 684-698. DOI:10.1080/00934690.2016.1234897.

ten Bruggencate, R. E., Milne, S. B., Park, R. W., Fayek, M., and Stenton, D. R. 2017. Combining chert provenance and least-cost pathway analyses to reconstruct Pre-Dorset and Dorset mobility on southern Baffin Island. *Journal of Archaeological Science: Reports*, *14*, 651-661.

Thompson, V. D., Arnold III, P. J., Pluckhahn, T. J., and Vanderwarker, A. 2011. Situating remote sensing in anthropological archaeology. *Archaeological Prospection*, 18, 195-213.

Urban, T. M. 2012. In the footsteps of J. Louis Giddings (1909–1964): archaeological geophysics in Arctic Alaska. *Antiquity*, 86, 332.

Urban, T. M., Anderson, D. D., and Anderson, W. W. 2012. Multimethod geophysical investigations at an Inupiaq village site in Kobuk Valley, Alaska. *The Leading Edge*, *31*(8), 950-956.

Urban, T. M., Vella, C., Bocancea, E., Tuttle, C. A., and Alcock, S. E. 2014a. A geophysical investigation of a newly discovered Early Bronze Age site near Petra, Jordan. *Journal of Archaeological Science*, *42*, 260-272.

Urban, T. M., Rowan, Y. M., and Kersel, M. M. 2014b. Ground-penetrating radar investigations at Marj Rabba, a Chalcolithic site in the lower Galilee of Israel. *Journal of Archaeological Science*, *46*, 96-106.

Wolff, C. B., and Urban, T. M. 2013. Geophysical analysis at the Old Whaling site, Cape Krusenstern, Alaska, reveals the possible impact of permafrost loss on archaeological interpretation. *Polar Research*, *32*(1), 19888.

Valls, A., García, F., Ramírez, M., and Benlloch, J. 2016. A combined use of GPR Data with historical archives for identifying pavement construction periods of Valencian Silos (16th century, Spain). *IEEE Journal of Selected Topics in Applied Earth Observations and Remote Sensing*, 9(1), 98-107.

Viberg A, Trinks I, Lidén K. 2009. Archaeological prospection in the Swedish mountain tundra region. *ArchéoSciences*, *33*. Rennes: Presses Université.

Watterson, A. 2015. Beyond digital dwelling: re-thinking interpretive visualisation in Archaeology. *Open Archaeology*, 1, 119-130.

Chapter 2

Eastern Arctic Prehistory, Study Area, and Remote Sensing and Geophysics in an Arctic Environment

This chapter presents background information on the Paleo- and Thule Inuit inhabitants of the Eastern North American Arctic. In addition, this chapter describes the study area, including the subsistence and material resources found in the interior regions of southern Baffin Island. The inland regional physiography, climate, and geology are an important element of this chapter as they help to understand the human use of the area. Moreover, they directly influence the use of the remote sensing and geophysical instrumentation that form the core of this study. The final sections of this chapter discuss the general methods used in the application of terrestrial laser scanning (TLS) and geophysical survey.

2.1 Human Occupation of Southern Baffin Island

Roughly 4,500 years ago, small groups of mobile hunter-gatherers began a rapid migration into the eastern Arctic during a period of Post-Glacial Warming. Site remains associated with these early movement are labeled by archaeologists as belonging to the Arctic Small Tool tradition (ASTt) (Bielawski 1988) in large part because of the incredibly small size of the stone tools found consistently among all of the related sites (Irving 1957). These nomadic people were well adapted to terrestrial and coastal environments, and made use of a small, compact, and easily transportable toolkit (Maxwell 1985; McGhee 1970). As the ASTt people spread throughout low, and high Arctic regions, along with northern and western Greenland, they began to develop regionally unique traditions that became manifest in their associated material cultures. These regional variants of the ASTt are recognized archaeologically as the Pre-Dorset

in the low Arctic (Collins 1954, 1956, Maxwell 1973, Taylor 1968, Milne and Park 2016), Independence I in the high Arctic (McGhee 1976, Knuth 1954) and Saqqaq along the western shores of Greenland (Meldgaard 1952).

Collins (1954) first used the term pre-Dorset to describe cultural occupations in the low Arctic that likely pre-dated the Dorset. Some sites discovered in the eastern low Arctic date as far back as 4,500 B.P. (e.g. Helmer 1991:302; Maxwell 1976b, 1985). Pre-Dorset occupations are recognized archaeologically by their use of unique microlithic chipped stone toolkits which include burins, burin spalls, chipped bifacial points, semi-circular blades, endscrapers, and microblades (Milne 2003a, 2003b; Milne and Park 2016). Diagnostic Pre-Dorset dwellings remains include bilobate arrangements of stones with possible axial features. Many large Pre-Dorset sites are suggested to have been re-organized and occupied by later cultural groups (Milne 2003:68; Dekin 1976). Pre-Dorset populations of southern Baffin Island are known to have been highly mobile, traveling seasonally between the coastal and deep interior regions of the island (Milne 2003). The Pre-Dorset appear to have used the interior during the summer months to acquire raw chert toolstone, hunt caribou and local waterfowl, and likely to socialize with other groups who lived in distant locales during the remainder of the yet (Milne 2003; 2005). The Pre-Dorset occupation of southern Baffin lasted for nearly 2,500 years, at which point a major climatic shift occurred.

Paleoclimatic data for this part of the eastern North American Arctic indicates these early Paleo-Inuit peoples experienced warmer than normal temperatures and reduced annual sea-ice cover (McGhee 2001:110). These warmer climatic conditions lasted until around 2,500 B.P. Thereafter, the Arctic climate began to dramatically cool resulting in harsher, longer winters, and a more expansive sea-ice cover, which appears to have proved ideal for hunting marine

mammals (Mudie et al. 2005:120-121). Briner et al. (2016) further note that the timing of this cooling event varied across the Arctic. These environmental changes, which included an expanded sea ice environment and more persistent cold temperatures, are believed to have prompted changes in the way humans adapted to their surrounding landscape (Barry et al. 1977:198-199; Maxwell 1976a:5; 1985:81-82). The change in lifeways is reflected by changes in material culture including what Maxwell considers the appearance of "cold adapted technologies" in the archaeological record including ice creepers, sled shoes, snow knives, among other items (Maxwell 1976a:5; 1985:81-82). These material remains that date in association with the noted climatic cooling event appear to coincide with the emergence of the Dorset culture in the archaeological record (2,500-1,000 B.P.; Barry et al. 1977; Fitzhugh 1997). Archaeologists have inferred a decrease in human mobility during this time, as settlements are larger and more permanent, given the larger associated middens and more complex dwellings (McGhee 2001:131). Meanwhile, subsistence strategies are suggested to have become more diversified since people had to rely on what was available while staying in one place for longer periods of time. There is however, a greater reliance on sea mammals at this time, notably ringed seals, and the development of storage technology further suggests people found ways to stockpile food to allow them to remain on the coasts (Darwent 2004; Fitzhugh 1976; Helmer 1996; Hodgetts et al. 2003; LeMoine and Darwent 1998; McGhee 2001; Maxwell 1997; Murray 1999; Nagy 2000; Odess 1998; Ramsden and Tuck 2001; Renouf and Bell 2010; Tuck and Fitzhugh 1986).

The Dorset used a variety of raw materials to produce an extensive toolkit. The toolkit was often characterized by both knapped and ground microliths, including triangular blades, burin-like-tools, end-scrapers, microblades, and larger ground blades (Maxwell 1985). Most

Dorset deposits are encased in permafrost, which appears to have created better conditions for the preservation of organic implements. These remains indicate that Dorset people used numerous types of bone, antler, and wooden implements; they also had an elaborate carving industry including both human and animal figures (Betts et al. 2015; Hardenberg 2013; McGhee 2001:144). Organic tools included a variety of harpoon heads, arrows, snow knives, and many others, often displaying diagnostic gouged holes. Dorset dwellings vary in size and composition and include tent rings, semi-subterranean dwellings, and long-houses (Friesen 2007:200-201; Harp 1976:129-135). Around 1,500 years ago, a second migration of people out of Alaska began and came to occupy the Eastern North American Arctic. This new population is referred to as the Thule, and they are direct historic ancestors of today's Inuit people (Raghavan et al. 2014:1020).

The Thule migration from Alaska to the east marks the start of the Neo-Inuit phase in the Eastern Arctic. Archaeologists have noted the occurrence of a global warming period associated with this migration (Dekin 1972; McGhee 1969; 1970; 1974). Material remains excavated from Thule sites were first described by Danish researcher Mathiassen (1930), who on the Fifth Thule Expedition named this archaeological culture after a settlement in northern Greenland of the same name – Thule. Remains of Thule sites have been found throughout the Eastern Arctic, including Quebec, Newfoundland, and Greenland. After European contact, the Thule transitioned into what are referred to as historic Inuit and are now known as the Inuit across the Eastern Arctic today (Maxwell 1960). This transition to Inuit culture coincided with the Little Ice Age around 1600 AD. It is during this time that the Inuit focused their attention on hunting seals at their breathing holes on the winter sea ice (Dawson 2016).

2.2 Study Sites

2.2.1 LdFa-1

LdFa-1 is a large, multi-component site with evidence of Pre-Dorset, Dorset and Thule/Inuit cultural occupations. The site was first recorded in 1991 by Stenton, and later investigated by Milne and Park (Milne 2005; Milne 2008; Milne 2013; Park 2008). LdFa-1 is situated at the base of the Mingo Lake esker, approximately 209 kilometers from Frobisher Bay, on southeast coast of southern Baffin Island. The local geology consists of fossiliferous limestone of the Upper Ordovician Amadjuak Formation (Sandford and Grant 2000). This site is situated 2 km to the north of the contact point between this unit and Proterozoic monzogranite of the Cumberland batholith (St Onge et al., 2007).

LdFa-1 is separated into five spatially distinct areas (see Figure 2.1). The central portion of the site, referred to as Area 3 and 4, has yielded evidence associated with a Pre-Dorset occupation. Across a small stream in Area 1, excavations have exclusively yielded lithic and organic remains diagnostic of the Late Dorset period (690 A.D. ± 40 – 880 A.D. ± 40) (Milne et al 2012:278).

There are at least 33 visible stone tent rings within the LdFa-1 site area as well as several stone caches that were likely used to store caribou meat. The tent rings vary in size and shape, as well as in the nature of the construction (i.e. lightly rocked versus heavily rocked). On the nearby esker, Stenton (1991a; see also Milne 2005, 2008) identified several hunting blinds that are strategically situated to hunt caribou. Extensive subsurface testing and more limited excavation was undertaken by Milne in 2004, 2007, 2014, and Park in 2008 resulting in the recovery of large lithic assemblages including diagnostic artifacts for both Pre-Dorset and Dorset cultures. Numerous delicate bone needles and needle fragments suggest hide working occurred (Milne

2008). Large amounts of bone debitage further attest to the production of organic implements at LdFa-1 (Park 2008:30). An extensive and exceptionally well-preserved faunal assemblage, near-exclusively made-up of caribou, was excavated from both the Pre-Dorset and Dorset components at LdFa-1 (McAvoy 2014; Milne et al. 2012, 2013).

Lithic debitage analysis from Area 1, a Late Dorset component, suggested that chert nodules were transported to this site from a local source, and that lithic reduction activities in this area of the site were focused on the production of tool preforms and blanks (Landry 2013). Associated faunal remains further suggest caribou hunting occurred during the Late Dorset occupation of the site (Landry 2013:77). Lithic and faunal remains excavated from the Pre-Dorset component of the site are near identical suggesting cultural continuity in how LdFa-1 was used by both cultures over time.

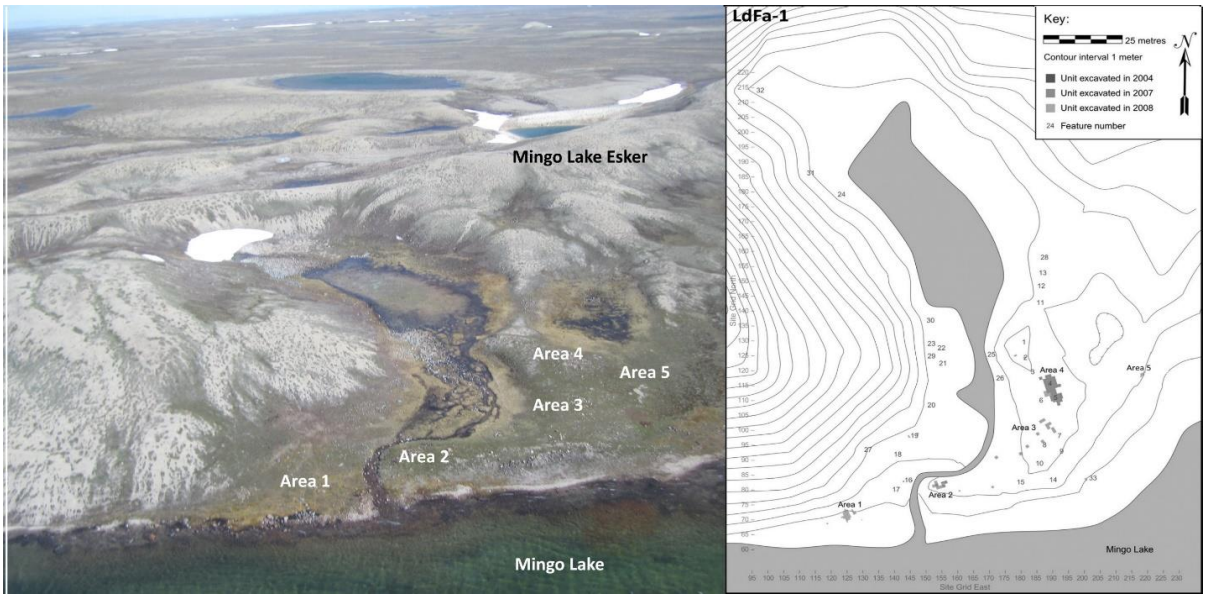

Figure 2.1 Photograph taken from above the northern part of Mingo Lake looking across the LdFa-1 site (left) (Photo credit: Dr. Brooke Milne). The topographic site map (right) derived from the 2008 total station survey of the site, covers the foreground area of the photograph.

2.2.2 LeDx-42

LeDx-42 is a smaller Paleo-Inuit site than LdFa-1 both in terms of its areal extent and total number of visible features. It is located approximately 12 km east of LdFa-1. It too is a multi-component site, having been occupied by the Pre-Dorset and Dorset, yet there is no evidence suggesting a later Thule occupation (Milne et al. 2012, Milne 2013). LeDx-42 is situated on top of a raised bedrock outcrop that looks out over the Mingo River (Figure 2.2). Unlike LdFa-1, LeDx-42 has no visible tent ring features. The site was identified originally because of the extensive scatters of lithic tools and debitage, and fragmented faunal remains (Milne 2005).

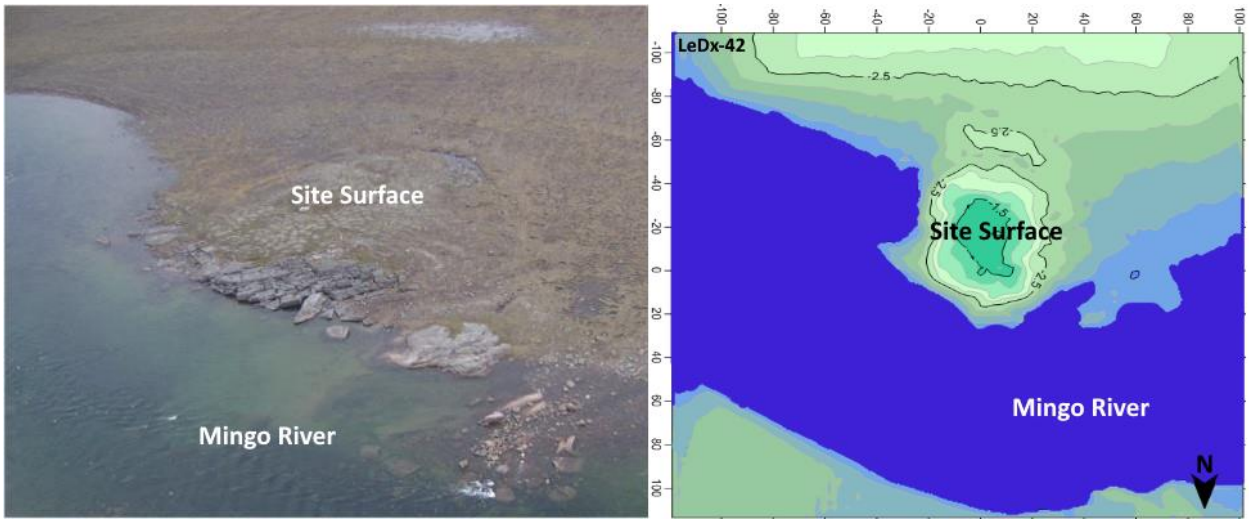

Figure 2.2 Photograph taken from above the northern part of Mingo River across from LeDx-42 site area (left) (Photo credit: Dr. Brooke Milne). The topographic site map (right) derived from the 2013 TLS survey of the site (Scale in meters). A portion of the river's edge has been topographically mapped during the TLS survey, and can be seen in the site map.

The surface cover of LeDx-42 is a mix of exposed bedrock, thick sod, moss, and lichen (Milne et al. 2012:418). The raised central area of the site is surrounded by low-lying wet

hummocky tundra, and numerous mud-boils. A total of 35, 1 m x 1 m units were excavated at the site and yielded dozens of diagnostic Pre-Dorset and Dorset stone tools, and delicate organic remains including bone needles (Milne 2005; Milne et al. 2012). Lithic debitage and faunal remains were collected from each unit. As with LdFa-1, caribou bone dominates the LeDx-42 faunal assemblage indicating an intense and focused exploitation of this resource during the occupation of the site (Milne et al. 2012:418).

2.2.3 LbDt-1

LbDt-1 was first identified in 2013 during an aerial survey along the Hone River. Given the sheer size of the site, it was divided into two separate components to facilitate investigation. They include the upper and lower components (see Figure 2.3). The upper component consists of a wide, elevated plateau. One of two notable features of the upper component is a massive chert flake deposit that is situated at the edge of the bluff that overlooks the Hone River and covers approximately one hectare in its overall size. Further east of the chert deposit is a long row of boulders and rocks that resemble the remains of tent ring dwellings. It is possible five tent rings are present and in 2013, two test small pits measuring 25 cm^2 were excavated in an effort to determine cultural affiliation. Unfortunately, no diagnostic artifacts were found, but hundreds of chert flake were recovered, suggesting toolstone reduction was occurring in or near these boulder features (Milne 2015:5-6).

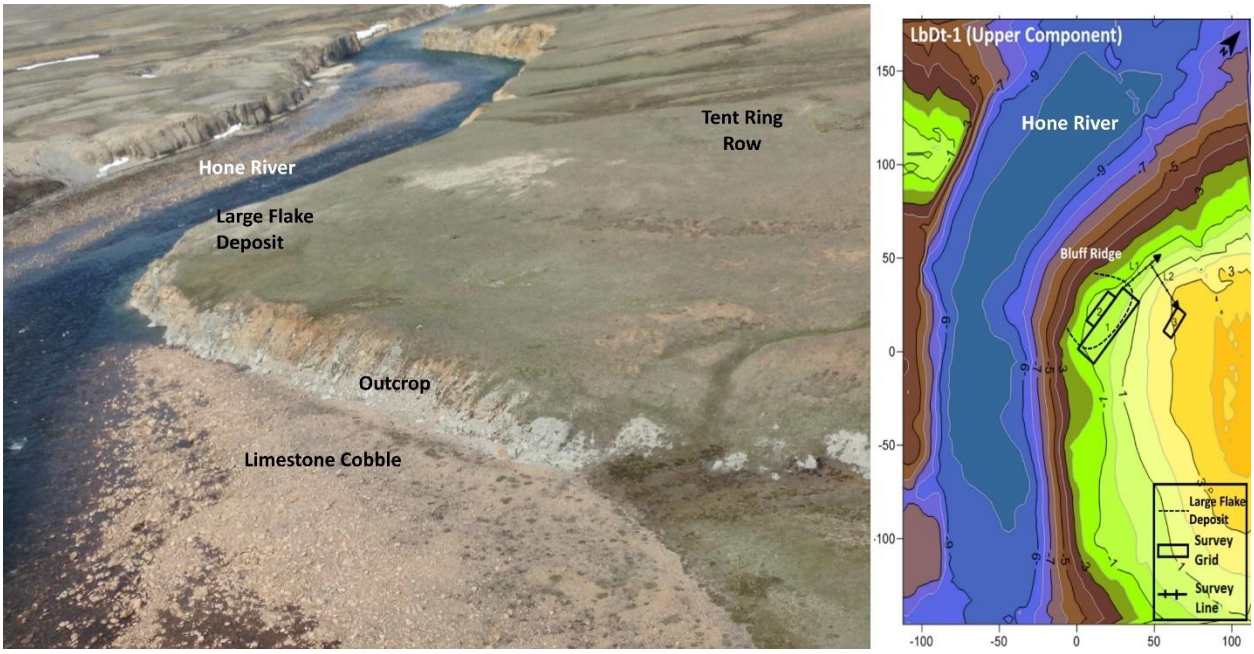

Figure 2.3 Photograph taken from above the eastern shore of the Hone River, across from LbDt-1 (left) (Photo credit: Dr. Brooke Milne). The upper component topographic site map (right) derived through TLS surveys from 2015 (Scales in meters). A portion of the river's edge has been topographically mapped during the TLS survey and can be seen in the site map.

LbDt-1's lower component is situated along a point bar on the south eastern shore of the Hone River. The ground surface in this area is covered in dense vegetation and is more difficult to traverse. There are many deeply buried boulders in the area, which hint at the possibility that tent rings exist beneath the vegetation cover. The northern-most portion of the lower component is defined by a large limestone exposure and cobble beach. Chert can be found within the layers of the exposed rock and is easily acquired as eroded nodules mixed in amongst the boulders (see Figure 2.4). Four small test pits were excavated within the lower component, but all failed to yield any culturally diagnostic artifacts. However, chert flakes were abundant and could be seen eroding out of the edge of the site deposit that is being undercut by the fast-moving waters of the Hone River.

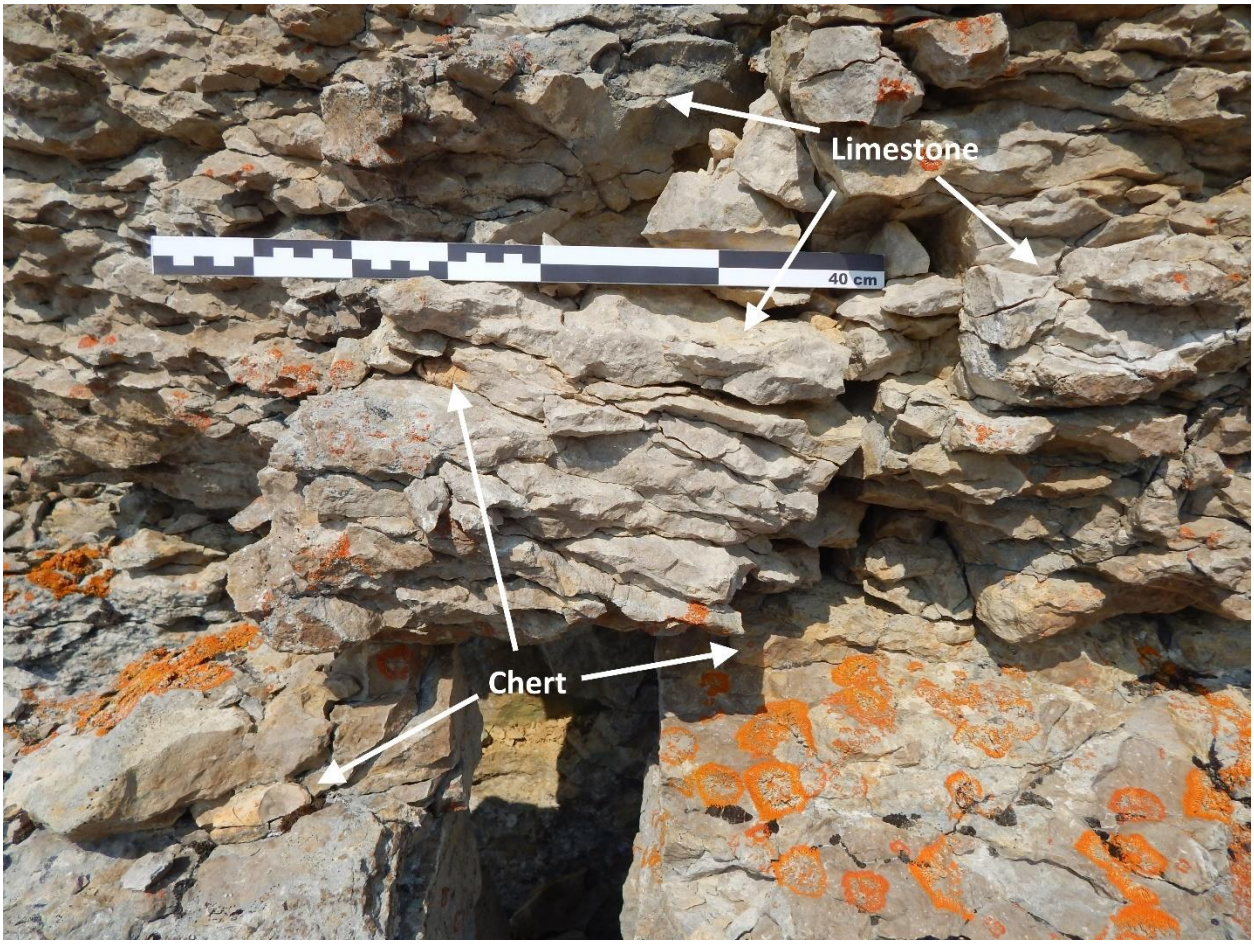

Figure 2.4 Photograph of naturally occurring chert nodules within the limestone layers that outcrops at LbDt-1.

The size and extent of the chert flake deposit at LbDt-1 suggest the site was an important location for Paleo-Inuit toolmakers to acquire lithic material and that visits to do so occurred regularly for a long period of time. While no culturally diagnostic artifacts have been recovered to date, we can be certain site occupants were Paleo-Inuit since chert was the most important lithic raw material in their technological inventory throughout the eastern Arctic. Moreover, Thule Inuit rarely if ever made use of chert toolstone (Park 1993; 2000).

Analysis of the debitage assemblage acquired from subsurface testing at the site was conducted in 2015 (Milne 2015). Results indicate primary reduction and raw material testing were the principal technological activities during the site's occupation. It also appears that Paleo-Inuit toolmakers were removing the stone in a minimally modified state for further reduction at a secondary location, likely a large habitation such as LdFa-1 or LeDx-42 (ten Bruggencate et al 2016, 2017).

2.3 Physical Environment of Interior Southern Baffin Island

2.3.1 Physiography

Baffin Island is the largest island in Canada and fifth largest in the world. The most notable features of the interior region of southern Baffin Island are the three large lakes: Mingo, Amadjuak, and Nettling, and the many tributaries and rivers that connect them (Milne 2003; Soper 1928; Stenton 1989). Surface vegetation consists of large patches of hummocky grass and moss, and a variety of low-lying flowers growing within a near-surface matrix of fine-grained sands, small stones, and thin layer of rich, organic soil. Erosion of exposed limestone bedrock has formed large patches of surface gravel and small-to-mid-sized rocks.

2.3.2 Climate

The modern climate around Amadjuak Lake, ranges from an average February temperature of -34º C to an average July temperature of 9º C (Jacobs et al. 1997). The large lakes and their tributary systems, which characterize the interior of southern Baffin Island, create a

moderating effect wherein during the Arctic summer, fall, and early winter, the local climate is warmer and more stable in comparison with surrounding regions (Jacobs and Grondin 1988). Summer months on the Baffin Island coast are often warm and dry; however, in recent years this has not been the case. As recently as the summer of 2015, in the vicinity of Iqaluit, rainfall levels surpassed their highest point in modern recorded history (CBC 2015).

Continuous permafrost zone extends across all of southern Baffin Island (Brown et al. 1998). The permafrost depth near Iqaluit, for the period 1998-2004 was 1.4 to 2.3 m (Throop 2010; Throop et al. 2010). In 2015 at LbDt-1, the permafrost surface depth was determined by geophysical imaging to be approximately 1.5 m (Landry et al. 2018). Above the permafrost is the active zone, a subsurface layer that goes through an annual near surface freeze-thaw process. As average global surface air temperatures continue to rise, permafrost layers are rapidly thawing across the Arctic, increasing the thickness of the active zone and destabilizing the surface through massive cracking, upheaval, and intensified erosion along coastal regions. These processes have been known to damage archaeological sites throughout the Arctic (Hollesen et al. 2017; Konopczak et al. 2016; Matthiesen et al. 2014); however, in comparison, the permafrost degradation and active-layer thickening in the more protected inland region of southern Baffin Island is likely to exhibit a low to moderate physical response (Smith and Burgess 2004).

2.3.3 Geology

Examination of geology of southern Baffin Island is useful for two reasons. First, it helps to establish the utility of geophysical and remote sensing instrumentation used in this study. An understanding of the local geological properties helps provide parameters for optimizing

instrument and survey configuration. Second, understanding how potential chert-bearing units are distributed provides information on the likely availability to Paleo-Inuit peoples.

The geology of the interior southern Baffin region consists of two main types of rocks: the Precambrian Cumberland batholith, and a sequence of Ordovician sedimentary rocks. The faulted margin of the Ordovician rocks with the Cumberland batholith (St. Onge et al. 2007) occurs about 50 kilometers south of Amadjuak Lake, and about 800 meters south of LbDt-1 (see Figure 2.5). All of the sites included in this study – LdFa-1, LeDx-42, LbDt-1 – are either atop, or near Ordovician rocks. The spatial distribution of the Paleozoic stratigraphy south of Amadjuak Lake including the Ordovician layers of southern Baffin Island was first established by Blackadar (1967). Layering within the stratigraphy is described by Sanford and Grant (2000) and has been recently updated by Zhang and Lavoie (2013). These geological strata form part of the Foxe Basin, are found exposed on Southampton Island, and also related to formations in the Hudson Bay Basin. The geological stratigraphy consists of the Ship Point Formation, Frobisher Bay Formation, Amadjuak Group, and the Akpatok Formation (see Figure 2.6). Both LdFa-1 and LbDt-1 are located on the Amadjuak Group bedrock.

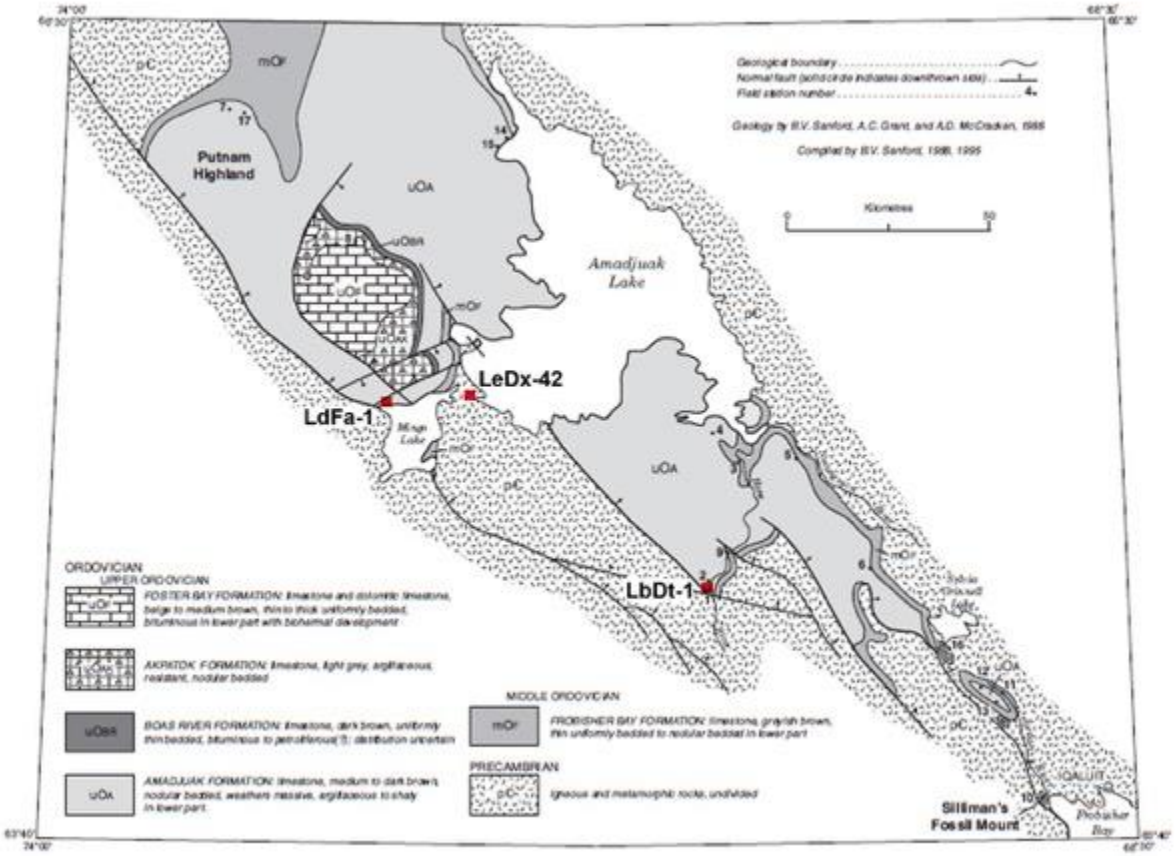

Figure 2.5 Map indicating the locations of archaeological sites LdFa-1, LeDx-42, and LbDt-1 within the spatial geological context of the Precambrian Batholith and the Ordovician sedimentary bedrock (Sandford and Grant 2000).

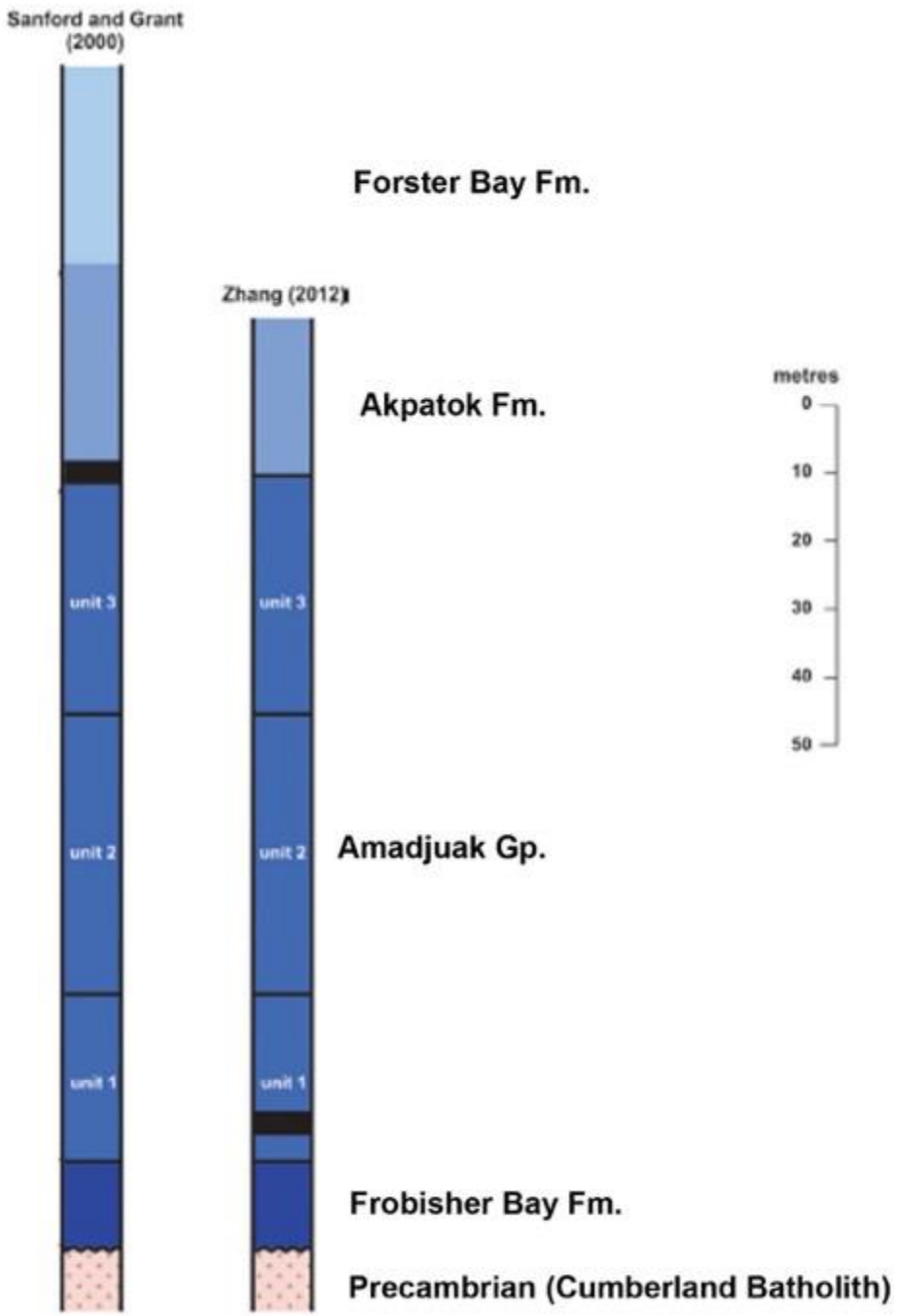

Figure 2.6 Correlation at the formation level of the Ordovician stratigraphy on southern Baffin Island and northeastern Melville Peninsula (Zhang and Lavoie 2013).

Sanford and Grant (2000) describe the Amadjuak Group based on the examination of a number of sites from Netilling Lake, Sylvia Grinnell Lake, and on the Hone River. Their descriptions define Unit 1 (20-28 m thick) as a base layer sitting non-conformably on the Frobisher Bay Formation (Sanford and Grant 2000). This unit comprises a uniform to nodular bedded light grey to dark brown limestone, and interbedded dark grey and black shales. Unit 2 of the Amadjuak Group (20-40 m thick), comprises a nodular, rubbly weathered limestone with only minor beds of shale. Unit 3 (28-35 m thick) consists of massive nodular bedded limestone and dolomite limestone in light to medium brown colour, and often forms an abrupt escarpment on the landscape (see Figure 2.7). Units 2 and 3 of the Amadjuak Group are the units most likely to be exposed near or at the surface level at sites like LdFa-1 and LbDt-1 (see Figure 2.7). The flat-lying, limestone makes these sites ideal locations for the successful application of geophysical instrumentation.

Sanford and Grant (2000) describe a location several kilometers south of Amadjuak Lake, along the Hone River known as GSC site O-104188. This site is located approximately 350 m southwest from LbDt-1 and contains both sections of Unit 2 and Unit 3. Here, Sanford and Grant (2000) describe lower beds of light greyish brown limestone that weathers blue-grey and yellowish orange upon exposure, and an upper light greyish brown limestone in nodular beds that also weathers yellowish orange upon exposure. In total, they note that 17 m of the Amadjuak Group are exposed along this Hone river location. Although Sanford and Grant (2000) do not explicitly mention chert nodules embedded within the limestone layers, their survey was fortunately situated nearby LbDt-1 and can be used as a proxy to identify the type of geological structures within which chert could be available.

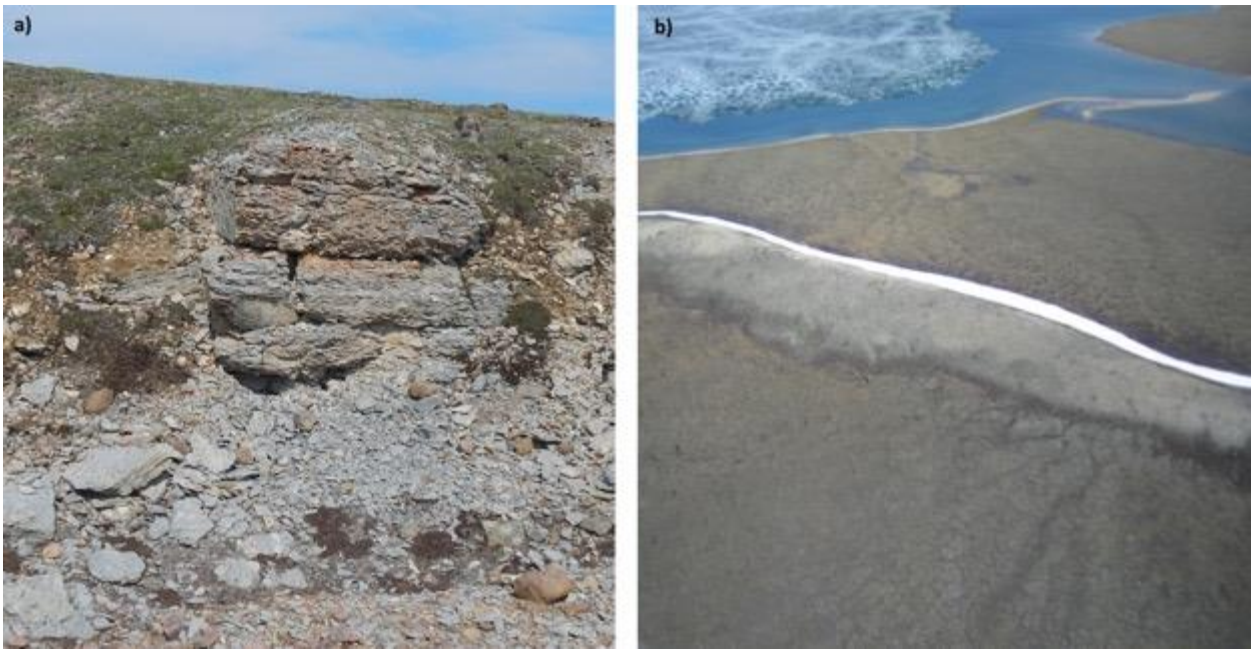

Figure 2.7 Photographs of Units 2 and 3 from the Amadjuak Group with identification of the units based on the descriptions by Sandford and Grant (2000). a) Eroded and exposed limestone outcrop of Unit 2 at LbDt-1. The height of the outcrop is ~5 m. The outcrop includes embedded chert nodules. b) Photograph of an outcrop of Unit 3, near LdDx-2. Photograph is taken looking north towards Amadjuak Lake. The height of the ridge formed by the limestone outcrop is ~10 m and the length of the ridge on the photograph is ~1.0 km.

Surface exposures of the mid and lowermost layers of stratigraphy are common within this region due to a process of weathering, upheaval with contact with the Precambrian rocks, and frost-shattering (Harris 1982). The low levels of natural magnetization from near surface limestone makes mapping anthropogenic magnetic anomalies somewhat more reliable in this region, and the equally low resistivity of limestone bedrock is also an important indication for the utility of functional radar survey (Landry et al. 2015). Additionally, based on the observation of *in situ* chert at low stratigraphic positions within the lower component of LbDt-1, it is interpreted that chert nodules may occur within these units of the Amadjuak Group.

2.4 Subsistence and Material Resources

The interior region of southern Baffin Island supports large herds of caribou (*Rangifer tarandus*) throughout the late summer and early fall (Boas 1964:26-27; Brody 1976; Soper 1928:64; Stenton 1986:14). Caribou played a significant role in the subsistence, social, and economic systems of the Paleo-Inuit and later Thule Inuit peoples, and they remain a vitally important species to today's Inuit communities (Burch 1972; 1978; Ferguson 1992; Ferguson et al. 1998; 2001; Stenton 1991a/b). Caribou provide meat, raw material in the form of bone, antler, and sinew, and hides essential for clothing, tents, and bedding (Burch 1972; Friesen 2013; Stenton 1991b; Stewart et al. 2004). The resident caribou populations in this region fluctuate in number over an estimated 10-to-20 year period; however, since the early 1990s, their numbers have been in constant decline (Ferguson et al. 1998).

In addition to caribou, migratory birds and waterfowl (e.g. snow geese [*Chen caerulescens*]) migrate to the inland Baffin area to nest for the summer months (Milne and Donnelly 2004), and tributary rivers connecting the large inland lakes where arctic char (*Salvalinus alpines*) are available during the fall months, making them another valuable subsistence resource. Lastly, plants growing during the summer months provide a source of vitamin C. These plants include blackberries (*Empetrum nigrum*), mountain sorrel (*Oxyria digyna*), and netted willow (*Salix reticulata*) (Kuhnlein et al. 1991). The overall abundance, diversity, and reliability of these resources throughout the summer seasons make the inland region of southern Baffin Island an attractive place for human habitation by both the Paleo- and Thule-Inuit.

Chert is the dominant toolstone used in Paleo-Inuit lithic technology. It is not readily available throughout southern Baffin Island, and where it is available, it is not accessible all year

round. Therefore, people had to move across the landscape at specific times of year to find available sources to acquire what they needed to meet their tool using needs. When trying to reconstruct a populations' technological organization, it is essential to know where the stone originates (Nelson 1991; Andrefsky 1994). Since southern Baffin Island has not yet been systematically surveyed for chert source locations, locating where exactly Paleo-Inuit toolmakers acquired their stone remains difficult. Limited survey and preliminary geochemical studies in this region have identified two chert quarries – LbDt-1 and LdDx-2 – and linked them to four inland and two coastal sites (ten Bruggencate et al. 2016; 2017) thus demonstrating that people carried this lithic raw material with them as the moved between coastal and inland areas.

The localized availability of chert is further attested to by local Inuit oral histories where the word Amadjuak is an English corruption of the Inuktitut word "ammaq," which loosely translated means "chert" (Milne et al. 2011:122; Stenton and Park 2003:25). Geological formations on the southern Baffin Island coast are not chert-bearing so it is highly unlikely that chert occurs naturally there (Milne et al. 2013).

2.5 Remote Sensing and Geophysical Methods

2.5.1 Arctic Geophysical and Remote Sensing Studies

Archaeogeophysists have successfully applied and optimized geophysical methodologies to investigate numerous archaeological sites around the world (e.g., Aspinall et al. 2008; 2009; Conyers 2010; Conyers and Leckebusch 2010; Conyers et al. 2008; Gaffney and Gater 2006; Johnson 2006; Kvamme 2003a; Linford 2006; Smekalova et al. 2008; Thompson et al. 2011; Urban et al. 2016). Used primarily as a tool for archaeological prospection, geophysical

techniques have been developed for over half a century for the near-surface mapping of archaeological sites (Scollar and Krückeberg 1966). The earliest attempts at prospection were focused on large scale archaeological anomalies such as brick or stone foundations and walls, or detecting geophysical responses in soils resulting from anthropogenic manipulation (Le Borgne 1955; 1965). The second type of activity includes magnetic mapping to locate ferromagnetic bodies, such as metals, or residual remnant magnetic anomalies caused by extensive burning or firing events (Le Borgne 1965).

Magnetics, GPR, and resistivity measurements have often been used to define large architectural features such as walled structures, buried foundations, or ditch constructions. These features produce obvious anomalies, making it easier to accurately locate and identify domestic spaces in the archaeological record (Thacker and Ellwood 2002:563). Despite the success of archaeogeophysics at larger-scale sites, smaller-scale hunter-gatherer sites, which tend to be more ephemeral with lower site visibility, require different geophysical procedures and methodologies to detect, isolate, and interpret their remains (Jones and Munson 2005).

Geophysics provides a useful tool to survey and map hunter-gatherer sites, especially in Arctic regions. A significant challenge, however, is that complex topography, uneven ground surfaces, and the glacial geologies of the Arctic can complicate the accurate collection of geophysical measurements at these types of sites (Urban et al. 2016; Wolff et al. 2013). Common magnetic and radar responses used to identify sub-surface archaeological features elsewhere can be obscured in Arctic surveys due to highly heterogeneous glacial fill and rapidly shifting terrain caused by frost cracking and the annual freeze-thaw-cycle (Hodgetts et al. 2011). The difficulties of archaeological geophysical surveys in the Arctic may be further exacerbated when extreme

environmental conditions cause malfunctions in the equipment (Wolff and Urban 2013), resulting in unwanted variations in data (Robinson et al. 2004).

More recently, some researchers have overcome these technical challenges and have successfully identified small subsurface features, including, for example, Dorset dwelling structures identified beneath more recent midden deposits during a magnetic mapping survey in Labrador, Newfoundland (Easthugh and Taylor 2005). Urban et al. (2016) have conducted several geophysical surveys across varying Arctic landscapes spanning from Alaska to Greenland. They have used magnetics and GPR survey to locate anthropogenic anomalies in the near surface as well as defining the depth of significant natural subsurface layers (i.e., permafrost and active layers). Often, successful applications of geophysics in the Arctic included the use of techniques to image midden deposits and pits, and to define the locations and extent of hearths (Easthaugh and Taylor 2005; 2011; Hodgetts et al. 2011; Urban et al. 2016; Viberg et al. 2009; 2013; Wolff and Urban 2013).

2.5.2 Terrestrial Laser Scanning Surveys

TLS surveys are designed to measure the reflection, range, intensity, colour, and texture of above-ground surfaces. Three categories of laser scanners are used for a variety of long and short-range surveys: time-of-flight, phase, and, triangulation (Vosselman and Maas 2010:3-8). In all three categories, light radiation is emitted from a source sensor at a constant speed and angle. The individual light ray is reflected when it reaches the surface of an object and returns back to the sensor. Upon returning, data for each point is collected for distance, angle, and reflection intensity of the object's surface and stored in the internal memory of the device. Collectively, the millions of points collected that make up a laser scan are referred to as a point cloud.

3D laser scanning technologies have recently been implemented by archaeologists working in the Canadian Arctic with the detailed documentation of large Thule Inuit whalebone houses (Dawson and Levy 2005) and the historic Fort Conger site (Dawson et al. 2013). These projects have significant implications for documenting and digitally recording northern heritage resources, particularly as the Arctic continues to be impacted by the effects of climate change (see Barber et al. 2012; Stocker et al. 2013) causing ongoing concerns about site preservation and stability in the circumpolar world (Blankholm 2009; Hald 2009). This project builds on those applications by using terrestrial laser scanning to record Arctic archaeological features, yet it is distinguished from them by concentrating on features with substantially lower visibility than the Fort Conger building or Thule sod houses. Instead, this study focuses on tent rings, small cache features, and surface artifact deposits at LdFa-1, LeDx-42, and LbDt-1.

A Lecia C10 ScanStation was used to collect point cloud data from these sites using multiple static reflective targets as reference points. Five designated areas (1 – 5) of LdFa-1 were scanned in detail (<0.05 m point spacing) using the TLS in 2013. A total of six station positions were used to capture and create a full point cloud. During the same field season, the surface of LeDx-42 was scanned in detail (<0.05 m point spacing) using the TLS. Three station positions were used to capture and create a full point cloud of the site. Both the Upper and Lower components of LbDt-1 were scanned using the TLS (<0.05 m point spacing) in 2013, and the upper component was rescanned in finer detail (<0.01 m point spacing) in 2015 in order to integrate the results into the geophysical grid surveys. Data processing was completed using a combination of automated and manual classification methods through open access software such as CouldCompare, and semi-access software LAStools (Landry et al. 2016; Milne and Landry 2016).

2.5.3 Magnetometer and Gradiometer Surveys

Magnetometers and gradiometer surveys are designed to measure the induced and remnant magnetization of objects in the subsurface. Both magnetometers and gradiometers are used extensively in small-scale hunter-gatherer contexts. Magnetometers are designed to map spatial variations in the Earth's magnetic field produced through natural and anthropogenic sources. Gradiometer magnetometers map at a higher spatial resolution, making them more ideal for discriminating between small-scale magnetic targets and the background magnetic field (Landry et al. 2015:2). Magnetometers and gradiometers are built with either one, two, or four magnetic sensors placed in either a vertical or horizontal arrangement. Total magnetic field (magnetometer) surveys require the use of an isolated base-station to allow removal of time-varying signals. Duo- and quarto-sensor magnetometers provide measures of the gradient of the magnetic field that are not impacted by the time-variation o the field (Ard et al. 2015:4). Magnetic measurement instruments provide a reliable tool for archaeologists to map small-scale changes in the subsurface, those most likely to be linked to hunter-gatherer sites.

Since magnetometers measure the overall variation in the Earth's magnetic field, data corrections must be made in order to provide an accurate reading. Urban (2012) credits J. Louis Giddings unpublished experiments with a proton magnetometer at an early hunter-gatherer site in the Alaskan Arctic as the first in the region; however, notes that the survey yielded erratic results and contained no particular trends. Giddings' results were affected by the rapid diurnal fluctuations typical of Arctic latitudes, which caused numerous errors in the magnetic readings. Corrections for these fluctuations can be made with the addition of a magnetic base-station that tracks the diurnal magnetic fluctuations. These can then be removed from the survey data (Landry et al. 2015:7). Gradiometer data do not suffer from these same problems. Gradiometer

measurements are independent of the magnetic field fluctuations because each sensor is subject to the same diurnal fluctuation and their difference will be free of the fluctuations (Ard et al. 2015:4).

In a number of archaeological studies, magnetic surveys have been used to locate features with enhanced magnetism caused by thermo-remanent magnetization (Gibson 1986:559; Hodgetts et al. 2011:1755; Jones and Munsen 2005:32; Kvamme 2003b:134; Prentiss et al. 2008:67; Weymouth and Nickel 1977; Wolff and Urban 2013:10; Wiewel and Kvamme 2014:266). Common naturally-occurring and weakly-magnetic hematite iron oxides in soils convert into magnetically enhanced maghemite when heavily heated or burned. Since hearths are most likely to be found in abundance on hunter-gatherer sites, many archaeologists use magnetometers to locate these types of small-scale features. Other features that have been detected magnetically are dugout pits, individual posts, and larger domestic depressions, and earthlodge construction sequences. Some of the earliest North American examples of these surveys come from North Dakota (Weymouth and Nickel 1977). These features are magnetically anomalous because of two differing anthropogenic influences. The first influence is the removal of magnetically charged topsoil from the centre of the pit to the exterior rim. The removal of magnetically positive soils can cause negative anomalies in the magnetic response (Hodgetts et al. 2011:1761; Jones and Munsen 2005:32). The second influence is the filling of pits by rocks, organics, and other refuse may create magnetic anomalies (Ard et al. 2015:7; Gibson 1986:560).

A GSSI magnetometer-gradiometer survey system with a base-station setup was used during the collection of data from LdFa-1. Additionally, magnetic susceptibility measurements were acquired from both LdFa-1 and LbDt-1 through electromagnetic InPhase responses.

2.5.4 Electromagnetic Surveys

EM instruments can be used to measure two different physical properties. For instruments operating in the low induction number (LIN) range the InPhase component of the response is sensitive to the local magnetic susceptibility as well as to the electrical conductivity (Fitterman and Labson 2005). In areas of low conductivity, the InPhase response can be used to map the susceptibility without the need to correct for spatial variations in the conductivity. Mapping the spatial variations of the magnetic susceptibility is useful when comparing anomalies to the magnetic gradient or total field responses (Landry et al. 2015:8-9). In contrast to magnetometer surveys, the EM response depends only on the induced magnetization and the response is sensitive to a relatively small volume surrounding the instrument. The alternative quadrature component of an EM instrument measurement is used to map changes in the subsurface electrical conductivity. Results are sometimes presented in terms of the reciprocal property, electrical resistivity. The apparent conductivity data provide important geological information for sites in complex environments such as in circumpolar regions (Landry et al. 2015:9).

The depth sensitivity of EM instruments in the LIN range depends on the coil spacing and instrument configuration. Apparent conductivity depth-sensitivity functions for a particular coil spacing r $S_{\sigma HD}(r,z)$ and $S_{\sigma VD}(r,z)$ are well known (e.g., Fitterman and Labson 2005):

$$S_{\sigma HD}(r,z) = 2 - 4\left(\frac{z}{r}\right)\left(4\left(\frac{z}{r}\right)^2 + 1\right)^{-1/2} \qquad \text{Eq. 1}$$

and

$$S_{\sigma VD}(r,z) = 4\left(\frac{z}{r}\right)\left(4\left(\frac{z}{r}\right)^2 + 1\right)^{-3/2} \qquad \text{Eq. 2}$$

where z is the depth.

In horizontal dipole or HD mode (vertical coplanar coils), the sensitivity of the apparent conductivity response is highest at the surface. In vertical dipole or VD mode (horizontal coplanar coils), sensitivity increases from zero at the surface, to a maximum at 0.35 times the coil spacing before decreasing at larger depth.

LIN apparent susceptibility sensitivity functions $S_{\kappa HD}(r,z)$ and $S_{\kappa VD}(r,z)$ are given by McNeill and Bosnar (1999):

$$S_{\kappa HD}(r,z) = -12\frac{z}{r}\left(4\left(\frac{z}{r}\right)^2 + 1\right)^{-5/2} \qquad \text{Eq. 3}$$

and

$$S_{\kappa VD}(r,z) = 12\frac{z}{r}\left(3 - 8\left(\frac{z}{r}\right)^2\right)\left(4\left(\frac{z}{r}\right)^2 + 1\right)^{-7/2} \qquad \text{Eq. 4}$$

The sensitivity of the apparent susceptibility response has maximum at 0.25r for the HD mode and 0.18r for the VD mode but the sign is reversed. The VD sensitivity is also complicated by a change in the sign at depth z>0.612r.

The EM quadrature component was used effectively to map individual pithouses in the interior of British Columbia (Prentiss et al. 2008). The archaeological remains themselves were not conductive in any geophysical manner, but because the topographic relief associated with the slightly concaved features led to higher moisture content in the interior surface of the features, it increased the electrical conductivity while the lower moisture content on the exterior edge

decreased the conductivity (Prentiss et al. 2008:64-65). Alternatively, the EM InPhase component used to map magnetic susceptibility among regional Arctic applications includes Landry et al. (2015), Viberg et al. (2013), and Urban et al. (2012).

The subsurface electrical response can also be measured using DC-resistivity methods including multi-electrode electrical resistivity tomography systems. Resistivity meters are used less frequently in archaeological hunter-gatherer contexts as they tend to be more useful for mapping larger scale changes in soil resistivity. Despite having little success in certain circumstances, Kvamme's (2003b) multidimensional project in Great Plains village sites successfully applied resistivity instruments to locate the remains of compacted domestic house floors. In this case, the compacted soil layers yielded strong resistive contrasts from the general silt-loam soils of the surrounding area (Kvamme 2003b:135). Additionally, Thompson and Pluckhahn (2010) note the correlation between topographic mound construction and corresponding higher resistivity readings making the use of their resistivity surveying quite successful, albeit for locating slightly larger features then commonly associated with hunter-gatherer sites (Thompson and Pluckhahn 2010:39-40). Electrical resistivity survey for hunter-gatherer sites requires a good working knowledge of the local lithostratigraphy and geological context of the archaeological levels (Thacker and Ellwood 2002:569). In many cases, resistivity instrumentation surveys restrict themselves to shallow archaeological deposits due to the electrode spacing required for detecting small archaeological features, and necessitate a sufficient contrast between archaeological deposits and the surrounding sediment matrix (Thacker and Ellwood 2002:569). In these cases, the evenly spaced Wenner Array configuration is commonly employed (Thacker and Ellwood 2002:564). Overall, it is a rare occurrence to use electrical resistivity survey in small-scale archaeological contexts; however, its potential has

been demonstrated in certain cases when it has been combined with other geophysical instrumentation.

In 2014, a small 20 m x 20 m section of Area 5 at LdFa-1 was mapped using magnetic and EM survey, and in 2015, a section of the LbDt-1 chert deposit measuring 44 m x 13 m was gridded and mapped using an EM survey instrument. To collect the data from LdFa-1 and LbDt-1, a Geonics EM-31, and a GSSI EM-Profiler were used, respectively. Several steps were needed to process the data, which included correcting for time-variations by using a single base-line setup outside the survey grid. Additionally, data reduction and two-layered inversion methods were used to isolate signals in the subsurface, and to provide insight towards the anthropogenic anomalies located within those layers.

2.5.5 Ground Penetrating Radar Surveys

GPR detects the reflection, refraction, and diffraction of high frequency EM signals produced by sub-surface variations in the electrical permittivity, or dielectric constant. This physical property is closely related to the water content in the subsurface. The GPR response can also depend on the electrical conductivity (Wolff and Urban 2013:4). GPR instruments rely on a specific frequency transmitted from an external antenna. The depth of penetration and resolution of the data are dependent on the frequency of the antenna. When using a higher frequency (shorter wavelength) GPR antenna, greater feature resolution can be attained, but there is a smaller depth of penetration.

GPR is one of the easier instruments to use in the field, and can be used to efficiently map long stretches of open land. For hunter-gatherer contexts, commonly used antenna includes 200 MHz to 400 MHz units (Conyers 2016; Keay et al. 2009; Landry et al. 2018; Urban et al.

2016). The antenna is often pulled or pushed across the ground surface and measurements can be made either individually or continuously along the grid transect. Using a 400MHz GPR antenna, the outlined remains of a Seneca Iroquois longhouse were successfully located at the White Springs Site, NY (Peregrine et al. 2012:2045-2046). This feature is suggested to be at a lower depth than anticipated since the researchers were not able to detect the same feature using a magnetometer (Peregrine et al. 2012:2046). Alternatively using both a 270 MHz and 400 MHz antenna, archaeologists were able to demonstrate the ability of GPR methods for reconstructing past geomorphological landscapes, including palaeo-channels adjacent to Upper Palaeolithic hunter-gatherer sites in Portugal (Conyers et al. 2013:49). Lastly, GPR has been used in Alaska, and despite having issues with uneven surfaces and malfunctions, Wolff and Urban (2013) were able to detect the underlying permafrost layer. This layer of permanently frozen soil encompasses parts of the archaeological site at Cape Krusenstern, and through comparisons with earlier geophysical surveys, the authors have suggested that the permafrost is in fact thawing in this region, producing a new environmental concern for the archaeological site remains (Wolff and Urban 2013:10).

At LbDt-1, a GSSI 400MHz antenna was used to survey three separate grids established within the upper component of the site. This survey made us of the GSSI SIR3000 system, along with a RADAN processing software. Additionally, Conyers (2010) open access processing software packages, ‘gpr_process’ and ‘gpr_viewer’ were used for more accurate interpretation of the near-surface reflections and archaeological features.

2.6 Works Cited – Chapter 2

Andrefsky, W. 1994. Raw-material availability and the organization of technology. *American Antiquity*, *59*(1), 21-34.

Ard, V., Mathé, V., Lévêque, F., and Camus, A. 2015. A comprehensive magnetic survey of a Neolithic causewayed enclosure in West-central France for the interpretation of archaeological features. *Archaeological Prospection*, 22(1), 21-32. DOI: 10.1002/arp.1495

Aspinall, A., Gaffney, C., and Conyers, L. 2008. Archaeological prospection – the first fifteen years. *Archaeological Prospection*, 15(4), 241-245.

Aspinall, A., Gaffney, C., and Schmidt, A. 2009. *Magnetometry for archaeologists* (Vol. 2). Rowman Altamira.

Barber, D. G., Asplin, M. G., Papakyriakou, T. N., Miller, L., Else, B. G., Iacozza, J., Mundy, C. J., Gosslin, M., Asselin, N. C., Ferguson, S., Lukovich, J. V. 2012. Consequences of change and variability in sea ice on marine ecosystem and biogeochemical processes during the 2007–2008 Canadian International Polar Year program. *Climatic Change*, 115(1), 135-59.

Barry, R. G., Arundale, W. H., Andrews, J. T., Bradley, R. S., and Nichols, H. 1977. Environmental change and cultural change in the eastern Canadian Arctic during the last 5000 years. *Arctic and Alpine Research*, 9, 193-210.

Betts, M. W., Hardenberg, M., and Stirling, I. 2015. How animals create human history: relational ecology and the Dorset-polar bear connection. *American Antiquity*, *80*(1), 89-112.

Bielawski, E. 1988. Palaeoeskimo variability: The early Arctic Small-Tool Tradition in the central Canadian Arctic. *American Antiquity*, 53, 52–74.

Blackadar, R. G. 1967. Geological Reconnaissance, Southern Baffin Island, District of Franklin: (Report, Figure and Maps 16-1966, 18-1966). Geological Survey of Canada, 1967.

Blankholm, H. P. 2009. Long-term research and cultural resource management strategies in light of climate change and human impact. *Arctic Anthropology*, 46(1-2), 17-24.

Boas, F. 1964. *The central eskimo*. (Original Publication 1888.) Lincoln: University of Nebraska Press.

Briner, J. P., McKay, N. P., Axford, Y., Bennike, O., Bradley, R. S., de Vernal, A., Fisher, D., Francus, P., Fréchette, B., Gajewski, K. and Jennings, A., 2016. Holocene climate change in Arctic Canada and Greenland. *Quaternary Science Reviews*, 147, 340-364.

Brown, J., Ferrians Jr., O. J., Heginbottom, J. A., and Melnikov, E. S. 1998. Circumarctic map of permafrost and ground-ice conditions. Report, National Snow and Ice Data Center, World Data Center for Glaciol Boulder, CO.

Burch, E. S. 1972. The caribou/wild reindeer as a human resource. *American antiquity*, *37*(3), 339-368.

Burch, E. S. 1978. Caribou Eskimo origins: an old problem reconsidered. *Arctic Anthropology*, 1-35.

CBC. 2015. Iqaluit gets a month's worth of rain in 9 days: Nunavut's capital has had 66.6 millimetres of rain so far in July. http://www.cbc.ca/news/canada/north/iqaluit-gets-a-month-s-worth-of-rain-in-9-days-1.3147605.

Collins, H. B. 1954. Archaeological research in the North American Arctic. *Arctic*, 7(3-4), 296-306.

Collins, H. B. 1956. Archaeological investigations on Southampton and Coats Island, N.W.T. In Annual Reports of the National Museum of Canada for 1954-1955. *National Museum of Canada Bulletin*, 142, 82-113.

Conyers, L. B. 2010. Ground-penetrating radar for anthropological research. *Antiquity*, 84(323), 175-184.

Conyers, L. B. 2016. *Interpreting ground-penetrating radar for archaeology*. Routledge.

Conyers, L. B., and Leckebusch, J. 2010. Geophysical archaeology research agendas for the future: Some ground- penetrating radar examples. *Archaeological Prospection*, *17*(2), 117-123.

Conyers, L. B., Ernenwein, E. G., Grealy, M., and Lowe, K. M. 2008. Electromagnetic conductivity mapping for site prediction in meandering river floodplains. *Archaeological Prospection*, 15(2), 81-91.

Conyers, L. B., Daniels, J. M., Haws, J. A., and Benedetti, M. M. 2013. An upper Palaeolithic landscape analysis of coastal Portugal using ground- penetrating radar. *Archaeological Prospection*, 20(1), 45-51.

Darwent, C. M. 2004. The highs and lows of high Arctic mammals: temporal change and regional variability in Palaeoeskimo subsistence. In M. Mondini, S. Muñoz, and S. Wickler (Eds.), *Colonization, Migration, and Marginal Areas: A Zooarchaeological Approach* (pp. 62–73). Oxford: Oxbow Books.

Dawson, P. 2016. The Thule-Inuit Succession in the Central Arctic. In M. Friesen and O. Mason (Eds.), *The Oxford Handbook of the Prehistoric Arctic*. Oxford University Press.

Dawson, P., Levy, R., and Lyons, N. 2011. 'Breaking the fourth wall': 3D virtual worlds as tools for knowledge repatriation in archaeology. *Journal of Social Archaeology*, *11*(3), 387-402.

Dawson, P., Bertulli, M. M., Levy, R., Tucker, C., Dick, L., and Cousins, P. L. 2013. Application of 3D laser scanning to the preservation of Fort Conger, a historic polar research base on northern Ellesmere Island, Arctic Canada. *Arctic,* 66(2), 147-158.

Dekin, A. A. Jr. 1972. Climatic change and cultural change: A correlative study from eastern Arctic prehistory. *Polar Notes*, 12, 11-31.

Dekin, A. A. Jr. 1976. Elliptical analysis: An heuristic technique for the analysis of artifact clusters. In M. S. Maxwell (Ed.), *Eastern Arctic Prehistory: Paleoeskimo Problems* (pp. 79–88). Memoirs of the Society for American Archaeology No. 31. Society for American Archaeology, Washington, D.C.

Eastaugh, E., and Taylor, J. 2005. Geophysical survey of the Dorset Palaeoeskimo site of Point Riche. *Newfoundland and Labrador Studies*, 20(1), 157–173.

Eastaugh, E., and Taylor, J. 2011. Settlement size and structural complexity: A case study in geophysical survey at Phillip's Garden, Port au Choix. In M.A.P. Renouf (Ed.), *The Cultural Landscapes of Port au Choix, Interdisciplinary Contributions to Archaeology* (pp. 178-188). Springer Science + Business Media, LLC. DOI 10.1007/978-1-4419-8324-4_9.

Ferguson, M. A. 1992. Status and trends of Rangifer tarandus and Ovibos moschatus populations in Canada. *Rangifer*, *12*(3), 127-141.

Ferguson, M. A., Williamson, R. G., and Messier, F. 1998. Inuit knowledge of long-term changes in a population of Arctic tundra caribou. *Arctic*, 201-219.

Ferguson, M. A., Gauthier, L., and Messier, F. 2001. Range shift and winter foraging ecology of a population of Arctic tundra caribou. *Canadian Journal of Zoology*, *79*(5), 746-758.

Fitterman, D. V., and Labson, V. F. 2005. Electromagnetic induction methods for environmental problems. In D. K. Butler (Ed.), *Near-surface geophysics* (pp. 301-355). Society of Exploration Geophysicists.

Fitzhugh, W. W. 1976. Environmental factors in the evolution of Dorset culture: A marginal proposal for Hudson Bay. In M. S. Maxwell (Ed.), *Eastern Arctic Prehistory: Paleoeskimo Problems* (pp. 139–149). Memoirs of the Society for American Archaeology No. 31. Society for American Archaeology, Washington, D.C.

Fitzhugh, W. W. 1997. Biogeographical archaeology in the eastern North American Arctic. *Human Ecology*, *25*(3), 385-418.

Friesen, T. M. 2007. Hearth rows, hierarchies and Arctic hunter-gatherers: The construction of equality in the Late Dorset period. *World Archaeology*, 39(2), 194-214.

Friesen, T. M. 2013. *When worlds collide: hunter-gatherer world-system change in the 19th Century Canadian Arctic*. University of Arizona Press.

Gaffney, C. F., and Gater, J. 2006. *Revealing the buried past: geophysics for archaeologists*. Tempus.

Gibson, T. H. 1986. Magnetic prospection on prehistoric sites in Western Canada. *Geophysics*, 51(3), 553-560.

Hald, M. 2009. Past climate change and perspectives for archaeological research: Examples from Norway, Svalbard, and adjoining seas. *Arctic Anthropology*, *46*(1-2), 8-16.

Hardenberg, M. 2013. Trends and ontology of artistic practices of the Dorset culture 800 BC–1300 AD. Ph.D. dissertation, Department of Prehistoric Archaeology, University of Copenhagen, Copenhagen.

Harp, E. Jr. 1976. Dorset Settlement Patterns in Newfoundland and Southeastern Hudson Bay. In M. S. Maxwell (Ed.), *Eastern Arctic Prehistory: Paleoeskimo Problems* (pp. 119–138). Memoirs of the Society for American Archaeology No. 31. Society for American Archaeology, Washington, D.C.

Harris, S. A. 1982. Identification of permafrost zones using selected permafrost landforms. In Proceedings of the fourth annual Canadian Permafrost Conference, 49-58.

Helmer, J. W. 1991. The Palaeo-Eskimo prehistory of the North Devon lowlands. *Arctic*, 44, 307-317.

Helmer, J. W. 1996. A tale of three villages: Assessing the archaeological potential of three Late Dorset settlements on Little Cornwallis Island. In B. Grønnow, and J. Pind (Eds.), *The Palaeo-Eskimo Cultures of Greenland: New Perspectives in Greenlandic Archaeology* (pp. 295–308). Danish Polar Centre Publication No.1, Danish Polar Centre, Copenhagen, Denmark.

Hodgetts, L., Renouf, M. A. P., Murray, M. S., McCuaig-Balkwill, D. and Howse, L. 2003. Changing subsistence practices at the Dorset Palaeoeskimo site of Phillip's Garden, Newfoundland. *Arctic Anthropology*, 40(1), 106–120.

Hodgetts, L., Dawson, P., and Eastaugh, E. 2011. Archaeological magnetometry in an Arctic Setting: a case study from Maguse Lake, Nunavut. *Journal of Archaeological Sciences*, 38, 1754–1762. DOI:10.1016/j.jas.2011.03.007.

Hollesen, J., Matthiesen, H., and Elberling, B. 2017. The impact of climate change on an archaeological site in the Arctic. *Archaeometry*. DOI: 10.1111/arcm.12319.

Jacobs, J. D., and Grondin, L. D. 1988. The influence of an Arctic large-lakes system on mesoclimate in south-central Baffin Island, NWT, Canada. *Arctic and Alpine Research*, 212-219.

Jacobs, J. D., Headley, A. N., Maus, L. A., Mode, W. N., and Simms, E. L. 1997. Climate and vegetation of the interior lowlands of southern Baffin Island: long-term stability at the low arctic limit. *Arctic*, 167-177.

Johnson, J. K. 2006. *Remote Sensing in Archaeology: An Explicitly North American Perspective* (pp. 1-16). Tuscaloosa: The University of Alabama Press.

Jones, G., and Munson, G. 2005. Geophysical survey as an approach to the ephemeral campsite problem: Case studies from the northern plains. *Plains Anthropologist*, *50*(193), 31-43.

Keay, S., Earl, G., Hay, S., Kay, S., Ogden, J., and Strutt, K. D. 2009. The role of integrated geophysical survey methods in the assessment of archaeological landscapes: the case of Portus. *Archaeological Prospection*, *16*(3), 154-166.

Knuth, E. 1954. The Paleo-Eskimo culture of northeast Greenland elucidated by three new sites. *American Antiquity*, 19(4), 17-33.

Konopczak, A. M., Manson, G. K., and Lantuit, H. 2016. Coastal erosion and resulting impacts along the ice-rich permafrost coast of the Yukon Territory, Canada. XI. International Conference on Permafrost, Potsdam, 20 June 2016 - 24 June 2016.

Kuhnlein, H. V., and Turner, N. J. 1991. *Traditional plant foods of Canadian indigenous peoples: nutrition, botany, and use* (Vol. 8). Taylor & Francis.

Kvamme, K. 2003a. Geophysical surveys as landscape archaeology. *American Antiquity*, 68(3), 435–457.

Kvamme, K. L. 2003b. Multidimensional prospecting in North American Great Plains village sites. *Archaeological Prospection*, *10*(2), 131-142.

Landry, D. B. 2013. The organization of late Dorset lithic technology at the LdFa-1 site in southern Baffin Island, Nunavut. M.A. thesis, University of Manitoba, Winnipeg. MSpace.

Landry, D. B., Ferguson, I. J., Milne, S. B., and Park, R. W. 2015. Combined geophysical approach in a complex Arctic archaeological environment: A case study from the LdFa-1 site, southern Baffin Island, Nunavut. *Archaeological Prospection*, *22*(3), 157-170.

Landry, D. B., Milne, S. B., Park, R. W., Ferguson, I. J., and Fayek, M. 2016. Manual point cloud classification and extraction for hunter-gatherer feature investigation: A test case from two low arctic Paleo-Inuit sites. *Open Archaeology*, *2*(1), 232-242.

Landry, D. B., Ferguson, I. J., Milne, S. B., Serzu, M., and Park, R. W. 2018. Integrated geophysical techniques for the archaeological investigation of LbDt-1, a Paleo-Inuit quarry site in the interior of southern Baffin Island, Nunavut, Canada. *Journal of Archaeological Method and Theory*. DOI: https://doi.org/10.1007/s10816-018-9370-6.

Le Borgne, E. 1955. Susceptibilité magnétique anomale du sol superficiel. *Annals Géophysics*, 11, 399–419.

Le Borgne, E. 1965. Les propriétés magnétique du sol: application à la prospection des sites archéologiques. *Archaeo-Physika*, 1(15), 1–20.

LeMoine, G. M., and Darwent, C. M. 1998. The walrus and the carpenter: Late Dorset ivory working in the high Arctic. *Journal of Archaeological Science*, 25, 73–83.

Linford, N. 2006. The application of geophysical methods to archaeological prospection. *Reports on Progress in Physics*, 69: 2205–2257. DOI:10.1088/0034-4885/69/7/R04.

Mathiassen, T. 1930. The Question of the Origin of Eskimo Culture. *American Anthropologist*, 32(4), 591-607.

Matthiesen, H., Jensen, J. B., Gregory, D., Hollesen, J., and Elberling, B. 2014. Degradation of archaeological wood under freezing and thawing conditions - effects of permafrost and climate change. *Archaeometry*, *56*(3), 479-495.

Maxwell, M. S. 1960. The movement of cultures in the Canadian high Arctic. *Anthropologica*, 177-189.

Maxwell, M. S. 1973. Archaeology of the Lake Harbour district, Baffin Island. *Mercury Series No. 6*. Archaeological Survey of Canada, National Museum of Man, Ottawa, Ontario.

Maxwell, M. S. 1976a. Introduction. *Memoirs of the Society for American Archaeology, Eastern Arctic Prehistory: Palaeoeskimo Problems*, 31, 1-5.

Maxwell, M. S. 1976b. Pre-Dorset and Dorset artifacts: the view from Lake Harbour. *Memoirs of the Society for American Archaeology*, *Eastern Arctic Prehistory: Palaeoeskimo Problems*, 31, 58-78.

Maxwell, M. S., 1985. *Prehistory of the eastern Arctic*. Orlando, FL.: Academic Press.

Maxwell, M. S., 1997. The Canadian Arctic in transition: Pre-Dorset to Dorset. In R. Gilberg, and H. C. Gulløv (Eds.), *Fifty Years of Arctic Research. Anthropological Studies from Greenland to Siberia* (pp. 205–208). National Museum Ethnographical Series No. 18. The National Museum of Denmark, Department of Ethnography, Copenhagen, Denmark.

McGhee, R. 1969. Speculations on climatic change and Thule culture development. *Folk*, 11, 173-184.

McGhee, R. 1970. Excavations at Bloody Falls, NWT, Canada. *Arctic Anthropology*, 6(2), 53-72.

McGhee, R. 1974. A Current Interpretation of central Canadian Arctic Prehistory. *Inter-Nord*, 13-14, 171-180.

McGhee, R. 1976. Paleoeskimo occupation of central and high Arctic Canada. In M. S. Maxwell (Ed.), *Eastern Arctic Prehistory: Paleoeskimo Problems* (pp. 15-39). Memoirs of the Society for American Archaeology No. 31. Society for American Archaeology, Washington, D.C.

McGhee, R. 2001. *Ancient people of the Arctic*. British Columbia: UBC Press.

Meldgaard, J. 1952. A Paleo-Eskimo culture in west Greenland. *American Antiquity*, 17(3), 222-230.

Milne, S. B. 2003a. Peopling the Pre-Dorset past: a multiscalar study of early arctic lithic technology and seasonal land use patterns on southern Baffin Island. PhD Dissertation, Department of Anthropology, McMaster University, Hamilton, Ontario.

Milne, S. B. 2003b. Identifying Pre-Dorset structural features on southern Baffin Island: Challenges and considerations for alternative sampling methods. *Études/Inuit/Studies*, 27(1-2), 67-90.

Milne, S. B. 2005. Archaeological Investigations in the Mingo and Amadjuak Lake Districts of southern Baffin Island. Permit Report covering the work conducted under Nunavut Archaeologist Permit 04-06A. Unpublished permit report, Nunavut Ministry of Culture, Language, Elders and Youth, Igloolik.

Milne, S. B. 2008. Archaeological Investigations in the Mingo Lake District of southern Baffin Island: Assessing Palaeo-Eskimo Culture Continuity and Change. Permit report covering the work conducted under Nunavut Archaeologist Permit 07-014. Manuscript on file, Department of Culture, Language, Elders and Youth, Government of Nunavut, Igloolik, Nunavut.

Milne, S. B. 2013. Chert Sourcing and Palaeo-Eskimo Stone Tool Technology. Report on work conducted under Nunavut Archaeological Permit No. 2013-02A. Manuscript on file with the Department of Culture, Language, Elders and Youth, Government of Nunavut, Igloolik, Nunavut.

Milne, S. B. 2015. Chert Sourcing and Palaeo-Eskimo Stone Tool Technology. Report on work conducted under Nunavut Archaeological Permit No. 2015-21A. Manuscript on file with the Department of Culture, Language, Elders and Youth, Government of Nunavut, Igloolik, Nunavut.

Milne, S. B., and Donnelly, S. M. 2004. Going to the birds: examining the importance of avian resources to Pre-Dorset subsistence strategies on southern Baffin Island. *Arctic Anthropology*, 41(1), 90–112.

Milne, S. B., and Landry, D. B. 2016. Shedding new light on arctic archaeological sites through the use of HDS and point cloud feature extraction and enhancement. Paper presented at the Hexagon Lecia Geosystem Industry Conference, June 13-16, Anaheim, CA. (Invited Podium Paper).

Milne, S. B., and Park, R. W. 2016. Pre-Dorset Culture. In M. Friesen and O. Mason (Eds.), *The Oxford Handbook of the Prehistoric Arctic*. Oxford University Press. DOI: 10.1093/oxfordhb/9780199766956.001.0001.

Milne, S. B., Park, R. W., Hamilton, A. C., and Fayek, M. J. 2011. Chert sourcing and Palaeo-Eskimo raw material use in the interior of southern Baffin Island, arctic Canada. *Canadian Journal of Archaeology*, *35*(1), 117-142.

Milne, S. B., Park, R. W., and Stenton, D. 2012. Dorset culture land use strategies and the case of inland southern Baffin Island. *Canadian Journal of Archaeology/Journal Canadien D'Archéologie*, 36, 267–288.

Milne, S. B., Park, R. W., and Stenton, D. R. 2013. For caribou, chert, and company: understanding mobility among the Palaeo-Eskimos of Baffin Island, Arctic Canada. In Mobility, Transition, and Change in Prehistory and Antiquity. Proceedings of the Graduate Archaeology Organisation Conference on the Fourth and Fifth of April 2008 at Hertford College, Oxford, UK, Preston PR, Schorle K (eds). British Archaeological Reports, International Series, Archaeopress: Oxford; 49–61.

McNeill, J. D., and Bosnar, M. 1999. Application of 'dipole–dipole' electromagnetic systems for geological depth sounding. Technical Note TN-31, Geonics Limited: Mississauga, ON, Canada. http://www.geonics.com/pdfs/technicalnotes/tn31.pdf (as modified October 2007).

Mudie, P.J., Rochon, A., Levac, E. 2005. Decadal scale sea ice changes in the Canadian Arctic and their impacts on humans during the past 4,000 years. *Environmental Archaeology*, 10, 113126.

Murray, M. S. 1999. Local heroes. The long-term effects of short-term prosperity: An example from the Canadian Arctic. *World Archaeology*, 30, 466–483.

Nagy, M. I. 2000. From Pre-Dorset foragers to Dorset collectors: Palaeo-Eskimo culture change in Ivujivik, eastern Canadian Arctic. In M. Appelt, J. Berglund, and H. C. Gullov (Eds.), *Identities and Culture Contacts in the Arctic* (pp. 143–148). Danish Polar Centre Publication No. 8. Danish National Museum, Copenhagen, Denmark.

Nelson, M. C. 1991. The study of technological organization. *Archaeological method and theory, 3*, 57-100.

Odess, D. 1998. The archaeology of interaction: Views from artifact style and material exchange in Dorset society. *American Antiquity,* 63, 417–435.

Park, R. W. 1993. The Dorset-Thule succession in Arctic North America: assessing claims for culture contact. *American Antiquity, 58*(2), 203-234.

Park, R. W. 2000. The Dorset-Thule succession revisited. *Identities and cultural contacts in the Arctic.* Copenhagen: Danish National Museum and Danish Polar Center, 192205.

Park R. W. 2008. Archaeological Excavations at the LdFa-1 site, Mingo Lake, Baffin Island, Summer 2008. Report on work conducted under Nunavut Territory Archaeologist Permit No. 08-029A. University of Waterloo, ON, Canada.

Peregrine, A. G.- L., Rogers, M. B., and Jordan, K. A. 2012. Understanding the built environment at the Seneca Iroquois White Springs Site using large-scale, multi-instrument archaeogeophysical surveys. *Journal of Archaeological Science*, 39(7), 2042–48. DOI:10.1016/j.jas.2012.03.011.

Prentiss, A. M., Cross, G., Foor, T. A., Hogan, M., Markle, D., and Clarke, D. S. 2008. Evolution of a Late Prehistoric winter village on the interior plateau of British Columbia: geophysical investigations, radiocarbon dating, and spatial analysis of the Bridge River site. *American Antiquity*, 73(1), 59–81.

Raghavan, M., M. DeGiorgio, A. Albrechtsen, I. Moltke, P. Skoglund, T. S. Korneliussen, B. Grønnow, M. Appelt, H. C. Gulløv, T. M. Friesen, W. Fitzhugh, H. Malmström, S. Rasmussen, J. Olsen, L. Melchior, B. T. Fuller, S. M. Fahrni, T. Stafford Jr., V. Grimes, M. A. P. Renouf, J. Cybulski, N. Lynnerup, M. M. Lahr, K. Britton, R. Knecht, J. Arneborg, M. Metspalu, O. E. Cornejo, A-S. Malaspinas, Y. Wang, M. Rasmussen, V. Raghavan, T. V. O. Hansen, E. Khusnutdinova, T. Pierre, K. Dneprovsky, C. Andreasen, H. Lange, M. G. Hayes, J. Coltrain, V. A. Spitsyn, A. Götherström, L. Orlando, T. Kivisild, R. Villems, M. H. Crawford, F. C. Nielsen, J. Dissing, J. Heinemeier, M. Meldgaard, C. Bustamante, D. H. O'Rourke, M. Jakobsson, M. T. P. Gilbert, R. Nielsen, and E. Willerslev. 2014. The genetic prehistory of the New World Arctic. *Science*, 345(6200), 1255832.

Ramsden, P., and Tuck, J. A. 2001. A comment on the Pre-Dorset/Dorset transition in the eastern Arctic. *Anthropological Papers of the University of Alaska, New Series*, 1(1), 7–11.

Renouf, M. A. P., and Bell, T. 2010. Precontact population contraction and expansion in Newfoundland, 1200–1000 Cal BP. In H. Maschner, O. Mason, and R. McGhee (Eds.), *The Northern World AD 1100-1350* (pp. 263–278). Salt Lake City, Utah: University of Utah Press.

Robinson, D. A., Lebron, I., Lesch, S. M., and Shouse, P. 2004. Minimizing drift in electrical conductivity measurements in high temperature environments using the EM-38. *Soil Science Society of America Journal*, 68(2), 339-345.

Sanford, B. V., and Grant, A. C. 2000. Geological framework of the Ordovician System in the southeast Arctic platform, Nunavut. *Geological Survey of Canada, Bulletin*, *557*, 13-38.

Scollar, I., and Krückeberg, F. 1966. Computer treatment of magnetic measurements from archaeological sites. *Archaeometry*, 9(1), 61-71.

Smekalova, T. N., Voss, O., and Smekalov, S. L. 2008. *Magnetic surveying in archaeology: More than 10 years of using the Overhauser GSM-19 gradiometer, 2nd revised edition*, B. W. Bevan (Ed.). Højbjerg, Denmark: Wormianum.

Smith, S. L., and Burgess, M. 2004. *Sensitivity of permafrost to climate warming in Canada* (No. 579). Natural Resources Canada.

Soper, J. D., and Wilson, A. E. 1928. *A faunal investigation of southern Baffin Island* (Vol. 53). FA Acland, printer to the King.

Stenton, D. R. 1986. Mitigation of the Sandy Point Site (LlDv-10), Baffin Island, NWT. A Report Submitted to the Prince of Wales Northern Heritage Centre. On file at the Prince of Wales Northern Heritage Centre, Yellowknife, NWT.

Stenton, D. R. 1991a. The archaeology of terrestrial hunting systems: The Amadjuak Lake Project. Permit report on file with the Department of Culture, Elders, Language, and Youth. Government of Nunavut. Igloolik: Nunavut.

Stenton, D. R. 1991b. The adaptive significance of caribou winter clothing for arctic hunter-gatherers. *Etudes/Inuit/Studies*, 3-28.

Stenton, D. R., and Park, R. W. 2003. Archaeological Excavations at Igloolik (NiHf-57) Summer 2002. *Manuscript on file, Canadian Museum of Civilization, Gatineau, Québec*.

Stewart, A. M., Keith, D., and Scottie, J. 2004. Caribou crossings and cultural meanings: Placing traditional knowledge and archaeology in context in an Inuit landscape. *Journal of Archaeological Method and Theory*, *11*(2), 183-211.

Stocker, T. F., Qin, D., Plattner, G. K., Tignor, M. Allen, S. K., Boschung, J. Nauels, A. Xia, Y., Bex, V., and Midgley, P. M. IPCC, 2013: summary for policymakers. *Climate change*, 3-29.

St. Onge, M. R., Sanborn-Barrie, M., and Young, M. D. 2007. Geology. Mingo Lake, Baffin Island, Nunavut: Geological Survey of Canada, Open File 5433, scale 1:200 000.

Taylor, W. E. 1968. The Arnapik and Tyara sites: An archaeological study of Dorset culture origins. *Memoirs of the Society for American Archaeology*, (22), iii-129.

ten Bruggencate, R. E., Stup, J. P., Milne, S. B., Stenton, D. R., Park, R. W., and Fayek, M. 2016. A human-centered GIS approach to modeling mobility on southern Baffin Island, Nunavut, Canada. *Journal of Field Archaeology*, 41(6), 684-698. DOI:10.1080/00934690.2016.1234897.

ten Bruggencate, R. E., Milne, S. B., Park, R. W., Fayek, M., and Stenton, D. R. 2017. Combining chert provenance and least-cost pathway analyses to reconstruct Pre-Dorset and Dorset mobility on southern Baffin Island. *Journal of Archaeological Science: Reports*, *14*, 651-661.

Thacker, P. T., and Ellwood, B. B. 2002. The magnetic susceptibility of cherts: archaeological and geochemical implications of source variation. *Geoarchaeology*, *17*(5), 465-482.

Thompson, V. D., and Pluckhahn, T. J. 2010. History, complex hunter-gatherers, and the mounds and monuments of Crystal River, Florida, USA: A geophysical perspective. *Journal of Island & Coastal Archaeology*, *5*(1), 33-51.

Thompson, V. D., Arnold III, P. J., Pluckhahn, T. J., and Vanderwarker, A. 2011. Situating remote sensing in anthropological archaeology. *Archaeological Prospection*, 18, 195-213.

Throop, J. L. 2010. Spatial and temporal variability in permafrost conditions, northern Canada. Unpublished M.A. Thesis. Department of Geography, Faculty of Arts, University of Ottawa.

Throop, J. L., Smith, S. L., and Lewkowicz, A. G. 2010. Observed recent changes in climate and permafrost temperatures at four sites in northern Canada. In *GEO2010, 63rd Canadian Geotechnical Conference and the 6th Canadian Permafrost Conference, Calgary. GEO2010 Calgary Organizing Committee* (pp. 1265-1272).

Tuck, James A., and William Fitzhugh 1986. Palaeo-Eskimo Traditions of Newfoundland and Labrador: A Reappraisal. In Palaeo-Eskimo Cultures in Newfoundland, Labrador, and Ungava, pp. 161–167. Reports in Archaeology No. 1, Memorial University of Newfoundland, St. John's, Newfoundland

Urban, T. M. 2012. In the footsteps of J. Louis Giddings (1909–1964): archaeological geophysics in Arctic Alaska. *Antiquity*, 86, 332.

Urban, T. M., Anderson, D. D., and Anderson, W. W. 2012. Multimethod geophysical investigations at an Inupiaq village site in Kobuk Valley, Alaska. *The Leading Edge*, *31*(8), 950-956.

Urban, T. M., Rasic, J. T., Alix, C., Anderson, D. D., Manning, S. W., Mason, O. K., Tremayne, A. H., and Wolff, C. B. 2016. Frozen: The potential and pitfalls of ground-penetrating radar for archaeology in the Alaskan Arctic. *Remote Sensing*, 8, 1007.

Weymouth, J. W., and Nickel, R. 1977. A magnetometer survey of the knife river Indian villages. *Plains Archaeologist*, Memoir 13(2), 104-118.

Wiewel, A. S., and Kvamme, K. L. 2014. Magnetic investigations of nomadic group encampments at Fort Clark State Historic Site, North Dakota. *Plains Anthropologist*, *59*(231), 261-278.

Wolff, C. B., and Urban, T. M. 2013. Geophysical analysis at the Old Whaling site, Cape Krusenstern, Alaska, reveals the possible impact of permafrost loss on archaeological interpretation. *Polar Research*, *32*(1), 19888.

Viberg A, Trinks I, and Lidén K. 2009. Archaeological prospection in the Swedish mountain tundra region. *ArchéoSciences, 33*. Rennes: Presses Université de Rennes.

Viberg A, Berntsson A, and Lidén K. 2013. Archaeological prospection of a high altitude Neolithic site in the Arctic mountain tundra region of Northern Sweden. *Journal of Archaeological Science*, 40(6), 2579–2588.

Vosselman, G., and Maas, H. G. 2010. *Airborne and terrestrial laser scanning*. Whittles publishing.

Zhang, S., and Lavoie, D. 2013. Studies of Paleozoic stratigraphy and petroleum potential in the Hudson Bay and Foxe basins, Nunavut. *Summary of Activities*, 121-130.

Chapter 3

Combined Geophysical Approach in a Complex Arctic Archaeological Environment: A Case Study from the LdFa-1 Site, Southern Baffin Island, Nunavut

A peer-reviewed scientific research paper published in:

Archaeological Prospection, 22(3):157-170,

DOI: 10.1002/arp.1505

David B. Landry, Ian J. Ferguson, S. Brooke Milne, and Robert W. Park

Abstract: In 2014, we mapped the complex landscape of component Area 5 at LdFa-1, a 3000-year-old Palaeoeskimo site located in the deep interior of southern Baffin Island, using a combined magnetic and electromagnetic approach to define the physical characteristics of any large- or small-scale anthropogenic anomalies. Measurements were made using a GEM Systems Overhauser magnetometer-gradiometer and Geonics EM31 instrument, and a survey configuration designed to map in high resolution the total magnetic field, magnetic susceptibility and electrical conductivity responses of the underlying soils. Data-reduction methods were used for each survey, including, for example, removal of temporal drift, to produce final responses related closely to the subsurface physical properties. Six geophysical responses are presented in the results: total magnetic field, vertical magnetic gradient, horizontal- and vertical dipole-mode apparent susceptibility, and horizontal- and vertical-dipole-mode apparent conductivity. Spatial assemblages of small-scale (<2m) anomalies, correlated between the magnetic and magnetic susceptibility results and interpreted to be associated with groupings of igneous boulders in the shallow subsurface, define three areas of archaeological interest. One grouping is a roughly circular arrangement of anomalies with a diameter of 4m. Its spatial correlation with a productive excavation unit at the site suggests an anthropogenic origin. The complementarity of data acquired at this site reduces the chances of misidentifying anomalies, for example, the apparent conductivity results support interpretation of larger-scale anomalies observed at the site as being of lithogenic origin. This archaeogeophyiscal case study demonstrates the value of geophysical investigation in a complex Arctic archaeological environment and its role in providing information on subsurface archaeological features.

3.1 Introduction

Geophysicists have shared an interest in the investigation of archaeological artefacts and sites for over a century. As early as 1899, publications demonstrate the use of magnetic measurements from prehistoric ceramic vessels to map significant changes in the Earth's magnetic field (Evans and Heller, 2003, pp. 231). Since the mid-twentieth century work of Le Borgne (1955, 1965) on the magnetic properties of archaeological soils, however, geophysical techniques have become an exciting and unparalleled technique for archaeological prospection and non-invasive investigation. This case study combines the results of both magnetic and electromagnetic surveys over the Area 5 component at the LdFa-1 site in the interior of southern Baffin Island (Figure 3.1) in order to define and characterize near-surface anomalies in a geologically complex Arctic environment. The geophysical responses from this site inform our archaeological interpretations about possible underlying Palaeo-Eskimo site features and activity areas.

Archaeogeophysical surveys are used in a number of applications, including non-invasive mapping and prospection of archaeological landscapes, and for the identification and characterization of subsurface archaeological features and other forms of anthropogenic or lithogenic anomalies (e.g. Lepold et al., 2010; Peregrine et al., 2012; Rosendahl et al., 2014; Welham et al., 2014). Magnetometers map spatial variations in the Earth's magnetic field produced through both natural and anthropogenic sources, while vertical gradiometer magnetometers measure the response of the magnetic field at a higher spatial resolution (e.g. Hansen et al., 2005). Electromagnetic surveying is designed to map the electrical conductivity of the near surface with the additional and complementary capability of mapping magnetic susceptibility (e.g. Tabbagh, 1986).

The wide use and success of geophysics in archaeology has been well documented in the literature (see Gaffney and Gater, 2006; Kvamme, 2003; Dalan, 2006; Johnson, 2006; Linford, 2006; Viberg et al., 2011), yet its contributions to Arctic archaeological research remain limited to a few specific areas in North America (Eastaugh and Taylor, 2005, 2011; Hodgetts et al., 2011; Urban, 2012; Eastaugh et al., 2013; Wolff and Urban, 2013), and the tundra mountains of Arctic Sweden (Viberg et al., 2009, 2013). This dearth of geophysical applications has been attributed to the small-scale nature and commonly organic composition of hunter–gatherer remains in Canada and, specifically, in northern tundra regions where natural soil development processes are extremely slow and limited to a few centimetres thickness (Viberg et al., 2009; Hodgetts et al., 2011; Eastaugh et al., 2013). The variable thickness of the soils and the near-surface bedrock can create significant magnetic and electrical anomalies, making it more difficult to discern and separate anthropogenic signals in the data and leading to difficulties in the interpretation of the results. Through the application of careful data reduction techniques, including removal of temporal drifts from the data, and correlation of magnetic and electromagnetic responses, this case study addresses these difficulties of applying archaeogeophysics to a geologically complex Arctic archaeological site.

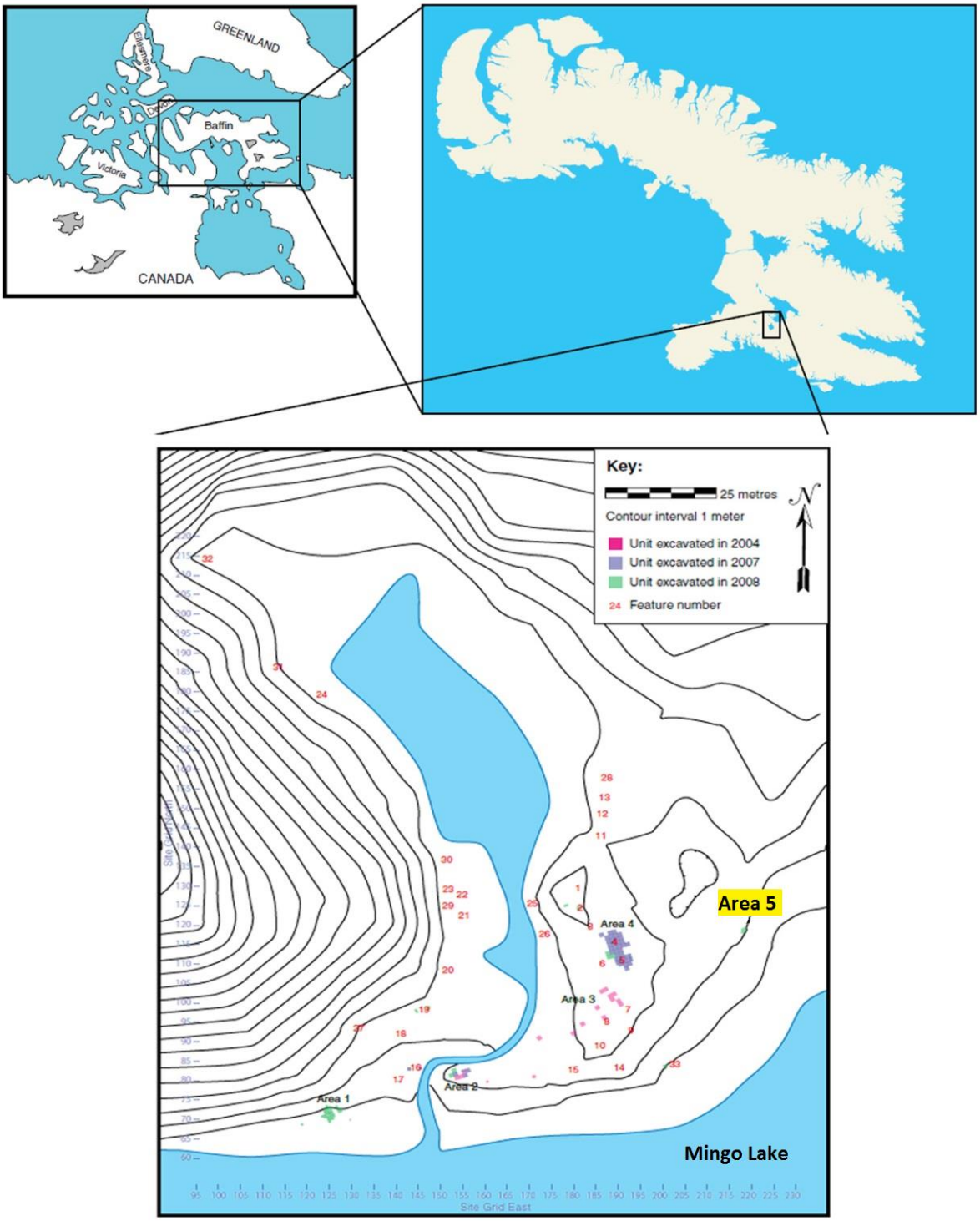

Figure 3.1 Northern Canada and Greenland, with Baffin Island and LdFa-1 site map inset (modified from Park, 2008). The LdFa-1 map shows the areas defined at the complex site and defined features of interest and excavation units. The current study is located in Area 5.

3.2 Southern Baffin Island and the LdFa-1 Area 5 Survey Site

The geological landscape significantly influences the magnetic and electrical properties of archaeological subsurface soils (LeBorgne, 1965). Prior to this research, there had been no investigation of the near-surface geophysical properties of the LdFa-1 survey site. However, a number of studies provide geological information. The interior of southern Baffin Island is characterized by three large Lakes: Amadjuak, Mingo and Nettling. The regional terrain is relatively flat with marshy tundra and networks of glacial moraines and eskers along the edges of large rivers, and inlets (Soper, 1923; Stenton, 1989; Milne, 1999, 2003; Milne and Donnelly, 2004). The LdFa-1 site is situated on the northwest shore of Mingo Lake (Figure 3.1). The bedrock geology at the site consists of flat-lying, fossiliferous, limestone of the Upper Ordovician Amadjuak Formation (St Onge et al., 2007). The site lies only 2km to the north of the contact between this unit and Proterozoic monzogranite of the Cumberland batholith (St Onge et al., 2007) and the limestone bedrock at the site probably forms only a thin veneer overlying Proterozoic rocks. The site is located on the lower parts of an esker adjacent to Lake Mingo (Milne, 2005, 2007, 2013; Utting et al., 2007; Park, 2008; Milne et al., 2012, 2013) and the surficial geology consists of glacial and organic deposits. The glacial drift contains abundant granitic cobbles and boulders (Utting et al., 2007) reflecting the proximity of the margin with the Proterozoic granitic rocks. In this geological setting, the larger scale (tens of metres and greater) magnetic field response in the study area will be influenced by the Proterozoic rocks, because the overlying limestones will be almost non-magnetic. On a small scale (1m and less), granitic inclusions in the glacial drift are expected to have a stronger magnetic response than the surrounding glacial materials (e.g. Hansen et al., 2005; Nabighian et al., 2005; Sanborn-Barrie et al., 2008).

The archaeological site of LdFa-1 was first identified by Stenton in 1991, and investigated by Milne in 2004 and 2007, and Park in 2008. The site is multicomponent, yielding evidence for Palaeoeskimo (Pre-Dorset, Dorset), and Neoeskimo (Thule Inuit) occupations. Site LdFa-1 is large and topographically complex, and has been divided into five component areas (Figure 3.1). Visible surface features include at least 33 stone tent rings, stone caches and possible hearth areas. The size and shape of the stone tent rings vary across the site, however, they are defined as roughly circular to oval arrangements of boulders ranging from 2.0m to 5.0m in diameter. The geophysical survey in this case study was conducted at Area 5, located in the eastern portion of the site. Area 5 has been tested only preliminarily and, therefore, limited information is available about its archaeological features.

Park (2008) describes Area 5 as heavily vegetated with no large archaeological surface features (Figure 3.2). The northwest corner is partially inundated with thickly vegetated, wet soil, however, the area drains and flattens near the middle section before sloping to the southeast corner. Several caribou trails have been cut deeply into the surface, running east–west across the survey grid, exposing a number of pieces of lithic debitage (i.e. stone waste flakes), formal and informal stone tools, and faunal remains. In 2008, a total of 1.25m2 were excavated in Area 5, resulting in the recovery of a remarkable number of lithic debitage, burins, burin-spalls and microblades. Park (2008, pp. 20) illustrates the stratigraphy from these units as consisting of 10cm of black loam, 4–6 cm of sandy loam, 10cm of gravely loam, overlying 3 cm of sterile sand. Several near-surface rocks were uncovered during the excavation, however, it remains unclear whether they are part of a structure (Park, 2008). Unlike all other similar concentrations of archeological items excavated at LdFa-1, the one in Area 5 is of particular interest because of the absence of any known associated features. The geophysical survey conducted in this study

was designed to examine evidence for the presence of subsurface anthropological features surrounding the excavation unit.

Figure 3.2 Photograph of LdFa-1 Area 5 showing the 20m by 20m geophysical survey grid. Note the relatively thick vegetation covering parts of the surface.

3.3 Geophysical Methods

3.3.1 Magnetometer/Gradiometer

Geophysical magnetic applications in Arctic archaeological research have been successful in identifying several types of anthropogenic remains, including middens, hearths and sunken turf houses (Eastaugh and Taylor, 2005, 2011; Viberg et al., 2009; 2013; Hodgetts et al., 2011; Urban, 2012; Wolff and Urban 2013). Magnetic anomalies are caused by localized increases or decreases in magnetization, measured as variations from the background magnetic field. They may be created by both lithogenic and anthropogenic sources (Fialová et al., 2006). In many locations, anthropogenic anomalies may be obscured by lithogenic anomalies associated with spatial variations in shallow bedrock, soil types, soil erosion rates and climate change (Fialová et al., 2006; Linford, 2006, pp. 2220).

There are two forms of magnetization measured in magnetic surveys (e.g. Evans and Heller, 2003; Hansen et al., 2005). Remanent magnetization is permanent magnetization that persists in materials even when they are distant from any external magnetic sources. In contrast, induced magnetization occurs only when a body is located in the vicinity of an external magnetic source. The ability to be magnetized is measured by the magnetic susceptibility. The induced magnetization also depends on the direction and strength of the external magnetic field. In most small-scale magnetic surveys, a large component of the response will be the induced magnetization caused by the spatial distribution of magnetically susceptible materials (e.g. magnetic topsoil). It is often difficult to discriminate between remanent and induced magnetization, particularly if the remnant magnetization is parallel to the Earth's magnetic field.

In total magnetic field (TMF) surveys the strength of the local magnetic field is measured using an instrument such as a single-sensor Overhauser magnetometer (e.g. Martín et al., 2009; Smekalova et al., 2008). Responses measured in TMF surveys may be obscured by temporal variations in the Earth's magnetic field associated with diurnal fluctuations and geomagnetic storms. It is necessary to correct for the temporal variations using recordings from a stationary location such as a magnetic observatory or a magnetic base-station. In gradiometer surveys, the magnetic field gradient is measured using two magnetometer sensors separated in the vertical or horizontal direction. Gradiometer measurements are not affected by temporal field variations, removing the need for a base-station recording. The gradiometer response is a high-pass filtered form of the TMF response that emphasizes the short wavelength (high spatial frequency) features, often of most interest in archeological surveys, and reduces the response of longer wavelength features, that are more commonly of lithogenic origin.

3.3.2 EM31

Frequency-domain electromagnetic (FEM) surveys have been applied in archeological field studies to provide estimates of the shallow electrical conductivity of survey sites (Tabbagh, 1986; Welham et al., 2014). Instruments operating at low induction number (LIN; i. e. at frequencies for which the signal penetration greatly exceeds the coil spacing), provide a response that is proportional to the apparent or depth-averaged conductivity at the measurement point (McNeill, 1980, 1990; Tabbagh, 1986; Fitterman and Labson, 2005). The apparent conductivity is derived from the quadrature component of the response. The InPhase component of the same response provides a measure of the apparent magnetic susceptibility at the measurement point (Tabbagh, 1986; McNeill and Bosnar, 1999; Dalan, 2006; McNeill, 2012), but the InPhase response may also be affected by electric polarization properties or very high conductivity in the subsurface.

The sensitivity of the LIN response to the subsurface properties depends on the separation of the transmitter and receiver coils and the instrument configuration (McNeill and Bosnar, 1999; Fitterman and Labson, 2005; Figure 3.3). When operated with the coils in a vertical coplanar configuration, that is, in horizontal dipole (HD) mode, the sensitivity of the apparent conductivity response is highest at the surface and decreases with depth. When operated with the coils in a horizontal coplanar configuration, in vertical dipole (VD) mode, the sensitivity increases from zero at the surface, to a maximum at a depth of 0.35 times the coil spacing, and then decreases at greater depth. The sensitivity of the InPhase response to magnetic susceptibility has maximum magnitude at 0.25 times the coil spacing for the HD mode and 0.18 times the spacing for the VD mode, but the sign of the response is the opposite in the two cases. The

sensitivity function of the VD mode is complicated by a change in the sign at depths exceeding 0.6 coil spacings (Figure 3.3; Dalan, 2006).

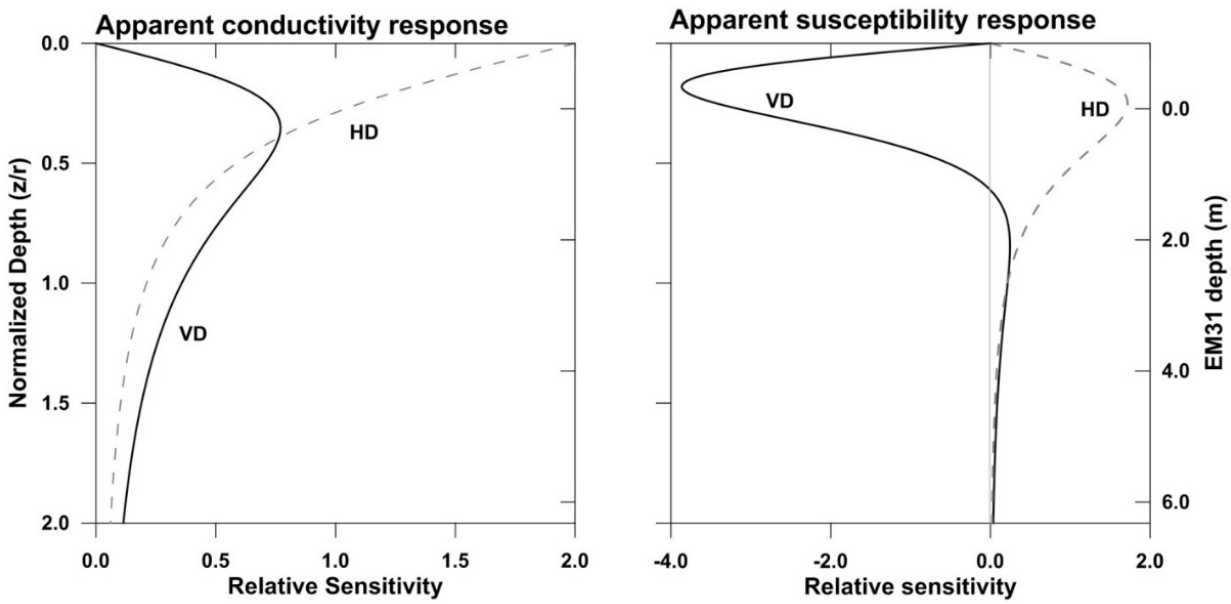

Figure 3.3 Relative sensitivity of the apparent conductivity and apparent susceptibility response of a LIN instrument: left-hand vertical axes show normalized depth, the ratio of the depth to coil spacing, and right-hand vertical axes show the equivalent depths for an EM31 instrument operated at 1m elevation. Equations for the sensitivity functions can be found in Fitterman and Labson (2005).

3.4 Survey and Configuration

The LdFa-1 geophysical fieldwork was initially designed as a multiday, multi-instrument project, with the site to be accessed each day from Iqaluit by Twin Otter aircraft, but the total field time was reduced to only 8 h at the site because of difficulties in aircraft landings. As a result, the survey area size was restricted, and the geophysical instrumentation used was limited to the Overhauser magnetometer-gradiometer and EM31 instruments that had been transported to the site on the first trip in order to provide an overview of the magnetic and electrical responses:

additional geophysical instrumentation shipped to Iqaluit to be used in the project could not be deployed.

The geophysical survey area was established at a location surrounding the excavation unit in Area 5 and consisted of a 20m×20m square grid. Individual measurement locations were established using tapes extended between non-magnetic measuring pegs at the grid margin.

The TMF and vertical magnetic gradient survey was carried out using a GSM-19 Overhauser magnetometer gradiometer with sensors at 0.5m and 0.75m height on the measuring rod. Measurements were acquired at a line spacing of 0.5min the east–west direction and a station spacing of 0.2m along north–south lines with the lines traversed in a zig-zag pattern. The position accuracy is approximately 0.05m. The configuration produced 101 individual survey points on each line, and a total of 4144 measurements.

A single sensor GEM Systems magnetometer base station was deployed 260m northeast from the survey grid to record diurnal background magnetic field fluctuations. The base-station and roving magnetometers were time-synchronized to ±1ms using GPS UTC to ensure an accurate correction of the field data following the survey. Magnetic field readings were recorded during the survey cycling every 10s.

The electromagnetic survey at LdFa-1 used a GEONICS EM31 instrument (McNeill, 1979), which was carried at 1m (hip) height and aligned parallel to the line direction. Prior to the survey the instrument was prepared using standard field functional checks (McNeill, 1979); because of the extremely low conductivity at the site, the phasing could be completed at only an approximate level, requiring post-survey correction of the data. The survey used a line spacing of 1m in the east–west direction and a station spacing of 0.5 m, with each line traversed from south

to north. Readings were taken with the mid-point of the coils centred over the specified measurement location and have an estimated positioning accuracy of positioning is 0.2m laterally and 0.1m vertically. Readings were acquired in both VD and HD modes and recorded digitally, providing accurate InPhase and quadrature responses. InPhase (apparent susceptibility) and quadrature (apparent conductivity) VD and HD measurements were made a total of 861 locations for a total of 3444 individual data points.

3.5 Data Reduction and Results

The TMF data were corrected for temporal variations using linear interpolation between the recorded base station values. Figure 3.4 shows the time variations in the magnetic field during the survey as well as contour maps of the raw and corrected TMF data. Over the duration of the survey the magnetic field varied by 80 nT with shorter term micropulsations of 10 to 20 nT magnitude. The larger-scale spatial variations in the magnetic field in the survey area have a magnitude of only 120 nT, so the time-variations create significant distortion in the raw TMF response. In particular, they create linear features parallel to the line direction, for example, along the 15.5m east line and distort the true form of other spatial variations, for example, around 3 to 5m east and 7–12m north. The base-stationcorrected data do not exhibit lineations and show the position of small-scale anomalies more clearly.

It is of interest to compare the Mingo Lake base station recordings with the magnetic field variations recorded at the Iqaluit Magnetic Observatory, 190km east-southeast of the LdFa-1 study area (Figure 3.4a). The traces clearly exhibit the same general fluctuations but there are significant frequency-dependent differences in the magnetic field variations at the two locations. These differences can be attributed to spatial changes in the magnetic source fields and to

changes in magnetic field response associated with large-scale electromagnetic induction in the Earth by these source fields (e.g. Lilley et al., 1984; Vallée et al., 2006). The comparison indicates that although the observatory data would have allowed an approximate correction of the TMF data, the results would not have been as accurate as when a local base-station was used.

Several processing steps were required for preparation of final EM31 responses. Contour maps of the raw HD and VD InPhase data (not shown) are characterized by linear striping parallel to survey lines. This striping is parameterized by small offsets of 0.1 to 0.6 ppt between adjacent survey lines. The effect may be explained by jarring of the instrument during its transport to the start of each line, however, the offsets are consistently positive, so it is more reasonably explained by instrumental drift, as has been observed previously for InPhase surveys (e.g. Simpson et al., 2009). Rather than using a linear drift correction, as suggested by Dalan (2006), the data were corrected using a piece-wise approach in which the median HD and VD InPhase response for each line was adjusted to equal the corresponding values for the first line. This process greatly reduced the striping. The InPhase data were converted to apparent volume susceptibility values using an approach that allows for the decrease in response due to the elevation of the instrument (e.g. Huang et al., 2003; Dalan, 2006). The transformation was applied to the difference of each response from the minimum HD or VD response in the data set so that the apparent susceptibility values represent values that are relative to the minimum value.

Raw apparent conductivity responses for both the HD and VD modes included negative values because of the inexact phasing of the EM31 instrument and extremely low values of conductivity at the survey site. The data were corrected by converting the apparent conductivity and InPhase responses into a single complex-valued response, rephasing the responses so that the minimum phase corresponded to that for a reading over a 1 mS m_1 uniform half-space, and

converting back to standard apparent conductivity and InPhase responses. This correction means that the absolute value of the HD and VD apparent conductivity responses is not defined, but spatial changes in the data are still correctly resolved.

The final geophysical data sets were inspected using variograms to choose optimal parameters for interpolation and contouring. The TMF, magnetic gradient and apparent susceptibility variograms could be fitted by a sum of two model functions: a linear or exponential function related to larger-scale variations at the site plus an exponential function with a length scale of 0.5 to 1.0 m, related to a decrease in the variance to zero at small distance lag. This decrease is explained by the averaging effect of the sensor height. In contrast to the other parameters, variograms of the apparent conductivity data had non-zero variance at the smallest distance lag, indicating a significant random variation between adjacent data points. This response is interpreted to reflect a limit in the resolution of the apparent conductivity of ~±0.1 mS m_1, consistent with that determined in other studies (e.g. Beamish, 2011). Figure 3.5 shows the final contour maps of the six geophysical responses.

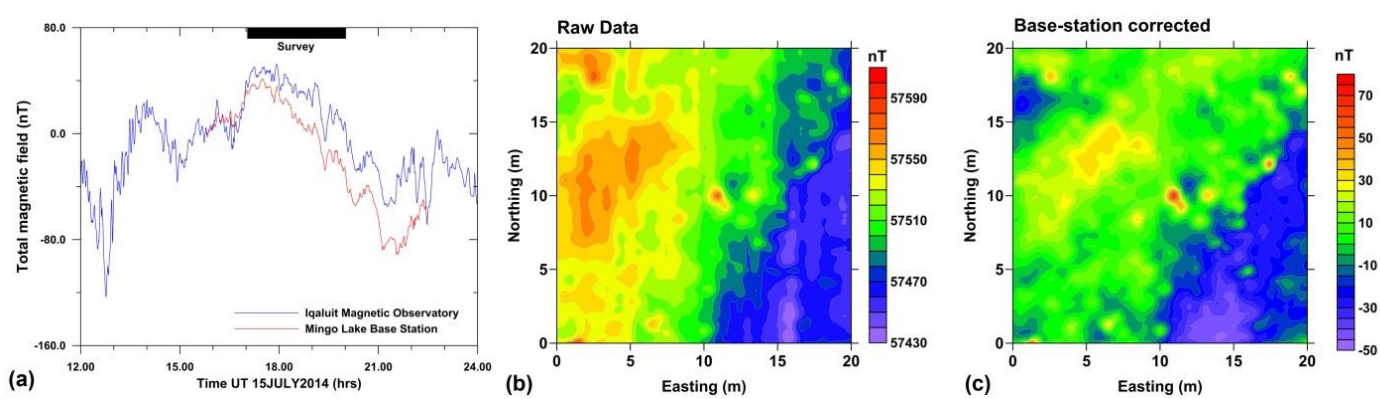

Figure 3.4 (a) Temporal magnetic field fluctuations recorded at the Mingo Lake base station and the Iqaluit Magnetic Observatory on 15 July 2014. The black bar along the top shows the time of the actual magnetic field survey. (b) Contour map of raw TMF data over the survey grid. (c) Contour map of corrected TMF data over the survey grid.

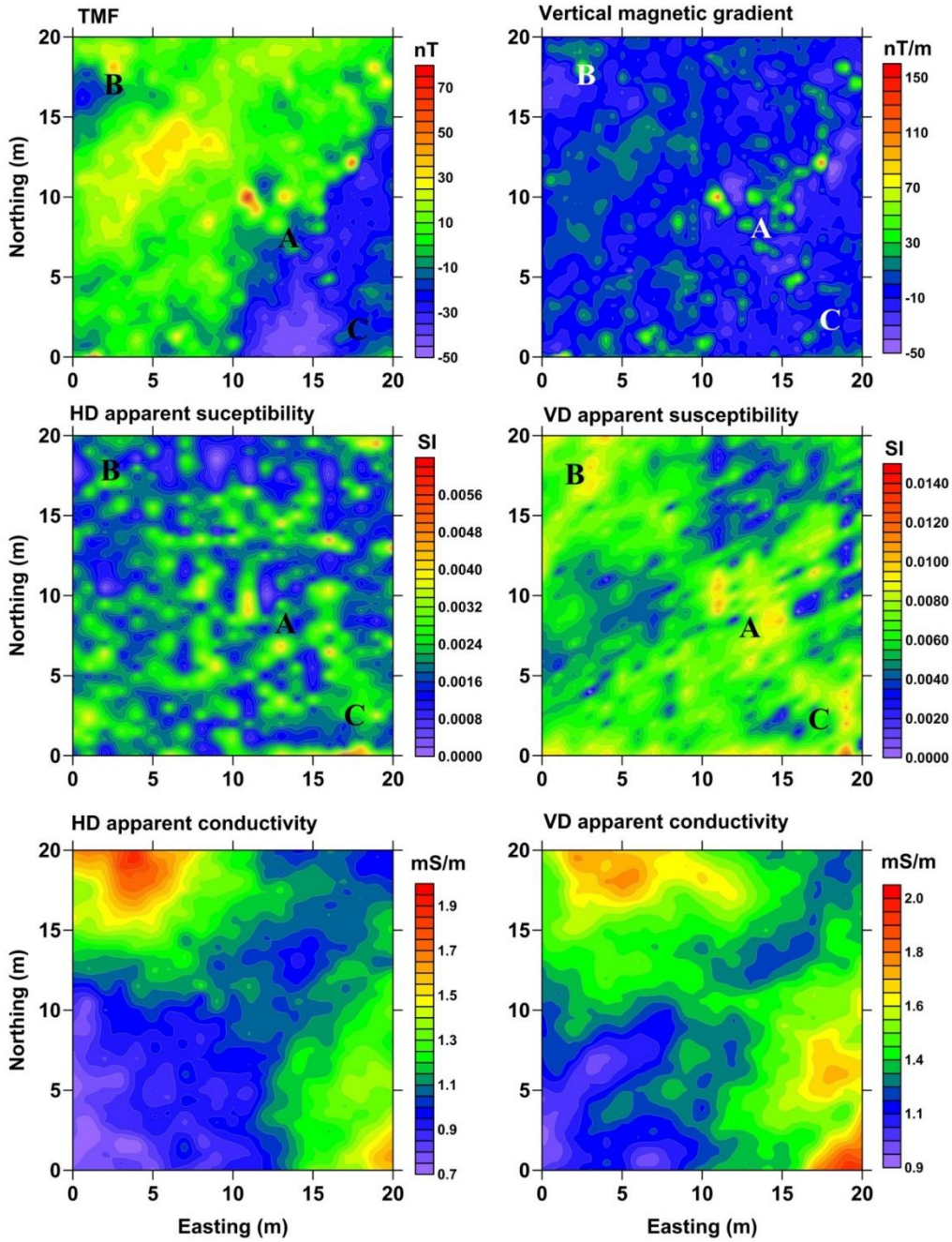

Figure 3.5 Contour maps of the final geophysical survey results from LdFa-1 Area 5. The maps show the TMF, magnetic gradient, apparent susceptibility and apparent conductivity responses. The interpolation and contouring is based on variogram analysis of the data and the apparent conductivity maps include a nugget effect variance of approximately 10% of the scale. Apparent magnetic susceptibility values were derived from the InPhase responses using conversion factors of ka (SI) = 2.95 × 10_3ΔI (ppt) for the HD mode and ka (SI) = 9.51 × 10_3ΔI (ppt) for the VD mode. These factors provide an exact susceptibility for a uniform Earth model. Apparent susceptibility and apparent conductivity maps show only the relative values of the parameters. “A”, “B” and “C” denote locations of interest.

3.6 Geophysical Responses

3.6.1 Apparent Conductivity

The LdFa-1 site is electrically resistive and although the exact absolute values of apparent conductivity could not be determined because of the imperfect phasing of the EM31 instrument, the values can be confidently limited to less than a few mS m_1. The HD and VD results exhibit well-resolved spatial variations of ~1 mS m_1 across the site (Figure 3.5). The responses for both modes are similar and include slightly more conductive zones in the northeast and southwest parts of the survey area and a more resistive zone trending in a southwest–northeast direction through the area. The similarity of the HD and VD responses suggests that the observed features extend over several metres depth. Smaller-scale variations within these resistive and conductive zones are not well resolved because of the small magnitude of these variations relative to the maximum resolution of the instrument.

3.6.2 TMF and Vertical Magnetic Gradient

The TMF response exhibits both large-scale and small-scale variations within the survey area (Figure 3.5). On the large-scale the TMF varies by 120 nT across the survey site, with low values observed in the northwest and southeast parts and higher values extending in a southwest to northeast pattern across the site. This large-scale pattern is spatially correlated with the apparent conductivity response, with the higher magnetic response associated with more resistive areas.

The TMF exhibits a number of short wavelength anomalies with length scale of <2m within the study area. Many of these are isolated positive anomalies with a magnitude of ~40 nT, however, there are several sets of paired positive and negative anomalies, such as at 12E–12 N,

6E–1N and 17E–13 N. The inclination of the Earth's field at the site is 81°, so the paired anomalies are indicative of a magnetic source with a component of remanent magnetization oblique to the Earth's field (e.g. Hansen et al., 2005). There is a very clear concentration of the magnetic anomalies centred on 12E–10N and the location has been designated "A" in Figure 3.5. There are several other locations with multiple anomalies, such as those designated "B" and "C".

The vertical magnetic gradient response resolves the short wavelength anomalies noted in the TMF results more clearly, the anomalies have values of up to 100 nT m_1 higher than background values. It also includes negative anomalies of up to 50 nT m_1 lower than background values. The gradient response provides only a weak indication of the large-scale changes across the study site that was observed in the TMF response. The gradient results thus exhibit the expected enhancement of short-wavelength features and suppression of long-wavelength features in the TMF response.

3.6.3 Apparent Susceptibility Responses

The VD apparent susceptibility (InPhase) response includes a number of features that correlate with the TMF and vertical magnetic gradient responses (Figure 3.5). At the largest scale there is an inverse correlation between a zone of low magnetic susceptibility values trending in a southwest–northeast direction through the study area and a zone of high TMF responses in the same area. Noting that the VD inphase sensitivity changes sign at a depth of ~1m (Figure 3.3), the observations indicate a source consisting of enhanced magnetic susceptibility at depths exceeding 1m. Such a source will create a positive response in the TMF and, because of the negative sensitivity at these depths, a negative response in the apparent susceptibility. The apparent susceptibility response indicates that the source has a susceptibility of around 0.005 SI,

but because the response is from a discrete body, this value is only an order of magnitude estimate.

At a smaller scale the VD apparent susceptibility response contains a number of anomalies, for example in locations A, B and C, that correlate with anomalies in the TMF and vertical magnetic gradient response. These features have quite high apparent susceptibility values of up to 0.005 SI (or 0.6 ppt in the InPhase response) but because of the three-dimensional geometry the susceptibility is again only an order of magnitude estimate (e.g. Tabbagh, 1986). In some situations (e.g. in the northwest part of location A), there is an apparent susceptibility anomaly coincident with paired positive and negative anomalies in the TMF, indicating a source with both induced and remanent magnetization. The VD apparent susceptibility map contains several additional anomalies not noted in the TMF response (e.g. in the eastern part of location C).

The HD apparent susceptibility response is characterized by an abundance of small-scale point and linear anomalies. A small proportion of these anomalies correlate with anomalies in the VD apparent susceptibility and TMF responses, but there are many additional anomalies present. At first appearance the response may be interpreted as being noisy, but it is of note that the presence of the linear anomalies is supported by larger correlation scales determined in the variogram analysis and by the fact that many of these anomalies cross multiple survey lines.

3.7 Interpretation

The combined geophysical results (Figure 3.5) indicate the presence of a larger-scale resistive and magnetic feature trending in a southwest-northeast direction across the survey area. This feature is the main response in the apparent conductivity results. The negative VD apparent

susceptibility response of this feature allows the source to be constrained to depths of more than 1m. It is therefore interpreted to be a natural geological feature at the site rather than being of anthropogenic origin. Two possible interpretations are that it represents a southwest–northeast trending body of elevated bedrock extending upwards into surrounding surficial sediments, or that it presents a zone of moremagnetic bedrock, such as a mafic dyke, located between less magnetic and more porous or weathered, conductive bedrock.

The magnetic susceptibility contrast of the body and the surrounding material is in the order of 0.005 SI, suggesting that the body is composed of a moderately magnetic igneous rock (e.g. Hansen et al., 2005) rather than the less magnetic limestone. The magnetic results resolve a number of 1–2-mscale anomalies across the study area, with a particular concentration at location A and less well defined concentrations at locations B and C. The small wavelength and positive apparent VD apparent susceptibility response of these features indicate that their sources are located at shallow depth (<1 m). The absence of any clear corresponding response in the apparent conductivity indicates that they are probably relatively small and resistive bodies. These combined geophysical results
allow the small-scale anomalies to be confidently interpreted as being caused by igneous cobbles and boulders in the shallow (<1m depth) subsurface.

In order to provide an enhanced visualization of the distribution of smaller-scale geophysical anomalies in Area 5 of LdFa-1, Figure 3.6 shows the magnetic and EM31 VD apparent susceptibility responses in alternative image formats. The shaded-relief images in particular show that the anomalies in area A form an approximately circular pattern with a diameter of approximately 4m. This pattern is similar to that of other interpreted anthropogenic surface groupings of rocks found across LdFa-1 (e.g. features 2, 19 and 33 in Figure 3.1). These

surface features have been interpreted as tent rings, while associated excavations have produced collections of lithic and bone artefacts within their limits (Milne, 2007; Park, 2008). Therefore, comparison of the assemblage of the anomalies at Location A in Area 5 and the rough circular pattern that they form with the archaeological results elsewhere in area LdFa-1, provides an indication that the distribution of rocks in this location may have an anthropogenic origin. In this situation, the concentrations of magnetic anomalies at locations B and C also prompts increased interest, however, the distribution of anomalies in these other two areas appears to have a less structured form than at location A (see Figures 3.5 and 3.6).

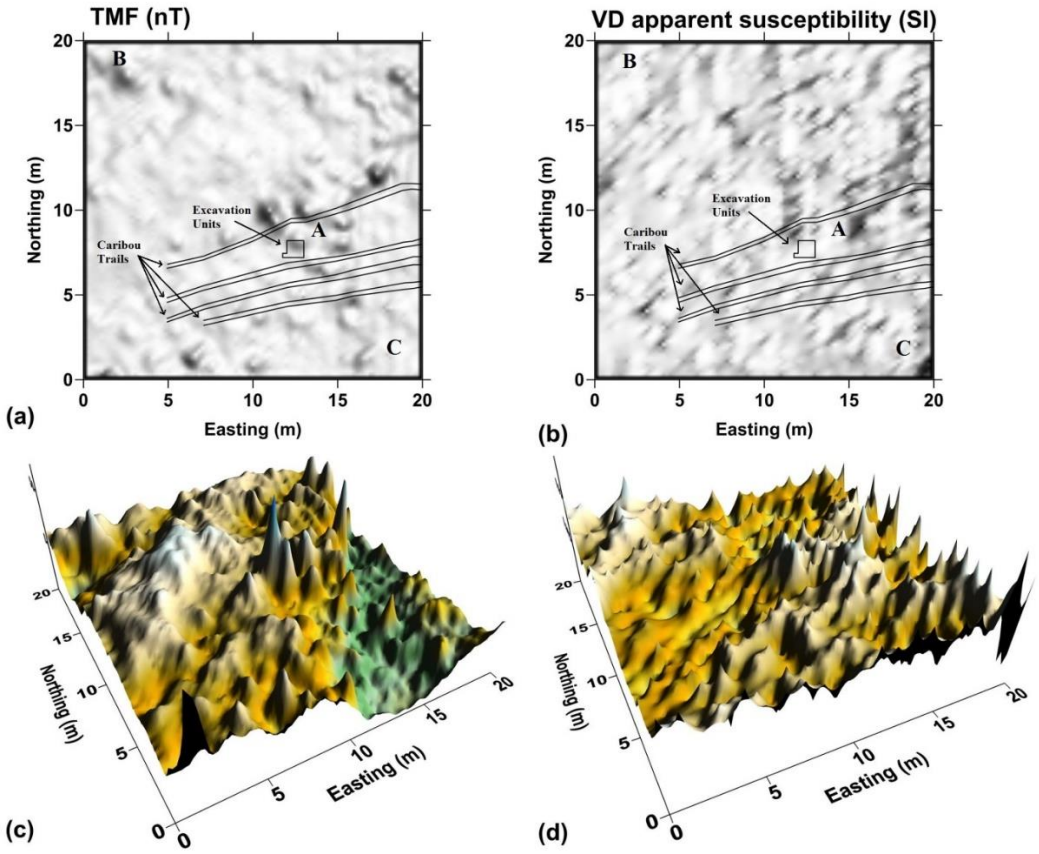

Figure 3.6 (a and b) Shaded relief maps of the TMF and VD apparent susceptibility in LdFa-1 Area 5 with base-map overlay indicating the location of the previous test units, caribou trails and response areas of interest A, B and C. (c and d) Surface map of the TMF and VD apparent susceptibility response.

3.8 Discussion

3.8.1 Archaeological Studies at LdFa-1

Taken in isolation, the geophysical results obtained in the present study suggest the presence of significant archaeological activity in LdFa-1 Area 5. The geophysical responses provide a very strong indication of the presence of a 4m diameter, roughly circular, arrangement of igneous boulders or cobbles in the shallow subsurface. Elsewhere at LdFa-1 similar patterns of exposed rocks have been interpreted as tent rings (Stenton, 1991; Milne, 2005, 2008; Park, 2008).

It is of significance that the main geophysically identified feature in Area 5 coincides spatially with the 2008 excavation unit. The spatial coincidence of the geophysical anomalies with these archaeologically productive excavation units provides increased support for the interpretation that the geophysically defined feature was produced by Palaeo-Eskimo activity, however, further ground-truthing at the site will be required for a more comprehensive interpretation. For example, it remains unclear as to whether burning of materials at the site could have produced the remanent magnetization indicated by the paired positive and negative magnetic anomalies.

The distribution of the geophysical anomalies in Area 5 and the identification of two additional clusters of anomalies provide important information on the impacted subsurface and will facilitate planning for future excavations in Area 5. Anomalies B and C occur in sections of the site where there has been no previous evidence for Palaeo-Eskimo activity.

3.8.2 Implications for Archaeological Studies in a Complex Arctic Environment

The current study provides an assessment of the role of archeogeophysics at a hunter–gatherer site in a complex Arctic environment. The magnetometer and gradiometer results illustrate the value of these approaches. Both responses were able to identify several clusters of relatively strong localized anomalies of archeological interest. The vertical gradient response provided the clearest mapping of these features, but the TMF data, when corrected with temporal recordings, also provided a clear indication of their presence. Comparison of Figures 3.5 and 3.6 shows that the display of the TMF data using methods such as shaded relief or surface plots that highlight shorter wavelength features is particularly useful. The TMF data provide additional information on the larger wavelength magnetic variations that are related to a lithogenic source. This information may be useful in a fully integrated interpretation of a site survey.

Results of the current study also show the need for TMF surveys in this region to be carried out using a local base-station. Distant magnetic observatories will provide recordings that allow approximate removal of the temporal variations but the process will not be as accurate in comparison with instances when good quality local base-station records are available.

At the LdFa-1 archeological site, the apparent conductivity data available from the EM31 recordings provided limited information on anthropogenic features. However, they did help identify the long wavelength magnetic variation in the survey area as a lithogenic feature. As noted previously, the EM31 was included in equipment taken to the LdFa-1 site for the first day of fieldwork in order to obtain an overview of the electrical resistivity at the site, and the apparent conductivity response provides two useful results in this context. First, the very low resistivity identified by the EM31 data provides an important indication of the utility of future ground-penetrating radar (GPR) surveys at the LdFa-1 site. There should be no problem

achieving the required signal penetration. Second, the similarity of the VD and HD apparent conductivity results suggests the presence of lateral conductivity variations that penetrate over to at least 1m depth. Such variations may complicate the ability to resolve the surface of the permafrost layer in climate-change related studies at the site and suggest the need for methods such as GPR or multi-electrode DC resistivity imaging that can simultaneously define both the lateral and depth variation of subsurface features.

A number of previous studies have compared magnetic and electromagnetic InPhase measurements in an archeological context (e.g. Tabbagh, 1986; Simpson et al., 2009), but there have been fewer studies in complex geological environments (e.g. Viberg et al., 2009, 2013) or at hunter–gatherer sites (Martin et al., 1991; Prentiss et al., 2008). The results of the present study demonstrate the value of electromagnetic measurement of apparent susceptibility in such a complex Arctic environment. The VD dipole apparent susceptibility response clearly resolves the anomalies observed in the TMF and vertical magnetic gradient data (e.g. Figure 3.6). As noted in previous studies, it is necessary to include a careful correction for drift in the data reduction for the InPhase response (e.g. Dalan, 2006; Simpson et al., 2009).

In contrast to the VD apparent resistivity results for Area 5, the HD results appear quite poor and include many features not seen in the other magnetic anomaly maps. Previous studies have suggested that there is greater noise interference with the instrument in this configuration (e.g. Dalan, 2006), however, the LdFa-1 site is extremely remote, so there will be minimal electromagnetic noise at this site. Also, as noted above, some of the additional anomalies in the HD apparent susceptibility response appear to be coherent across multiple survey lines (Figure 3.5). Additional field testing is required to identify the origin of these additional anomalies.

3.9 Conclusions

The combined results of the two geophysical survey datasets indicate the possible presence of large circular Palaeo-Eskimo features in Area 5 of LdFa-1, previously unknown to the researchers. The magnetic and magnetic susceptibility survey results agree positively with prior test units excavated in 2008 and define new areas of interest for further testing and ground truthing. The use of magnetic and electromagnetic methods has contributed to our overall understanding of the lithogenic responses and subsurface properties at LdFa-1. For example, we now have an improved understanding of the range of magnetic features that can be identified in this complex geological environment. Although the apparent conductivity results did not resolve the small-scale anomalies observed in the magnetic responses, they provide valuable information on the larger-scale lithogenic responses. They also revealed that the soils at the site are highly resistive, and so are ideal for future studies at LdFa-1 that aim to use GPR and multiprobe resistivity meters to acquire additional complementary, high-resolution data. Overall, this case study has provided valuable information for the geophysical study of small-scale hunter–gatherer remains at the LdFa-1 site, and provided new evidence for the value of archaeogeophysical applications in extremely remote, complex geological environments, such as the Arctic.

3.10 Works Cited – Chapter 3

Beamish, D. 2011. Low induction number, ground conductivity meters: A correction procedure in the absence of magnetic effects. *Journal of Applied Geophysics*, 75(2), 244–253.

Dalan, R. A. 2006. Magnetic susceptibility. In J. K. Johnson (Ed.), *Remote Sensing in Archaeology: An Explicitly North American Perspective*, (pp. 161-203). Tuscaloosa: The University of Alabama Press.

Eastaugh, E., and Taylor, J. 2005. Geophysical survey of the Dorset Palaeoeskimo site of Point Riche. *Newfoundland and Labrador Studies*, 20(1), 157–173.

Eastaugh, E., and Taylor, J. 2011. Settlement size and structural complexity: A case study in geophysical survey at Phillip's Garden, Port au Choix. In M. A. P Renouf (Ed.), *The Cultural Landscapes of Port au Choix, Interdisciplinary Contributions to Archaeology* (pp. 178-188). Springer Science + Business Media, LLC. DOI 10.1007/978-1-4419-8324-4_9.

Eastaugh, E., Ellis, C., Hodgetts, L., and Keron, J. 2013. Problem based magnetometer survey at the Late Archaic Davidson Site (AhHk-54) in Southwestern Ontario. *Canadian Journal of Archaeology/Journal Canadien D'Archaéologie*, 37, 274–301.

Evans, M. E., Heller, F. 2003. *Environmental Magnetism: Principals and Applications of Enviromagnetics*. Academic Press, Elsevier Science.

Fialová, H., Maier, G., Petrovskyá, E., Kapička, A., Boyko, T., and Scholger, R. 2006. Magnetic properties of soils from sites with different geological and environmental settings. *Journal of Applied Geophysics*, 59, 273–283.

Fitterman, D. V., and Labson, V. F. 2005. Electromagnetic induction methods for environmental problems. In D. K. Butler (Ed.), *Near-Surface Geophysics*, (pp.301-356). Tulsa, OK.: Society of Exploration Geophysicists.

Gaffney, C. F., and Gater, J. 2006. *Revealing the buried past: geophysics for archaeologists*. Tempus.

Gibson, T. H. 1986. Magnetic prospection on prehistoric sites in Western Canada. *Geophysics*, 51(3), 553-560.

Hansen, R. O., Racic, L., and Grauch, V. J. S., 2005. Magnetic methods in near-surface geophysics. In D. K. Butler (Ed.), *Near-Surface Geophysics* (pp. 151-175). Tulsa, OK.: Society of Exploration Geophysicists.

Huang, H., Won, I., and San Filipo, B. 2003. Detecting buried nonmetal objects using soil magnetic susceptibility measurements. In R. S. Harmon, J. H. Holloway Jr., and J. T. Broach (Eds.), *Detection and Remediation Technologies for Mines and Mine-like Targets* (pp.1181-1188). Proceedings of International Society for Optics and Photonics VIII, 5089.

Hodgetts, L., Dawson, P., and Eastaugh, E. 2011. Archaeological magnetometry in an Arctic setting: a case study from Maguse Lake, Nunavut. *Journal of Archaeological Sciences*, 38, 1754–1762. DOI:10.1016/j.jas.2011.03.007.

Johnson, J. K. 2006. *Remote sensing in archaeology: An explicitly north American perspective.* The University of Alabama Press: Tuscaloosa; 1–16.

Kvamme, K. 2003. Geophysical surveys as landscape archaeology. *American Antiquity*, 68(3), 435–457.

Le Borgne, E. 1955. Susceptibilité magnétique anomale du sol superficiel. *Annals Géophysics*, 11, 399–419.

Le Borgne, E. 1965. Les propriétés magnétique du sol: application à la prospection des sites archéologiques. *Archaeo-Physika*, 1(15), 1–20.

Leopold, M., Plöckl, T., Forstenaicher, G., and Völkel, J. 2010. Integrating pedological and geophysical methods to enhance the informative value of an archaeological prospection – the example of a Roman Villa Rustica near Regensburg, Germany. *Journal of Archaeological Science*, 37(7), 1731–1741.

Lilley, F. E. M., Sloane, M. N., and Ferguson, I. J. 1984. An application of total-field fluctuation data to geomagnetic induction studies. *Journal of Geomagnetism and Geoelectricity*, 36, 161–172.

Linford, N. 2006. The application of geophysical methods to archaeological prospection. *Reports on Progress in Physics*, 69, 2205–2257. DOI:10.1088/0034-4885/69/7/R04.

Martin, W. A., Bruseth, J. E., and Huggins, R. J. 1991. Assessing feature function and spatial patterning of artifacts with geophysical remote-sensing data. *American Antiquity*, 56(4), 701–720.

Martín, A., Padín, J., Anquela, A. B., Sánchez, J., and Belda, S. 2009. Compact integration of a GSM-19 magnetic sensor with high-precision positioning using VRS GNSS technology. *Sensors*, 9, 2944–2950. DOI:10.3390/s90402944.

McNeill, J. D. 1979. Operating manual for EM-31 noncontacting terrain conductivity meter. Mississauga, ON, Canada: Geonics Limited; 42.

McNeill, J. D. 1980. Electromagnetic terrain conductivity measurement at low induction numbers. Technical Note TN-6, Geonics Limited, Mississauga, ON, Canada. http://www.geonics.com/pdfs/technicalnotes/ tn6.pdf

McNeill, J. D. 1990. Use of electromagnetic methods for groundwater studies. In S. H. Ward (Ed.), *Geotechnical and Environmental Geophysics, Vol. I Review and Tutorial* (pp.191-218). Tulsa, OK.: Society of Exploration Geophysicists.

McNeill, J. D. 2012. Archaeological mapping using the geonics EM38B to map terrain magnetic susceptibility (With Selected Case Histories). Technical Note TN-35. Canada: Geonics Limited, Mississauga, ON.

McNeill, J. D., and Bosnar, M. 1999. Application of ‘dipole–dipole’ electromagnetic systems for geological depth sounding. Technical Note TN-31, Geonics Limited: Mississauga, ON, Canada. http://www.geonics.com/pdfs/technicalnotes/tn31.pdf (as modified October 2007).

Milne, S. B. 1999. Pre-Dorset lithic technology: a study of lithic assemblage variability in an inland Pre-Dorset site. MA Thesis, Department of Anthropology, University of Trent, Peterborough, ON.

Milne, S. B. 2003. Peopling the Pre-Dorset past: a multiscalar study of early arctic lithic technology and seasonal land use patterns on southern Baffin Island. PhD Dissertation, Department of Anthropology, McMaster University, Hamilton, Ontario.

Milne, S. B. 2005. Archaeological Investigations in the Mingo and Amadjuak Lake Districts of Southern Baffin Island. Permit Report covering the work conducted under Nunavut Archaeologist Permit 04-06A. Unpublished permit report, Nunavut Ministry of Culture, Language, Elders and Youth, Igloolik.

Milne, S. B. 2007. Archaeological Investigations in the Mingo Lake District of Southern Baffin Island: Assessing Palaeo-Eskimo Culture Continuity and Change. Permit report covering the work conducted under Nunavut Archaeologist Permit 07-014. Manuscript on file, Department of Culture, Language, Elders and Youth, Government of Nunavut, Igloolik, Nunavut.

Milne, S. B. 2013. Chert Sourcing and Palaeo-Eskimo Stone Tool Technology. Report on work conducted under Nunavut Archaeological Permit No. 2013-02A. Manuscript on file with the Department of Culture, Language, Elders and Youth, Government of Nunavut, Igloolik, Nunavut.

Milne, S. B., and Donnelly, S. M. 2004. Going to the birds: examining the importance of avian resources to Pre-Dorset subsistence strategies on southern Baffin Island. *Arctic Anthropology*, 41(1), 90–112.

Milne, S. B., Park, R. W., and Stenton, D. 2012. Dorset culture land use strategies and the case of inland southern Baffin Island. *Canadian Journal of Archaeology/Journal Canadien D'Archéologie*, 36, 267–288.

Milne, S. B, Park, R., and Stenton, D. 2013. For caribou, chert, and company: understanding mobility among the Palaeo-Eskimos of Baffin Island, Arctic Canada. In P. R. Preston, and K. Schorle (Eds.), *Mobility, Transition, and Change in Prehistory and Antiquity* (pp. 49-61). Proceedings of the Graduate Archaeology Organisation Conference on the Fourth and Fifth of April 2008 at Hertford College, Oxford, UK,. British Archaeological Reports, International Series. Oxford: Archaeopress.

Nabighian, M. N., Grauch, J. S., Hansen, R. O., LaFehr, T. R., Li1, Y., Peirce, J. W., Phillips, J. D., and Ruder, M. E. 2005. 75th anniversary: The historical development of the magnetic method in exploration. *Geophysics*, 70(6), 33–61.

Park, R. W. 2008. Archaeological Excavations at the LdFa-1 site, Mingo Lake, Baffin Island, Summer 2008. Report on work conducted under Nunavut Territory Archaeologist Permit No. 08-029A. University of Waterloo, ON, Canada.

Peregrine, A. G-L., Rogers, M. B., and Jordan, K. A. 2012. Understanding the built environment at the Seneca Iroquois White Springs site using large-scale, multi-instrument archaeogeophysical surveys. *Journal of Archaeological Science*, 39(7), 2042–48. DOI:10.1016/j.jas.2012.03.011.

Prentiss, A. M., Cross, G., Foor, T. A., Hogan, M., Markle, D., and Clarke, D. S. 2008. Evolution of a Late Prehistoric winter village on the Interior Plateau of British Columbia: geophysical investigations, radiocarbon dating, and spatial analysis of the Bridge River Site. *American Antiquity*, 73(1), 59–81.

Rosendahl, D., Lowe, K. M., Wallis, L. A., and Ulm, S. 2014. Integrating geoarchaeology and magnetic susceptibility at three shell mounds: A pilot study from Mornington Island, Gulf of Carpentaria, Australia. *Journal of Archaeological Science*, 49, 21–32. DOI:10.1016/j.jas.2014.04.017.

Sanborn-Barrie, M., St-Onge, M. R., Young, M. D., and James, D. T. 2008. Bedrock geology of southwestern Baffin Island, Nunavut: expanding the tectonostratigraphic framework with relevance to mineral resources. *Geological Survey of Canada, Current Research*, 6, 1–16.

Simpson, D., Lehouck, A., Verdonck, L., Vermeersch, H., Van Meirvenne, M., Bourgeois, J., Thoen, E. and Docter, R., 2009. Comparison between electromagnetic induction and fluxgate gradiometer measurements on the buried remains of a 17th century castle. *Journal of Applied Geophysics*, *68*(2), 294-300.

Smekalova, T. N., Voss, O., and Smekalov, S. L. 2008. *Magnetic surveying in archaeology: More than 10 years of using the Overhauser GSM-19 gradiometer, 2nd revised edition*. B. W. Bevan (Ed.). Højbjerg, Denmark: Wormianum.

Soper, J. D. 1923. Faunal Investigation of Southern Baffin Island. Ottawa: Bulletin 53, Canada Department of Mines, National Museum of Canada.

Stenton, D. R. 1989. Terrestrial adaptations of Neo-Eskimo coastal-marine hunters on southern Baffin Island, NWT. PhD Dissertation, Department of Anthropology, University of Alberta, Edmonton, Alberta.

Stenton, D. R. 1991. The Archaeology of Terrestrial Hunting Systems: The Amadjuak Lake Project. Permit report on file with the Department of Culture, Elders, Language, and Youth. Government of Nunavut. Igloolik: Nunavut.

St Onge, M. R., Sanborn-Barrie, M., and Young, M. D. 2007. Geology. Mingo Lake, Baffin Island, Nunavut. Geological Survey of Canada, Open File 5499, scale 1:200 000.

Tabbagh, A. 1986. Applications and advantages of the Slingram electromagnetic method for archaeological prospecting. *Geophysics*, 51(3), 576–584.

Urban, T. M. 2012. In the footsteps of J. Louis Giddings (1909–1964): archaeological geophysics in Arctic Alaska. *Antiquity*, 86, 332.

Utting, D. J., Gosse, J. C., Hodgson, D. A., Trommelen, M. S., Vickers, K. J., Kelley, S. E. and Ward, B., 2007. Report on ice-flow history, deglacial chronology, and surficial geology, Foxe Peninsula, southwest Baffin Island, Nunavut. *Current Research-Geological Survey of Canada*.

Vallée, M. A., Craven, J. A., Newitt, L., Keating, P., Dumont, R., and Ferguson, I. J. 2006. Guidelines for location and use of base station data in aeromagnetic survey processing. Society of Exploration Geophysicists Annual Meeting, New Orleans, October 2006.

Viberg, A., Trinks, I., and Lidén, K. 2009. Archaeological prospection in the Swedish mountain tundra region. *ArchéoSciences*, 33. Rennes: Presses Université de Rennes.

Viberg, A., Trinks, I., and Lidén, K. 2011. A review of the use of geophysical archaeological prospection in Sweden. *Archaeological Prospection*, 18, 43–56.

Viberg, A., Berntsson, A., Lidén, K. 2013. Archaeological prospection of a high altitude Neolithic site in the Arctic mountain tundra region of Northern Sweden. *Journal of Archaeological Science*, 40(6), 2579–2588.

Welham, K., Fleisher, J., Cheetham, P., Manley, H., and Steele, C. 2014. Geophysical survey in Sub-Saharan Africa: magnetic and electromagnetic investigation of the UNESCO world heritage site of Songo Mnara, Tanzania. *Archaeological Prospection*, 21(4), 255–262. DOI:10.1002/arp.1487.

Wolff, C. B., and Urban, T. M. 2013. Geophysical analysis at the Old Whaling site, Cape Krusenstern, Alaska, reveals the possible impact of permafrost loss on archaeological interpretation. *Polar Research*, 32, 19888.

Chapter 4

Manual Point Cloud Classification and Extraction for Hunter-Gatherer Feature Investigation: A Test Case from Two Low-Arctic Paleo-Inuit Sites

A peer-reviewed scientific research paper published in:
Open Archaeology, Topical Issue on Advances in Arctic Archaeology, 2(1):232-242,
DOI 10.1515/opar-2016-0017

David B. Landry, S. Brooke Milne, Robert W. Park, Ian J. Ferguson, Mostafa Fayek

Abstract: For archaeologists, the task of processing large terrestrial laser scanning (TLS)-derived point cloud data can be difficult, particularly when focusing on acquiring analytical and interpretive outcomes from the data. Using our TLS lidar data collected in 2013 from two compositionally different, low Arctic multi-component hunter-gatherer sites (LdFa-1 and LeDx-42), we demonstrate how a manual point cloud classification approach with open source software can be used to extract natural and archaeological features from a site's surface. Through a combination of spectral datasets typical to TLS (i.e., intensity and RGB values), archaeologists can enhance the visual and analytical representation of archaeological hunter gatherer site surfaces. Our approach classifies low visibility Arctic site point clouds into independent segments, each representing a different surface material found on the site. With the segmented dataset, we extract only the surface boulders to create an alternate characterization of the site's prominent features and their surroundings. Using surface point clouds from Paleo-Inuit sites allows us to demonstrate the value of this approach within hunter-gatherer research as our results illustrate an effective use of large TLS datasets for extracting and improving our analytical capabilities for low relief site features.

4.1 Introduction

The application of three-dimensional (3D) terrestrial laser scanning (TLS) in archaeological research has benefited from the fast-paced technological developments increasing both the resolution and scale of data, along with changing modern field survey methodologies (i.e., static, mobile, and/or drone scanners). As the application of TLS and collection of point cloud datasets continues to increase (e.g., Lerma et al. 2010; Huimin et al. 2012; Dawson et al. 2013; Romero and Bray 2014; Larsen et al. in press), critical attention is shifting towards the development of complementary analytical and interpretive processes (Huggett 2015: 80; Watterson 2015: 120). Even though techniques used for presenting point cloud datasets produce visually impressive results, they are entirely outpacing those used for data processing and analysis in archaeological research. While a small number of recent studies have successfully demonstrated the value of point cloud data processing and analysis on high relief archaeological sites and features (e.g., Schreiber et al. 2012: 16-17; Romero and Bray 2014: 30-34; Larsen et al. in press: 6-7), along with smaller-targeted prehistoric rock-art sites (Rüther et al. 2009: 1853-1854; Güth 2012: 3110-3113), the investigation of the low relief features common to prehistoric hunter-gatherer sites using TLS-derived datasets has remained limited, with the exception of Hakonen et al.'s (2015: 232-233) recent study of Finish stone cairn sites. As such, we present a simple open-source manual point cloud classification approach for convenient surface feature extraction from two low Arctic multi-component site datasets: LdFa-1 and LeDx-42 (Figure 4.1). These point clouds were acquired in 2013 using a Leica C10 ScanStation terrestrial light and detection ranging (lidar) laser scanner.

Complex automated TLS point cloud classification systems have been developed by engineers, geoscientists, and environmental scientists to analyse specific elements in large point

clouds of both urban and rural landscapes (e.g., Brodu and Lague 2012; Niemeyer et al. 2012; Buckley et al. 2013 etc.). The CANUPO classification system developed by Brodu and Lague (2012: 13-15), for example, uses a complex algorithm to define classes based on the geometry of objects in a point cloud at multiple scales. It is a useful and accessible tool for defining different materials in heterogeneous environments; however, we have found that for identifying low relief hunter-gatherer archaeological features in an Arctic environment, where only slight changes in the material makeup and colour are of primary importance, an alternative manual point cloud classification approach is beneficial for both quick in-field and more involved laboratory investigations. Depending on the type of laser scanner in use, the collected TLS data that can be used for this include X, Y, Z Cartesian coordinates, 8 or 16 bit RGB colour pixel data, and pseudo-infrared intensity values (Abbas et al. 2014: 116). This digital approach provides archaeologists with control over an analytical tool aimed at investigating the layout, orientation, and distribution of surface elements and their surrounding objects in a low Arctic environment.

Low Arctic sites in North America (i.e., those lying south of the Parry Channel) present some unique challenges in terms of surface survey because wetlands, hummocky terrain, and thick vegetation obstruct archaeological surface remains, while annual freeze-thaw cycles can act to displace or destroy them entirely (Milne 2003: 67-68). Additionally, in sites occupied for millennia, the low relief surface structures were sometimes cannibalized for building materials by subsequent groups camping in the same locations, leaving the original surface features in disarray (Bielawski 1988; Milne 2003). Our manual point cloud classification approach uses a ground point classifier from LAStools to first separate ground points from non-ground points. Commonly functioning as a bare-earth process in airborne lidar processing, we use this tool to separate our TLS dataset into two data groups: low-lying features (e.g., grass, snow) and taller

surface features (e.g., boulders, tall grasses, etc.). Then, using a combination of two spectral data value ranges – intensity and red/green/blue (RGB) pixel data – we isolate the location of each material on the surface within the point clouds. The results are then used to map individual surface materials, fingerprint each by their spectral value ranges, extract them from their original point clouds, and finally demonstrate how this approach improves the analytical capacity – in and out of the field – of large 3D digital datasets representing low relief surface structures in Arctic hunter-gatherer contexts.

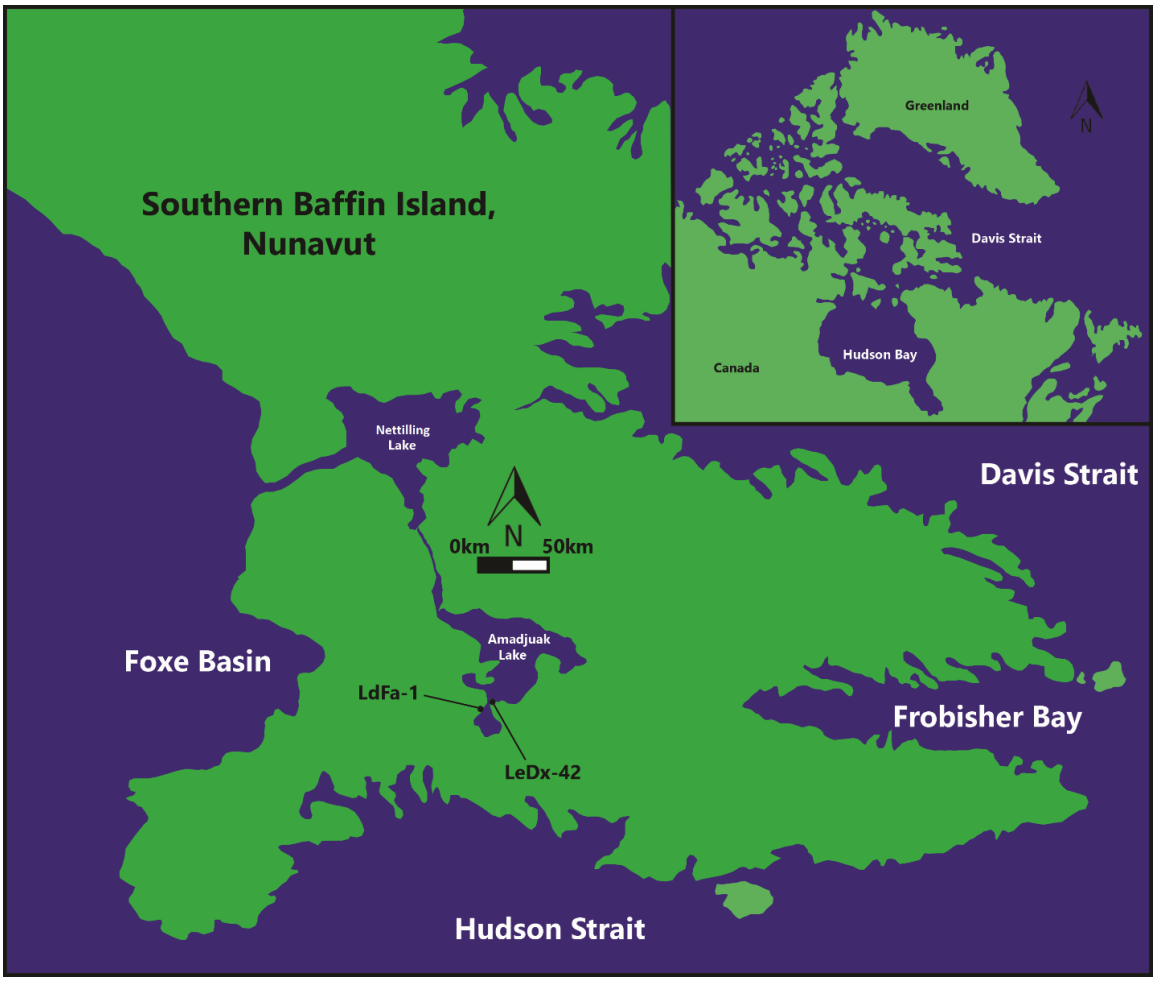

Figure 4.1 Archaeological sites LdFa-1 and LeDx-42 situated on a Google Earth landsat image with southern Baffin Island inset. Sites are located near lakes Mingo and Amadjuak, southern Baffin Island, NU.

4.2 Study Sites and Methods

4.2.1 LdFa-1 and LeDx-42

LdFa-1 is a large, multi-component site with evidence of Pre-Dorset (2250-800 BC), Dorset (800 BC-1200 AD) and Thule/Inuit (1200-1500 AD) cultural occupations, located in the interior of southern Baffin Island. The site is situated at the base of the Mingo Lake esker (Milne 2005; Milne 2008; Milne 2013; Park 2008) and was first recorded in 1991 by Stenton with subsequent investigations by Milne (2005, 2008, 2013) and Park (2008). Stone tent rings – boulder rock formations used to hold down the edges of ancient skin tents – represent an important surface feature for locating and investigating Arctic archaeological sites. There are at least 33 visible tent ring features at LdFa-1 (Park 2008). Other visible surface remains include stone caches used for meat storage, and widespread scatters of lithic artifacts and faunal remains. Archaeogeopysical surveying has been conducted in a section of the site to locate potential sub-surface remains and with the eventual aim to investigate the combined surface and sub-surface spatial datasets (Landry et al. 2015). TLS data were acquired at LdFa-1 in 2013, during our first field tests of the instrument in the Arctic. The point cloud registration at LdFa-1 derives from three station scanning positions around the site. For the purpose of this paper, only a small section of the point cloud measuring approximately 30 m x 10 m was selected given the level of detail and accuracy of the point cloud registration.

LeDx-42 is a smaller archaeological site both in terms of its areal extent and its total number of surface features. It too is multi-component, having been occupied by the Pre-Dorset and Dorset (Milne et al. 2012, Milne 2013) – who together are referred to archaeologically as Paleo-Inuit (see Friesen 2015). LeDx-42 is located on a bedrock outcrop that looks out over the Mingo River. The landscape surrounding the site is characterized as flat, hummocky tundra.

Unlike LdFa-1, LeDx-42 has no visible tent ring features yet the site was identified originally because of the extensive scatters of lithic tools and debitage, and fragmented faunal remains (Milne 2005). Widespread test excavations at the site yielded dozens of diagnostic Pre- Dorset and Dorset stone tools, and delicate organic remains including bone needles (Milne 2005; Milne et al. 2013). This site was also scanned during the 2013 field season. Two lidar stations were used to register the central portion of this site. Our novice use of the equipment is demonstrated in the data by the lack of overlap on the station platforms, resulting in circular shaped gaps in the data. The point cloud included in this study derives from an area measuring 45 m x 25 m.

The Arctic tundra characterising these sites is made up of a combination of thick low-lying and medium height vegetation including grasses, small Arctic flowers, and areas of high vegetation and shrubbery. The natural surface can exhibit large patches of gravel, snow, melt ponds, exposed stone outcrops, and small and large stone boulders. LdFa-1 and LeDx-42 represent two archaeological sites with compositionally different surfaces, illustrating a small portion of the heterogeneity exhibited among Arctic archaeological landscapes across this region. Their differences are highlighted by their density of surface boulders, vegetation growth, nearby water, snow cover, and even lichen growth that can obscure materials found on the surface making the identification of colour ranges as part of our approach more difficult.

4.2.2 Parameter Values

Intensity and RGB pixel data are used to create the classification parameters in this process. Unaccompanied, neither value provides enough detailed information about each surface material to accurately identify it within the point cloud. Intensity has been defined by Song et al. (2002: 259) as the ratio of strength of reflected light from a material to that of the emitted light of

the laser. In theory, reflective materials should have a known value to represent this ratio; however, several natural factors influence the reflectance value of every material, including the surface roughness, the angle of incidence, the transit length, and the aggregate laser optics and receiver characteristics, among others (Reyes et al. 2009: 16). These factors are problematic in almost all natural environments as the materials in question are not uniform and, therefore, cause a greater range of intensity value fluctuations across a completed point cloud. The process to correct and normalize intensity data continues to be a highly active area of technical research (see Humair et al. 2015) that we do not intend to discuss in this paper. For the purposes of our simplified procedure and tests, we decided to account for fluctuations by using a wide intensity range for each material and combining it with a complementary RGB range to refine the classification outcome.

The second parameter value used in this test is 8-bit RGB pixel data. These values represent the colour combination in red, green, and blue, of each individual pixel that make up the digital image within the point cloud. By using RGB values we identify a range of colour classes most likely to fall within the material in question (e.g., Snow: R=205-255, G=250-255 B=225-255). Using RGB values alone has its limitations as changes in the daily sky conditions can cause shadowing and shifts in the spectral colours captured by the scanner's digital camera. However, using visible colours to match materials is beneficial for refining a heterogeneous surface, including some of those found in these low Arctic environments. A combination of the intensity and RGB datasets is a simple and effective way to create a range of values for each surface material at these sites to define a classification outcome.

4.2.3 Processing Sequence

This processing sequence is modeled after several urban and rural area classification systems (Brodu and Lague 2012; Bandyopadhyay et al. 2013; Penasa et al. 2014). Our lidar site scans were originally stored as .PTS format files exported from Cyclone software. They were combined using a static target-based system (Abbas et al. 2014: 117), registering millions of points and 360-degree digital images to create a full 3D representation of the two separate sites. The following procedures were conducted using open-source software available for educational purposes, with a focus on non-technical, user-friendly methods.

In LAStools – a well-designed, active, and frequently updated software created by Martin Isenburg (2015) with a simple operating graphical user interface (GUI) – we were able to convert, manipulate, and filter the large point cloud datasets. The software has a two part license (part one OPEN source, part two CLOSED source), but remains 'freely' available to use for educational purposes, which is integral for our applications in this study. Almost all processing was conducted using its automated GUI tools. Manual script amendments are also made using this software to filter changes in the parameter values at each archaeological site. This software is designed to conveniently convert the large point cloud data file formats into the more openly accessible and compact .LAS/.LAZ formats. The conversion process is conducted in the software's *txt2las.exe* GUI and included the translation of the intensity data to 16 bit and a rescaling of the X, Y, Z coordinates to 0.001 m. The manually edited script for this step is shown here:

txt2las –v –i "input.txt" –skip 1 –parse xyziRGB –translate_intensity 2048 –rescale 0.001 0.001 0.001–odir "output" -olas

Following this step, the quantity of points in the dataset is reduced to 1.5 million using a random point remover while duplicate points caused by combining multiple scans were removed from the point cloud files to increase the efficiency during the processing stages within this software.

Next, the software suite is used to create a preliminary ground classification for objects that lay above the natural ground surface (>0.02 m at LdFa-1 and >0.05 m at LeDx-42) based on an automated point sampling algorithm in the software suite. Using the existing script in *lasground_new.exe*, we classify the "ground surface" and additionally classify all objects above them as "not ground." Following the point separation between "ground" and "not ground," we identify the parameter values for each separate material we wanted to classify. This is done using CloudCompare software (2015).

CloudCompare is another open-source program easily accessible to archaeologists learning to work with and process point cloud data. This software is used to manually sample data from the surface materials (e.g. stones, grass, water, outcrops etc.) we want to classify. Approximately 30 points are picked at random from each material. A range MAX/MIN of intensity and RGB is established and used to create the filtering parameters for each (Table 4.1). These parameters are then extracted out of the point cloud using the *las2las. Exe* GUI in the LAStools software suite, and saved as individual files. The final script and amendments are shown below:

las2las -v -i "input.las" –drop_intensity_below ### –drop_intensity_above ### -keep_RGB_red ### ### -keep_RGB_green ### ### -keep_RGB_blue ### ### -olas

All subsequent processing is completed in CloudCompare, including a spatial outlier reduction process we use to clean and remove outlying points from the newly segmented files,

and reduce noise and isolated points. This step is important for removing single data points from the cloud that fall within the same parameter range as for instance, stone boulders, yet do not specifically represent a common material type. The complete step-by-step process is outlined in Figure 4.2.

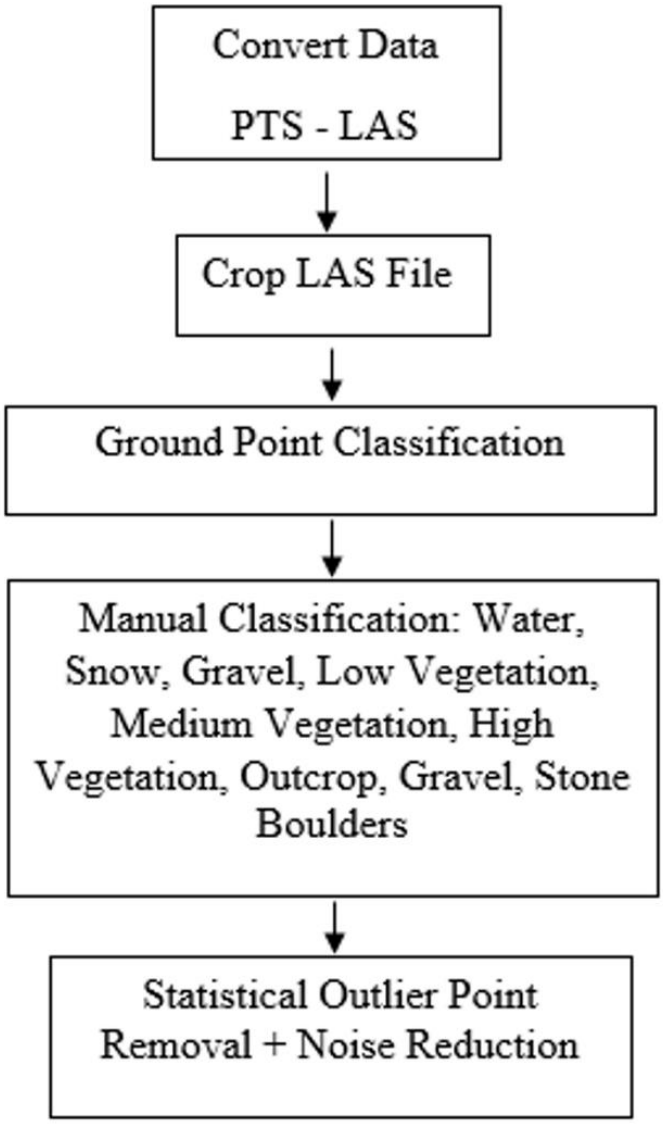

Figure 4.2 Step-by-step classification sequence from original point cloud dataset to the individually classified elements, using open source LAStools and CloudCompare software.

Table 4.1 Parameters and ranges used to fingerprint and define each surface material from LdFa-1 and LeDx-42. A combination of the four parameters can identify and isolate each material from the original point clouds.

	Water*	**Snow**	**Gravel**	**Stone Boulders – Above Ground Points**	**Exposed Outcrop***	**Low Vegetation**	**Medium Vegetation – Above Ground Points**	**High Vegetation – Above Ground Points**
LdFa-1								
Intensity	500-700	878-978	1029-1462	716-943		714-920	737-920	503-699
Red	69-95	250-255	177-255	155-255		69-95	75-130	80-188
Green	71-120	250-255	170-255	155-255		55-130	55-130	55-130
Blue	65-120	225-255	166-215	120-255		31-100	31-100	31-100
LeDx-42								
Intensity		878-978	819-1107	730-945	500-636	714-920	711-1015	314-690
Red		250-255	160-255	100-255	40-93	69-95	69-97	88-135
Green		250-255	167-255	95-255	56-142	55-130	44-132	53-134
Blue		225-255	190-220	70-252	40-106	31-100	29-109	40-106

4.3 Results

Using this classification approach, eight different material classes commonly found across Arctic hunter gatherer sites have been successfully fingerprinted, and segmented from

their original point cloud. These classifications, especially the *stone boulders* class, are used to map potential features in the site point clouds, and investigate them along with any associated objects in their nearby surroundings. LdFa-1 was successfully classified into: Water; Snow; Gravel; Stone Boulders; Low Vegetation; Medium Vegetation; and High Vegetation. LeDx-42 was successfully classified into: Snow; Gravel; Stone Boulders; Exposed Outcrop; Low Vegetation; Medium Vegetation; and High Vegetation. Figure 4.3 illustrates the site point clouds in their original forms and the finalized classification of surface materials. Each surface material in these files can be individually extracted, or alternatively, combined so that two or three layers can be represented at the same time while removing overlying objects or materials. At LdFa-1, water and snow were easily identified and classified in the point cloud. Gravel was primarily located near the edges of the point cloud dataset. The stone boulders segment was extracted from the point cloud and layered on top of a contour map of the surface area to illuminate any features. Figure 4.4 highlights some of the obvious stone features located on the surface of the site, while also providing a detailed map of all stone boulder placements and distributions of all shapes and sizes. The dense stone boulder area shown on the map was initially obstructed by a mix of medium and high vegetation and grasses on the site, while in other areas the boulders had begun to sink into the surrounding hummocky soils adjacent to the water.

LeDx-42 had less medium and high vegetation growth on the surface, but did exhibit exposed stone outcrops and numerous patches of gravel near the previous unit excavations. In comparison to LdFa-1, the visibility of stone features is low even when stone boulders were extracted and layered onto a contour map (Figure 4.5). The classification and extraction process was successful, yet due to lichen growth on the surfaces of the boulders, a slightly wider range of intensity and colour values was used. The file segment shows a wide distribution of surface

boulders in this area of the site. While many of the stones are small in size (<0.30 m) and isolated from each other, some larger surface scatters are visible and may prove useful for further investigation. There was no water in this point cloud of LeDx-42, yet small patches of snow remained on the surface of the site.

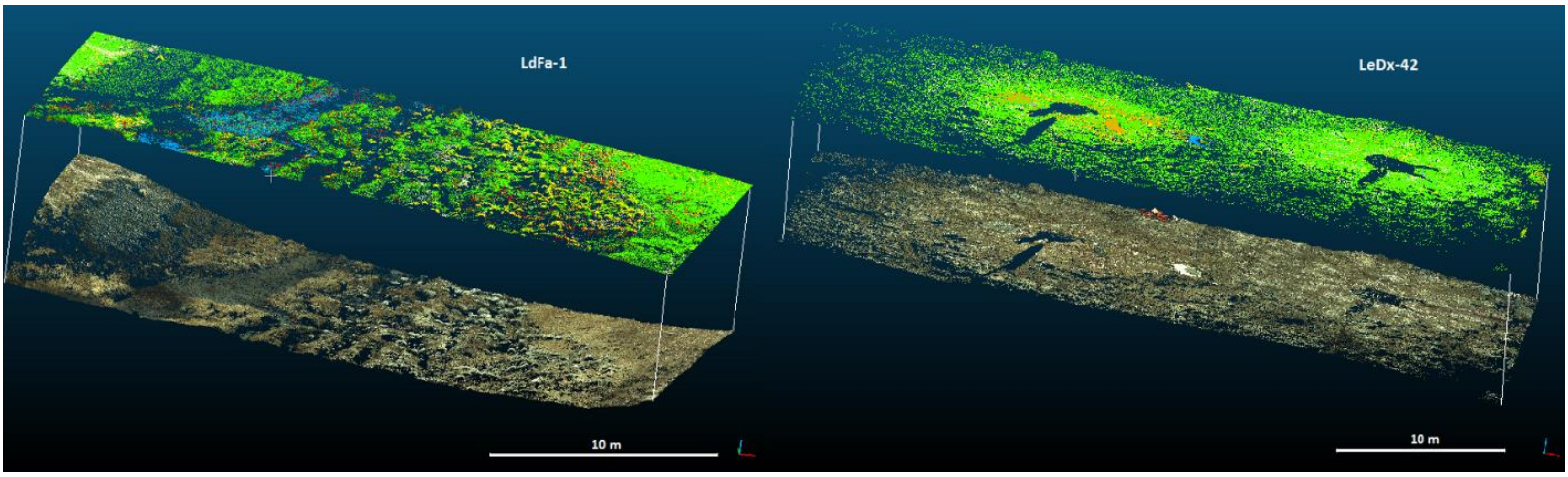

Figure 4.3 Bottom: Original colour point clouds of LdFa-1 and LeDx-42. Top: Colour classified point clouds using our processing sequence. Colours correspond to the following materials: Blue – Water/Snow; Light Green – Low-vegetation; Dark Green – Medium-vegetation; Red – High-vegetation; Grey – Gravel; Orange – Exposed Outcrop; Yellow – Stone Boulders. Note that the scanner positioning in LeDx-42 caused the shadowed areas in the point clouds.

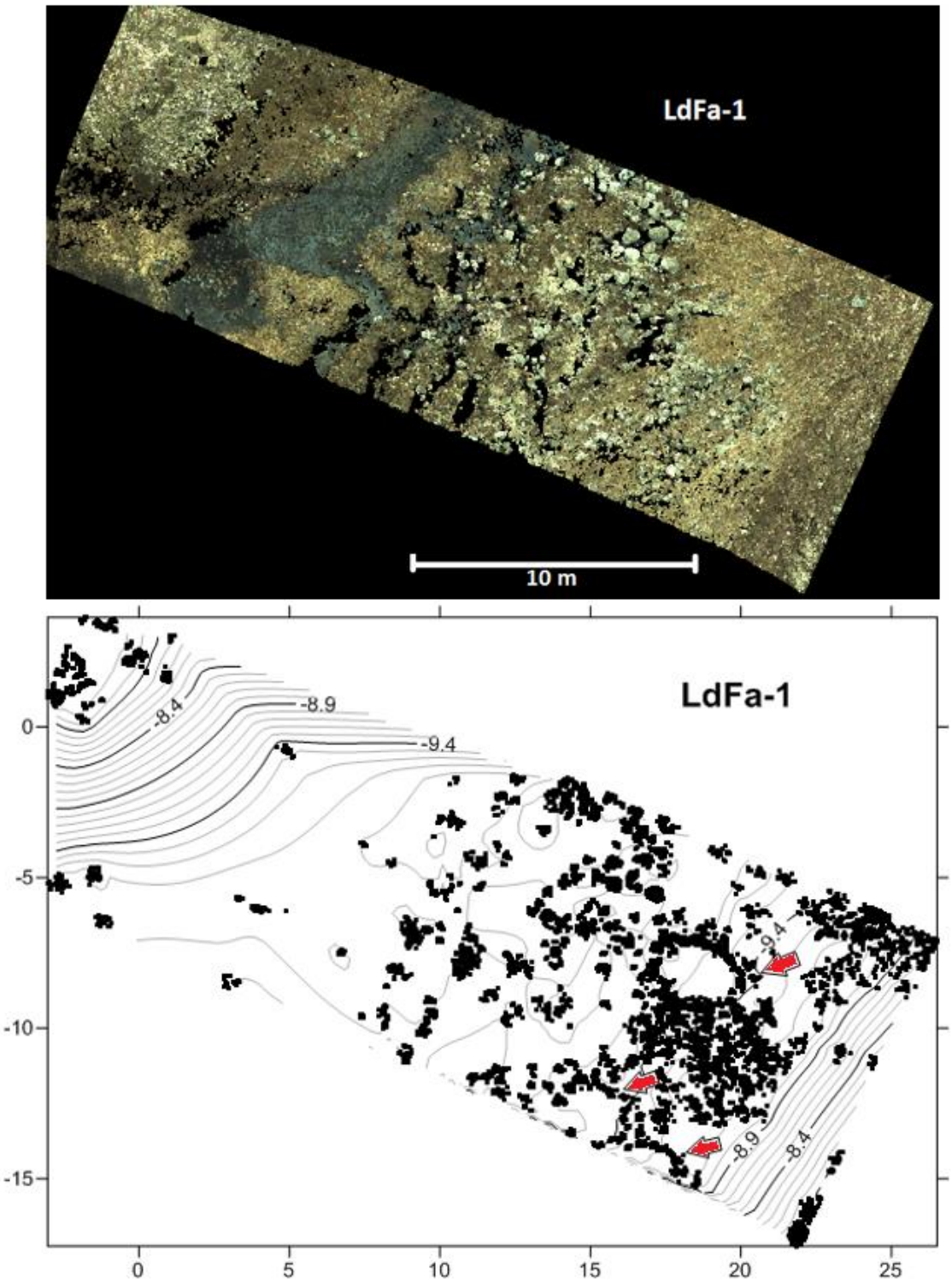

Figure 4.4 Top: Original point cloud sample from LdFa-1. Bottom: Extracted stone boulders from the point cloud and layered on top of a surface contour map. Arrows indicating the location of stone tent rings near the right side of the map. Scale is in meters.

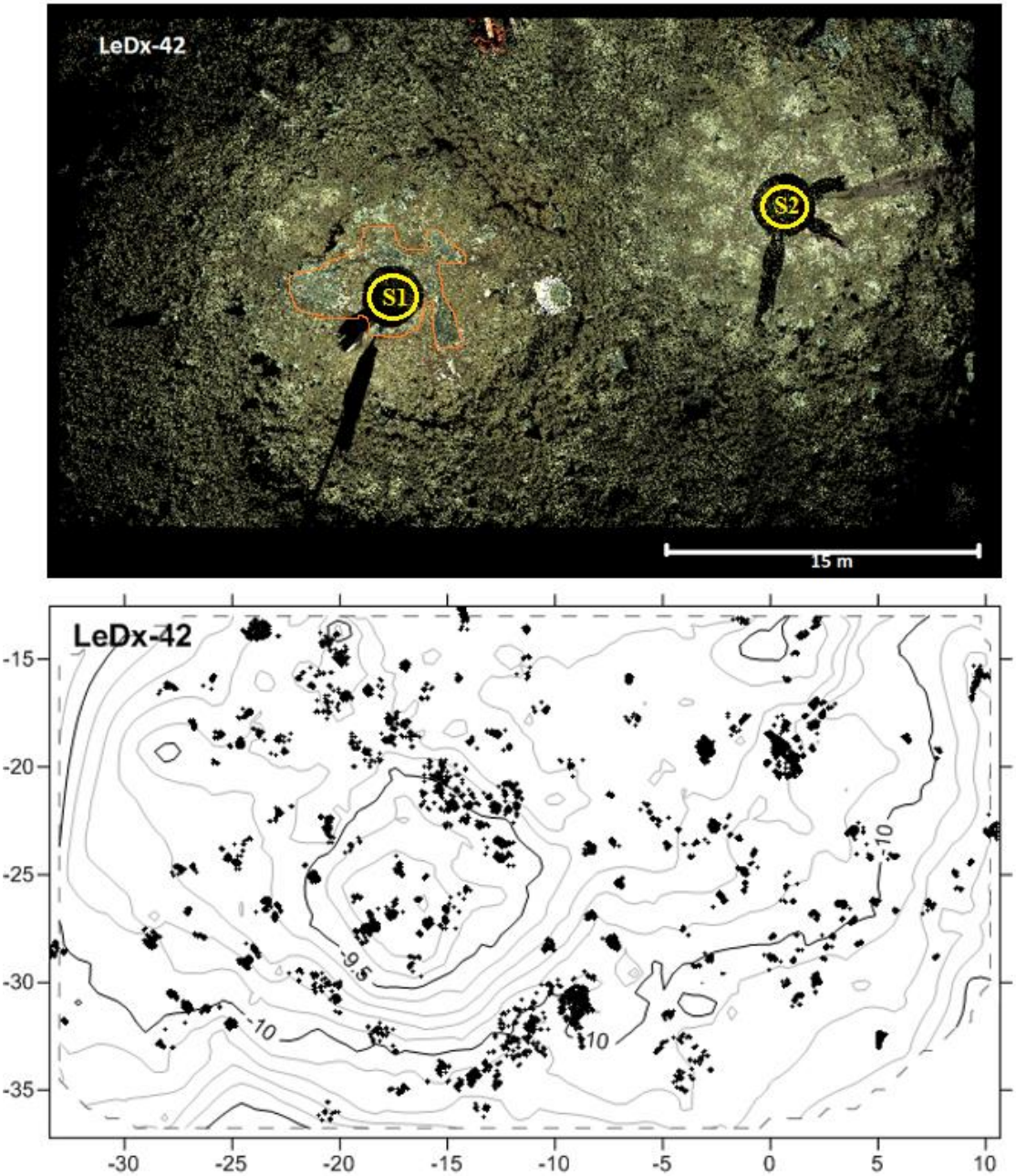

Figure 4.5 Top: Original point cloud sample from LeDx-42. Gaps in the data represent the location of the laser scanner stations and are indicated by S1 and S2. The exposed stone outcrops on the surface are also outlined in orange. Bottom: Extracted stone boulders from point cloud and layered on top of surface contour map. Stone clusters are found radiating from the points of highest elevation near the left side of the map, away from the hummocky tundra seen on the right. Scale is in meters.

4.4 Discussion

This classification and extraction approach proved to be an effective means of using large digital point clouds to enhance our ability to map and investigate Arctic hunter-gatherer sites. Specifically, it demonstrates how discrete elements can be extracted from low relief hunter gatherer sites with different surface compositions. This approach was designed to accomplish two goals: (1) to fingerprint specific materials found on diverse small scale archaeological surfaces in order to isolate them from their original 3D point clouds, and (2) to provide archaeologists with a new visual and spatial analytical tool that can be used for future feature investigation and interpretation of similar low visibility sites.

The low relief surface stone boulders at LdFa-1 were successfully extracted from the rest of the point cloud. Three prominent archaeological stone features are best highlighted within this new dataset while layered over top of a contour map and isolated from the mix of vegetation at the site. Extracting materials that make up the most common Arctic archaeological structures helps enhance the visual representation of these features at the site in order to measure, orient, and locate potential patterns in the surrounding debris. Using the distributions of materials in these extracted datasets can lead to the identification of subsequent areas of archaeological interest and also help in planning future fieldwork.

The results from LeDx-42 were equally successful in fingerprinting and extracting stone boulders from the original point cloud. No obvious stone features are identified in the new dataset, although in combination with the collection of artifact deposits, the distribution of larger clusters of stone boulders may suggest the location of former, dismantled stone features on this known Paleo-Inuit site. In addition, the extracted point cloud data illustrate a tendency for stone clusters to occur near areas of highest elevation (see Figure 4.5), suggesting potential preference

in occupation area situated away from the lower-lying hummocky terrain. Investigating the stone boulders in context with the surface outcrop exposure may also suggest a combined use of building materials (i.e., stone boulders and natural outcrop) at this site. However, this does require further excavation in those adjacent areas.

The overall results demonstrate how a manual TLS point cloud classification approach can be a valuable tool in the analysis of low relief archaeological features on two Arctic hunter-gatherer sites. The manual classification process demonstrates the ability to fingerprint and extract specific materials on two compositionally different site surfaces. This digital approach is entirely processed in openly available software, making it a more accessible and flexible tool for non-specialists in the archaeological sciences. The resulting digital datasets provide us with a new starting point from which to record and interpret the distribution of both the natural and anthropogenic elements across the surface of a site. Using the segmented classifications provides a more objective and accurate way to record and compare archaeological surface features and other natural objects at sites like LdFa-1 and LeDx-42, and additionally creates a new dataset from which we can discuss the spatial organization of an Arctic hunter-gather site.

Using TLS analytical processes like this one allows researchers to accurately evaluate a site in real time while still in the field. This has important implications for effective use of resources, namely time and money, when working in remote locations that are affected by unpredictable seasonal conditions like the interior of southern Baffin Island. Having the ability to identify important areas for investigation that were previously unknown or unclear due to surface obstructions allows researchers to shift site investigations to focus on those areas that are more likely to yield meaningful data. TLS analytical processes also provide researchers with the ability to continue a site analysis in a 3D digital space even if they do not have the funds to support

returns to the physical site, which, again, is an important consideration when working in remote field locations like the Arctic.

During our tests of this approach, we encountered a few issues in our data that will be addressed in our future site investigations using this technology. Upon noticing some areas of overlapping classifications, this, and any other RGB and intensity-based approach, would benefit from a consistent data normalization process available for any type of terrestrial scanner. Additionally, better scanner positioning would have provided greater detail in shadowed areas on the site, benefiting both the intensity values and RGB colourization. Finally, even greater material classification accuracy could be achieved having used a higher quality digital camera, and image meshing procedures. Overall, given the methodological challenges of conducting this type of research in Arctic sites, this simple analytical process can provide a valuable addition to TLS research in the north.

4.5 Conclusions

Our results illustrate the potential of a manual TLS point cloud classification approach for extracting materials that make up Arctic hunter-gatherer archaeological features. We present a simple, but effective classification technique adopted from existing scripts, and available to any non-expert in the field of archaeology. Although simple in method, using manual classification processes provides an alternative to other existing, more robust procedures like CANUPO. Manual classification gives an archaeologist complete control to identify a combination of colours exhibited on often ambiguous and extremely low relief hunter gatherer features on the surface of the low Arctic tundra, and makes it possible to locate and examine these potential features while still in the field. Using the extracted data to characterize the surface of the site in a

unique way provides us with a new analytical tool for investigating and analysing low relief Arctic hunter gatherer sites. TLS point clouds of LdFa-1 and LeDx-42 have been successfully segmented into several parts where both the natural and anthropogenic elements of the surface have been extracted in the resulting digital datasets. Using this classification approach, we were able to produce datasets composed of low relief archaeological elements to allow for unique measurements, and larger scale analysis to take place. In providing a meaningful use for Arctic hunter-gatherer contexts, these results help us to move beyond the simple large-scale acquisition and visualization of 3D digital point clouds at archaeological sites. Our classification method provides a novel contribution to the field of digital archaeology as its focus shifts from data collection to data analysis and interpretation. Implementing this analytical approach in both a field and lab setting, demonstrates the value of large digital dataset procurement, processing, and analysis.

4.6 Works Cited – Chapter 4

Abbas, M. A., Luh, L. C., Setan, H., Majid, Z., Chong, A. K., Aspuri, A., Idris, K. M., and Ariff, M. F. M. 2014. Terrestrial laser scanners pre-processing: Registration and georeferencing. *Jurnal Teknologi*, 71(4), 115-122.

Bandyopadhyay, M., van Aardt, J. A. N., and Cawse-Nicholson, K. 2013. Classification and extraction of trees and buildings from urban scenes using discrete return LiDAR and aerial colour imagery. In M. D. Turner, and G. W. Kamerman (Eds.), *Laser Radar Technology and Applications* XVIII, Proceedings of SPIE 2013, Vol. 8731, 873105.

Bielawski, E. 1988. Paleoeskimo variability: The early Arctic Small-Tool tradition in the central Canadian Arctic. *American Antiquity*, 53, 52-74.

Brodu, N., and Lague, D. 2012. 3D terrestrial lidar data classification of complex natural scenes using a multi-scale dimensionality criterion: applications in geomorphology. *ISPRS Journal of Photogrammetry and Remote Sensing*, 68, 121-134.

Buckley, S. J., Kruz, T. H., Howell, J. A., and Schneider, D. 2013. Terrestrial lidar and hyperspectral data fusion products for geological outcrop analysis. *Computers and Geosciences*, 54, 249-258.

CloudCompare (version 2.6.1) [GPL software]. 2015. Retrieved from http://www.cloudcompare.org/

Dawson, P. C., Bertulli, M. M., Levy, R., Tucker, C., Dick, L., and Cousins, P. L. 2013. Application of 3D laser scanning to the preservation of Fort Conger, a historic polar research base on northern Ellesmere Island, Arctic Canada. *Arctic*, 66(2), 147–158.

Friesen, T. M. 2015. On the naming of Arctic archaeological traditions: The case for Paleo-Inuit. *Arctic*, 68(3), iii-iv.

Güth, A. 2012. Using 3D scanning in the investigation of Upper Palaeolithic engravings: first results of a pilot study. *Journal of Archaeological Science*, 39(10), 3105-3114.

Hakonen, A., Kuusela, J-M., and Okkonen, J. 2015. Assessing the application of laser scanning and 3D inspection in the study of prehistoric carin sites: The case study of Tahkokangas, Northern Finland. *Journal of Archaeological Science: Reports*, 2, 227-234.

Huggett, J. 2015. Challenging Digital Archaeology. *Open Archaeology*, 1(1), 79-85.

Huimin, H., Yanmin, W., Chunmei, H., and Guoli, H. 2012. Application of terrestrial LiDAR technology in digital surveying and mapping of the Hall of Preserving Harmony of Forbidden City. *Journal of Beijing University of Civil Engineering and Architecture*, 3, 009.

Humair, F., Abellan, A., Carrea, D., Matasci, B., Epard, J-L., and Jaboyedoff, M. 2015. Geological layers detection and characterisation using high resolution 3D point clouds: Example of a box-fold in the Swiss Jura Mountains. *European Journal of Remote Sensing*, 48, 541-568.

Isenburg, M. 2015. LAStools efficient tools for LiDAR processing. (Version 1.3). Retrieved from http://lastools.org.

Landry, D. B., Ferguson, I. J., Milne, S. B., and Park, R. W. 2015. Combined geophysical approach in a complex arctic archaeological environment: A case study from the LdFa-1 site, southern Baffin Island, Nunavut. *Archaeological Prospection*, 22(3), 157-170.

Larsen, B. P., Holdaway, S. J., Fanning, P. C., Mackrell, T., and Shiner J. I. 2017. Shape and an outcome of formation history: Terrestrial laser scanning of shell mounds from far north Queensland, Australia. Quaternary International, 427(A), 5-12.

Lerma, J. L., Navarro, S., Cabrelles, M., and Villaverde, V. 2010. Terrestrial laser scanning and close range photogrammetry for 3D archaeological documentation: The Upper Palaeolithic Cave of Parpalló as a case study. *Journal of Archaeological Science*, 37(3), 499-507.

Milne, S. B. 2003. Identifying Pre-Dorset structural features on southern Baffin Island: Challenges and considerations for alternative sampling methods. *Inuit Studies*, 27(1-2), 67-90.

Milne, S. B. 2005. Archaeological investigations in the Mingo and Amadjuak Lake districts of southern Baffin Island. Permit report covering the work conducted under Nunavut Territory Archaeologist Permit No. 04-06A. Nunavut Ministry of Culture, Language, Elders and Youth, Igloolik, Nunavut.

Milne, S. B. 2008. Archaeological investigations in the Mingo lake district of southern Baffin Island: Assessing Palaeo-Eskimo culture continuity and change. Permit report covering the work conducted under Nunavut Territory Archaeologist Permit No. 07-014. Department of Culture, Language, Elders and Youth, Government of Nunavut, Igloolik, Nunavut.

Milne, S. B. 2013. Chert sourcing and Palaeo-Eskimo stone tool technology. Permit report covering the work conducted under Nunavut Territory Archaeologist Permit No. 2013-02A. Department of Culture, Language, Elders and Youth, Government of Nunavut, Igloolik, Nunavut.

Milne, S. B., Park, R. W., and Stenton, D. R. 2012. Dorset culture land use strategies and the case of inland southern Baffin Island. *Canadian Journal of Archaeology/Journal Canadien D'Archéologie*, 36(2), 267-288.

Milne, S. B., Park, R. W., Fayek, M., Stenton, D. R., and Landry, D. B. 2013. Toolstone availability near Frobisher Bay, NU and its implications for Palaeo-Eskimo lithic technological organization. Proceedings of the Canadian Archaeological Association Conference 15-19 May 2013, Whistler, British Columbia. Canada.

Niemeyer, J., Rottensteiner, F., and Soergel, U. 2012. Conditional random fields for lidar point cloud classification in complex urban areas. *ISPRS annals of the photogrammetry, remote sensing and spatial information sciences*, 1(3), 263-268.

Park, R. 2008. Archaeological excavations at the LdFa-1 site, Mingo lake, Baffin Island, Summer 2008 Permit report on work conducted under Nunavut Territory Archaeologist Permit No. 08-029A. University of Waterloo.

Penasa, L., Franceschi, M., Preto, N., Teza, G., and Polito, V. 2014. Integration of intensity textures and local geometry descriptors from terrestrial laser scanning to map chert in outcrops. *ISPRS Journal of Photogrammetry and Remote Sensing*, 93, 88–97.

Reyes, R., Bellian, J., and Adams, E. W. 2009. Using statistical methods to correct lidar intensities from geological outcrops. Proceedings of the Digital Mapping ASPRS/MAPPS Annual Conference, 16-19 November 2009, San Antonio, Texas. United States of America.

Romero, B. E., and Bray. T. L. 2014. Analytical applications of fine-scale terrestrial lidar at the imperial Inca site of Caranqui, northern highland Ecuador. *World Archaeology*, 46(1), 25-42.

Rüther, H., Chazan, M., Schroeder, R., Neeser, R., Held, C., Walker, S. J., Matmon, A., and Horwitz, L. K. 2009. Laser scanning for conservation and research of African cultural sites: the case study of Wonderwerk Cave, South Africa. *Journal of Archaeological Science*, 36(9), 1847-1856.

Schreiber, S., Hinzen, K. G., Fleischer, C., and Schütte, S. 2012. Excavation-parallel laser scanning of a medieval cesspit in the archaeological zone of Cologne, Germany. *Journal on Computing and Cultural Heritage*, 5(3), 12.

Song, J-H., Han, S-H., Yu, K. Y., and Kim, Y-I. 2002. Assessing the possibility of land-cover classification using lidar intensity data. *International Archives of Photogrammetry Remote Sensing and Spatial Information Sciences*, 34(3/B), 259-262.

Stenton, D. R. 1991. The archaeology of terrestrial hunting systems: The Amadjuak Lake Project. Permit report on file with the Department of Culture, Elders, Language, and Youth. Government of Nunavut. Igloolik: Nunavut.

Watterson, A. 2015. Beyond digital dwelling: re-thinking interpretive visualisation in Archaeology. *Open Archaeology*, 1, 119-130.

Chapter 5

Integrated Geophysical Techniques for the Archaeological Investigation of LbDt-1, a Paleo-Inuit Quarry Site in the Interior of Southern Baffin Island, Nunavut, Canada.

An original scientific research manuscript published in:

Journal of Archaeological Methods and Theory,

DOI: https://doi.org/10.1007/s10816-018-9370-6

David B. Landry, Ian J. Ferguson, S. Brook Milne, Mulu Serzu, Robert W. Park

Abstract: In 2015, we mapped surface and near-surface physical properties of a Paleo-Inuit lithic quarry site, LbDt-1, located in the interior of southern Baffin Island, Nunavut, Canada using a multi-method approach. The survey site is characterised by a dense chert flake deposit. The purpose of the survey was to document this survey site's surface features using three-dimensional laser scanning and to investigate the utility of active remote sensing and geophysical methodologies at prehistoric lithic quarry sites. Manual and automated data reduction, interpretation and inversion methods were applied across each dataset to isolate the surface and subsurface distribution of flakes. Laser scanning results demonstrate a remarkable dispersal of surface chert flakes confined to a general area of the geophysical survey. To define the base of the lithic deposit layer, a combination of enhanced radar reflections and two-layer inversion models of magnetic responses obtained using electromagnetic measurements was used. Radar results suggest the deposit has a thickness of around 10–20 cm and indicate that there are no additional parts of the deposit masked by soil in this area. The magnetic susceptibility data define an upper layer of ~ 20 cm thickness and susceptibility (0.004–0.008 SI) overlying a less magnetic (< 0.004 SI) lower layer, with the spatial variations in the upper layer suggesting debitage and gravel deposits have lower magnetisation than the topsoil at the site. Overall, this study demonstrates the capacity of remote sensing and geophysical methods to non-invasively investigate some prehistoric activities without the need for full-scale excavation and the collection of large material assemblage characteristic of lithic quarry sites.

5.1 Introduction

Archaeological investigation of prehistoric lithic quarry sites remains both a methodological and interpretive challenge. The broad and often ambiguous scale—both in geographic and stratigraphic extent—of lithic quarries combined with extensive layering, and mixed anthropogenic and natural deposits, make designing an investigative framework extremely difficult. Moreover, the ability to isolate individual events or behaviours related to the prehistoric activities is laborious and often relies on discovery of diagnostic artefact types or discrete activity areas associated with specific knapping events (Ericson 1984).

A lithic quarry represents the first component of a stone tool using people's technological system. Archaeological investigation at these sites can provide information concerning raw material selection, extraction and knapping techniques through analysis of on-site activity areas and archaeological features (Ericson 1984, pp. 2). Moreover, the results of these analyses can provide insight concerning the duration of site occupation, the types of flaking activities and reduction conducted on site and the potential existence of on-site habitation.

Efforts to link lithic quarries to secondary reduction and habitation sites typically rely on the identification and comparison of macroscopic traits identified on lithic raw materials including colour, texture, quality, texture and cortex cover, among others (e.g., Byrd et al. 2009; Brumbach 1987; Goodyear and Charles 1984; Kessler et al. 2009; Milne et al. 2011; Wilke and Schroth 1989). Advances in provenance sourcing techniques involving physical and chemical techniques have, however, enabled archaeologists to more assess the movement of raw material over time within a region (e.g., Burke 2007; Hull et al. 2008; Parish 2013; ten Bruggencate et al. 2015, 2016a; Tripcevich and Contreras 2013).

This study has the somewhat different goal of understanding the internal structure of a single lithic quarry in the interior of southern Baffin Island, Nunavut. Specifically, we assess the efficacy of using a non-invasive multi-method approach to define and measure the surface and subsurface extent of lithic reduction activities at a Paleo- Inuit chert quarry site known as LbDt-1 (Figure 5.1; Milne 2013, Milne 2015). This archaeologically exploited lithic quarry exhibits available chert raw material in the form of an eroded river bank limestone outcrop, along with massive chert debitage scatters across the site. Investigation at this site is particularly important for stone tool using hunter-gatherers in the Arctic since few lithic source areas are presently known (e.g., Erwin 2010; Gramly 1978; Lazenby 1980; ten Bruggencate et al. 2016a). Thus our understanding of how Paleo-Inuit peoples acquired lithic raw material at quarries is limited.

Characterising surface and near-surface layering using a combination of terrestrial laser scanning (TLS), ground penetrating radar (GPR) and electromagnetic geophysical surveys, provides data on the distribution and depth of both natural and anthropogenic features at the LbDt-1 site. In addition, lithic debitage results presented in this study help provide insight into the lithic quarrying and early-stage reduction for transport at this site. From this, inferences regarding lithic transport and land use can be deduced. Perhaps most importantly, the non-invasive nature of this approach demonstrates howthis large lithic quarry can be investigated without using traditional site excavations, which are logistically complex and generate massive artefact assemblages that pose challenges for analysis and storage post-excavation (e.g., Andrews et al. 2004; Bamforth 2006; Minchak 2010).

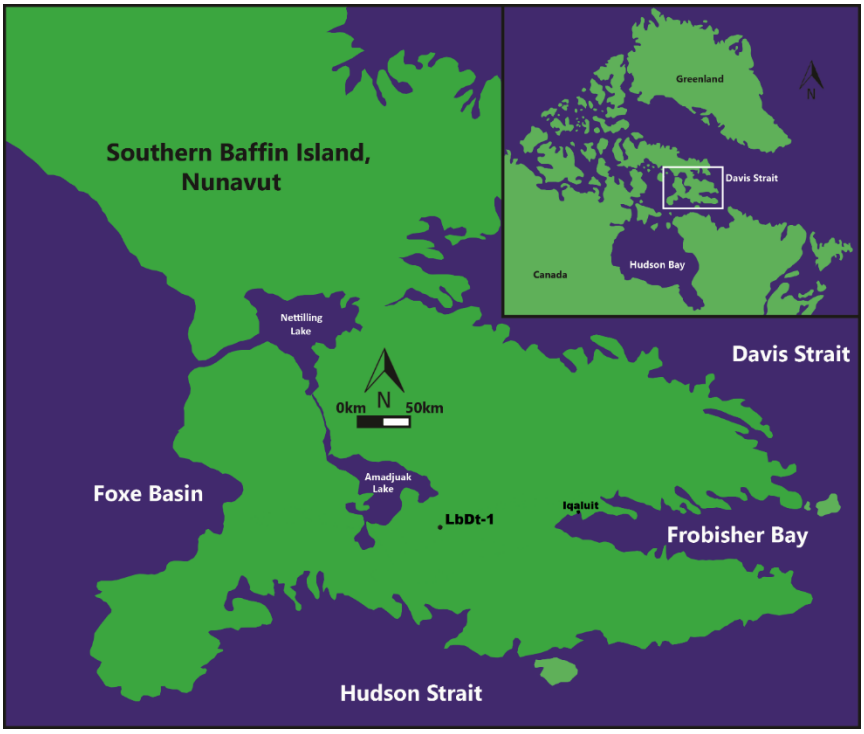

Figure 5.2 Map of southern Baffin Island indicating the location of the archaeological site, LbDt-1, inset with map of northern Canada and Greenland.

5.2 LbDt-1

LbDt-1 is situated along the eastern bank of the Hone River, 42 km south of Amadjuak Lake and 115 km west of Iqaluit (see Figure 5.1). The site was discovered in 2013 via aerial survey (Milne 2013) and was further investigated by Milne in 2015. LbDt-1 is divided into two components to facilitate description and investigation (see Figure. 5.2). The Upper Component is approximately 5 m above the river and adjacent to a steep bluff. It consists of several features including an extensive deposit of chert debitage near the edge of the bluff and a row of large well-defined boulder tent rings approximate 300 m east of the deposit. The site's lower component is covered in a dense vegetation layer making it difficult to identify the surface expression of similar boulder tent rings. The river banks at the margin of the lower component are being actively eroded by the Hone River, and large deposits of chert debitage and some

caribou remains can be seen slumping into the water. There are several large limestone outcrops where chert can be readily found in situ and as eroded nodules. This important lithic raw material can be easily picked up and transported elsewhere. Paleo-Inuit toolmakers presumably moved the raw chert material from the lower to the upper component of LbDt-1 to work the stone as evidenced by the large debitage deposit in the upper component.

The survey conducted for this study focused on the upper component of LbDt-1, specifically, on areas near the steep bluff where the debitage deposit is most visible (see Figure 5.2). The chert deposit has an approximate aerial extent of 20 m×25 m as defined during initial visual inspection in 2013. In 2015, the upper component was surveyed systematically. Three small test pits (0.25×0.25 m) were excavated (see Figure 5.3) to determine cultural affiliation for the site and yielded thousands of lithic debitage and pieces of debris yet no diagnostic artefacts. An analysis of over 5000 lithic debitage acquired from the test units found evidence associated near exclusively with early-stage reduction activities. Interestingly, more than 50% of the analysed flakes retained surface cortex further indicating a focus on decortication and early-stage reduction of chert nodules available at the site (Milne 2015, pp. 6). While no culturally diagnostic artefacts were recovered, we can be certain that those peoples using LbDt-1 for lithic acquisition purposes were Paleo-Inuit since their toolkits are dominated by chert artefacts whereas later Thule Inuit toolmakers did not make extensive use of this material in their technological inventories throughout the eastern Arctic (Stenton and Park 1998; ten Bruggencate et al. 2016b).

The debitage deposit is most dense at the edge of the river bluff where flake aggregations are virtually devoid of any surface soil or vegetation. As one moves away from the bluff towards the tent ring row, the surface scatter of flakes becomes more diffuse within a densely covered

grassy area (Figure 5.3a, b). In test pit 1, the chert layer is observed to be 15–20 cm thick (see Figure 5.3c). It comprises >90% chert fragments with the remaining 10% consisting of fine grain sand and soil. In test pit 2, a thin surface layer of gravel, grass and sparse chert pieces overlies at least 10 cm of uniformly textured organic-rich brown soil, which is noted as a sterile background layer for the purposes of this study (see Figure 5.3d). At the time of the survey in July 2015, the soil was observed to be completely unfrozen in both test pits.

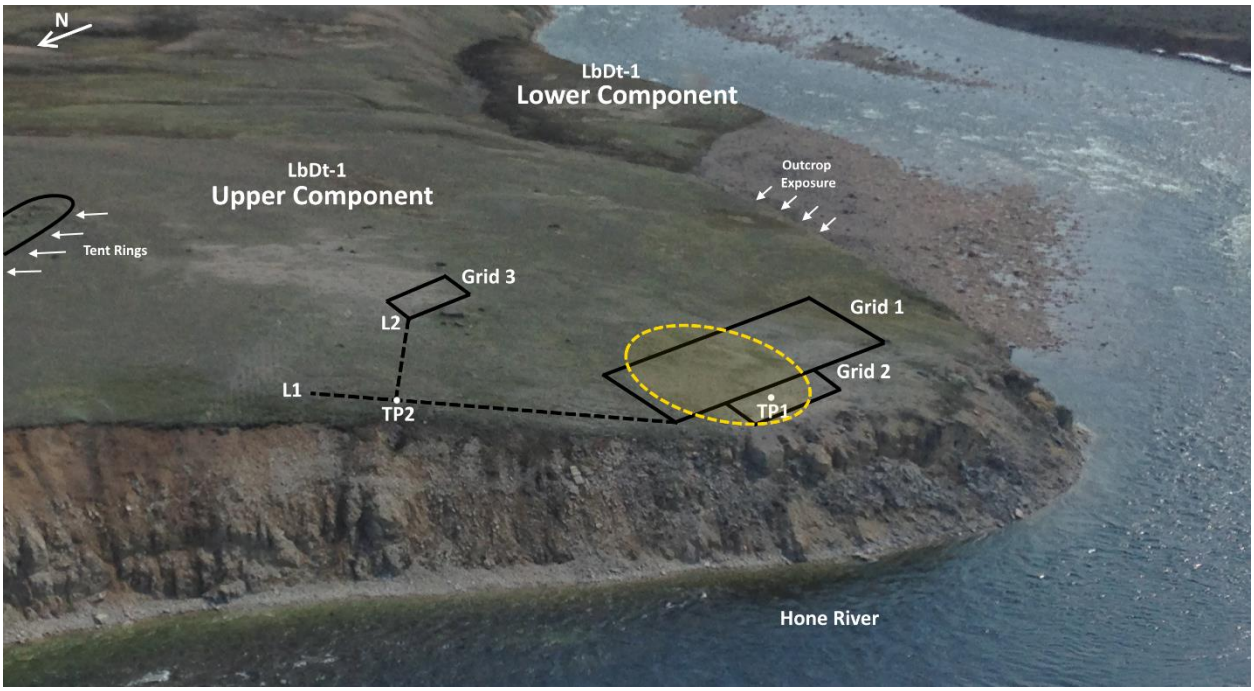

Figure 5.2 Oblique aerial photograph of LbDt-1 showing the upper and lower site components. Survey grid 1 (13 m×44 m), grid 2 (6 m×20 m) and grid 3 (8 m×15 m) are noted, along with the survey lines (L) 1 and 2 and the locations of test pits (TP) 1 and 2. The extensive surface chert deposit appears within the yellow dashed ellipse.

The surface gravel seen in areas around the debitage deposit has a light-coloured appearance that is superficially similar to the chert. However, the gravel deposits are characterised by a more significant variation in particle size than the chert deposit and contain thinly cracked particles ranging from 0.03 to >0.20 m. These deposits have likely formed

through a process of weathering, upheaval and frost shattering of the underlying limestone bedrock. Harris (1982) reports the common presence of this process at the nearby Amadjuak Lake. The gravel areas are notably free of grass, but there are small patches of moss and lichen present throughout.

Figure 5.3 Photographs from LbDT-1. **a** Surface view of the chert flake deposit. Note the grass growing within the deposit. **b** Photograph of 0.25×0.25 m area of the surface chert deposit. Scale bar divisions are centimeters. **c** Test pit 1, located in grid 2 within the dense chert flake deposit. **d** Test pit 2 which is located on line 1 outside the chert flake deposit.

5.3 Remote-sensing and Geophysical Methods

5.3.1 Terrestrial Laser Scanning

TLS is a three-dimensional (3D) remote-sensing technology that measures the range of a target, including two angles (inclination and azimuth) providing the horizontal and vertical

coordinates of the data point. This process is done simultaneously across a wide field of view to accurately map large landscapes or structural surfaces in minutes. A mid-length scanner such as the one used in this study, employs a source transmitter/receiver arrangement in which light radiation is emitted from a rotating console at wavelengths between 500 and 1050 nm (Landry et al. 2016, pp. 61). This energy is reflected off target surfaces and measured on its return. Data are captured in the hundreds of thousands of points per second and stored as individual coordinate (x,y,z), colour and reflectance values (Bellian et al. 2005), creating a large database of responses known collectively as a point cloud.

3D laser scanning technologies are known for their ability to create extremely detailed and accurate wide area landscape maps and structural models, along with smaller-scale 3D images used for numerous analytical and visual procedures (Güth 2012, pp. 3110–3113; Landry et al. 2016, pp. 234–237; Larsen et al. 2017, pp. 6–7; Romero and Bray 2014, pp. 30–34). In addition, point cloud data have been used to manually classify surface elements and structures on landscape surfaces. The method has been applied in a number of archaeological studies, including at two nearby Paleo-Inuit sites in the interior of southern Baffin Island (Landry et al. 2016, pp. 237–239). In our study from 2016, the TLS site surface image was classified into various materials based on their point colour and reflective properties, measured as RGB and intensity data. The classification process was conducted manually using a combination of LAStools (Isenburg 2015) and CloudCompare (CloudCompare 2015) processing and visualisation software. The TLS parameters were averaged over small samples of points (~30) and classified as specific materials (e.g., grass, snow or bedrock).

This TLS classification approach was used in the present study to map surface characteristics and the lateral distribution of the debitage deposit. To achieve the first objective,

the colour and reflectance response of the deposit are examined along with the general uniformity and texture of these responses. These results are also used to determine whether there is any internal variation within the deposit. If different parts of the deposit were created at different times, such spatial variation could provide information on recurring occupations and discrete knapping episodes. The second objective is achieved by comparing the distribution of chert flakes as defined by TLS with the distribution determined by observation at the site. Aspects to be considered include the definition of reflectance characteristics that allow chert to be discriminated from other materials at the site and determination of the reliability with which the surface distribution of chert can be mapped using TLS. The results of this part of the study have implications for the ability to rapidly map chert flake deposits in other locations.

5.3.2 Ground Penetrating Radar Imaging

GPR is used in this study as a non-invasive method to characterise the vertical and lateral extent of the debitage deposit at LbDt-1. The use of traditional large-scale archaeological excavation practices for this purpose is impractical at this type of site due to their size and the time it would take, and also due to the voluminous resulting assemblage that would be generated. Therefore, GPR mapping of near-surface reflections, including imaging the base of the chert layer, is an important step in understanding the complexity of this Arctic chert quarry. A previous electromagnetic study at a site near Amadjuak Lake indicated that the near surface was very resistive (<3 mS m−1), suggesting that archaeological sites in the region would be well suited for GPR imaging applications (Landry et al. 2015, pp. 166).

GPR theory is well established and described in detail elsewhere (e.g., Annan 2005; Conyers 2016) so will be considered only briefly here. GPR responses depend primarily on the

dielectric constant k of the sub-surface materials, which is, in turn, strongly influenced by the liquid water content. In periglacial environments, the dielectric constant of common Earth materials will typically vary from k=10 to >30 for saturated, unfrozen, porous soils and sands to k=8–15 in low-porosity bedrock and to k=4–6 in dry or frozen soils or sands (e.g., Annan 2005; Kneisel et al. 2008; Gacitúa et al. 2012). The velocity of the radar signals is defined by the speed of light divided by the square root of k, and reflections and diffractions of GPR signals will be caused by interfaces between materials with different dielectric constant.

GPR operates by transmitting a pulse with a length dependent on the system frequency from a transmitter antenna and recording responses associated with direct transmission, reflections and diffractions using a receiver antenna. In a horizontallayered environment, the first signals to be recorded will be a direct wave traveling through the air and a direct wave through the ground (e.g., Grote et al. 2010). For systems in which the transmitter and receiver antennae are closely spaced, as used in the present study, these signals may overlap. Subsequent signals will come from reflections between sub-surface layers of different dielectric constants (e.g., a bedrock or permafrost surface). As the GPR system is moved along the surface, these reflections will image variations in the depth to the reflector. When larger localised 3D objects are present, the increasing lateral component of the travel path occurring as the system moves away from the object causes the response to have the form of a hyperbolic reflection. Such responses are often referred to as diffraction hyperbolae since they involve a plane-wave front interacting with a point source (e.g., Yilmaz 1987). When there are multiple 3D objects in the sub-surface, more extensive scattering occurs.

The response of GPR in Arctic and periglacial regions has been examined in a number of studies (e.g., Brosten et al. 2009; Gacitúa et al. 2012; Hinkel et al. 2001; Kneisel et al. 2008;

Moorman et al. 2003; Snegirev et al. 2003; Schwamborn et al. 2008). Studies in northern Canada include those of Dallimore and Davis (1992) and Pilon et al. (1992). Several studies have also applied GPR in Arctic archaeological sites including Wolff and Urban (2013) and Urban et al. (2016).

The specific objectives for applying GPR in the LbDt-1 study were to (i) examine the reflection and scattering responses of the chert flake deposit, (ii) map the thickness of the deposit across the site, (iii) identify any additional areas of the deposit that may be covered by soil or vegetation and (iv) extract information on the geological and permafrost structure at the site. The GPR system available for the survey was GSSI SIR 3000 system and monostatic 200 and 400 MHz antennae. The 400-MHz antenna was chosen for the survey as it provides the better near-surface depth resolution. The typical wavelength of this system in the study environment is estimated to be between 15 and 25 cm. Prior to the survey, it was expected that the GPR system would be able to identify the thickness of the chert deposit if it was more than about 20 cm thick and a reflection from the base of the layer would therefore be distinct from the direct arrivals.

The reflective and scattering properties of the debitage deposit were unknown before the study. The circumference of the chert flakes is >20% of the wavelength suggesting that scattering may be significant (Annan 2005). Such scattering could degrade reflections from the base of the deposit. However, the scattering could also potentially produce a distinct signature that allowed for recognition of the presence of chert even where the deposit is thinner than 20 cm. Previous archaeological studies have made use of spectral GPR responses associated with such scattering (e.g., Valls et al. 2016).

5.3.3 Electromagnetic Imaging

An electromagnetic survey was completed at LbDt-1 to image the sub-surface electrical conductivity and magnetic susceptibility of the chert flake deposit complementing the information on the electrical permittivity derived from the GPR survey. A number of previous studies have demonstrated the value of electromagnetic imaging in archaeological surveys in periglacial environments (e.g., Landry et al. 2015; Urban et al. 2012; Viberg et al. 2009).

As previously noted, it was expected that the site would be an electrically resistive site due to the high resistivity observed at the LdFa-1 site located approximately 110 km northwest of LbDt-1 (see Landry et al. 2015); similar results have been observed in other Arctic settings (e.g., Kneisel et al. 2008; Urban et al. 2012). In resistive environments, appropriately designed electromagnetic instruments provide a low induction number (LIN) response in which the relationships between the response and ground properties become simplified (e.g., McNeill 1980; Beamish 2011; Dalan 2006; Tabbagh 1986; Everett and Meju 2005; Mester et al. 2011). The quadrature (Q) response from LIN electromagnetic instruments provides a direct estimate of the depthaveraged or apparent electrical conductivity σa and, in resistive environments, the inphase (IP) response provides a direct measure of the depth-averaged or apparent magnetic susceptibility κa.

The exploration depth for LIN responses depends the coil spacing and on whether the instruments are operated in vertical dipole (VD) mode (horizontal coils) or horizontal dipole (HD) mode (vertical coils). For the LbDt-1 survey, we used a GSSI EMP- 400 LIN instrument that has a coil spacing of 1.219 m. Figure 5.4 shows the sensitivity functions for the Q and IP responses for both modes and the relative contributions to the responses from each layer in a two-layer structure. The sensitivity functions for the low induction number responses are

provided by a number of authors. For example, McNeill (1980), Fitterman and Labson (2005) and Mester et al. (2011) note the apparent conductivity functions and Tabbagh (1986), McNeill and Bosnar (1999), Huang et al. (2003) and Dalan (2006) note the apparent susceptibility functions.

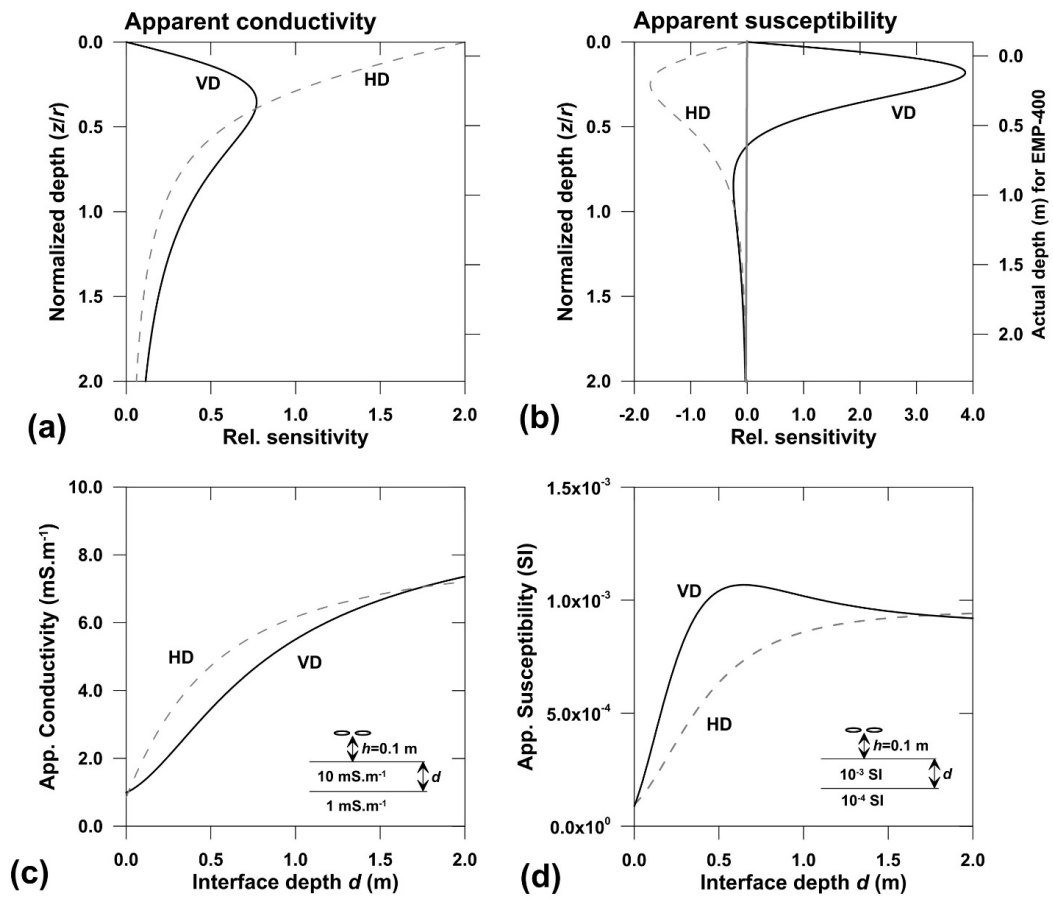

Figure 5.4 LIN apparent conductivity and apparent susceptibility sensitivity functions and two-layer responses. **a, b** The relative sensitivity of apparent conductivity and apparent susceptibility responses for the vertical dipole (VD) and horizontal dipole (HD) modes. The left axis shows normalised depth, and the right axes show the actual depth for an EMP-400 instrument operated at 10 cm elevation. Note that all responses are plotted using the convention that the sign of the transmitter signal at the receiver coil is positive. **c, d** The apparent conductivity and apparent susceptibility responses for a two-layer structure containing an upper layer of increasing thickness for an EMP-400 instrument operated at 10 cm elevation. The conductivity and susceptibility of the upper layer are a factor of ten higher than the same parameters in the lower layer.

The two-layer responses show that the HD apparent conductivity has greatest sensitivity to a thin upper layer (as it is affected more than the VD apparent conductivity by thin upper layers) (Dafflon et al. 2013; Everett and Meju 2005). In contrast, the VD apparent susceptibility response exhibits significantly larger sensitivity to a thin upper layer than the corresponding HD response. Because of the sign of the sensitivity functions, the HD and VD responses will have the opposite sign when the main contribution to the magnetic susceptibility comes from depths below the instrument of <0.612 times the coil spacing (Dalan 2006; McNeill 2012). The theory represented by the sensitivity functions and two-layer responses in Figure 5.4 can be used to invert a set of observed HD and VD responses into equivalent two-layer conductivity or susceptibility structures assuming that the height of the instrument operation is known and the thickness of the upper layer is known or can be assumed (e.g., Dafflon et al. 2013; McNeill 1980; Mester et al. 2011).

5.4 Survey Configuration and Measurements

On the 12th and 13th of July 2015, we investigated LbDt-1 using geophysics, remote sensing, surface survey and limited test pitting (Figure 5.2). The site was accessed via helicopter from Iqaluit (Figure 5.1), and while we had planned for a more extensive and comprehensive 7-day geophysical and archaeological survey, weather conditions restricted site access to just 2 days. The 2-day period was sufficient to allow high-density terrestrial laser scans to be completed over the whole upper component of the LbDt-1 site, including the debitage deposit. However, the limitations on field time required the geophysical objectives be modified from extensive coverage of the upper and lower LbDt-1 site to detailed coverage of representative grid areas and test lines.

Three survey grids were established in locations considered suitable to cover areas of archaeological interest and to include nearby natural background surfaces (Figure 5.2). Grid 1 is the primary survey grid and measures 44 m in the north-south direction by 13 m in the east-west direction. The grid overlooks the Hone River in the site's upper component and includes areas both within and outside the visible debitage deposit. Grid 2 is a small, 20-m north-south by 6-m east-west area directly adjacent to the west side of grid 1 and closer to the bank of the Hone River. It provides further assessment of the debitage deposit; TP1 is located within grid 2. Figure 5.5 shows the layout and ground surface of grids 1 and 2. Grid 3 measures 15 m by 8 m and was established over a gravel deposit surrounding a large, flat glacial erratic boulder about 30 m east of grids 1 and 2. Test lines 1 and 2 connect grids 1 and 2 with grid 3; TP2 is located at the intersection of these lines (Figure 5.3). Our discussion focuses primarily on results obtained from the grid 1 survey; however, we do include some results from grids 2 and 3 in our analysis.

A total of six full TLS point clouds were combined across the Upper Component of LbDt-1 using a Leica ScanStation C10. Individual stations consisted of a 360° x–y-axis digital image, a point scan at 0.1 m point spacing with a 45-m range and a focused point scan at 0.05 m point spacing with a 30-m range. The instrument height averaged 1.20 m for each scan. All surface scan data for this area were digitally combined using Leica Cyclone software; additional data processing was accomplished using LAStools and CloudCompare.

A 3D survey using a GSSI 400 MHz GPR system was conducted over grid 1 using a 1-m line spacing. To allow optimal coupling of the GPR signal with the slightly uneven ground, the antenna was towed using an extendable handle and survey wheel attachment. The real-time survey was run and viewed in GSSI's SIR3000 QUICK3D Grid Mode. Lines were completed in a continuous zig-zag pattern, with the antenna position being defined by the survey wheel

measurements. Soundings were collected at ~2 cm intervals along each line, and each sounding consisted of a 512 sample time series of ~ 50 ns, providing a depth penetration of around 2 m. GPR data were also acquired in grids 2 and 3, using a similar configuration to that in grid 1 and along test lines 1 and 2 (see Figure 5.2).

Electromagnetic data were only collected on grid 1. Measurements with the EMP-400 profiler were made using 1 m line and 1 m station spacing with the instrument 10 cm above the ground surface. IP and Q responses for three frequencies (1000, 4000 and 16,000 Hz) were recorded using the data logger. In order to minimise thermal drift, particularly in the IP measurements, the instrument was started about 20 min prior to beginning the survey (e.g., Robinson et al. 2004) and in order to assess the effects of thermal drift, repeat data were collected along a short test line at the start and end of each survey. Complete surveys were done with the instrument in VD mode and HD mode.

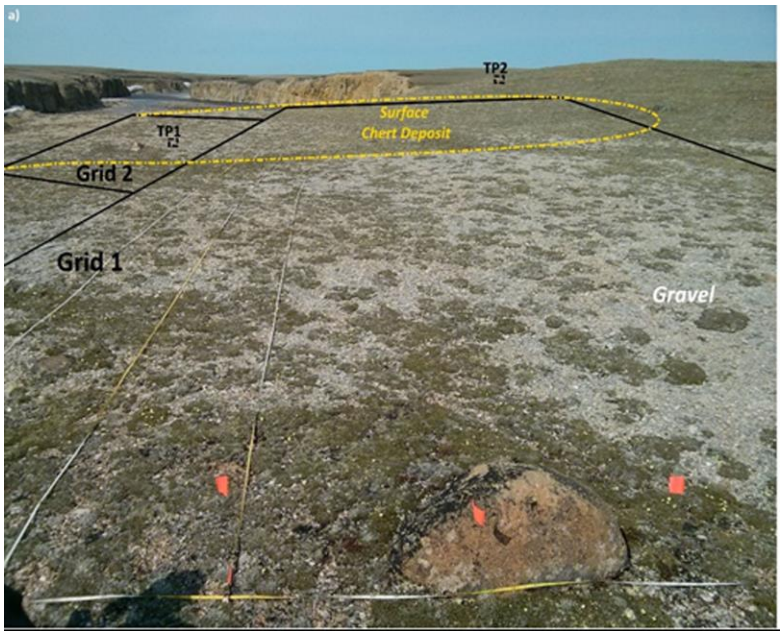

Figure 5.5 Photograph looking north from near the (0 N, 3 E) on grid 1. The locations of grid 2 and test pits TP1 and TP2 are shown. Note the absence of grass from the surface deposits of gravel.

5.5 TLS Data Processing and Results

TLS scans were used to create a detailed gridded point cloud image (see Figure 5.6a) and topographic surface map of grid 1 (see Figure 5.7). Along with field notes and photographs, this image was used to define the visible locations of important surface features for referencing to the sub-surface non-visible geophysical results. The surface of the debitage deposit is visible in the TLS point cloud image. The chert flakes and interspersed grass (see Figure 5.3) create a mottled texture. On the eastern side of grid 1, this visual estimation of the deposit extends from 15 to 32 N. The deposit continues across the grid and along the western side, extends from approximately 20 to 40 N.

A surface gravel deposit in the southern part of grid 1 appears as a lightly coloured region. This area is lighter and less mottled in appearance than the debitage deposit. It extends from 0 to ~15 N and is most prominent towards the middle of the grid. Sinuous narrow zones of

darker coloured areas in Figure 5.6 correspond to slightly low topography areas in grid 1. These areas contain thicker grass so are not easily evident in the topographic map derived from the point cloud data (see Figure 5.7). Finally, the TLS point cloud image also shows the side of a large boulder at the edge of the grid (at 0 N, 4 E) that is visible in Figure 5.5.

The TLS point cloud data are processed using a manual classification approach (see Landry et al. 2016, pp. 235–237). For this study, our primary classification scheme focused on isolating surface areas most intensely covered by debitage. This objective was met by identifying distinctive differences in surface colours and reflectivity of the materials in question.

In the first classification approach, we isolated the response of the cortical surface chert (see Figure 5.6b). The response was based on averaging the colour and reflective property parameters of the residual cortex present on many of the visible surface flakes (intensity-1492-1726; R-200-255; G-170-255; B-150-255). This response corresponds to a relatively high reflectivity (bright colour) and an overall light tan-ecru colour (as is visible in the photographs of the chert flakes in Figure 5.3b, c). This approach provides an effective indication of the major distribution areas of cortical surface chert (see Figure 5.6). The chert deposit is well outlined by the region in which there is a high density of points corresponding to the cortical chert responses. Allowing for the change in intensity with distance from the laser scanner, the results in Figure 5.6 suggest that the chert deposit has a relatively uniform distribution.

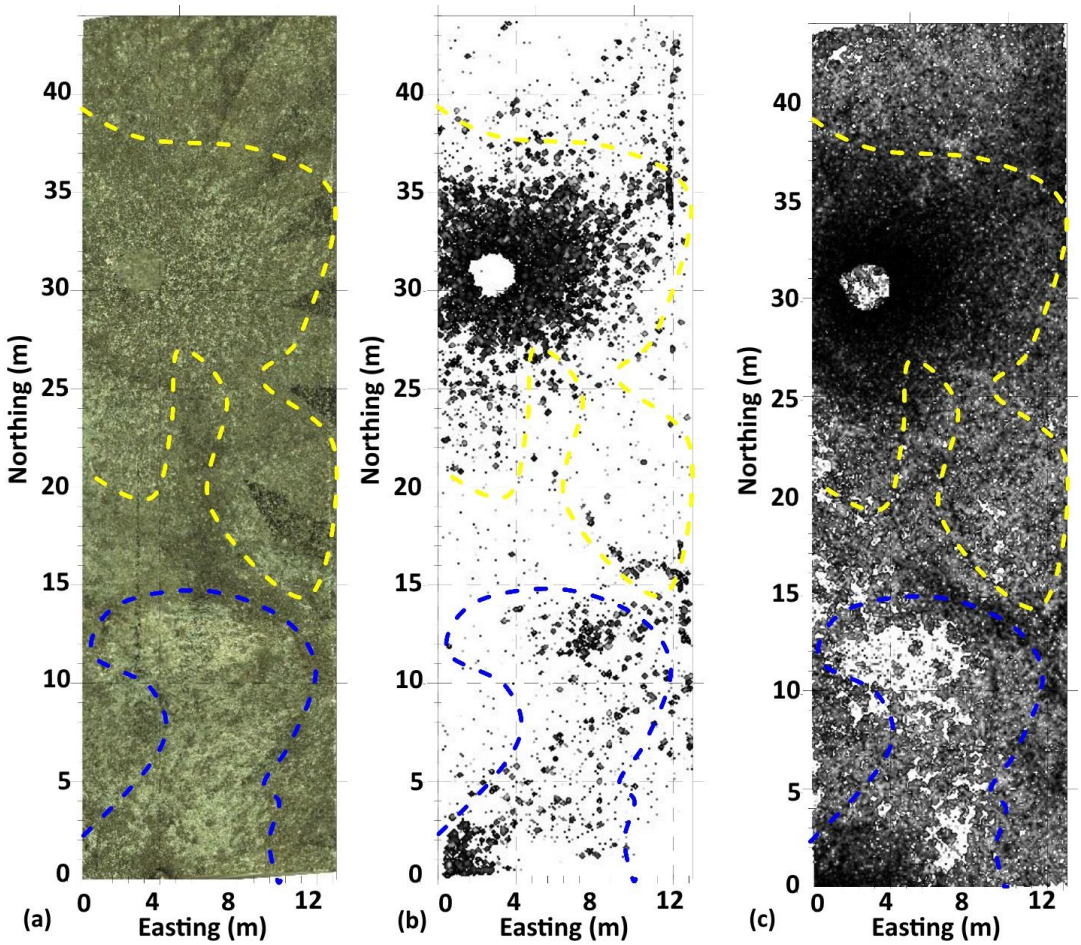

Figure 5.6 TLS images of grid 1. **a** Restored colour image of the grid. The yellow dashed line indicates the surface outline of the visible chert flake deposit, and the blue dashed line indicates the surface outline of the visible gravel deposit. **b** Density image of point classifications representing chert flakes with surface cortex. **c** Density image of point classifications representing grass. The circular gap in data centred on (31 N, 3 E) indicates the area where the TLS instrument was situated and points did not consistently overlap. Darker shade points indicate greater density of nearby neighbours in (**b**) and (**c**).

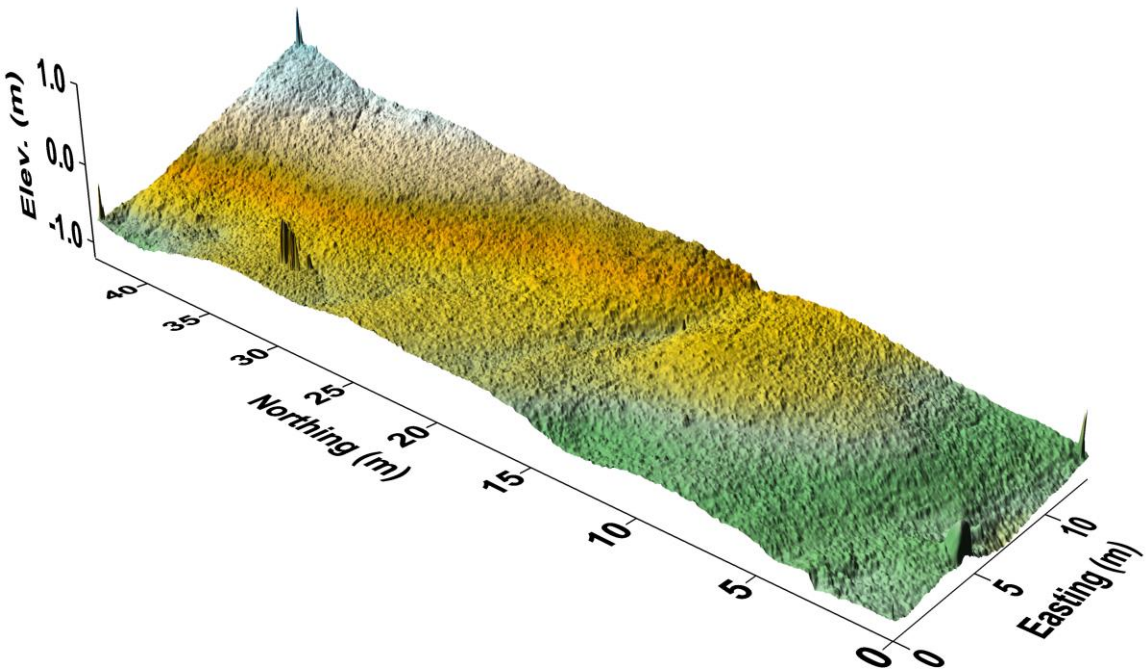

Figure 5.7 Topographic surface map of grid 1, using the TLS point cloud relative x,y,z, coordinate data. Gridding is based on natural neighbour interpolation and 5-cm cell sizes. The local topographic lows (around 15 N) correlate with the dark patches on the restored colour image seen in Figure 5.6**a**. A larger reflector is visible at (4–5 E, 0 N), along with a few residual data artefacts at the scanner position (0E, 34 N).

The initial point cloud does have some limitations and this result is to be expected when defining areas based on the response of relatively small-scale features (i.e., flakes of ~0.03 m). The classification also incorrectly detected several additional areas where there was no chert present (e.g., centred on 8 E, 12 N in Figure 5.6b). These areas are interpreted to contain gravel fragments with a similar texture and colour to the cortical chert fragments. Most of the gravel deposit has a distinct response relative to the chert, but there are some areas of gravel with overlapping characteristics.

In a secondary classification approach, we isolated the chert deposit more accurately by defining the area with points corresponding to both the cortical chert response and to grass. As

noted above, the chert deposits are observed to have grass growing between patches of chert flakes whereas the gravel deposits do not include similar patches. The grass was classified using the parameters (intensity-1492-1726; R-200-255; G-170- 255; B-150-255) corresponding to a range of green colours. Figure 5.6c shows the resulting density of point classifications. Most of the incorrectly identified areas of cortical chert in the south part of the grid lie in areas of thin to no grass allowing them to be excluded as parts of the chert flake deposit.

Overall, the results of the current study have defined the TLS response of the chert flake deposit. The spatial consistency of the TLS chert flake response is high in the northern half of grid 1. The colour overlap of the gravel and chert cortex caused some inconsistencies in the southern half; however, the classification of dark green grass surrounding the deposit served as an important detail to isolate parameters of reflection intensity in this area.

5.6 GPR Data Processing and Results

5.6.1 Unprocessed GPR responses

The GPR data collected at LbDt-1 were downloaded from the GSSI system and examined and processed using RADAN (GSSI) and GprViewer (J. Lucius and L. Conyers) software. Inspection of raw radagrams from the different areas of the site reveals a very complex response. Figure 8 shows the GPR responses from adjacent to TP1 in grid 1 and from adjacent to TP2 on test line 1. After zero-time correction of the traces, the results show the direct arrival and semi-continuous reflections at early two- Integrated Geophysical Techniques for the Archaeological... way travel times (<5 ns), low reflectivity between 5 and 20 ns and a significant increase in semi-continuous reflectivity at 20–30 ns. There is another zone of semi-continuous reflections at ~40 ns two-way travel time. When plotted at a high vertical scale, it is evident that the GPR

responses are strongly affected by scattering and a crowded sequence of closely spaced diffraction hyperbolas. The cusps of many of the hyperbolas occur at or close to zero time allowing them to be attributed to the debitage deposit and surface gravel at the site, confirming the presence of the scattering expected ahead of the survey. There are also a number of deeper hyperbolas with their apices associated with the deeper reflections.

Close inspection of the results the chert deposit indicates that the diffraction hyperbolas produce a dense clutter that degrades reflections from greater depth (labelled B in Figure 5.8a). The form of the hyperbolas can be seen most clearly in the relatively non-reflective zone between 5 and 20 ns. The hyperbola have a higher frequency response than the sub-horizontal reflections. On higher resolution plots than the one shown in Figure 5.8, the density of the hyperbola limbs is relatively uniform with around four to five limbs every metre. This density appears to be limited by the signal wavelength. The amplitude of the hyperbola signals is relatively uniform. At the scale of the image shown in Figure 5.8, these characteristics cause the response the GPR signals to appear as a fuzzy diffuse zone. The response shown in Figure 5.8 also contains several areas with more prominent scattering signals: in the area of the test pit (A in Figure 5.8a), which had been infilled prior to the GPR survey, and from an area about 10 m south of the test pit (C in Figure 5.8a). The slopes of the hyperbola limbs are relatively uniform with measurements of 10 individual limbs from the profile shown in Figure 5.8 yielding a slope of $S=0.113\pm0.01$ m ns^{-1}. The slope is related to the radar velocity by

$$v \sim 2S \qquad \text{Eq. 5}$$

yielding a velocity of 2.26 m ns^{-1} corresponding to a dielectric constant of 1.8.

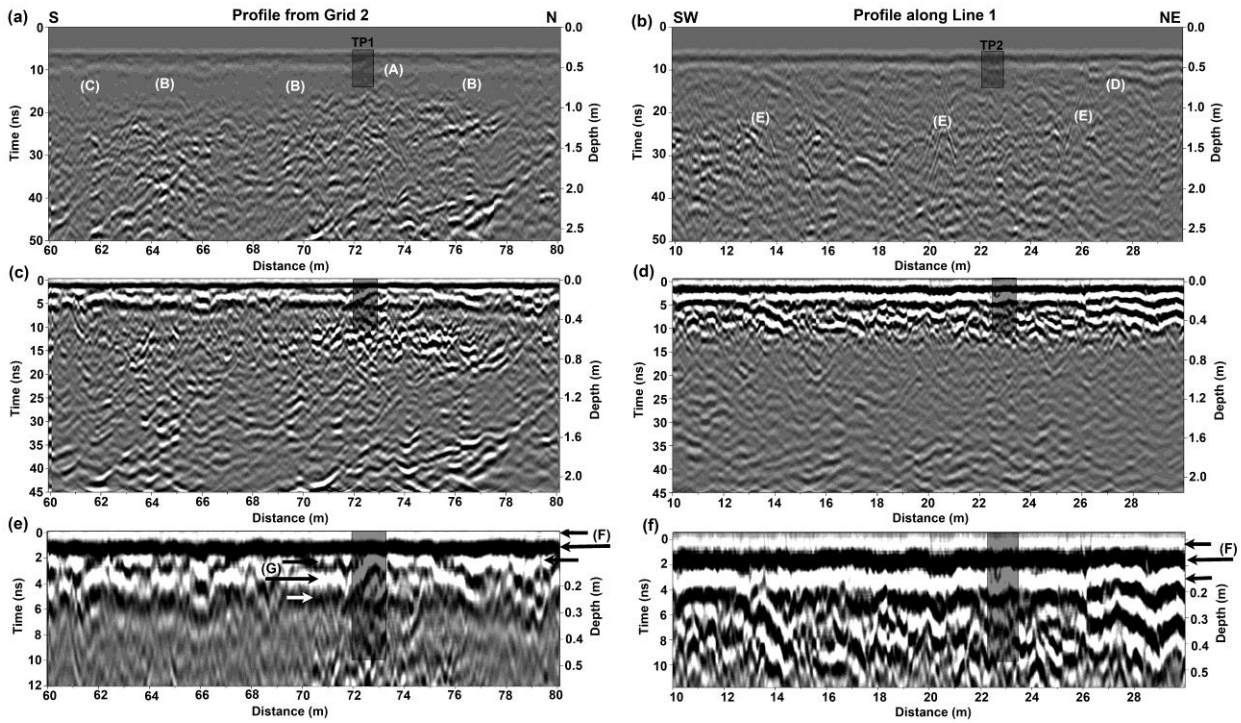

Figure 5.8 Raw and processed GPR responses from near Test Pits TP 1 and TP2 shown using a gray-shaded display. Shaded rectangles show approximate extent of each test pit. The depth scale is based on a dielectric constant of k=9. **a**, **b** Raw GPR data for 20 m long profiles containing TP1 (left) in an area of the chert deposit and TP2 (right) in a background area (see Figure 5.2). Labels indicate particular features of the GPR response: A, diffraction hyperbolas created by heterogeneities in the in-filled test pit; B, zone of extremely dense clutter caused by scattering at the ground surface creates a fuzzy texture when plotted at the scale shown; C, a zone of more discrete diffraction hyperbolas with cusps at the surface; D, diffractions from termination of a subhorizontal reflector; E, zones of more discrete diffraction hyperbolas with cusps at the surface. **c**, **d** The same profiles following standard GPR processing. Note the increase in the continuity of the deeper reflections. **e**, **f** Early time part of the processed GPR radargrams (0–15 ns). Arrows labelled F indicate the direct arrival with the long arrow pointing to the positive central peak of the recorded pulse and the short arrows to the negative side-lobes. Arrows labelled G indicate an early-time negative-polarity reflection with the long arrow pointing to the negative main peak and the short arrows to the positive side-lobes.

The strong scattering response observed in the unprocessed GPR data can be attributed to the assemblage of chert particles in the debitage deposit (Figure 5.3b, c) and is a characterising feature of the deposit. GPR studies from other locations have been characterised by scattering

from surface features. For example, a lower frequency GPR study from Turtle Mountain, Alberta, Canada showed strong diffractions from surface rocks (Theune et al. 2006). The diffraction velocities observed at the LbDt-1 debitage deposit are relatively fast and the corresponding dielectric constants are low. This observation supports the interpretation that the diffractions are due mainly to surface particles. The dielectric constant of chert is taken to be similar to that of quartz (k=4.5–4.7) (Knight and Nur 1987) and, assuming a simple complex refractive index mixing model (CRIM) (e.g., Annan 2005), the observed dielectric constant of 1.8 can be explained by a mixture of air and just a few percent chert. The high-frequency content of the diffraction response also supports the interpretation that the signals are travelling close to the surface and have undergone minimal absorption.

There is a larger variation of the amplitude of the diffraction signals in the background area near TP2, and this variation is interpreted to be due to the more sparse distribution and greater variation in the size of the rocks at the surface in that location. This variation can be seen in Figure 5.3d and in close inspection of exposed cliff edge beneath line 1 in Figure 5.2. The diffraction signals again have higher frequency than the semi-horizontal reflections. The slopes of the prominent hyperbola limbs (E in Figure 5.8b) indicate a signal velocity of 0.11–0.15 m ns−1 and a dielectric constant of k=4–7. The lower diffraction velocity in this area compared with in the debitage deposit is explained by an increased effect of a relatively dry soil layer. There is a zone of strong diffractions associated with the lateral termination of a sub-horizontal reflector about 4 m northeast of TP2 (labelled D in Figure 5.8b). Comparison of the GPR response with features seen on Figure 5.2 suggests that this feature is associated with slumping of the upper soil layers towards the cliff-face.

5.6.2 GPR data processing steps

Based on the initial inspection of the GPR responses, a data processing sequence (e.g., Conyers 2015, 2016) was established using the methods available in RADAN and GprViewer to improve the visibility of reflections in the results. The steps involved in the processing are as follows:

1. Correction of zero-time using the leading negative side-lobe of the superimposed air and ground wave.
2. High-pass filtering using a cut-off of 300 MHz.
3. Background removal by subtraction of a defined trace based on an average trace across the grid.
4. Diffraction migration to remove the effects of surface diffractions. This step was performed in RADAN. The migration is based on the parameters of hyperbolas fitted to observed diffractions in the various grids or profiles.
5. Display using formats and gain functions available in RADAN and GprViewer.

Because the area of the main grids is relatively flat (Figure 5.7), no correction is made for topography. Figure 5.8 shows the results of applying the processing to the GPR data near the two test pits. The processing scheme greatly improves the continuity and visibility of the horizontal reflections in the GPR sections. The diffractions are not completely removed and it is possible that further experimentation with a range of migration velocities may lead to further improvement in the sections.

Figure 5.9 shows the processed GPR responses from grid 1 displayed using the 3D display mode in RADAN and using section and depth slices in GprViewer. The data processing, and particularly the migration phase, leads to a significant improvement in the responses. In order to display the GPR sections from grid 1 using a depth scale, it is necessary to use a characteristic dielectric constant. We established this value using diffractions that could be reliably associated with the deeper reflections in the data. The manual hyperbolic fitting

procedure in GprViewer was applied to ten different diffractions in the grid 1 data yielding values for the dielectric constant of 9.9±1.5 (and a typical radar velocity of 0.095 m ns−1). This value is typical of relatively unsaturated sands or low porosity bedrock (Annan 2005; Kneisel et al. 2008; Gacitúa et al. 2012).

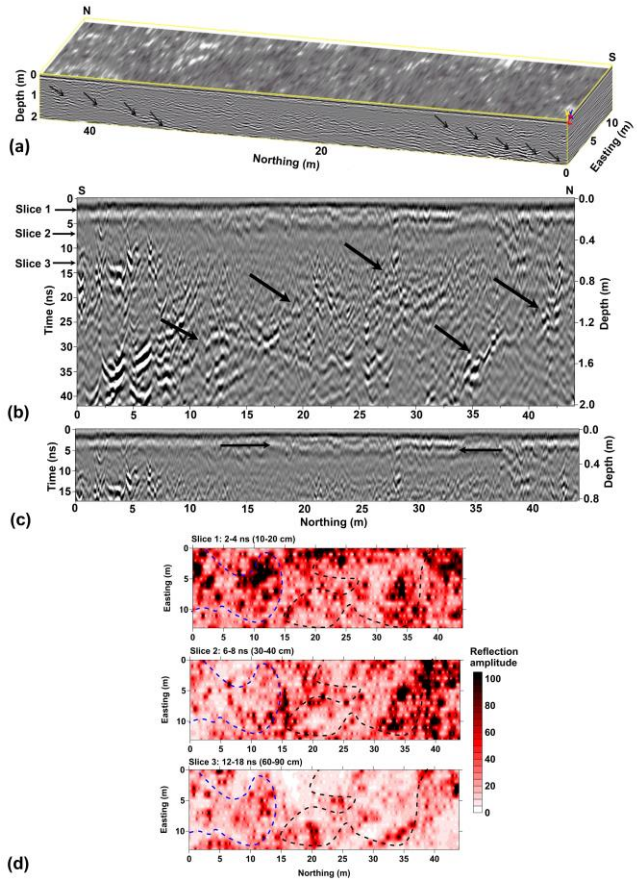

Figure 5.9 Processed GPR responses for grid 1. Depths are based on dielectric constant of k=9.9. a Perspective view from the southwest showing line 1. The upper surface corresponds to the amplitude response at 19 cm depth averaged over a depth range of 18 cm. Arrows on the vertical section indicate south-dipping reflectors. b View of line 1 at increased vertical exaggeration with the location of the top of additional depth slices marked. Arrows indicate south-dipping reflectors. c Enlarged view of first 16 ns of the line 1 response. Arrows indicate negative-polarity reflection interpreted to be the base of the debitage deposit. d Horizontal amplitude slices with black dashed line showing the surface distribution of chert and blue dashed line showing the distribution of gravel. The top of slice 1 is at 2 ns (or 10 cm depth) and the response averages over 2 ns. It highlights the amplitude of the negative polarity reflection. Slice 2 is at 6 ns (or 30 cm depth) and averages over 2 ns. Note the generally low amplitude reflections from the debitage and gravel deposits. Slice 3 is at 12 ns (or 60 cm depth) and averages over 6 ns. It highlights deeper reflections and shows the structures present at shallow depth in the north part of section (from 35 to 44 N) are mostly confined to more shallow depth.

5.6.3 GPR response of the chert flake deposit

There is a significant response in the early-time (upper 30 cm) GPR data that can be reliably associated with the chert flake deposit. As shown in enlarged early-time response in Figure 5.8, near TP1, there is an additional semi-continuous reflection (white coloured on the colour scale used in the figure) visible at ~1.5 ns or 8 cm depth that is clearly absent from the background area near TP2. A similar feature can be observed at ~2 ns or 15 cm depth in the enlarged early-time response in grid 1 (Figure 5.9c). On line 0 E, this feature extends from 15 to 33 N, and based on comparison with the location of the chert deposit (e.g., Figure 5.6), the feature can be confidently linked to the chert flakes. Similar correlations between the observed response and the mapped area of the deposit also occur for the other lines in grid 1.

After removal of surface diffractions, the early time GPR arrivals in the area of the debitage deposit are expected to consist of the air wave, the ground wave, internal diffractions from within the chert flake deposit, and a reflection from the base of the deposit. For a near-offset system such as the GSSI 3000, it is more difficult to discern between these signals as they will be superimposed on each other. The consistency of the sign and the uniformity of the amplitude of the chert deposit signal seen in Figures 5.8 and 5.9 suggest that it is not a diffraction signal and, therefore, that it is a reflection from the base of the debitage deposit.

In order to examine whether this signal is indeed a reflection from the base of deposit, it is necessary to examine the GPR responses in closer detail. Figure 5.10 shows the GPR wiggle trace response for several representative locations at LbDt-1. The response in background areas of grid 1 and elsewhere such as near TP2 consists of a single positive pulse (with its peak to the left as plotted in Figure 5.10) that can be related to the superposition of a direct arrival through the air and a direct arrival through the ground. We use the maximum of this pulse as the zero-

time reference in the analysis. In areas of the surface gravel deposit and the chert flake deposit, a strong negative arrival is visible with its peak at 2 to 4 ns after the direct arrival. The sign of this arrival is consistent with that of a reflection caused by a decrease in the radar velocity (i.e., an increase in the dielectric constant) (e.g., Annan 2005). A transition from predominantly debitage to background soils would create a reflection with this sign. The time of the negative pulse in areas adjacent to TP1 is 3 ns, and using the dielectric constant determined from grid 1, this time would correspond to a depth of 14.5 cm. This depth matches the observed thickness of chert in TP1 (15–20 cm) very well. Finally, following the main negative pulse, there are a series of positive and negative peaks that can be explained by multiple reflections from within the chert deposit. The large apparent amplitude of the multiples in Figure 5.10 is due to the gain factor applied.

Overall, the spatial correlation of the signal with the observed extent of the debitage deposit, the sign of the signal, the uniformity of the signal and the agreement of its timing with the observed thickness of the chert deposit in TP1 allow us to confidently attribute the signal to a reflection from the base of the debitage deposit. The interpretation was also further confirmed using an experimental survey with the same radar system in which the reflections from the base of an increasing thickness of concrete paving blocks was studied (Campbell 2016). The basal reflection from the chert deposit, indicates that across much of the mapped area the chert is 10 to 15 cm thick.

To examine the spatial extent of the reflection from the base of the debitage deposit, we used GprViewer to view the reflection amplitude through three 2–4 ns time slices (Figure 5.9d). The result shows patches of increased amplitude within the areas of the debitage deposit, but it provides a relatively poor mapping of the lateral extent of the reflector. Alternative time slices

(e.g., 0–2, 3–5, and 4–6 ns) were less effective at outlining the deposit. The lateral variation in the depth and amplitude of the reflection means that the response is most accurately defined in section view. The distribution of the chert is examined in more detail below.

There are also near-surface reflections observed in the southern part of grid 1 corresponding to the area of the surface gravel deposit. These can be seen in the wiggle trace display in Figure 5.10 and in the line 1 sections and the 2–4-ns time slice in Figure 5.9. These reflections are typically more shallow (3–7 cm) than the reflections from the base of the debitage deposit (>9 cm) and are less spatially uniform. The observations suggest the gravel deposit consists of a concentration of gravel particles in a relatively thin (<10 cm) surface layer that likely formed as a result of cryoturbation processes.

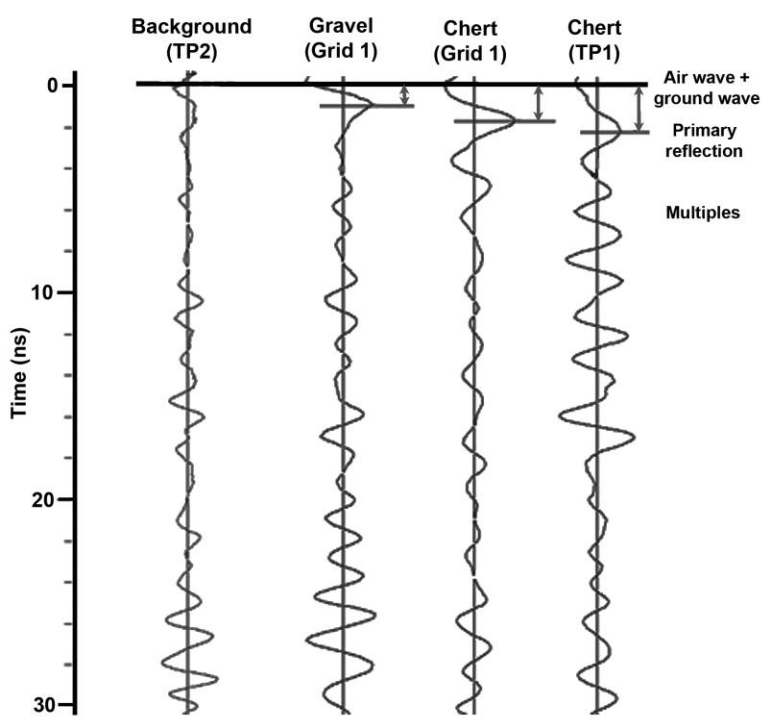

Figure 5.10 Comparison of GPR signals from representative locations of LdBt-1 using wiggle trace format. The background results are for an area with mainly soil at the surface whereas the remaining plots are for areas with gravel or chert flakes at the surface. Note that a deflection to the left corresponds to a black colour in Figures 5.8 and 5.9.

5.6.4 Deeper GPR responses

At greater depths, the GPR data define a sequence of shallowly south-dipping reflections (Figure 5.8). We interpret these reflections as being associated with more reflective units in the limestone bedrock underlying the site. The bedrock is visible along the banks of the Hone River (Figure 5.2) although it is not possible to define a clear dip in the observed rocks. The GPR reflections increase in depth by ~1 m over horizontal scales of ~20 m corresponding to apparent southward dips of 2° to 3°. The GPR results from grids 2 and 3 also show similar south-dipping reflections. The deeper reflections produce an irregular zone of increased signal amplitude in the 12–18-ns (60–90 cm) time slice (Figure 5.9d). The results suggest a very irregular bedrock surface which is consistent with the observations of bedrock in the cliffs of the Hone River. Where it is visible, the bedrock consists of consolidated blocks of several-metre scale and occasional boulders interspersed with extensively weathered material.

It is noted that the bedrock reflections from beneath the debitage deposit are very poorly resolved. Decreased reflection amplitudes are seen in the area of the debitage and gravel deposits in the 6–8-ns time slice (see Figure 5.9d). Examination of the grid 1 section response in Figure 5.9b shows that the deeper reflections in these areas are obscured by the strong scattering at shallow depth. Reflections were affected by the migration applied in the GPR processing and are further obscured by residual diffractions. These observations suggest that the debitage deposit can be additionally characterised in GPR studies by the effects of its scattering (in a similar approach to the use of scattering responses by Valls et al. 2016).

5.7 Electromagnetic Survey Data Processing and Results

5.7.1 Raw IP and Q responses

The EMP-400 IP data were first corrected for thermal drift using linear interpolation and repeat base station measurements. The EMP-400 Q data were also checked for drift, but no correction was necessary. Comparison of the EMP-400 results at different frequencies showed that the lower frequency responses were relatively noisy as may be expected in a very resistive environment (see Bonsall et al. 2013). The remaining analyses were therefore restricted to the higher frequency 16,000 Hz data set. The EMP-400 Q responses were converted into equivalent apparent conductivity values using the standard formulae (e.g., Fitterman and Labson 2005). The raw IP data provided in the files downloaded from the instrument consist of the ratio of the secondary IP magnetic field to the primary magnetic field (HsIP/Hp). Denoting the in-phase component of the ratio for the HD and VD components as IHD and IVD, respectively, the results can be converted into equivalent apparent susceptibility values using:

$$\kappa_{aHD} = 2I_{HD} \cdot \left(I_{HD} + 1\right)^{-1} \qquad \text{Eq. 6}$$

and

$$\kappa_{aVD} = 2I_{VD} \cdot \left(I_{VD} - 1\right)^{-1} \qquad \text{Eq. 7}$$

(e.g., Dalan 2006; Huang et al. 2003). No corrections are made for instrument elevation in these conversions. In the raw EMP-400 IP data, the spatial variations in the HD and VD data have opposite signs but the conversion of the HD mode response into apparent susceptibility reverses the sign of that response (as shown in Figure 5.4d) (Dafflon et al. 2013; McNeill 1980).

Figure 5.11 shows variograms and contour maps of the electromagnetic responses. The mean and standard deviation of the HD response are 5.7 and 0.7 mS m−1, and for the VD response, they are 5.4 and 0.4 mS m−1. Figure 5.4a shows the depth penetration of these responses; the results define a relatively resistive response over the uppermost 1 m at LbDt-1 with no significant variation in conductivity with depth. The mean value for each response is well defined in a statistical sense. However, the patterns of the much smaller spatial variations in the responses (0.7 mS m−1 for the HD response and 0.3 mS m−1 for the VD response) are poorly defined. The apparent conductivity responses have variograms that are close to those of random data with only a small, approximately linear, decrease in variance between closely-spaced points. It is possible that the spatial patterning of the conductivity responses may in fact relate to isolated drainage and moisture properties in the soil. However, there is no visible association between the conductivity responses and the TLS topographic dataset depicted in Figure 5.7. The large-scale patterns in the HD response exhibit weak correlation with the distribution of the chert and gravel deposits. However, inspection of the raw data show that this pattern results from heavy spatial smoothing of a number of isolated resistive patches in these deposits so the result cannot be considered entirely reliable. The VD results suggest a slight increase in conductivity to the east of the grid but examination of the raw data again suggests that this result is not very reliable. Overall, the EMP-400 apparent conductivity results provide minimal information on the debitage deposit beyond providing evidence that the upper metre of soil at the LbDt-1 site is relatively uniformly resistive.

The EMP-400 apparent susceptibility shows evidence of more significant spatial variations in magnetisation than in electrical conductivity. The observed variograms for these responses can be fitted by two-component models consisting of a linear component and an

exponential component defining a strong decrease in variance between closely spaced points (see Figure 5.11). The length scale of the exponential function is 1.5 m for the HD response and 0.9 m for the VD response. Figure 5.11 shows contour maps produced using the fitted variogram models. The apparent susceptibility values range from ~10−4 (SI) to >10−3 (SI). For both responses, the highest values of susceptibility are observed in the northwest part of grid 1 and the lowest values in the south part of the grid. Overall, the HD response exhibits greater spatial uniformity and lower susceptibility values compared with the VD response.

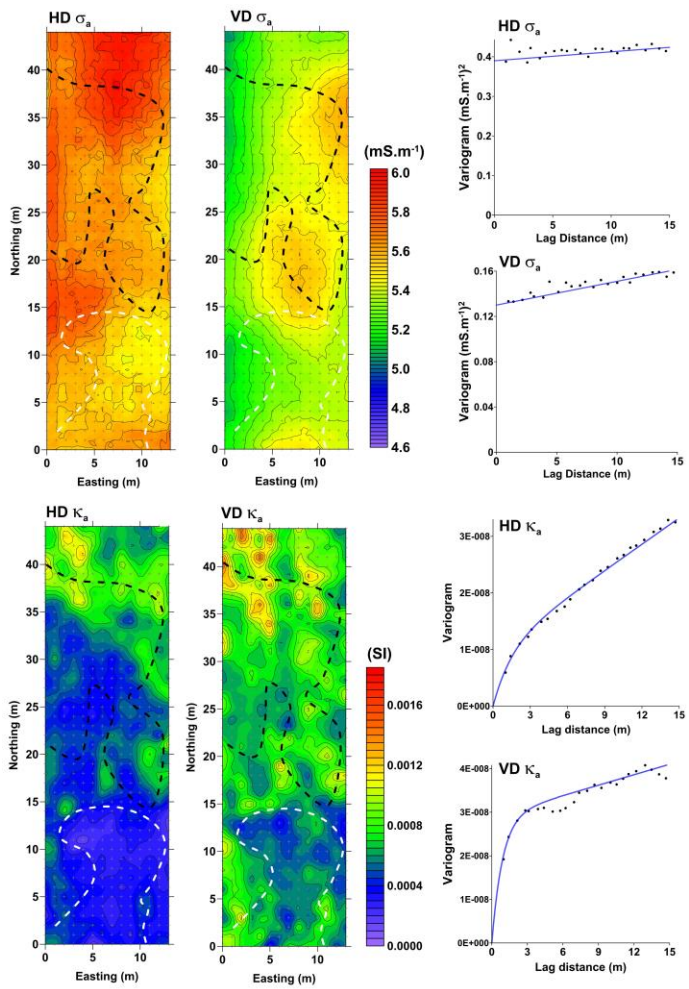

Figure 5.11 EMP-400 16,000 Hz Q and IP responses plotted in terms of apparent conductivity (upper panels) in mS m−1 and apparent susceptibility (lower panels) in SI.

5.7.2 Two-layer inversions of the IP data

To further interpret the magnetic results the pairs of HD and VD readings at each point were inverted using the corresponding sensitivity functions to yield a two-layer model of the susceptibility. The approach is simpler than simultaneous inversion of in-phase and quadrature responses to derive conductivity and magnetic susceptibility structure (e.g., Huang and Fraser 2003). As noted above, the very resistive environment and LIN condition means that it is possible to use the IP response in the independent evaluation of magnetic susceptibility. We use the approach of Dalan (2006) and others to partition the sensitivity of the LIN magnetic response into contributions from individual underlying layers, in our model, an air layer and two underlying earth layers. In the case of a two layer model with an interface depth z1 and the instrument at height h above the surface, the measured responses will be related to the true susceptibility of each layer by:

$$I_{HD} = \frac{-\kappa_1}{2+\kappa_1}\left[R_{\kappa HD}(r,h) - R_{\kappa HD}(r,h+z_1)\right] + \frac{-\kappa_2}{2+\kappa_2}\left[R_{\kappa HD}(h+z_1)\right] \qquad \text{Eq. 8}$$

and

$$I_{VD} = \frac{-\kappa_1}{2+\kappa_1}\left[R_{\kappa VD}(r,h) - R_{\kappa VD}(r,h+z_1)\right] + \frac{-\kappa_2}{2+\kappa_2}\left[R_{\kappa VD}(h+z_1)\right] \qquad \text{Eq. 9}$$

where the functions RκHD(r,z) and RκVD(r,z) are cumulative sensitivity functions defined by the integrals of the sensitivity functions shown in Figure 5.4b. For moderate values of susceptibility, it is possible to neglect the value appearing in the denominator of each of these equations (since κ<2), and the result leads to two linear equations for the observed responses in

terms of the susceptibility of the two layers. It is straightforward to rearrange the resulting equations to obtain the susceptibility values in terms of the observed responses. So, for example, for a 20-cm-thick upper layer and a 10-cm instrument height, after substituting for the sensitivity functions, the result for the susceptibility of each layer is:

$$\kappa_1 = 1.706\, I_{HD} + 4.1096\, I_{VD} \qquad \text{Eq. 10}$$

and

$$\kappa_2 = -3.3334\, I_{HD} - 1.3589\, I_{VD} \qquad \text{Eq. 11}$$

For this particular model, it is evident that the susceptibility of the 20-cm-thick top layer will be most similar to the VD EMP-400 IP response (since the coefficient of that response is the larger term in Eq. 6) and the susceptibility of the underlying layer will be most similar to the negative of the EMP-400 HD IP response. The results match the sensitivity of the EMP-400 IP responses to thin surface layers shown in Figure 5.4d.

In order to complete the two-layer analysis of the magnetic data using only two measurements (HD and VD) of the IP response, it is necessary to know or assume the interface depth. As this depth was unknown in our study, we proceeded by calculating two-layer models for a range of specified interface depths. We selected the preferred result from the suite of resulting models by examining the spatial correlation of the susceptibility in the upper and lower layers and choosing the model exhibiting the least correlation. The basis for this approach is that it may be expected that there are different geological or archaeological factors controlling the magnetic susceptibility at shallow depth and at larger depth, and the model with the least

correlation between the layers will therefore have an interface depth that best separates these processes. Computations were completed for a large number of possible interface depths using an automated MATLAB code.

The results of the two-layer susceptibility determinations are shown in Figure 5.12. The optimal interface depth of 20 cm yielded almost zero spatial correlation between the upper and lower layers. Figure 5.12b, c shows the variograms and contoured maps of the susceptibility in each layer for the optimal model. The lower layer shows an approximately linear variogram model and yields relatively large spatial scale variations in the contoured results. In contrast, the susceptibility in the upper layer is dominated by relatively small scale spatial features. As expected, the shallow layer response most resembles the VD IP response and the deeper layer response most closely resembles the HD IP response. The two-layer susceptibility maps both show high values in the northern part of grid 1, between 37 and 44 N.

Comparison of the upper layer susceptibility for grid 1 with the distribution of the chert and gravel deposits reveals significant correlations. The susceptibility tends to be higher (>0.006 SI) and more spatially variable outside the areas where chert or gravel is situated on the surface (which have susceptibility of ~0.004 SI). This result is consistent with the shallow soil having higher susceptibility than the chert or dominantly limestone gravel particles. There is a weaker indication of the same pattern in the results for the lower layer (with susceptibility values of 0.002 SI outside the deposits and < 0.0005 SI inside the deposit), suggesting that the two-layer model may be an oversimplification of the actual structure. For example, the true structure may involve a more gradual decrease in susceptibility rather than a sharp interface. However, it is of note that the 20-cm interface depth determined in the analysis matches with the GPR defined base of the chert deposit.

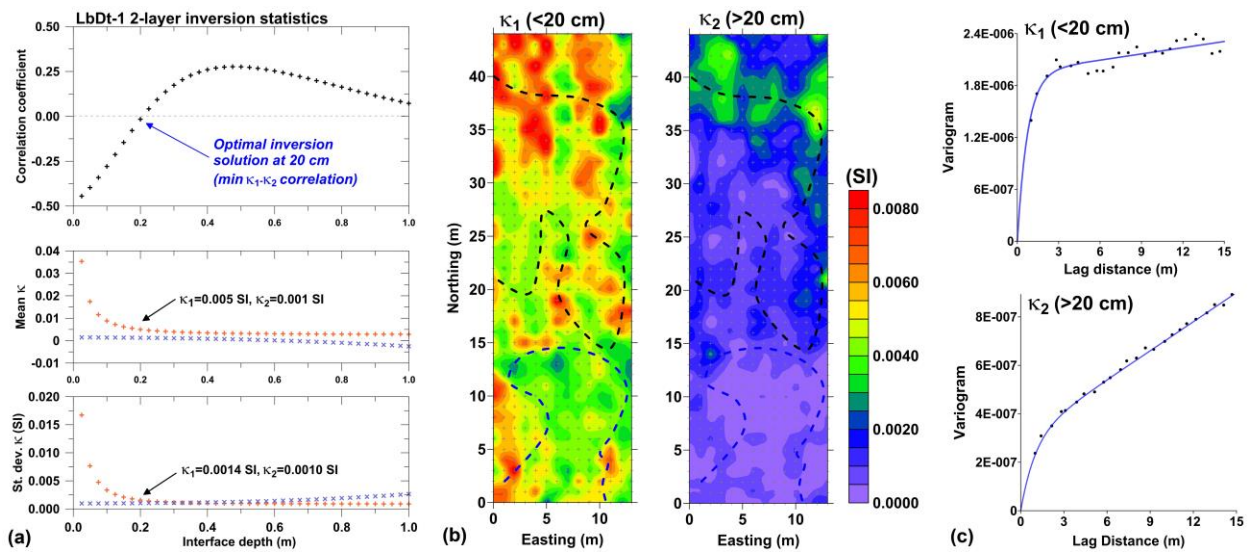

Figure 5.12 Results of two-layer magnetic susceptibility inversions. **a** Statistics of the inversion process showing for the different interface depths the correlation of susceptibility in the two layers (upper panel), the mean value of susceptibility in each layer and the standard deviation of susceptibility in each layer. **b** The contours of susceptibility in each layer for the optimal model with an interface depth of 20 cm. **c** Variograms of the spatial variation of susceptibility in the upper and lower layer. The fitted variograms were used to produce the contoured results in (b).

5.8 Integration of remote sensing and geophysical results

The TLS results from grid 1 produce a detailed record of the in situ distribution of chert as seen above the surface. These results illustrate three major surface components: (1) surface gravel coverage in the southern-most areas, (2) surface grass coverage across most of the central and northern parts of the grid and (3) surface chert deposit coverage. It provides us with important spatial information concerning the visible extent, possible frequency and preferential use of the landscape for transport and primary reduction. Ultimately, the scan results suggest that the highest coverage of surface chert is in the central and north-western portion of grid 1. This coincides with an area more generally covered with patches of grass and a thinner underlying soil layer than in surrounding areas as shown through the lower susceptibility values in the susceptibility inversion results. The southern-most area lacks any intensive chert coverage

suggesting that tool stone reduction and deposit activities were mainly occurring near the central and uppermost parts of this grid.

The GPR reflection results as seen over grids 1 and 2 provide a detailed outline of the variability of depth and distribution of the base reflection layer across this area. The depth to the early-time reflection was determined from the processed radargrams at multiple points along each line in the two grids, and the values were then collated and contoured to form a map of the depth to the base of the surface layer (Figure 5.13). At some locations on grid 1, there is a faint first reflection, and then a stronger second one. The fainter one was interpreted to be an internal reflection from the chert deposit and the stronger reflection to be the base of the chert layer.

Two specific areas are noted in Figure 5.13. Most of the chert deposit that covers both grids 1 and 2 (labelled A in the figure) has a surface layer thickness of over 9 cm. In some areas of the chert deposit, this depth exceeds 11.5 cm. Comparison of the GPR results and the TLS point cloud images of this area shows moderate consistency between the area of the debitage deposit as defined by the remote sensing method and the relative depth and distribution of the deposit beneath the surface as defined by the GPR method (Figure 5.13). Test pit TP1 (Figure 5.3b) is located in grid 2 in one of the thickest areas of the debitage deposit. Much of the area surrounding the debitage deposit has a relatively thin surface layer. Beneath the area of the gravel deposit, the surface layer (labelled B in Figure 5.13) is thinner than in the debitage deposit and is typically only 4–7 cm thick.

The integration of surface and subsurface imaging of the debitage deposit permits quantitative characterisation of the significant size of the deposit. Using the TLS and depth-to-reflector information, we calculate a size of ~450 m2 and a volume of ~37 m3for the chert deposit.

The GPR time slice results and magnetic susceptibility provide some additional support for the interpretations of the TLS and GPR reflection data and show areas of high reflection amplitude and relatively low susceptibility in the area of the debitage deposit (see Figure 5.13). Individually, these responses are not as diagnostic as the TLS and reflection depth information for imaging the deposit and they do not provide effective discrimination between the debitage and gravel deposits (see Figure 5.13). For the GPR response, experimentation with different slice depths and thicknesses shows that it is difficult to define a slice depth and thickness that adequately captures the response of the whole deposit. For the magnetic response, spatial variation observed in the apparent susceptibility results is likely due to variable amounts of top soil mixed with the chert fragments and departures of the structure from the assumed two-layer model.

The two-layer susceptibility maps show high values in the northern part of grid 1, where it is of note that the GPR results also show significant reflections at less than 50 cm depth (see Figure 5.14). This correlation is clearest at the 35 N point on line 1 and can also be observed on adjacent lines (e.g., compare the reflection amplitude and upper layer magnetic susceptibility in Figure 5.9c, d). The high susceptibility is observed in both the shallow (<20 cm) and deeper (>20 cm layers). It seems fairly unlikely that the responses are due to the bedrock as the limestone rocks underlying the site will have only weak magnetisation. It is possible that the correlated responses are related to cryoturbation processes and movement of more highly magnetic topsoil to increased depth. However, the spatially correlated increase in the susceptibility in the top layer and the location of the features adjacent to the margin of the chert flake deposit suggest that the responses represent anthropogenic features.

There are several anthropogenic activities that can increase the magnetic susceptibility of the soil including the use of fires and disposal of organic material in a midden (e.g., Evans & Heller 2003; Dalan 2006; McNeill 2012). Campfires in this area of the observed anomalies would make sense as raw material acquisition and primary flintknapping activities of this scale would have to occur outdoors during the summer months, where a fire would not only provide warmth, but also deter the presence of animals and mosquitoes in this area. It is of note that the location of the possible campfires is just outside the chert flake deposit. Urban et al. (2012) also attribute zones with similar magnetic susceptibility (~0.0032 SI) and about the same, 5 m spatial scale, at an Inupiaq village site in Kobuk Alaska to a region of burning.

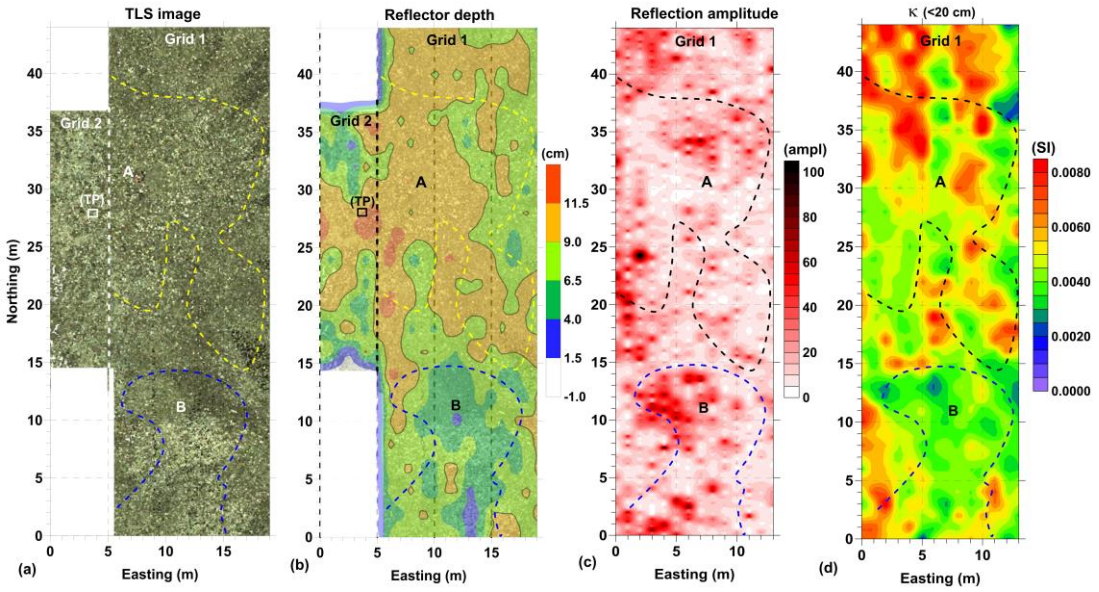

Figure 5.13 Multi-method imaging of the debitage deposit. Areas labelled (a) and (b) represent the estimated surface extent of the chert debitage and gravel distributions, respectively. a TLS surface point cloud image of grid 1 and grid 2. b Depth to the base of surface layer as indicated by primary reflection in the GPR response. The reflector depth results show a wider distribution of a thick (>9 cm) layer beneath the visible debitage deposit. In contrast, the depth of the reflector beneath the visible gravel deposit is relatively shallow (<4 to 7 cm) and is fairly distinct in the southern portion of grid 1 and parts of grid 2. c Near-surface radar slice (2– 4 ns) showing location of reflections from the base of the chert layer. d Magnetic susceptibility in upper 20 cm showing relatively low values in the debitage and gravel deposits.

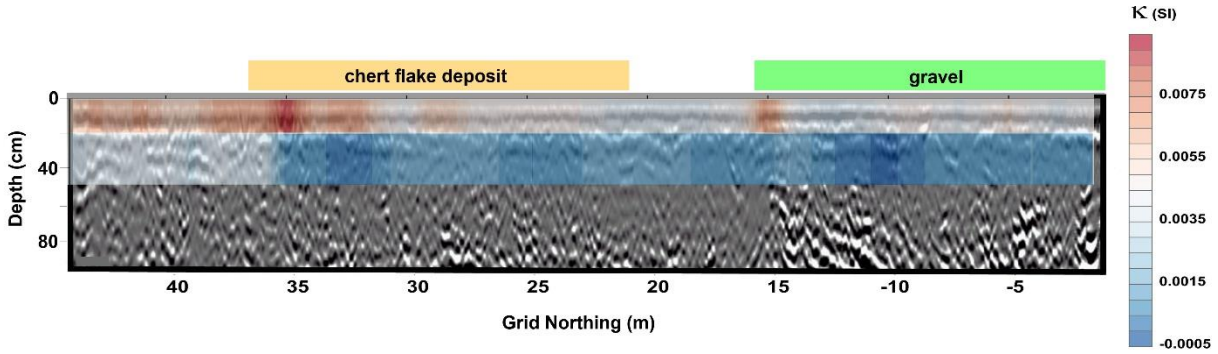

Figure 5.14 Two-layer magnetic susceptibility results overlain on the GPR section for the 3-m E line of grid 1. The high susceptibility values in the lower layer at the north end of the line are spatially correlated with deepening GPR reflections and high susceptibility values in the upper layer**.**

5.9 Discussion and Conclusions

The combination of TLS and geophysical datasets from LbDt-1 provides a non invasive investigative approach for lithic quarry sites in the Arctic. An examination of the surface and sub-surface data provides insight into the extent and depth of a large debitage deposit and provides the opportunity to further explore this prominent feature of the LbDt-1 quarry without the need for invasive wide-scale site excavation. The Figure 5.14 Two-layer magnetic susceptibility results overlain on the GPR section for the 3-m E line of grid 1. The high susceptibility values in the lower layer at the north end of the line are spatially correlated with deepening GPR reflections and high susceptibility values in the upper layer surface data collected using TLS indicates that the largest surface distribution and density of chert flakes is found within the central to northwestern portion of grid 1. This result suggests that the greatest deposits of chert layers in the sub-surface likely occur in this location and tells us where the most recent prehistoric activities and deposits of this area exist. The GPR data include a number of diffractions and reflections defining subsurface layering at the site. However, the interpretations

of the GPR responses were not apparent until migration and filtering of the GPR data occurred. A signal occurring in the early part of the GPR response was identified confidently as a primary reflection from the base of a surface layer and could be used to map the thickness of the surface chert and gravel deposits. Finally, a two-layer susceptibility model fit to the electromagnetic data from LbDt-1, demonstrates a decreased susceptibility in the upper 20 cm at locations where chert or gravel are present on the surface. Additionally, the electromagnetic data indicate an apparent high level of magnetic susceptibility along the northernmost portion of grid 1 and may in fact correlate to the use of fire in this area (Dalan 2006).

5.9.1 Remote Sensing and Geophysical Interpretations

Through the integration of these non-invasive remote sensing and geophysical methods, we were able to map the surface distribution and the base of the debitage deposit and the background responses throughout the survey grids.

The individual particles in the chert deposit cause the raw GPR response to be characterised by a dense set of diffractions. The relatively high velocity of these diffraction signals indicates that the diffractions are caused by the surface chert particles. These diffractions give the radargrams an almost fuzzy appearance in the 30 cm to 1 m depth range. Outside the chert deposit, there are additional surface diffractions in the gravel deposit and elsewhere. The amplitude of these diffractions tend to be more variable than those in the chert deposit, suggesting there is less variation in the particle size within the deposit. The diffractions from the surface particles can be minimised by the diffraction migration of the response.

To convert the GPR responses into depth sections we made use of velocity estimates derived from deeper diffractions with hinges on sub-surface reflections. A velocity of 0.095

m.ns−1 corresponding to a dielectric constant of 9.9 was used. The zone between about 20 cm and 1 m depth, corresponding to the unfrozen active zone, has relatively low reflectivity in the GPR response perhaps due to long-term cryoturbation processes. An increase in the reflectivity and diffraction density occurs at 1 m depth. This response dips downwards towards the river in the grid 2 GPR data. It is interpreted to correspond with the depth to the top of the permafrost layer in this region (see Vickers 2011). This layer is important to note as degradation on the parts of the LbDt-1 site nearest to the eroding river's edge could impact the future stability of the site. Longer-term monitoring of this response and other properties within the upper layer will provide insight into the pace of erosion and potential loss of the LbDt-1 debitage deposit. At greater depth, the GPR results define a sequence of bedrock layers that dip gently to the south.

The results of this study demonstrate the successful combined investigative application of remote sensing and geophysical methods among archaeological sites in the Arctic. The TLS data collection and results are useful for objectively categorising the surface materials and response at the LbDt-1 quarry. While the TLS results were more complex than we had previously expected they would be, the limitations encountered were due to the intermixing of surface materials and the general similarities between the surface properties of the chert and the weathered limestone gravel. Improved results were obtained by using the properties of the residual cortex present on surface debitage and raw chert rather than relying only on those parameters attributed to the chert in general and the spectral responses of the vegetation associated with the chert deposit.

The GPR data provided significant results throughout this study including positively identifying the subsurface depth and distribution of the entire debitage deposit. However, there is a need to develop an appropriate data processing scheme and to use caution when interpreting the resulting data to achieve these objectives. Had we used a higher-frequency antenna, we

believe we could have isolated the nearest layers in the data with even greater precision. That said, the responses would have been affected more significantly by scattering from the particles in the chert deposit. We strongly suggest that future studies use a combination of 400 and 1000 MHz in order to fully characterise the near sub-surface layers, in addition to the deeper permafrost and bedrock layers. Additional techniques such as elevating the GPR instrument to separate the air wave from the ground reflections could also be investigated.

The electrical conductivity results derived from the electromagnetic responses are not very useful except for defining a relatively uniform resistive structure at LbDt-1. Similar limitations have been observed in other Arctic surveys (see also Landry et al. 2015) and are in agreement with the high resistivity often observed in cryosolic soils in Canada (Tarnocai and Bockheim 2011). In contrast, the magnetic susceptibility results derived from the electromagnetic data did provide new and useful site information and were appropriate for determining the general spatial variabilities and layering in the subsurface, albeit at a lower resolution when compared with the GPR data when attempting to isolate the debitage deposit.

5.9.2 Archaeological Significance and Conclusions

The combined results of grids 1 and 2 provide evidence for localised reduction activities within grid 1 at this quarry site. The repeated use of this same location suggests liberated nodules of chert that eroded out of the limestone bedrock exposure were gathered by Paleo- Inuit toolmakers in the site's lower component and then brought to the upper component where reduction occurred in the open area near the bluff that overlooks the Hone River. The debitage analysis indicates the nodules were minimally modified, if at all, before they were transported to the upper component and the deposition of thousands of large primary cortical flakes around

these grids suggests modification was limited to raw material testing and primary reduction. The survey results indicate that the aerial extent of the deposit is ~450m2 and its total volume is ~37 m3, suggesting that the Paleo-Inuit used this quarry extensively during their travels inland. However, no evidence of middle- to late-stage tool reduction occurring or any sign of discarded tools indicates short-term occupations at the site as they collected new raw materials for future use.

The use of a multiple method non-invasive investigative approach has contributed to our overall understanding of this extensive quarry deposit without the need for wide scale archaeological excavation. That we were able to use the resulting data to measure the overall surface extent of the debitage deposit, estimate variations in its depth across the site and calculate the volume of resulting knapping debris is a major contribution to archaeological studies on lithic quarries. In applying this method of investigation to other quarry sites in this region of Baffin Island, we can begin to compare how intensively these sites were used over time and how they correlate to the large inland and coastal habitation sites where chert acquired from them, including LbDt-1 (see ten Bruggencate et al. 2016a), has been found. If archaeologists can begin to use this approach or one inspired by it, it will go a long way to reducing the ambivalence many researchers have towards investigating quarry sites, thus allowing us to better understand the pivotal role these lithic acquisition sites play in the technological organisation of hunter-gatherer lithic toolkits over time (Andrefsky 2009; Bamforth 2006).

5.10 Works Cited – Chapter 5

Andrefsky, W. 2009. The analysis of stone tool procurement, production, and maintenance. *Journal of Archaeological Research*, 17(1), 65–103.

Andrews, B. W., Murtha, T. M., and Scheetz, B. 2004. Approaching the Hatch Jasper quarry from a technological perspective: a study of prehistoric stone tool production in Central Pennsylvania. *Midcontinental Journal of Archaeology*, 29(1), 63–101.

Annan, A. P. 2005. Ground-penetrating radar. In D. K. Butler (Ed.), *Near-surface geophysics* (pp. 357–438). Society of Exploration Geophysicists.

Bamforth, D. B. 2006. The Windy Ridge quartzite quarry: hunter-gatherer mining and hunter-gatherer land use on the North American continental divide. *World Archaeology*, 38(3), 511–527.

Beamish, D. 2011. Low induction number, ground conductivity meters: a correction procedure in the absence of magnetic effects. *Journal of Applied Geophysics*, 75(2), 244–253.

Bellian, J. A., Kerans, C., and Jennette, D. C. 2005. Digital outcrop models: applications of terrestrial scanning LiDAR technology in stratigraphic modeling. *Journal of Sedimentary Research*, 75(2), 166–176.

Bonsall, J., Fry, R., Gaffney, C., Armit, I., Beck, A., and Gaffney, V. 2013. Assessment of the CMD miniexplorer, a new low-frequency multi-coil electromagnetic device, for archaeological investigations. *Archaeological Prospection*, 20(3), 219–231. https://doi.org/10.1002/arp.1458.

Brosten, T. R., Bradford, J. H., McNamara, J. P., Gooseff, M. N., Zarnetske, J. P., Bowden,W. B., and Johnston, M. E. 2009. Estimating 3D variation in active-layer thickness beneath Arctic streams using ground penetrating radar. *Journal of Hydrology*, 373(3–4), 479–486.

Brumbach, H. J. 1987. A quarry/workshop and processing station on the Hudson River in Pleasantdale, New York. *Archaeology of Eastern North America*, 15, 59–83.

Burke, A. L. 2007. Quarry source areas and the organization of stone tool technology: a view from Quebec. *Archaeology of Eastern North America*, 35, 63–80.

Byrd, B. F., Young, D. C., and McGuire, K. R. 2009. Pavement, quarries, gypsum period residential stabiltity, and trans-Holocene settlement systems of the Mohave Desert: a case study at Fort Irwin. *Journal of California and Great Basin Anthropology*, 29(2), 121–144.

Campbell, R. 2016. Experimental approach to the resolution and detection limit of the GSSI SIR3000 GPR system with a 400 MHz antenna in a scattering and non-scattering medium. Unpublished report to Dept. Geological Sciences, University of Manitoba.

Conyers, L. B. 2015. Analysis and interpretation of GPR datasets for integrated archaeological mapping. *Near Surface Geophysics*, 13(6), 645–651.

Conyers, L. B. 2016. *Ground-penetrating radar for geoarchaeology*. Wiley-Blackwell.

Dafflon, B., Hubbard, S. S., Ulrich, C., and Peterson, J. 2013. Electrical conductivity imaging of active layer and permafrost in an Arctic ecosystem, through advanced inversion of electromagnetic induction data. *Vadose Zone Journal*, 12(4). DOI: https://doi.org/10.2136/vzj2012.0161.

Dalan, R. A. 2006. Magnetic susceptibility. In J. K. Johnson (Ed.), *Remote sensing in archaeology: an explicitly North American perspective* (pp. 161–203). The University of Alabama Press: Tuscaloosa.

Dallimore, S. R., and Davis, J. L. 1992. Ground penetrating radar investigations of massive ground ice. In J. Pilon (Ed.), *Ground penetrating radar* (pp. 41–48), Geological Survey of Canada, Paper 90(4).

Ericson, J. E. 1984. Towards the analysis of lithic production systems. In J. E. Ericson and B. A. Purdy (Eds.), *Prehistoric quarries and lithic production. New directions in archaeology* (pp. 1–10). Cambridge: Cambridge University Press.

Erwin, J. C. 2010. Dorset Palaeoeskimo quarrying techniques and the production of little pots at Fleur de Lys, Newfoundland. In M. Brewer-LaPorta, A. Burke, and D. Field (Eds.), *Ancient mines and quarries: a trans-Atlantic perspective* (pp. 56–66). Oxbow Books: Oxford.

Evans, M., and Heller, F. 2003. *Environmental magnetism: principles and applications of enviromagnetics*. San Diego, USA: Elsevier Science.

Everett, M. E., and Meju, M. A. 2005. Near-surface controlled-source electromagnetic induction: background and recent advances. In Y. Rubin and S. S. Hubbard (Eds.), *Hydrogeophysics* (pp. 157–183). Springer: Dordrecht, the Netherlands.

Fitterman, D. V., and Labson, V. F. 2005. Electromagnetic induction methods for environmental problems. In D. K. Butler (Ed.), *Near-surface geophysics* (pp. 301–355). Society of Exploration Geophysicists.

Gacitúa, G., Tamstorf, M. P., Kristiansen, S. M., and Uribe, J. A. 2012. Estimations of moisture content in the active layer in an Arctic ecosystem by using ground-penetrating radar profiling. *Journal of Applied Geophysics*, 79, 100–106.

Goodyear, A. C., and Charles, T. 1984. An archaeological survey of chert quarries in western Allendale County, South Carolina. Research Manuscript Series, 187.

Gramly, R. M. 1978. Lithic source areas in Northern Labrador. *Arctic Anthropology*, 15, 36–47.

Grote, K., Crist, T., and Nickel, C. 2010. Experimental estimation of the GPR groundwave sampling depth. *Water Resources Research*, 46(10).

Güth, A. 2012. Using 3D scanning in the investigation of Upper Palaeolithic engravings: first results of a pilot study. *Journal of Archaeological Science*, 39(10), 3105–3114.

Harris, S. A. 1982. Identification of permafrost zones using selected permafrost landforms. In *Proceedings of the fourth annual Canadian permafrost conference*, 49–58.

Hinkel, K. M., Doolittle, J. A., Bockheim, J. G., Nelson, F. E., Paetzold, R., Kimble, J. M., and Travis, R. 2001. Detection of subsurface permafrost features with ground-penetrating radar, Barrow, Alaska. *Permafrost and Periglacial Processes*, 12(2), 179–190.

Huang, H., and Fraser, D. C. 2003. Inversion of helicopter electromagnetic data to a magnetic conductive layered earth. *Geophysics*, 68(4), 1211–1223.

Huang, H., Won, I. J., and San Filipo, B. 2003. Detecting buried nonmetal objects using soil magnetic susceptibility measurements. *AeroSense*, 1181–1188.

Hull, S., Fayek, M., Mathien, F. J., Shelley, P., and Durand, K. R. 2008. A new approach to determining the geological provenance of turquoise artifacts using hydrogen and copper stable isotopes. *Journal of Archaeological Science*, 35(5), 1355–1369.

Isenburg, M. 2015. LAStools efficient tools for LiDAR processing. (Version 1.3). Retrieved from http://lastools.org.

Kessler, R. A., Beck, C., and Jones, G. T. 2009. Trash: The Structure of Great Basin Palaeoarchaic Debitage Assemblages in Western North America. In B. Adams and B. S. Blades (Eds.), *Lithic Materials and Paleolithic Societies* (pp. 144–159). New York: Wiley-Blackwell.

Kneisel, C., Hauck, C., Fortier, R., and Moorman, B. 2008. Advances in geophysical methods for permafrost investigations. *Permafrost and Periglacial Processes*, 19(2), 157–178.

Knight, R. J., and Nur, A. 1987. The dielectric constant of sandstones, 60 kHz to 4 MHz. *Geophysics*, 52(5), 644–654.

Landry, D. B., Ferguson, I. J., Milne, S. B., and Park, R. W. 2015. Combined geophysical approach in a complex Arctic archaeological environment: A case study from the LdFa-1 site, southern Baffin Island, Nunavut. *Archaeological Prospection*, 22(3), 157–170.

Landry, D. B., Milne, S. B., Park, R. W., Ferguson, I. J., and Fayek, M. 2016. Manual point cloud classification and extraction for hunter-gatherer feature investigation: a test case from two low Arctic Paleo-Inuit sites. *Open Archaeology*, 2(1), 232–242.

Larsen, B. P., Holdaway, S. J., Fanning, P. C., Mackrell, T., and Shiner, J. I. 2017. Shape and an outcome of formation history: Terrestrial laser scanning of shell mounds from far north Queensland, Australia. *Quaternary International*, 427(A), 5–12.

Lazenby, M. E. C. 1980. Prehistoric Sources of Chert in Northern Labrador: Field Work and Preliminary Analyses. *Arctic*, 33(3), 628–645.

McNeill, J. D. 1980. Electromagnetic terrain conductivity measurement at low induction numbers. Tech. Note TN-6. Geonics Ltd., Mississauga, ON.

McNeill J. D. 2012. Archaeological mapping using the Geonics EM38B to map terrain magnetic susceptibility (with selected case histories). Tech. Note TN-35, Geonics Ltd., Mississauga, ON.

McNeill, J and Bosnar M. 1999. Application of ‘dipole–dipole’ electromagnetic systems for geological depth sounding. Tech. Note TN-31, Geonics limited: Mississauga, ON.

Mester, A., van der Kruk, J., Zimmermann, E., & Vereecken, H. 2011. Quantitative two-layer conductivity inversion of multi-configuration electromagnetic induction measurements. *Vadose Zone Journal*, 10(4), 1319–1330. https://doi.org/10.2136/vzj2011.0035.

Milne, S. B. 2013. Chert sourcing and Palaeo-Eskimo stone tool technology. Report on work conducted under Nunavut Archaeological Permit No. 2013-02A. Manuscript on file with the Department of Culture, Language, Elders and Youth, Government of Nunavut, Igloolik, Nunavut.

Milne, S. B. 2015. Chert sourcing and Palaeo-Eskimo stone tool technology: permit report on work conducted under Nunavut archaeological permit no. 2015-21A. Department of Culture, Language, Elders and Youth, Government of Nunavut, Igloolik, Nunavut.

Milne, S. B., Park, R. W., Hamilton, A. C., and Fayek, M. J. 2011. Chert sourcing and Palaeo-Eskimo raw material use in the interior of southern Baffin Island, Arctic Canada. *Canadian Journal of Archaeology*, 35(1), 117–142.

Minchak, S. A. 2010. A microwear study of Clovis blades from the Gault Site, Bell County, Texas (Doctoral dissertation, Texas A & M University).

Moorman, B. J., Robinson, S. D., and Burgess, M. M. 2003. Imaging periglacial conditions with ground penetrating radar. *Permafrost and Periglacial Processes*, 14(4), 319–329.

Parish, R. M. 2013. The application of reflectance spectroscopy to chert provenance of Mississippian symbolic weaponry. Doctoral dissertation, University of Memphis.

Pilon, J. A., Allard, M., and Séguin, M. K. 1992. Ground probing radar in the investigation of permafrost and subsurface characteristics of surticial deposits in Kangiqsualujjuaq, Northern Quebec. In J. Pilon (ed.), *Ground penetrating radar* (pp. 165–175), Geological Survey of Canada, Paper 90(4).

Robinson, D. A., Lebron, I., Lesch, S. M., and Shouse, P. 2004. Minimizing drift in electrical conductivity measurements in high temperature environments using the EM-38. *Soil Science Society of America Journal*, 68(2), 339–345.

Romero, B. E., and Bray, T. L. 2014. Analytical applications of fine-scale terrestrial lidar at the imperial Inca site of Caranqui, northern highland Ecuador. *World Archaeology*, 46(1), 25–42.

Schwamborn, G., Wagner, D., and Hubberten, H. W. 2008. The use of GPR to detect active layers in young periglacial terrain of Livingston Island, Maritime Antarctica. *Near Surface Geophysics*, 6(5), 331–336.

Snegirev, A. M., Velikin, S. A., Istratov, V. A., Kuchmin, A. O., Skvortsov, A. G. and Frolov, A. D. 2003. Geophysical monitoring in permafrost areas. In *Permafrost: 8th international conference on permafrost*, Zurich, pp. 1079–1084.

Stenton, D. R., and Park, R. W. 1998. Ancient Harpoon Heads of Nunavut: An Illustrated Guide [in English and Inuktitut]. Parks Canada, Department of Canadian Heritage, Government of Canada, Iqaluit. 108 pp.

Tarnocai, C., and Bockheim, J. G. 2011. Cryosolic soils of Canada: genesis, distribution, and classification. *Canadian Journal of Soil Science*, 91(5), 749–762.

Tabbagh, A. 1986. Applications and advantages of the Slingram electromagnetic method for archaeological prospecting. *Geophysics*, 51(3), 576–584.

ten Bruggencate, R. E., Milne, S. B., Fayek, M., Park, R. W., and Stenton, D. R. 2015. Characterization of chert artifacts and two newly identified chert quarries on southern Baffin Island. *Lithic Technology*, 40(3), 189–198.

ten Bruggencate, R. E., Milne, S. B., Fayek, M., Park, R. W., Stenton, D. R., and Hamilton, A. C. 2016a. Characterizing southern Baffin Island chert: a cautionary tale for provenance research. *Journal of Archaeological Science: Reports*. https://doi.org/10.1016/j.jasrep.2016.03.016.

ten Bruggencate, R. E., Stup, J. P., Milne, S. B., Stenton, D. R., Park, R. W., & Fayek, M. 2016b. A humancentered GIS approach to modeling mobility on Southern Baffin Island, Nunavut, Canada. *Journal of Field Archaeology*, 41(6), 684–698.

Theune, U., Rokosh, D., Sacchi, M. D., and Schmitt, D. R. 2006. Mapping fractures with GPR: A case study from Turtle Mountain. *Geophysics*, 71(5), B139–B150.

Tripcevich, N., and Contreras, D. A. 2013. Archaeological approaches to obsidian quarries: investigations at the Quispisisa source. In N. Tripcevich and K. J. Vaughn (Eds.), *Mining and quarrying in the Ancient Andes, interdisciplinary contributions to archaeology*. New York: Springer Science+Business Media.

Urban, T. M., Anderson, D. D., and Anderson, W. W. 2012. *Multimethod geophysical investigations at an Inupiaq village site in Kobuk Valley, Alaska*. The Leading Edge, 31(8), 950–956.

Urban, T. M., Rasic, J. T., Alix, C., Anderson, D. D., Manning, S. W., Mason, O. K., Tremayne, A. H., and Wolff, C. B. 2016. Frozen: the potential and pitfalls of ground-penetrating radar for archaeology in the Alaskan Arctic. *Remote Sensing*, 8(12), 1007.

Valls, A., García, F., Ramírez,M., and Benlloch, J. 2016. A combined use of GPR data with historical archives for identifying pavement construction periods of Valencian Silos (16th century, Spain). *IEEE Journal of Selected Topics in Applied Earth Observations and Remote Sensing*, 9(1), 98–107.

Viberg, A., Trinks, I., and Lidén, K. 2009. Archaeological prospection in the Swedish Mountain tundra region. *ArchéoSciences* 33, *Presses Université de Rennes*, 33 (suppl.), 167, 169.

Vickers, K. J. 2011. Quaternary geology of Bluegoose Prairie, Baffin Island, Nunavut. M.Sc. thesis, Simon Fraser University, Canada.

Wilke, P. J., and Schroth, A. B. 1989. Lithic raw material prospects in the Mojave Desert, California. *Journal of California and Great Basin anthropology*, 11(2), 146–174.

Wolff, C. B., and Urban, T. M. 2013. Geophysical analysis at the old whaling site, Cape Krusenstern, Alaska, reveals the possible impact of permafrost loss on archaeological interpretation. *Polar Research*, 32(1).

Yilmaz, O. 1987. *Seismic data processing*. Tulsa: Society of Exploration Geophysicists.

Chapter 6

Combining Remote Sensing, Geophysics, and Lithic Provenance and Reduction to Understand Long-Term Continuity in Paleo-Inuit Chert Quarrying and Seasonal Inland Travels on Southern Baffin Island, NU

An original scientific research manuscript accepted for publication in a special issue of:

Quaternary International

David B. Landry, S. Brooke Milne, Rachel E. ten Bruggencate

Abstract: In 2013, we identified a large chert quarry located in the intermediate zone between southern Baffin Island's coast and interior. In 2015, we used a combination of remote sensing and geophysical technology to assess how intensively Pre-Dorset and Dorset populations (collectively known as Paleo-Inuit) used the site. This paper presents the results of those investigations, and explains how they articulate with geochemical and lithic reduction data from two large inland Paleo-Inuit habitation sites on southern Baffin Island. Our findings suggest that, despite a dramatic shift in the Arctic climate c. 5000 – 2500 BP, human populations in this region maintained seasonal patterns of intensive resource exploitation in the interior regions of Baffin Island. This was likely a result of ongoing need for vital resources only available in the interior, including chert toolstone.

6.1 Introduction

Lithic technology is a reductive process wherein stone is systematically removed until tools are exhausted. Thus, toolmakers required a constant supply of stone to meet their technological needs. For archaeologists aiming to reconstruct lithic technological organization for mobile, stone-tool using hunter-gatherer populations, the logical place to begin is at quarries (Ericson, 1984; Frank et al., 2015). The earliest stages of tool production are concentrated at quarries as stone is acquired, tested, shaped, and prepared for future use elsewhere (Trepcevich & Contreras, 2013, pp. 25). These activities create a baseline for interpreting lithic reduction sequences, which archaeologists use to trace the circulation of toolstone, and by extension, people across landscapes (Andrefsky, 2008, 2009). Thus, quarries are unique nexus points that link sites throughout a region (Nash et al., 2016). While archaeologists recognize their analytical importance, quarries remain understudied and poorly understood (Minchak, 2010).

Arguably, archaeologists are ambivalent about studying quarries because they are spatially massive and comprise mixed reduction episodes often spanning millennia; they are devoid of stratigraphy, lack temporally diagnostic tool types and other datable materials, yield voluminous assemblages dominated by lithic debris and shatter, and are logistically challenging to excavate (Ericson, 1984; Daniel, 2001; Andrews et al., 2004; Bamforth, 2006; Minchak, 2010; Gopher & Barkai, 2014; Sykes et al. 2017; see Milne 2016a) Yet, by avoiding investigation of these sites because of the noted challenges they present, archaeologists cannot accurately reconstruct human mobility and settlement using lithic technology as a proxy since they cannot "anchor" the beginning of reduction sequences (Goodyear & Charles, 1984; Burke, 2007; Nash et al., 2016, see Milne 2016a).

The first human occupants of the North American Arctic are known archaeologically as Paleo-Inuit (4,500 – 1,200 BP). The artifact assemblages found in association with Paleo-Inuit sites are typically dominated by lithic artifacts made using chert toolstone; however, comparatively little is known about where these peoples procured this raw material, how, and at what time of year. In 2012, Milne began a multi-year project focused on identifying chert quarries on southern Baffin Island. In 2013, the first chert quarry in this region, LbDt-1, was identified and immediately presented a conundrum of how best to investigate the site so as to understand its influence on regional Paleo-Inuit land use and technological organization.

Conducting archaeological fieldwork in the Arctic is logistically difficult – field seasons are short, expenses are high, and inclement weather can make remote sites very difficult to reach. For all of these reasons, along with the prospect of transporting, shipping, and storing a massive lithic assemblage, it was deemed impractical to launch a full-scale excavation at LbDt-1. Therefore, we devised a minimally invasive investigative approach combining remote sensing, geophysics, and limited test excavation to ascertain the size and scope of the LbDt-1 lithic quarry (Landry et al., 2018), which proved highly successful. In this paper, we consider the data acquired from LbDt-1 in conjunction with existing chert provenance and lithic technological data to examine the relationship between LbDt-1 and two large Paleo-Inuit habitation sites, LdFa-1 and LeDx-42, located further inland on southern Baffin Island (see Figure 6.1). Both provenance and technological data link the three sites, suggesting that chert available at LbDt-1 made it an important waypoint on Paleo-Inuit journeys to the interior.

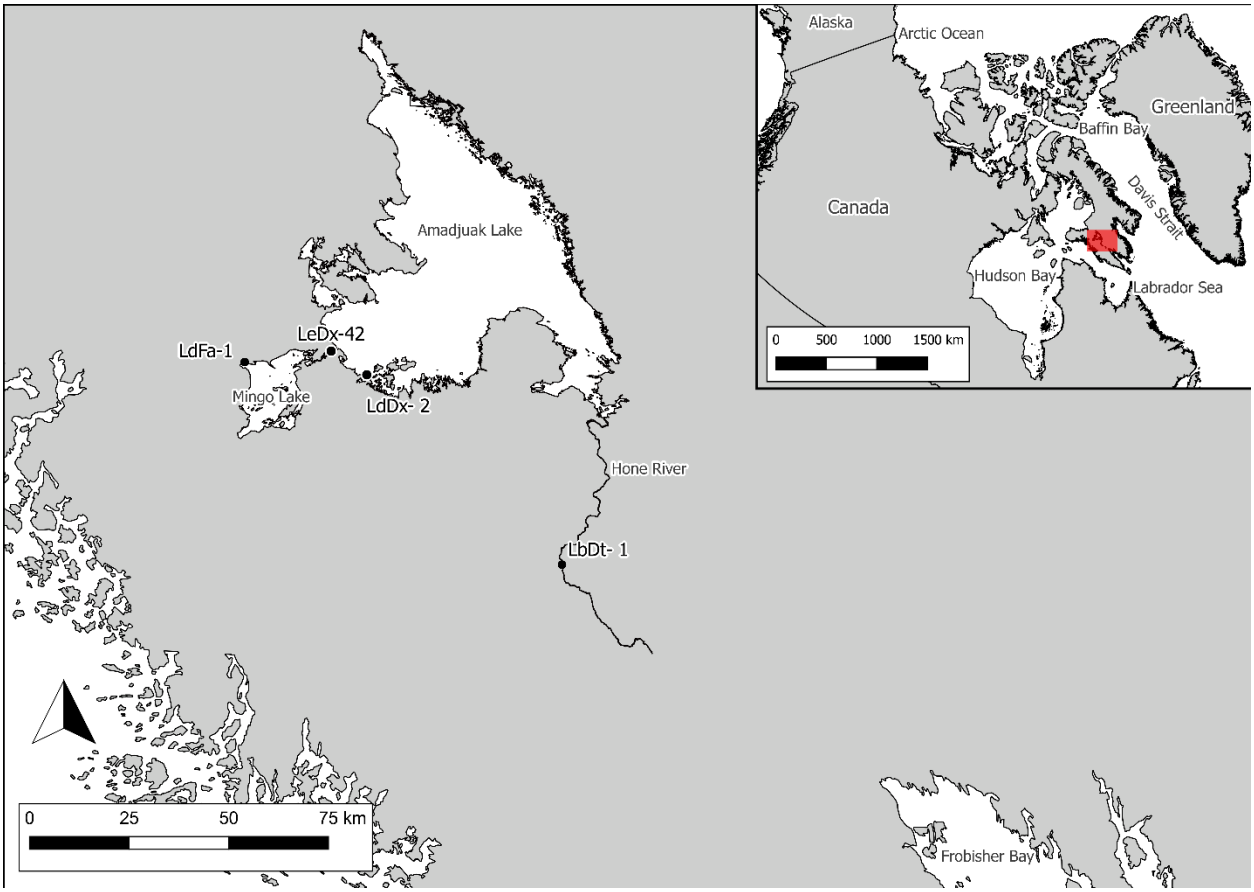

Figure 6.1 Location of sites LbDt-1, LdDx-2, LdFa-1, and LeDx-42 situated within inland southern Baffin Island.

6.1.1 Archaeological Background

Nearly three decades of archaeological research on southern Baffin Island indicate that the region's Paleo-Inuit peoples traveled seasonally between the coast and interior to acquire chert, along with other food and material resources (Stenton, 1990, 1991a/b/c; Milne, 2003; 2005; Park, 2008; Milne et al., 2012, 2013). Evidence in support of this includes geochemical data from quarry and artifact samples, which confirms that chert debitage found at sites on the coast of southern Baffin Island is chemically consistent with chert from sources in the interior (ten Bruggencate et al., 2016, 2017). In other regions of the Arctic, long-distance coastal-inland seasonal mobility does not occur through the entire Paleo-Inuit period. Rather, Pre-Dorset appear

to be mobile between coastal and inland regions, while the Dorset display a more sedentary, marine-focused way of life. One explanation given for this cultural discontinuity is the timing of major paleoclimatic events during the Holocene epoch (Barry et al., 1977; Mudie et al., 2005). It is thought that in response to longer, harsher winters and an expanded sea ice environment (c. 5,000-2,500 BP), human populations adapted by developing a more sedentary way of life focused on the exploitation of sea mammal resources (e.g. Maxwell, 1985; Bielawski, 1988; McCartney and Helmer, 1989; McGhee, 1996; Murray, 1999; Darwent, 2004; Milne et al., 2012; Betts et al., 2015). As this way of life spread, archaeologists inferred that long-distance seasonal travel to neighbouring interior regions must necessarily have declined or ceased altogether (Milne et al., 2012). In the interior of southern Baffin Island, however, large and exceptionally well-preserved multi-component Paleo-Inuit sites indicate that Dorset in this region continued a way of life seemingly unchanged from that of their predecessors (Milne et al., 2012).

6.1.1.1 Chert on southern Baffin Island

Paleo-Inuit lithic assemblages on southern Baffin Island are overwhelmingly dominated by chert tools and debitage (Milne, 2003, 2005, 2008; Landry, 2013; Milne, 2014). Until recently, however, archaeologists were uncertain how and where Paleo-Inuit in the region were acquiring this important lithic resource. Decades of archaeological survey along the Precambrian igneous bedrock of southern Baffin Island's coast had failed to locate any reliable sources of chert (Maxwell, 1973), while survey among the potentially more productive limestone formations of the interior had yet to be carried out. During the early 2010s, an interdisciplinary team of archaeologists and geologists initiated survey of inland southern Baffin Island with the specific goal of identifying chert procurement sites (Milne, 2013). Within a year, two chert

quarries – LbDt-1 and a second, smaller quarry, LdDx-2 – were identified (Figure 6.2; Milne, 2014).

At both of these quarry sites, chert cobbles are located in or eroding out of Amadjuak formation Ordovician limestone bedrock that only occurs in a small area south of Amadjuak Lake and northeast of Mingo Lake (Milne, 2013, 2015; ten Bruggencate et al., 2015, 2016; Landry et al., 2015; Landry et al., 2018). Acquisition of chert at sites such as LbDt-1 would have been seasonally constrained by deep snow cover common from late autumn through to early spring on southern Baffin Island. Therefore, Paleo-Inuit people would have needed to time journeys to the interior to arrive at chert bearing exposures during the warmer months between late spring and early autumn. Spatial and temporal limitations on access to chert – a vital component of daily toolkits – would likely have made quarries important resource acquisition sites, and therefore important nodes shaping Paleo-Inuit seasonal travel.

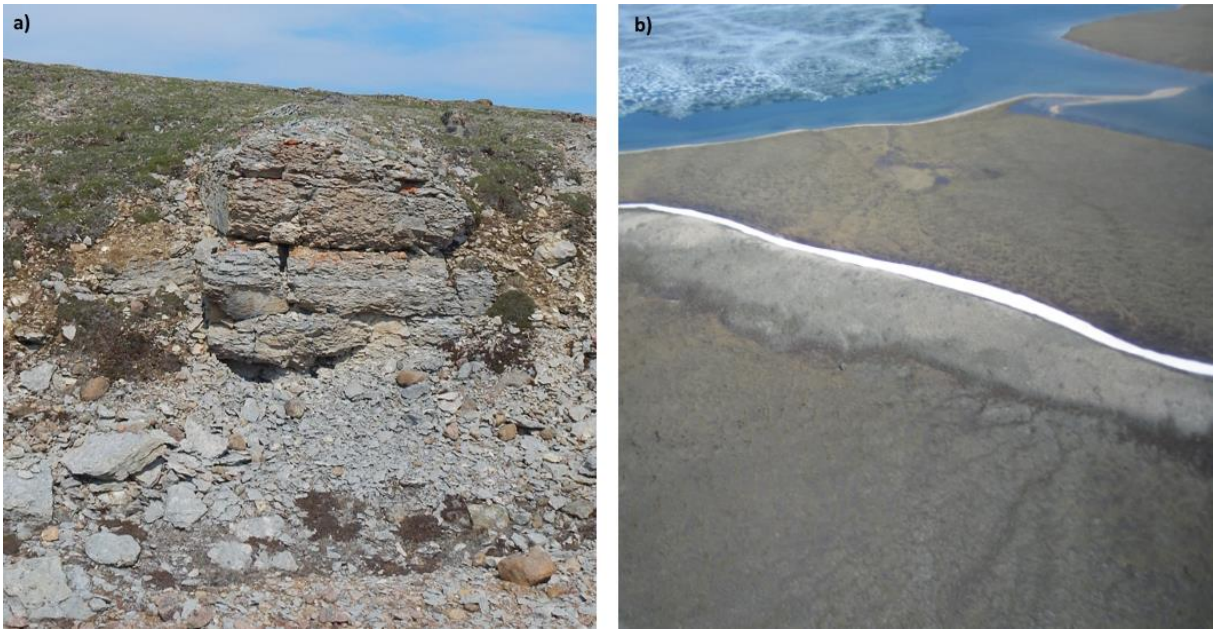

Figure 6.2 Photographs of Units 2 and 3 from the Amadjuak Group with identification of the units based on the descriptions by Sandford and Grant (2000). a) Eroded and exposed limestone outcrop of Unit 2 at LbDt-1. The height of the outcrop is ~5 m. The outcrop includes embedded chert nodules. b) Photograph of an outcrop of Unit 3, near LdDx-2. Photograph is taken looking north towards Amadjuak Lake. The height of the ridge formed by the limestone outcrop is ~10 m and the length of the ridge on the photograph is ~1.0 km.

6.1.1.2 Quarries and Lithic Technology

Lithic reduction is generally understood as a sequential, spatially staged continuum of activities involving different percussors, techniques, and force loads, each of which have different outcomes for lithic assemblages, and individual flake and tool attributes (Collins, 1975, pp. 17; Andrefsky, 2009, pp. 66-67). Different patterns of mobility and lithic resource availability have reasonably predictable effects on reduction strategies (e.g. Andrefsky, 1994; Shott, 1994). This makes reconstruction of reduction sequences through analysis of lithic assemblages an important tool for understanding these aspects of past lives and landscapes

The crucial first step in reconstructing reduction sequences is determining how toolstone was initially extracted and reduced at the quarry (Burke, 2007). Archaeologists have documented

evidence of both intensive mining of toolstone from *in situ* bedrock outcrops (e.g., Gramly, 1978; Bamforth, 2006; Burke, 2010; Erwin, 2010) and exploitation of secondary sources where chert occurs as liberated nodules and weathered pebbles (e.g., Wenzel & Shelley, 2001; Ekshtain et al., 2014). Very often, stone is then transported to an adjacent area where it is reduced into tool blanks, preforms, and prepared cores, resulting in the generation of massive quantities of debitage (e.g., Gramly, 1978; Lazenby, 1980). The intensity of early stage reduction carried out at quarries – which can be reconstructed through analysis of said debitage – positively correlates to the distance people had to travel with their newly acquired toolstone before reaching other resources (Beck et al., 2002; Kessler et al., 2009). If raw material abundance in an area is restricted, quarry activities may even include the complete replacement of existing toolkits in anticipation of future needs, and the focused production of bifaces to serve as specialized cores to ensure the availability of sufficient useable toolstone. None of these behaviours, or their impact on subsequent reduction strategies, can be reconstructed without analysis of quarry assemblages.

Limited inferences about lithic technological organization can also be made from the opposite end of the reduction continuum using distance-decay or fall-off models to arrive at reasoned, inductive interpretations of an assemblage (e.g., Ricklis & Cox, 1993; Milne & Donnelly, 2004; Milne, 2005; Tremayne, 2015; cf. Burke, 2007). Our early reconstructions of Pre-Dorset and Dorset lithic technological organization on southern Baffin Island were based on these interpretive models, because actual quarry data did not yet exist (Milne, 2003, 2005). We did know, however, that large scatters of chert gravel could be found throughout the interior, and that chert was absent on the coast (Milne et al., 2009, 2011). We also knew that lithic assemblages at coastal sites tend to be dominated by products of late stage tool production,

toolstone liquidation, and artifact recycling (Milne, 2003, 2005; cf. Ricklis & Cox, 1993). Therefore, our reconstructions placed coastal sites at the terminal end of the Paleo-Inuit reduction sequence. On the other hand, interior sites in close proximity to chert gravels yielded comparatively massive lithic assemblages with high flake-to-tool ratios (Milne, 2014). These were inferred to be lithic workshops where intensive tool production activities occurred in anticipation of traveling long distances (i.e., 100-200 km) back to the coast (Milne, 2003, 2005, 2011). Prior to the documentation of inland chert quarries in 2013 (Milne, 2014), the surface scatters of chert gravel were interpreted as the main toolstone source. Now, with the identification of archaeologically exploited chert sources – including LbDt-1 – in the interior of southern Baffin Island, we are able to properly situate quarries and other sites within Paleo-Inuit reduction sequences and arrive at better supported conclusions regarding technological organization.

6.1.1.3 Southern Baffin Island Quarries

In 2013, we identified the first true chert quarries on southern Baffin Island, LbDt-1 and LdDx-2. Through analysis of over 5000 pieces of lithic debitage recovered from the larger quarry, LbDt-1 (Milne, 2016b), we know that our preliminary reconstructions of Paleo-Inuit reduction sequences were not entirely accurate, as they were missing this initial step. The lithic assemblage from LbDt-1, along with its geological context, also indicates a pattern of quarry exploitation and toolstone transport that seems to defy existing economization models. Chert at LbDt-1 is available as fist-sized nodules weathering out of limestone bedrock exposed along the course of the Hone River (see Figure 6.3). These nodules can be picked up along the river's shoreline, or extracted by hand from the crumbling limestone.

Figure 6.3 Exposed chert embedded in the limestone outcrop at LbDt-1. Arrows point to loose nodules weathered out of the limestone.

Analysis of debitage from the upper component of LbDt-1 (Figure 6.4) tells us that early stage reduction, as expected, was the focus of toolmakers on site. However, evidence normally associated with quarrying beyond initial extraction and testing of materials is totally absent; Paleo-Inuit toolmakers were not making blanks, preforms, or bifacial cores, or replacing existing lithic toolkits while at LbDt-1. It appears chert was being carried away in minimally modified form for journeys in excess of 60 km, the distance threshold at which archaeologists expect additional reduction to occur at quarries (Beck et al., 2002; see also Kessler et al., 2009; Garvey, 2015). To understand the potential ramifications of this pattern of acquisition and transport for subsequent stages of lithic reduction at other sites, a broader understanding of the significance of LbDt-1 to chert lithic technological organization on southern Baffin Island is necessary. To achieve this, we collected remote sensing, geophysical, and text excavation data to ascertain the

spatial extent of debitage deposits at LbDt-1, and contextualize these using technological and provenance data from nearby sites.

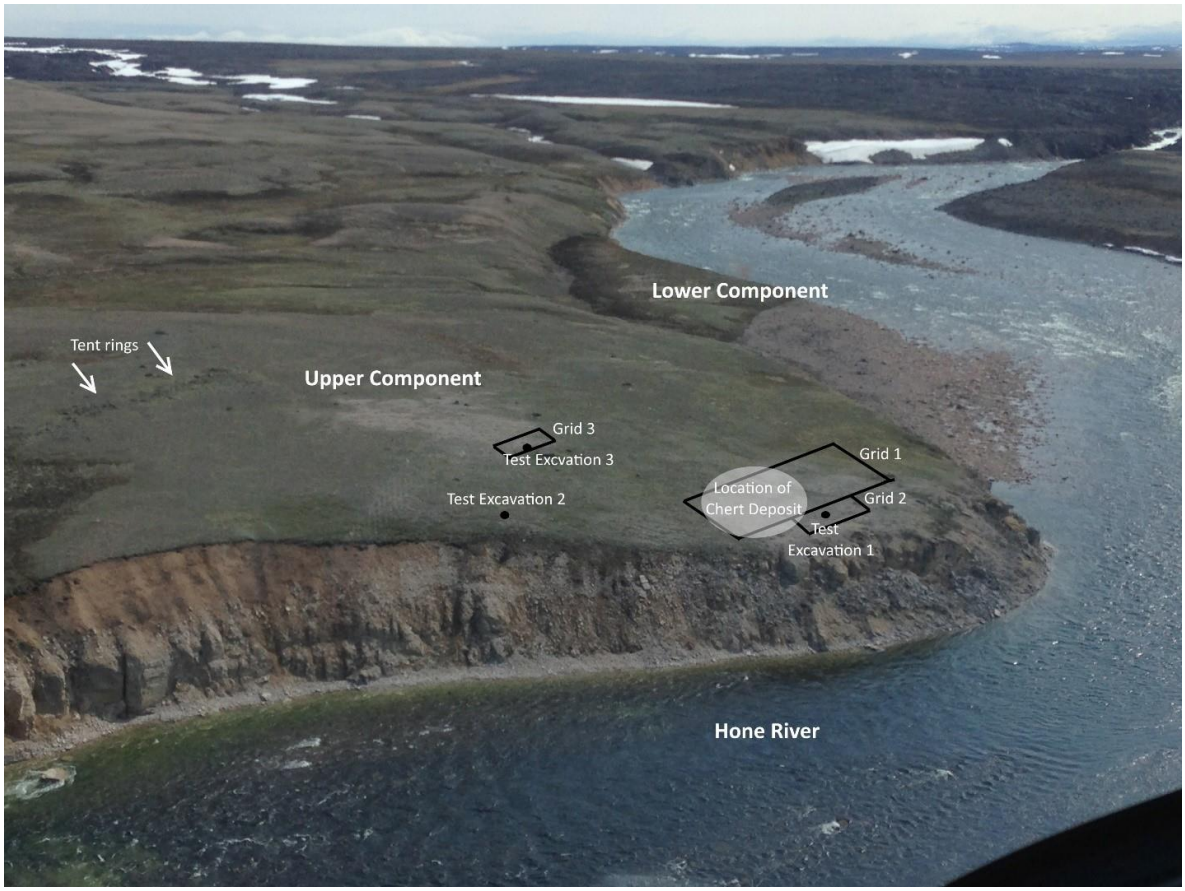

Figure 6.4 Oblique aerial image of the LbDt-1 quarry site. The focus of this study takes place within the Upper Component noted on the image; however, the exposed limestone outcrop is featured within the Lower Component.

6.2 Materials and Methods

6.2.1 Sites

6.2.1.1 LbDt-1

The LbDt-1 chert quarry is located on the eastern shore of the Hone River, approximately 40 km south of Amadjuak Lake (Figure 6.1). The site was identified in 2013 when what appeared to be a row of stone tent rings was noted during aerial survey. The site is divided into

two separate components: upper and lower. The upper component includes the row of tent rings, and an extensive chert flake deposit located approximately 300m to the east (Milne, 2013; Figure 6.4 and Figure 6.5).

Figure 6.5 Photograph showing a small close-up section of the dense chert flake deposit at the LbDt-1 quarry site.

The site's lower component is located along the shore of the Hone River (Figure 6.4), and features prominent limestone bedrock exposures containing nodules of chert. Chert nodules are rendered easily accessible by erosion and other weathering processes occurring along the river's edge. Annual freeze-thaw cycles break down these nodules to the point that their surfaces and interior structures can be easily evaluated and tested without much added effort. Chert nodules can be picked up along the river's shoreline or extracted from the outcrop itself if needed, by hand from areas where limestone is severely weathered, or using simple tools where it is not.

LbDt-1 is situated only a few kilometres north of the contact point between the Amadjuak formation and the Cumberland Batholith, which means it was likely one of the first chert exposures encountered by Paleo-Inuit moving inland from the southeast coast to the interior – or one of the last encountered on trips in the opposite direction (Figure 6.6). It should be noted that there are a series of isolated outcrops of the Amadjuak Group extending over a distance of 100 km from LbDt-1 to a location adjacent to Frobisher Bay. In 2013, we landed nearby one of these outcrops. After examination and pedestrian survey of the location, our project geologist concluded that it did not display any evidence of chert-bearing layers. In addition, there was little to no expectation of finding archaeological remains in this location, as it would have been near impossible to access due to the extremely steep sloping sides of these formations.

In 2015, LbDt-1 was revisited for further investigation. Two grids were established along the edge of the upper component and surveyed using ground penetrating radar and magnetic survey. The aim of the survey was to ascertain the distribution and depth of the upper level chert flake deposit, and thus gain insight into the intensity of procurement and reduction activities occurring at this site. Our non-invasive geophysical approach meant that we could do this within project constraints on time, cost, and transport. To ground truth our geophysics results, three $25cm^2$ test pits were excavated within the survey grids.

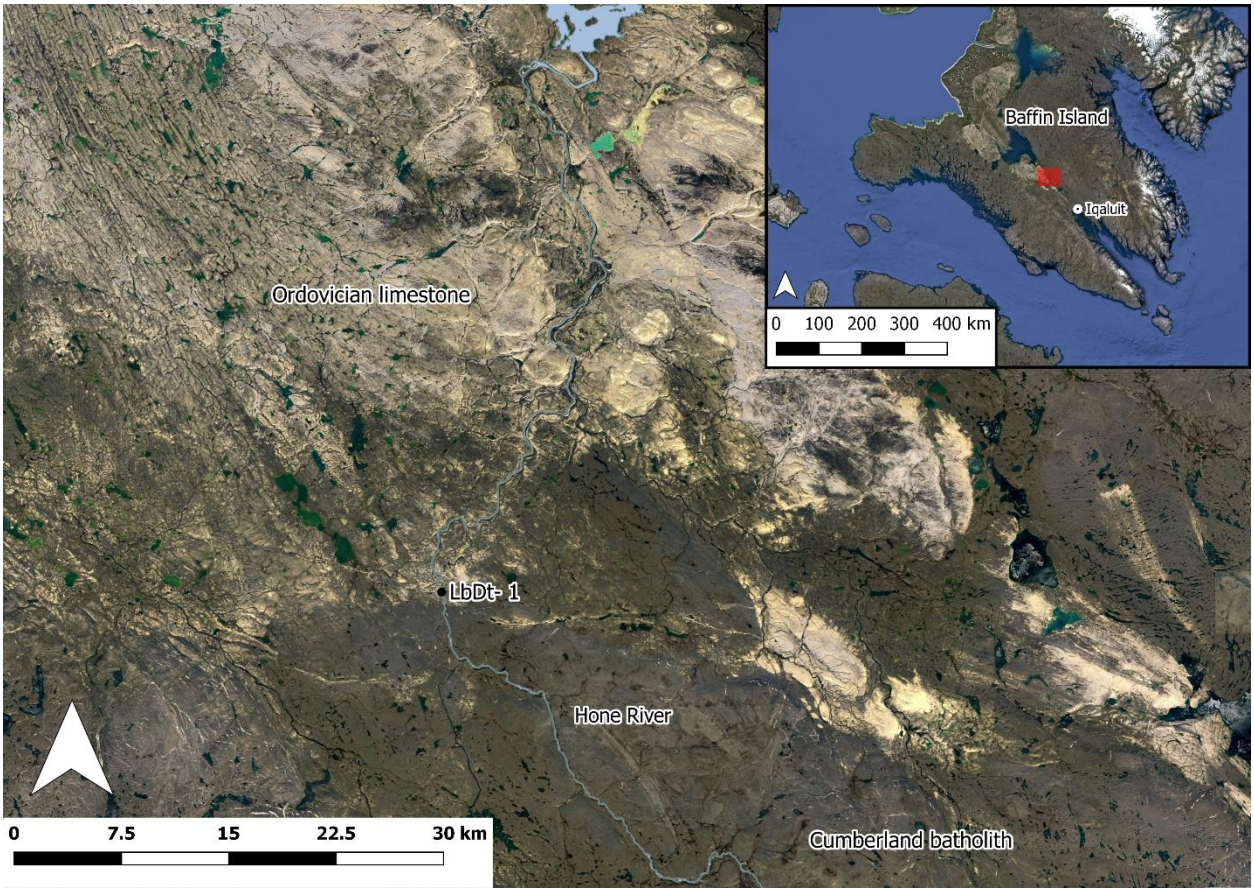

Figure 6.6 Satellite image indicating the approximate location of the LbDt-1 lithic quarry. Note that it sits within the Upper Ordovician Amadjuak Formation, approximately 1 km north of the Cumberland Batholith. Inset map of southern Baffin Island is included at top right.

6.2.1.2 LdFa-1

LdFa-1 is a large, multi-component habitation site located on the northwest shore of Mingo Lake (see Figure 6.1). The site, Paleo-Inuit and later Thule-Inuit occupied, includes 33 visible stone tent rings, large stone meat caches, and widespread surface and subsurface deposits of lithic and faunal remains (Milne, 2005, 2008, Park, 2008; Milne, 2013). Identifiable faunal remains recovered at LdFa-1 are overwhelmingly from caribou, which was likely a staple food for Paleo-Inuit during their time in the interior (McAvoy, 2014). The excavated lithic assemblage from LdFa-1 comprises more than 100,000 pieces of lithic debitage, and dozens of formal and

informal tools. A detailed analysis of more than 7000 chert flakes excavated from one area of LdFa-1 indicates intensive tool production activities occurred on site (Landry, 2013). Specifically, reduction strategies were focused on preparing tool preforms and blanks for transport to another location, possibly distant coastal sites, where they would be completed as formal tools (Landry, 2013; see also Milne, 2003).

6.2.1.3 LeDx-42

LeDx-42 is located on top of a rocky outcrop overlooking the Mingo River approximately 10 km southwest of LdFa-1 (Figure 6.1). Its view of the surrounding landscape would have made the site ideal for staging caribou hunts, as well-worn pathways attest to the repeated and habitual crossing of the animals nearby. There are no visible tent rings at LeDx-42; however, extensive surface and subsurface deposits of lithic debitage and faunal remains confirm Paleo-Inuit occupation of the site. Surface and subsurface collection at LeDx-42 yielded over 20,000 chert flakes, dozens of diagnostic Paleo-Inuit stone tools, and organic artifacts, including bone and antler tool-handles (Milne, 2005; Milne et al., 2013). As at LdFa-1, a well-preserved, caribou-dominated faunal assemblage indicates caribou hunting was an important activity for occupants of LeDx-42 (Milne et al., 2012, 2013).

6.2.2 Geophysical analysis and test excavation at LbDt-1

Two instruments were used for geophysical imaging at LbDt-1, one of which is designed to provide near-surface magnetic susceptibility and resistivity measurements, and the other to provide near-surface electrical permittivity, enabling archaeologists to assess and interpret

variability in stratigraphic measurements across a site. These instruments include a multi-channel GSSI Profiler EMP-400 magnetometer and a GSSI ground-penetrating-radar system, respectively. Survey data were collected on three established grids situated along the magnetic northerly axis. Grid 1 measures 44 by 14 meters. Grid 2 measures 20 by 6 meters and adjoins the western-most edge of Grid 1. The third survey grid was situated approximately 30 meters east of the first two grids, and measured only 15 by 8 meters. Data collected were processed using a series of manual and automated steps (see Landry et al., 2018 for a description of these methods).

Ground-penetrating-radar was used to survey all three grids at LbDt-1. This instrument is designed to measure subsurface features and layering. GPR systems emit a radar signal from an antenna (in this case, a 400Mhz antenna), and measure the time, and shape of subsurface reflections to provide a profile used for interpreting subsurface features. It was used in this project to measure the near-surface layering thickness of the quarry deposit, and the deeper subsurface permafrost layer.

The electromagnetic profiler was used to survey only grid 1, however, it was conducted twice, using both vertical and horizontal orientations. EMP survey maps the horizontal extent of the deposit area providing complementary spatial data to the vertical imaging of the GPR.

Through our archaeogeophysical investigation at LbDt-1, we were able to determine the area and thickness of the chert flake scatter on the upper level of the site. Considering the low population density of the precontact Arctic, this deposit is truly massive, measuring approximately 30 m x 15 m (Landry et al., 2018) with an estimated thickness of between 6.5cm and 11.5cm. The total volume of chert present at the site can be estimated at roughly 37m^3.

Test excavations at the site included three 25 cm^2 units located within the geophysical survey grids. The test pits were troweled to sterile soil, and all artifacts were collected. These test pits were excavated both to ground truth stratigraphic data provided by geophysical survey, and to provide artifacts for a preliminary lithic technological analysis of the site. All of the 3923 artifacts recovered during test excavation were pieces of chert debitage. 40% (n = 1583) of this debitage is over ¾" in size. No formal tools or diagnostic artifacts were collected from the test pits.

6.3 LbDt-1, quarrying, and inland mobility on southern Baffin Island

Our work at LbDt-1 indicates that non-invasive geophysical survey can be instrumental to archaeological investigation of voluminous quarry deposits with large surface areas. Using the GPR and EMP results, the extent of the deposit at LbDt-1 can be estimated without time consuming, expensive, invasive subsurface techniques (Landry et al., 2018). The sheer size and thickness of the flake deposit documented using the geophysical equipment suggests that intensive chert reduction occurred at LbDt-1. Given the low population density of Arctic peoples throughout the precontact era (McGhee, 1975, pp. 60; Odess, 1998, pp. 420), this reduction almost certainly occurred during multiple quarrying events over the course of hundreds to thousands of years.

This depth of use is mirrored at nearby Paleo-Inuit occupation sites LdFa-1 and LeDx-42. ^{14}C dates from both sites demonstrate repeated occupation from the earliest Pre-Dorset through later Dorset periods (Milne, 2007; Milne et al., 2008). While this congruence only tenuously indicates that chert from LbDt-1 was a major contributor to toolkits at inland occupation sites,

other lines of evidence – including chert provenance and technological data – provide more solid support for this hypothesis.

The test pits located within the survey grid at LbDt-1 yielded thousands of relatively large chert flakes. Notably, there are no recorded diagnostic tools from these units, nor any located within surface collections from the site, resulting in a completely one-sided flake-to-tool ratio. This ratio is significant in that it indicates an extreme, if not exclusive focus on early-stage reduction at LbDt-1 (Milne, 2011, pp. 106). There is no evidence to suggest that later stages of reduction (e.g. preform or biface manufacture) were occurring on site. Rather, chert nodules were being carried away from LbDt-1 after undergoing minimal testing and/or modification (e.g. decortication).

Technological data from LbDt-1 interleaves neatly with similar data from LdFa-1 and LeDx-42. Most notably, flake-to-tool ratios from Paleo-Inuit components of LdFa-1 and LeDx-42 are extremely high (436:1 and 341:1 respectively; Milne, 2011, pp. 106), though not as high as at LbDt-1, where no tools whatsoever have been collected. Further, at LdFa-1 and LeDx-42, there is evidence for manufacture of preform tools, and it appears that finished diagnostic tools were discarded and replaced at both sites (Milne, 2007, 2011; Park, 2008; Landry, 2013) This indicates that reduction undertaken at the two occupation sites likely falls into the stages immediately following those carried out at LbDt-1. This is precisely the outcome that would be expected if chert quarried at LbDt-1 was extensively utilized by toolmakers at LdFa-1 and LeDx-42.

Further support for the potential significance of LbDt-1 as a source for toolmakers at inland occupation sites is provided by geochemical provenance analysis of chert from southern Baffin Island (ten Bruggencate et al., 2016, 2017). A geochemical signature for chert from inland

quarries was generated through trace element analysis of samples from LbDt-1 and LdDx-2. Trace element results were obtained for debitage from LeDx-42 and LdFa-12, 13, and 14 (smaller occupation sites adjacent to LdFa-1) using the same technique, and compared to the quarry signatures. This comparison strongly suggests that the occupants of these inland sites extensively used chert from one or both of the inland quarries – or, possibly some other, chemically similar source nearby (ten Bruggencate et al., 2017).

Taken together, these lines of evidence strongly indicate that analysis of assemblages at LbDt-1 constitutes a rational first step toward understanding Paleo-Inuit lithic reduction sequences and technological organization on southern Baffin Island. Geophysical, geochemical, and technological data from the quarry, in the context of complementary data from inland occupation sites, firmly establishes LbDt-1 as a significant node for Paleo-Inuit travel across this landscape.

6.4 Conclusion

Using quarry data collected through a minimally invasive investigative approach combining remote sensing, geophysics, and limited test excavation, we set out to understand the initial steps of Paleo-Inuit lithic reduction sequences and technological organization across the inland region of southern Baffin Island. In conjunction with pre-existing technological and geochemical provenience data from two large Paleo-Inuit habitation sites, the results from LbDt-1 allow us to examine the technological relationship between the quarrying of chert at this site and its reduction and manufacture into preforms and finished tools further inland.

Geophysical data collected from the quarry was used to measure the extent, and depth of a large chert flake deposit. The results of this survey demonstrate the intensity and scope of

reduction occurring at the site. Analysis of chert debitage acquired from three excavated test pits at the site indicates that only the earliest stages of reduction took place at LbDt-1. This, along with evidence for preform, biface, and formal tool manufacture at LdFa-1 and LeDx-42, strongly indicates that LbDt-1 was the first link in a progressive sequence of lithic reduction continued at inland occupation site. Finally, geochemical provenance data further demonstrates the importance of LbDt-1 as a quarry site for toolmakers on southern Baffin Island, as it directly links chert from the quarry to chert debitage recovered from inland occupation sites.

Ultimately, the data we obtained using minimally invasive methods at LbDt-1 allow us to more accurately reconstruct Paleo-Inuit mobility and technological organization on southern Baffin Island, especially when contextualized using complementary datasets from LdFa-1 and LeDx-42. It is our hope that in presenting these methods, we promote quarry studies by providing a practical alternative for analysis of these challenging, but interpretively crucial sites.

6.5 Works Cited – Chapter 6

Andrefsky Jr., W., 1994. Raw Material Availability and the Organization of Technology. *American Antiquity*, 59(1), 21-34.

Andrefsky Jr., W., 2008. An Introduction to Lithic Technology and Stone Tool Life History. In Andrefsky Jr., W. (Ed.), *Lithic Technology: Measures of Production, Use and Curation*. Cambridge University Press, Cambridge, pp. 1-22.

Andrefsky Jr., W., 2009. The analysis of stone tool procurement, production, and maintenance. *Journal of Archaeological Research*, 17(1), 65-103.

Andrews, B. W., Murtha, T. M., and Scheetz, B., 2004. Approaching the Hatch Jasper quarry from a technological perspective: a study of prehistoric stone tool production in central Pennsylvania. *Midcontinental Journal of Archaeology*, 29(1), 63-101.

Bamforth, D. B., 2006. The Windy Ridge quartzite quarry: hunter-gatherer mining and hunter-gatherer land use on the North American Continental Divide. *World Archaeology*, 38(3), 511-527.

Barry, R. G., Arundale, W. H., Andrews, J. T., Bradley, R. S., and Nichols, H., 1977. Environmental Change and Cultural Change in the Eastern Canadian Arctic during the Last 5000 Years. *Arctic and Alpine Research*, 9(2), 193-210.

Beck, C., Taylor, A. K., Jones, G. T., Fadem, C. M., Cook, C. R., and Millward, S. A., 2002. Rocks are heavy: transport costs and Paleoarchaic quarry behavior in the Great Basin. *Journal of Anthropological Archaeology*, 21(4), 481-507.

Betts, M. W., Hardenberg, M., and Stirling, I., 2015. How animals create human history: relational ecology and the Dorset–polar bear connection. *American Antiquity*, 80, 89–112.

Bielawski, E., 1988. Palaeoeskimo variability: the early Arctic Small-Tool tradition in the central Canadian Arctic. *American Antiquity*, 53, 52–74.

Burke, A. L., 2007. Quarry source areas and the organization of stone tool technology: a view from Quebec. *Archaeology of Eastern North America*, 35, 63-80.

Burke, A. L., 2010. Extraction, Reduction, and Production at a Late Palaeoindian Chert Quarry in Eastern Quebec. In Brewer-LaPorta, M., Burke, A., Field, D. (Eds.), *Ancient Mines and Quarries: A Trans-Atlantic Perspective*. Oxbow Books, Oxford, pp. 85-96.

Collins, M. B., 1975. Lithic Technology as a Means of Processual Inference. In Swanson, E. (Ed.), *Lithic Technology: Making and Using Stone Tools*. Mouton Publishers, The Hague, pp. 15-34.

Daniel, I. R., 2001. Stone raw material availability and Early Archaic settlement in the southeastern United States. *American Antiquity*, 66(2), 237-265.

Darwent, C. M., 2004. The highs and lows of High Arctic mammals: temporal change and regional variability in Palaeoeskimo subsistence. In Mondini, M., Muñoz, S., Wickler, S. (Eds.), *Colonization, Migration, and Marginal Areas: A Zooarchaeological Approach*. Oxbow Books, Oxford, pp. 62–73.

Ericson, J. E., 1984. Towards the analysis of lithic production systems. In Ericson, J. E., Purdy, B. A. (Eds.), *Prehistoric quarries and lithic production. New directions in archaeology*. Cambridge: Cambridge University Press, pp. 1-10.

Erwin, J. C., 2010. Dorset Palaeoeskimo quarrying techniques and the production of little pots at Fleur De Lys, Newfoundland. In Brewer-LaPorta, M., Burke, A., Field, D. (Eds.), *Ancient Mines and Quarries: A Trans-Atlantic Perspective*. Oxbow Books, Oxford, pp. 56-66.

Frank, A. D., Skarbun, F., and Cueto, M. E., 2015. Tool Production Processes in Lithic Quarries from the Central Plateau of Santa Cruz, Argentina. *Quaternary International*, 375, 84-98.

Garvey, R., 2015. A Model of Lithic Raw Material Procurement. In Goodale, N., Andrefsky Jr., W. (Eds.), *Lithic Technological Systems and Evolutionary Theory*. Cambridge University Press, Cambridge, pp. 156-171.

Goodyear, A. C., and Charles, T., 1984. An archaeological survey of chert quarries in western Allendale county, South Carolina. Research Manuscript Series. Book 187.

Gopher, A., and Barkai, R. 2014. Middle Paleolithic open-air industrial areas in the Galilee, Israel: The challenging study of flint extraction and reduction complexes. *Quaternary International*, 331, 95-102.

Gramly, R. M., 1978. Lithic source areas in Northern Labrador. *Arctic Anthropology* 15, 36–47.

Kessler, R. A., Beck, C., Jones, G. T., 2009. Trash: The Structure of Great Basin Palaeoarchaic Debitage Assemblages in Western North America. In Adams, B., Blades, B.S. (Eds.), *Lithic Materials and Paleolithic Societies*. Wiley-Blackwell, New York, pp. 144-159.

Landry, D. B., 2013. The Organization of Late Dorset Lithic Technology at the LdFa-1 Site in Southern Baffin Island, Nunavut. M.A. Thesis, Department of Anthropology, University of Manitoba, Winnipeg, MB.

Landry, D. B., Ferguson, I. J., Milne, S. B., and Park, R. W., 2015. Combined geophysical approach in a complex Arctic archaeological environment: A case study from the LdFa-1 site, southern Baffin Island, Nunavut. *Archaeological Prospection*, 22(3), 157-170.

Landry, D. B., Milne, S. B., Park, R. W., Ferguson, I. J., and Fayek, M., 2016. Manual point cloud classification and extraction for hunter-gatherer feature investigation: A test case from two low arctic Paleo-Inuit sites. *Open Archaeology*, 2(1), 232-242.

Landry, D. B., Ferguson, I. J., Milne, S. B., Serzu, M., and Park, R. W., 2018. Integrated geophysical techniques for the archaeological investigation of LbDt-1, a Paleo-Inuit quarry site in the interior of southern Baffin Island, Nunavut, Canada. *Journal of Archaeological Method and Theory*, DOI: https://doi.org/10.1007/s10816-018-9370-6.

Lazenby, M. E. C., 1980. Prehistoric Sources of Chert in Northern Labrador: Field Work and Preliminary Analyses. *Arctic*, 33(3), 628-645.

Maxwell, M. S., 1973. Archaeology of the Lake Harbour district, Baffin Island. Mercury Series No. 6. Archaeological Survey of Canada, National Museum of Man, Ottawa, Ontario.

Maxwell, M. S., 1985. *Prehistory of the Eastern Arctic*. Academic Press, Orlando.

McAvoy, D. G., 2014. An Examination of the Pre-Dorset Caribou Hunters from the Deep Interior of Southern Baffin Island, Nunavut, Canada. M.A. Thesis, University of Manitoba, Winnipeg, MB.

McCartney, P. H., and Helmer, J. W., 1989. Marine and terrestrial mammals in the High Arctic Palaeoeskimo economy. *Archaeozoologia*, 3, 143–160.

McGhee, R., 1975. An individual view of Canadian Eskimo prehistory. Bulletin (Canadian Archaeological Association), (7), 55-75.

McGhee, R., 1996. *Ancient People of the Arctic*. UBC Press, Vancouver.

Milne, S. B., 2003. Peopling the Pre-Dorset Past: A Multi-Scalar Study of Early Arctic Lithic Technology and Seasonal Land Use Patterns on Southern Baffin Island. Ph.D. Dissertation, McMaster University, Hamilton, ON.

Milne, S. B., 2005. Archaeological investigations in the Mingo and Amadjuak Lake districts of southern Baffin Island. Permit report covering the work conducted under Nunavut Territory Archaeologist Permit No. 04-06A. Nunavut Ministry of Culture, Language, Elders and Youth, Igloolik, Nunavut.

Milne, S. B., 2007. Culture Continuity and Change in the Interior of southern Baffin Island: Revisiting the Pre-Dorset/Dorset Transition. Permit report covering the work conducted under Nunavut Archaeologist Permit 07-014A. Manuscript on file, Department of Culture, Language, Elders and Youth, Government of Nunavut, Igloolik, Nunavut.

Milne, S. B., 2008. Archaeological Investigations in the Mingo Lake District of southern Baffin Island: Assessing Palaeo-Eskimo Culture Continuity and Change. Permit report covering the work conducted under Nunavut Archaeologist Permit 07-014. Manuscript on file, Department of Culture, Language, Elders and Youth, Government of Nunavut, Igloolik, Nunavut.

Milne, S. B., 2011. Landscape Learning and Lithic Technology: Seasonal Mobility, Enculturation, and Tool Apprenticeship among the Early Palaeo-Eskimos. In A. Cannon, A. (Ed.), *Structured Worlds: The Archaeology of Hunter-Gatherer Thought and Action*. Equinox Publishing, Ltd., pp. 95-115.

Milne, S. B., 2013. Chert sourcing and Palaeo-Eskimo stone tool technology. Permit report covering the work conducted under Nunavut Territory Archaeologist Permit No. 2013-02A. Department of Culture, Language, Elders and Youth, Government of Nunavut, Igloolik, Nunavut.

Milne, S. B. 2016a. The Analytical Quandary of Chert Quarries: A Multi-Scalar Approach using GIS Modelling, Archaeo-Geophysics, Lithic Provenance, and Debitage Analysis to Understand Palaeo-Eskimo Lithic Technological Organization and Novice Skill on Southern Baffin Island. SSHRC Insight Grant Proposal.

Milne, S. B. 2016b. Chert Sourcing and Paleo-Eskimo Stone Tool Technology: Report on Work Conducted Under Nunavut Archaeological Permit No. 2015-21A. Department of Culture, Language, Elders and Youth, Government of Nunavut, Igloolik, Nunavut.

Milne, S. B., and Donnelly, S. M., 2004. Going to the birds: examining the importance of avian resources to Pre-Dorset subsistence strategies on southern Baffin Island. *Arctic Anthropology*, 41(1), 90–112.

Milne, S. B., Park, R. W., and Stenton, D. R., 2012. Dorset culture land use strategies and the case of inland southern Baffin Island. *Canadian Journal of Archaeology,* 36, 267–288.

Milne, S. B., Park, R. W., and Stenton, D. R., 2013. For caribou, chert, and company: understanding mobility among the Palaeo-Eskimos of Baffin Island, Arctic Canada. In Preston, P.R., Schorle, K. (Eds.), *Mobility, Transition, and Change in Prehistory and Antiquity*. Final Proceedings, Graduate Archaeology Organisation Conference 2008. Hertford College, Oxford, UK. British Archaeological Reports, International Series, Archaeopress, Oxford, pp. 49–61.

Milne, S. B., Park, R. W., Stenton, D. R., Fayek, M., and ten Bruggencate, R. E., 2014. Novice Flint Knapping, Seasonal Mobility, and Palaeo-Eskimo Lithic Raw Material Acquisition in the Interior of Southern Baffin Island, NU. Final Proceedings, Society for American Archaeology Annual Meetings. Austin, Texas, April 23 – 27.

Minchak, S. A., 2010. Subsistence Activities at Quarries and Quarry-Related Workshops: Testing Holmes and Bryan Alternatives with Blades from the Gault Site, Central Texas, USA. In Brewer-LaPorta, M., Burke, A., Field, D. (Eds.), *Ancient Mines and Quarries: A Trans-Atlantic Perspective*. Oxbow Books, Oxford, pp.120- 131.

Mudie, P. J., Rochon, A., and Levac, E., 2005. Decadal scale sea ice changes in the Canadian Arctic and their impacts on humans during the past 4,000 years. *Environmental Archaeology,* 10, 113-126.

Murray, M. S., 1999. Local heroes. The long-term effects of short-term prosperity-an example from the Canadian Arctic. *World Archaeology,* 30, 466–483.

Nash, D. J., Coulsen, S., Staurset, S., Ullyott, J. S., Babutsi, M., Smith, M. P., 2016. Going the Distance: Mapping Mobility in the Kalahari Desert During the Middle Stone Age Through Multi-Site Geochemical Provenancing of Silcrete Artefacts. *Journal of Human Evolution,* 96, 113-133.

Odess, D., 1998. The archaeology of interaction: Views from artifact style and material exchange in Dorset society. *American Antiquity,* 63, 417–435.

Park, R., 2008. Archaeological excavations at the LdFa-1 site, Mingo lake, Baffin Island, Summer Permit report on work conducted under Nunavut Territory Archaeologist Permit No. 08-029A. University of Waterloo.

Ricklis, R., and Cox, K., 1993. Examining Lithic Technological Organization as a Dynamic Cultural Subsystem: The Advantages of an Explicitly Spatial Approach. *American Antiquity,* 58(3), 444-461.

Sanford, B. V. and Grant, A. C., 2000. Geological framework of the Ordovician System in the southeast Arctic platform, Nunavut. *Geological Survey of Canada, Bulletin*, 557, 13-38.

Shott, M. J., 1994. Size and Form in the Analysis of Flake Debris: Review and Recent Approaches. *Journal of Archaeological Method and Theory,* 1(1), 69-110.

Stenton, D. R., 1990. Archaeological Investigations at the Tungatsivvik Site (KkDo-3), Baffin Island, N.W.T. Unpublished Report Prepared for the Government of the Northwest Territories, Iqaluit, NWT.

Stenton, D. R., 1991a. The archaeology of terrestrial hunting systems: The Amadjuak Lake Project. Permit report on file with the Department of Culture, Elders, Language, and Youth. Government of Nunavut. Igloolik: Nunavut.

Stenton, D. R., 1991b. Caribou population dynamics and Thule culture adaptations on southern Baffin Island, NWT. *Arctic Anthropology,* 1, 15-43.

Stenton, D. R., 1991c. The adaptive significance of caribou winter clothing for arctic hunter-gatherers. *Etudes/Inuit/Studies,* 1, 3-28.

Sykes, R. W., Delvigne, V., Fernandes, P., Piboule, M., Lafarge, A., Define, E., Santagata, C. and Raynal, J. P., 2017. “Undatable, unattractive, redundant”? The Rapavi silcrete source, Saint-Pierre-Eynac (Haute-Loire, France): Challenges studying a prehistoric quarry-workshop in the Massif Central mountains. *Journal of Archaeological Science: Reports*, 15, 587-610.

ten Bruggencate, R. E., Milne, S. B., Fayek, M., Park, R. W., and Stenton, D. R., 2015. Characterization of Chert Artifacts and Two Newly Identified Chert Quarries on Southern Baffin Island. *Lithic Technology*, 40, 189–198.

ten Bruggencate, R. E., Stup, J. P., Milne, S. B., Stenton, D. R., Park, R. W., and Fayek, M., 2016. A human-centered GIS approach to modeling mobility on southern Baffin Island, Nunavut, Canada. *Journal of Field Archaeology*, 41(6), 684-698. DOI:10.1080/00934690.2016.1234897.

ten Bruggencate, R. E., Milne, S. B., Park, R. W., Fayek, M., and Stenton, D. R., 2017. Combining chert provenance and least-cost pathway analyses to reconstruct Pre-Dorset and Dorset mobility on southern Baffin Island. *Journal of Archaeological Science: Reports*, 14, 651-661.

Tremayne, A. H., 2015. The Design of Arctic Small Tool Tradition Toolkits: An Example from the Matcharak Lake, Alaska. *North American Archaeologist*, 36(1), 1-31.

Tripcevich, N., Contreras, D. A., 2013. Archaeological Approaches to Obsidian Quarries: Investigations at the Quispisisa Source. In Tripcevich, N., Vaughn, K.J. (Eds.), *Mining and Quarrying in the Ancient Andes. Interdisciplinary Contributions to Archaeology*, Springer, New York, pp. 23-44.

Chapter 7

Discussion and Conclusions

7.1 Research Objectives and Results

This study had four objectives: (1) to evaluate the role of archaeogeophysical survey for the discernment of natural and anthropogenic features on hunter-gatherer archaeological sites in the deep interior of southern Baffin Island; (2) to develop and test an accessible method that allows archaeologists to spatially isolate and analyse surface elements from a massive 3D point cloud dataset produced by terrestrial laser scanning; (3) to use a combination of remote sensing and geophysical datasets (surface and subsurface) to develop methodologies that can be employed for a non-invasive study of hunter-gatherer quarry sites; and (4), to identify and understand long-term land and resource use patterns through the synthesis of three Paleo-Inuit site investigations in the deep interior of southern Baffin Island.

To meet these objectives, I used a combination of non-invasive survey and investigative techniques at three inland Paleo-Inuit sites on southern Baffin Island, and assessed their effectiveness in this challenging environment. The collection of local geological data and Paleo-Inuit archaeological remains were also integral to the completion of these tasks and assessment of the techniques in use. Three research manuscripts were developed with a focus in evaluating the application of these techniques in this region (Chapters 3, 4, and 5). The final manuscript (Chapter 6) presented the broader social significance of the cumulative results, which lend further support to patterns identified by Milne et al. (2012) that indicate the persistence of inland-coastal seasonal land-use patterns spanning the Pre-Dorset and Dorset periods on southern Baffin Island (2012).

Four remote sensing and geophysical survey methods were used to investigate site occupation and land-use patterns of the Paleo-Inuit of southern Baffin Island: TLS, GPR, EM, and Magnetic mapping. Overlapping datasets and integration of these four field methods provided multiple lines of evidence for interpreting of the surface and sub-surface natural and anthropogenic layering and anomalies (Landry et al. 2015, 2018). However, it is clear that not every method provided the same kind of data resolution or precision needed to accurately interpret the range of surface and sub-surface complexities and features in a low-Arctic environment.

The results from the archaeogeophysical case study conducted at LdFa-1, Area 5 (Chapter 3) successfully demonstrated the value of magnetic geophysical investigation in a complex low Arctic archaeological environment and its role in providing information on subsurface archaeological features. Data-reduction methods were highlighted in this study, including the importance of removing temporal drift from magnetic data to produce final responses related closely to the subsurface physical properties. Of the six geophysical responses presented in the results of this case study, spatial assemblages of small-scale (<2m) anomalies were found to correlate between the magnetic and magnetic susceptibility results. These magnetic anomalies were interpreted to be associated with groupings of igneous boulders in the shallow subsurface. One of these grouping is a roughly circular arrangement of anomalies with a diameter of 4 m, and is spatially correlated with a productive test unit at the site. This anomaly was interpreted to be the remains of a near-surface tent ring. Furthermore, magnetic susceptibility mapping data proved to be useful at the Paleo-Inuit lithic quarry site of LbDt-1 (see Chapter 5).

In Chapter 4, the TLS results illustrate an effective use of these large datasets for extracting and improving our analytical capabilities for low relief site features, such as those on Paleo-Inuit sites. Using a combination of spectral datasets common to TLS (i.e., intensity and RGB values), I was able to enhance the visual and analytical representation of archaeological hunter-gatherer site surfaces with a simplified digital, manual classification approach. This approach provided the means to non-invasively survey and map features in fine detail, and subsequently classify the point cloud data into independent segments, each representing a different surface material found on the site. With the segmented dataset, specific elements such as surface boulders were isolated to create an alternate characterization of the site's prominent features and their surroundings. This case study provided insight into how one could map small surface elements such as chert flakes at other sites like LbDt-1 with the goal of determining the surface distribution of less obvious or more ambiguous features.

Results of the third case study (Chapter 5) demonstrated the capacity of remote sensing and geophysical methods used to non-invasively investigate prehistoric activities at ephemeral hunter-gather quarry sites without the need for full-scale excavation and the collection of large material assemblages. At LbDt-1, a combination of surface remote sensing and sub-surface geophysics was used to investigate the extent of chert flakes within a general area of a quarry survey. The TLS classification approach presented in Chapter 4 provided a range of information discerning the surface distribution of the chert flake deposit, while GPR results from the site suggest the deposit has a thickness of around 10-20 cm, and indicate that there are no additional parts of the deposit masked by soil in this area. Lastly, the application of similar magnetic data reduction techniques, like those used at LdFa-1, helped to define two layers of ~20 cm thickness

within the chert deposit suggesting that areas of the chert and gravel deposits are attributable to differing levels of magnetization relative to the topsoil at the site.

The overall study of the lithic quarry site, and its relationship to other inland sites such as LdFa-1 and LeDx-42 (Chapter 6) provide insight in the use of the southern Baffin Island's interior region by both the Pre-Dorset and Dorset. Specifically, the results from this study suggest that Paleo-Inuit toolmakers were collecting raw chert nodules from specific inland quarry sites and carrying them further inland to larger habitation sites where they were more intensively reduced. These conclusions help to fill a gap in our understanding of Pre-Dorset and Dorset lithic technological organization in this region, as prior to this, little was known about the origins of the raw material and its earliest stages of reduction.

The four objectives of this dissertation have been met, resulting in both an important assessment of non-invasive archaeological techniques in the low Arctic, and a novel investigation of Paleo-Inuit quarrying and technological organization. The results of this study indicate that a combination of TLS, magnetic, and GPR survey can be useful in at least some complex Arctic environments. Their combination provided valuable information across a range of three hunter-gatherer sites and insight towards future development of new research questions based on their results.

The results of this study demonstrate the probable long-term extraction of raw chert toolstone from quarries sites like LbDt-1, and the subsequent transport of this material to larger, and more central sites like LdFa-1 and LeDx-42 for further reduction. These habitation sites are ideally situated to exploit locally available seasonal subsistence resources, namely caribou, while simultaneously meeting the need to socialize with other remotely located human populations (see Milne 2003, 2005, 2011; Milne et al. 2012, 2013). This strongly suggests continuity in land use

patterns, seasonal settlement, resource acquisition, and socialization among the Pre-Dorset and Dorset populations on southern Baffin Island.

7.2 Contributions to the Study of Archaeology and Arctic Sciences

This research project is the first of its kind to be conducted on southern Baffin Island, and was unique in its focus on a comprehensive analytical and interpretive application of remote sensing and geophysics in this region of the eastern Arctic. The resulting data and interpretations from this project contribute to the development of low-relief and ephemeral hunter-gatherer site investigations, and provide a wide range of testable archaeogeophysical and remote sensing applications in a complex environmental setting, perhaps, most notably, lithic quarry sites. The final results of this dissertation add to the limited literature focused on the invasive investigation of hunter-gatherer lithic procurement sites (i.e., quarries) as part of a system of technological organization (e.g., Bamforth 1991; 2006; Burke 2007; Byrd et al. 2009; Root 1997).

More broadly, the application of this multi-method approach dramatically shifts focus on future research design. Non-invasive investigative methods can decrease the amount of time spent manually mapping and testing archaeological sites, and provides a means to monitor and manipulate *in situ* features post investigation. The three field seasons that were foundational to this study were negatively impacted by unpredictable weather, among other logistical complications beyond the control of the research team. Due to these unforeseen circumstances, my complete field time for this project was reduced from 14 planned days to just 6 days in total. Even with these limitations, however, I was still able to design a fieldwork plan to acquire as much data as possible through remote sensing and geophysical survey, which, in the end,

provided enough information for me to work with to generate some important archaeological results.

Additionally, this kind of detailed collection of surface and subsurface data will serve as a baseline for future comparative mapping and targeted excavation. In turn, this will help monitor the stability of Arctic archaeological sites, which are increasingly threatened by the effects of climate change (e.g., Barr 2007, 2009; Colette and Cassar 2007; Heritage 2008; Hodgetts and Eastaugh 2017; Wolff and Urban 2013).

Lastly, whenever possible, I used openly sourced software to process and analyse data collected from all three sites. With the overall continued support, development, and inclusion of the kinds of techniques and programs presented throughout this project (i.e., LAStools; CloudCompare; grp_process), I believe that similar non-invasive approaches to archaeology will continue to gain popularity and become more accessible to a general audience. Moreover, the results will be readily comparable to those generated by people using similar approaches for archaeological investigation in other regions of the world.

7.3 Non-Invasive Approach to Archaeology and the Way of the Future

Stewardship of the archaeological record has long been a desire – and in recent decades – a mandate of all North American archaeologists (see SAA and CAA Principles of Archaeological Ethics). Given the potential to participate, and actively aid in the development of this collective goal, is one reason I found this project so appealing. Assessing the use of non-invasive digital survey and geophysical mapping techniques not only provides insight into an exciting future for archaeologists, but also helps us to explore new ways to investigate

archaeological remains without destroying the archaeological record through invasive excavation techniques. Archaeologists who have discussed and encouraged both the use of similar investigative technologies have ultimately help set the foundations for my project (Conyers 2010; Kvamme 2003; McCoy and Ladefoged 2009; Romero and Bray 2014; Thompson et al. 2011; Watterson 2015). These archaeologists note that as remote sensing and geophysics become more integrated into the principal research design of projects, our ability to answer more complex social questions through digital datasets will develop, and ultimately expand.

As remote sensing and geophysical techniques have become a more common component of North American Arctic archaeological projects (e.g., Dawson et al. 2011; Hodgetts and Eastaugh, 2017; Hodgetts et al. 2011; Wolff et al. 2015; Urban 2012; Urban et al. 2012; Easthaugh and Taylor 2005 etc.), examination of how to best apply instruments in the field, and more importantly how to generate the kinds of data that can be used to effectively interpret broader research questions within the prehistoric past, remains quite limited. Throughout this dissertation, I was able to test several combinations of instruments with the goal of understanding the kinds of information that can be derived from each complementary dataset at a range of Paleo-Inuit sites. Consequently, my assessment in this region led me to establish an effective approach to non-invasively investigate certain aspects of large scale lithic quarry sites. This ultimately proved to be of use in answering questions about the continuity of resource and land-use by both the Pre-Dorset and Dorset peoples of southern Baffin Island (Landry et al. 2018).

The use of TLS across all three sites (LdFa-1, LeDx-42, LbDt-1), was an effective and efficient method for mapping large-scale site features, and for further digital isolation of smaller surface elements for in-field examination. The major drawback of this method is the cost of the

instrument and supporting systems, transportation to and from the field, and its functionality in the extreme climate of the Arctic. For instance, using a bulky terrestrial laser scanner in the Arctic environment can be difficult to mount and maintain. Most importantly, the cold climate, and constant wind caused the instrument to repeatedly misalign, which rapidly drained the batteries of power. Fortunately, Leica has now released a much more compact, lightweight, and more cost-effective alternative, which also carries upgraded capturing and processing systems, and includes a lower operational temperature rating. Such a system would be ideal for future Arctic research.

For LdFa-1, the use of a magnetic gradiometer with a base-station was effective and appropriate for the objective of locating potential anthropogenic features in the near-surface. The base-station, with thermal and temporal drift corrections derived from its reading were essential to this project, and I would recommend this strategy for any future project. Although, one could consider using a simple baseline adjacent to the site to correct for thermal drift, while approximate correction of temporal drift could be made using the baseline data from the distant Iqaluit magnetic observatory, where we found that variations measured there were similar to those recorded on site. An EM31 instrument was also used at this site. While the InPhase component – measuring magnetic susceptibly – was effective in this environment, the resistivity imaging was less so; however, information about the near-surface characteristic derived from this instrument survey did inform me of the potential for effective radar use. In this regard, I believe that a combination of magnetics and radar would be ideal for future non-invasive investigation at LdFa-1 or other similar hunter-gatherer sites. In addition, the low resistivity means that the spatial variations in the InPhase response correspond closely to the spatial

variations in the magnetic susceptibility, meaning there is no need to correct for these variations in the conductivity when interpreting the magnetic susceptibility.

Lastly, at LbDt-1, the combined use of GPR and electromagnetic survey resulted in a successful investigation of a Paleo-Inuit lithic quarry deposit. The single antenna, 400 MHz GPR provided a sufficiently high-resolution dataset for processing and interpreting reflections in the uppermost near-surface layers. However, a second, lower-frequency wavelength antenna (i.e. 100 or 200MHz) may have provided better resolution of the deeper structures of the deposit, including the permafrost and bedrock layers. This would be recommended for future projects if the intended research design included understanding the stability of the subsurface layers.

The EM-400 Profiler survey at LbDt-1 also proved useful for determining areas of magnetic variation. These results, like those from LdFa-1, were derived from the InPhase magnetic susceptibility component of the EM survey. Once again, the quadrature component did not provide very useful results mainly due to the resistive nature of the subsurface. Since high resolution and high precision data collection is of particular importance for the investigation of ephemeral sites like those in this dissertation, it is important to take the proper steps to calibrate EM instruments prior to beginning a survey. Following Robinson et al. (2004) steps to warm-up the EM system prior to the survey proved useful in avoiding erroneous measurements during the early parts of the survey.

Any archaeologist aiming to investigate a quarry site would certainly benefit from these methods. In particular, TLS can be useful for identifying and quantifying certain types of raw material including diffuse surface scatters of chert debris or nodules of chert still embedded in a natural outcrop. If a researcher is interested in mapping and assessing the extent of an expansive deposit, like those often typifying lithic quarry sites, a combination of radar imaging (at varying

wavelengths) and magnetic susceptibly can provide valuable information about the characteristics of the near surface, and offer new insights into the site that would otherwise remain unknown or only be attainable through full-scale excavation. And finally, a combination of EM and radar methods invariably produces complementary datasets that can provide both horizontal and vertical mapping resolution, respectively, of the area surveyed.

Looking forward, important questions remain to be answered regarding Paleo-Inuit technological organization on southern Baffin. Geochemical data indicate there are other chert sources that were exploited by toolmakers (ten Bruggencate et al. 2016, 2017) thus it is important to locate these other sites and to understand how they were comparatively used over time to LbDt-1. Future survey planned by Milne in 2018 aims to do exactly that and once identified, application of the multi-method investigative approach presented in this dissertation will be a vital step in understanding Paleo-Inuit lithic procurement, reduction, and land use at the regional scale. Plans to investigate the lower component at LbDt-1 using magnetics and TLS survey will also provide complementary data to those presented in Case Study 3, which will facilitate a more thorough interpretation of the entire site. Moreover, such data might reveal the presence of features commonly found on Paleo-Inuit habitation sites, namely tent rings and hearth features. At present, LbDt-1 represents an interesting exception to the norm in that the site does not appear to have been inhabited by anyone for any length of time while toolstone was being procured (Milne 2016). Another avenue of investigation to understand why people were not apparently staying at LbDt-1 would be to look for indirect evidence for transport technology that would allow people to carry with them large amounts of useable toolstone without having to spend significant effort reducing it on site. This would allow people to get what they need in a shorter period of time so as to continue traveling further inland. Examples of such transport

technology might include skin bags or backpacks, or sledges could have been used but may not leave clear signs in the archaeological record of their use due to the limitations of organic preservations in some Paleo-Inuit sites (Maxwell 1985). However, indirect evidence such as polish or edge attrition on lithic cores or preforms may be identifiable (Young and Bamforth 1990; Bamforth et al. 1990).

Despite the initial costs, upkeep, transportation, and learning curve involved in the application of these technologies, I believe a multi-method approach that makes use of TLS, magnetics and magnetic susceptibility measurements, and GPR survey is suitable to map, examine, and interpret several aspects of early Arctic hunter-gatherer sites. Of particular importance to the broader archaeological community, this combination was successful in providing details and analytic information concerning a large quarry site deposit, and I believe this approach can be expanded to other lithic quarries around the world. By adopting this non-invasive multi-method approach, I have presented a more detailed examination of Paleo-Inuit chert use, specifically how and why chert was acquired in the inland regions of southern Baffin Island and how quarry acquisition sites may have related to other sites further inland.

7.4 Works Cited – Chapter 7

Bamforth, D. B. 1991. Technological organization and hunter-gatherer land use: a California example. *American Antiquity*, *56*(2), 216-234.

Bamforth, D. B. 2006. The Windy Ridge quartzite quarry: hunter-gatherer mining and hunter-gatherer land use on the North American continental divide. *World Archaeology*, 38(3), 511-527.

Bamforth, D. B., Burns, G. R., Woodman, C. 1990. Ambiguous use traces and blind test results: new data. *Journal of Archaeological Science*, 17(4), 413-430.

Barr, S. 2007. The effects of climate change on cultural heritage in the polar regions. In *Heritage at Risk*. ICOMOS World Report 2006/2007 on Monuments and Sites in Danger.

Barr, S. 2009. Protecting cultural heritage and community roots. In *Climate Change and Arctic Sustainable Development*. Paris, France: United Nations Educational, Scientific and Cultural Organization.

Bryd, B. F., Young, D. C., and McGuire, K. R. 2009. Pavement, quarries, Gypsum period residential stability, and Trans-Holocene settlement systems of the Mohave Desert: a case study at Fort Irwin. *Journal of California and Great Basin Anthropology*, 29(2), 121-144.

Burke, A. L. 2007. Quarry source areas and the organization of stone tool technology: a view from Quebec. *Archaeology of Eastern North America*, 35, 63-80.

Colette, A., and Cassar, M. 2007. Climate change and world heritage: report on predicting and managing the impacts of climate change on world heritage, and strategy to assist states parties to implement appropriate management responses.

Conyers, L. B. 2010. Ground-penetrating radar for anthropological research. *Antiquity*, 84(323), 175-184.

Dawson, P., Levy, R., and Lyons N. 2011. 'Breaking the fourth wall': 3D virtual worlds as tools for knowledge repatriation in archaeology. *Journal of Social Archaeology*, 11(3), 387-402.

Eastaugh, E., and Taylor, J. 2005. Geophysical survey of the Dorset Palaeoeskimo site of Point Riche. *Newfoundland and Labrador Studies*, *20*(1).

Heritage. 2008. *Climate Change and the Historic Environment.* London: English Heritage.

Hodgetts, L., and Eastaugh, E. 2017. The role of magnetometry in managing Arctic archaeological sites in the face of climate change. *Advances in Archaeological Practice*, *5*(2), 110-124.

Hodgetts, L., Dawson, P., and Eastaugh, E. 2011. Archaeological magnetometry in an Arctic setting: a case study from Maguse Lake, Nunavut. *Journal of Archaeological Sciences*, 38, 1754–1762. DOI:10.1016/j.jas.2011.03.007.

Kvamme, K. 2003. Geophysical surveys as landscape archaeology. *American Antiquity*, 68(3), 435–457.

Landry, D. B., Ferguson, I. J., Milne, S. B., and Park, R. W. 2015. Combined geophysical approach in a complex Arctic archaeological environment: A case study from the LdFa-1 site, southern Baffin Island, Nunavut. *Archaeological Prospection*, *22*(3), 157-170.

Landry, D. B., Milne, S. B., Park, R. W., Ferguson, I. J., and Fayek, M. 2016. Manual point cloud classification and extraction for hunter-gatherer feature investigation: A test case from two low arctic Paleo-Inuit sites. *Open Archaeology*, *2*(1), 232-242.

Landry, D. B., Ferguson, I. J., Milne, S. B., Serzu, M., and Park, R. W. 2018 Integrated geophysical techniques for the archaeological investigation of LbDt-1, a Paleo-Inuit quarry site in the interior of southern Baffin Island, Nunavut, Canada. *Journal of Archaeological Method and Theory*, DOI: https://doi.org/10.1007/s10816-018-9370-6.

McCoy, M. D., and Ladefoged, T. N. 2009. New developments in the use of spatial technology in archaeology. *Journal of Archaeological Research*, *17*(3), 263-295.

Maxwell, M. S., 1985. *Prehistory of the eastern Arctic*. Orlando, FL.: Academic Press.

Milne, S. B. 2003. Identifying Pre-Dorset structural features on southern Baffin Island: Challenges and considerations for alternative sampling methods. *Inuit Studies*, 27(1-2), 67-90.

Milne, S. B. 2005. Archaeological Investigations in the Mingo and Amadjuak Lake Districts of southern Baffin Island. Permit Report covering the work conducted under Nunavut Archaeologist Permit 04-06A. Unpublished permit report, Nunavut Ministry of Culture, Language, Elders and Youth, Igloolik.

Milne, S. B. 2011. Landscape learning and lithic technology: Seasonal mobility, enculturation and tool apprenticeship among the early Palaeo-Eskimos. In A. Cannon (Ed.), *Structured Worlds: The Archaeology of Hunter-Gatherer Thought and Action*, (pp. 95-115). Equinox Publications.

Milne, S. B. 2013. Chert Sourcing and Palaeo-Eskimo Stone Tool Technology. Report on work conducted under Nunavut Archaeological Permit No. 2013-02A. Manuscript on file with the Department of Culture, Language, Elders and Youth, Government of Nunavut, Igloolik, Nunavut.

Milne, S. B. 2016. Chert Sourcing and Paleo-Eskimo Stone Tool Technology: Report on Work conducted Under Nunavut Archaeological Permit No. 2015-21A. Department of Culture, Language, Elders and Youth, Government of Nunavut, Igloolik, Nunavut.

Milne, S. B., Park, R. W., and Stenton, D. R. 2012. Dorset culture land use strategies and the case of inland southern Baffin Island. *Canadian Journal of Archaeology/Journal Canadien D'Archéologie*, 36(2), 267-288.

Robinson, D. A., Lebron, I., Lesch, S. M., and Shouse, P. 2004. Minimizing drift in electrical conductivity measurements in high temperature environments using the EM-38. *Soil Science Society of America Journal*, 68(2), 339-345.

Romero, B. E., and Bray. T. L. 2014. Analytical applications of fine-scale terrestrial lidar at the imperial Inca site of Caranqui, northern highland Ecuador. *World Archaeology*, 46(1), 25-42.

Root, M. J. 1997. Production for Exchange at the Knife River Flint Quarries, North Dakota. *Lithic Technology*, 22, 33-50.

ten Bruggencate, R. E., Stup, J. P., Milne, S. B., Stenton, D. R., Park, R. W., and Fayek, M., 2016. A human-centered GIS approach to modeling mobility on southern Baffin Island, Nunavut, Canada. *Journal of Field Archaeology*, 41(6), 684-698. DOI:10.1080/00934690.2016.1234897.

ten Bruggencate, R. E., Milne, S. B., Park, R. W., Fayek, M., and Stenton, D. R., 2017. Combining chert provenance and least-cost pathway analyses to reconstruct Pre-Dorset and Dorset mobility on southern Baffin Island. *Journal of Archaeological Science: Reports*, 14, 651-661.

Thompson, V. D., Arnold III, P. J., Pluckhahn, T. J., and Vanderwarker, A. 2011. Situating remote sensing in anthropological archaeology. *Archaeological Prospection*, 18, 195-213.

Urban, T. M. 2012. In the footsteps of J. Louis Giddings (1909–1964): archaeological geophysics in Arctic Alaska. *Antiquity*, 86, 332.

Urban, T. M., Anderson, D. D. and Anderson, W. W. 2012. Multimethod geophysical investigations at an Inupiaq village site in Kobuk Valley, Alaska. *The Leading Edge*, 31, 950-956.

Watterson, A. 2015. Beyond digital dwelling: re-thinking interpretive visualisation in Archaeology. *Open Archaeology*, 1, 119-130.

Wolff, C. B., and Urban, T. M. 2013. Geophysical analysis at the Old Whaling site, Cape Krusenstern, Alaska, reveals the possible impact of permafrost loss on archaeological interpretation. *Polar Research*, *32*(1), 19888.

Young, D., and Bamforth, D. B. 1990. On the macroscopic identification of used flakes. *American Antiquity*, 55(2), 403-409.

Appendix A: Contribution of Collaborating Authors

Chapter 3 (Manuscript 1)

The idea for the study in this chapter was my own. I participated in establishing the geophysical grid, and collected the magnetic data from LdFa-1 during the 2014 field season as part of a collaborative project run by Dr. Brooke Milne of the University of Manitoba. Dr. Ian Ferguson collected the electrical resistivity imaging data from LdFa-1 during that same field season. The archaeological data referred to in this manuscript was collected by Dr. Robert Park in 2008. I processed all of the geophysical data with the help of Dr. Ian Ferguson. The writing and interpretations are my own, however, Dr. Brooke Milne provided primary edits and guidance throughout the entire writing process. Dr. Ian Ferguson aided in the writing of the geophysical theory sections. Each co-author provided detailed feedback and discussions throughout.

Chapter 4 (Manuscript 2)

The idea for the study in this chapter was my own. I collected the laser scanning point cloud data during the 2013 field season with the help of Dr. Brooke Milne and Dr. Mostafa Fayek. I developed and performed the all classification processing for this research paper. The images and figures are all my own. The writing and interpretations are my own, however, Dr. Brooke Milne provided primary edits and guidance throughout the entire writing process. Drs. Ferguson, Park, and Fayek each provided valuable discussion and suggestions to better the manuscript.

Chapter 5 (Manuscript 3)

The idea for the study in this chapter was my own. I established the three geophysical grids at LbDt-1. Remote sensing and geophysical data was collected by both me and Mr. Mulu Serzu during the 2015 field season as part of Dr. Milne's collaborative project. I developed the surveys and research design for this fieldwork as well as the outline for the manuscript. Dr. Ian Ferguson provided me with valuable technical training and skills in order to developing the geophysical processing procedures for this manuscript. The writing and interpretations are my own, however, Dr. Ferguson provided the technical sections pertaining to complex geophysical theory. Once again, Dr. Brooke Milne provided primary edits and guidance throughout the entire writing process, while the additional co-authors each provided valuable insight and feedback before the manuscript submission.

Chapter 6 (Manuscript 4)

The idea for the study in this chapter was my own. The geophysical data from LbDt-1 was collected by me and Mr. Mulu Serzu in 2015, while the archaeological excavation data from the three sites was collected by Dr. Milne, spanning a decade of fieldwork. Dr. Rachel ten Bruggencate collected, and analyzed the geochemical samples, and conducted the provenance analysis as part of her ongoing research on Baffin Island, and in collaboration with Dr. Milne's overarching project. Some sections regarding quarries, and geochemical provenance studies on Baffin Island were a collaborative effort involving the writing of Dr. Brooke Milne and Dr.

Rachel ten Bruggencate. Both Dr. ten Bruggencate and Dr. Milne provided vital editing and review as part of this collaborative process.